DEPARTMENT OF MECHANICAL AND INDUSTRIAL ENGINEERING
LABORATORY FOR ERGONOMICS RESEARCH
ENGINEERING EXPERIMENT STATION
UNIVERSITY OF ILLINOIS AT URBANA - CHAMPAIGN
URBANA, ILLINOIS 61801

NASA CR-116873

A STUDY OF THE THERMAL BEHAVIOR OF LIVING BIOLOGICAL TISSUE WITH APPLICATION TO THERMAL CONTROL OF PROTECTIVE SUITS

by

A. SHITZER
J. C. CHATO
B. A. HERTIG

Technical Report No. ME-TR-207
January 1971

Supported by
National Aeronautics and Space Administration
under
Grant No. NGR-14-005-103

A STUDY OF THE THERMAL BEHAVIOR OF LIVING BIOLOGICAL TISSUE WITH APPLICATION TO THERMAL CONTROL OF PROTECTIVE SUITS

by

A. Shitzer

J.C. Chato

B. A. Hertig

Research Supported by

National Aeronautics and Space Administration

under

Grant No. NGR-14-005-103

Technical Report No. ME-TR-207

January 1971

Department of Mechanical and Industrial Engineering

Laboratory for Ergonomics Research

Engineering Experiment Station

University of Illinois at Urbana-Champaign

Urbana, Illinois 61801

ABSTRACT

A biothermal model of living tissue has been studied which allows for the inclusion of the effects of blood flow, local heat generation, conduction, and storage of heat on the heat transfer processes occurring in the living tissue. A second order, partial differential equation, the "bio-heat" equation, was obtained for the model. Due to the lack of reliable and detailed data on the thermophysical properties involved, the tissue was assumed to be isotropic and homogeneous and all properties were assumed to be constant. Transient, as well as steady-state, closed form, analytical solutions were obtained for cylindrical and rectangular geometries, and for various parameters.

Based on the analysis, a few observations were made:

(1) Blood flow plays a significant role in the transfer of heat inside the living tissue.

(2) Transient times for reaching a so-called "fully developed" temperature profile in the tissue were estimated to be of the order of 5-20 minutes. These transient times were found to be strongly dominated by a geometrical parameter.

(3) At elevated metabolic rates, maximum temperature may occur in the tissue rather than in the inner core.

(4) Knowledge of the exact shape of the heat flux on the skin was found to be unimportant for the determination of the temperature distribution away from the skin surface.

(5) Results obtained for the cylindrical and rectangular models were remarkably close for the practical range of variables. The rectangular geometry, however, was easier for computation.

The analysis was partially validated by measuring the temperature profiles on the skin of the thigh cooled by parallel tubes in contact with the skin.

Particular applications of the biothermal model were directed to the problem of extending the thermophysical capabilities of man. Providing a "micro-climate" to man by means of cooling tubes that are in direct contact with the skin, e.g., extravehicular space suits, was a major concern in this study. To this end, a cooling garment, including a cooling hood, was constructed. The garment consisted of sixteen individual pads made of Tygon tubes. These pads were grouped to provide independent supply of cooling water to six separate regions of the body: head, upper torso, lower torso, arms, thighs, and lower legs. Experiments with the cooling garment were directed at exploring the characteristics of independent control of temperature and removal of excess heat from separate regions of the body. Five activity schedules consisting of alternate sessions of standing and treadmill walking were used with five test subjects. Quasi-steady state and, to some extent, transient characteristics of the proposed scheme of independent regional cooling were studied. The results show that there are regions that require more cooling for this type of activity than others (thighs, lower legs, head). It was also demonstrated that heat strain was reduced as a result of wearing the cooling garment.

NOMENCLATURE†

a	half distance between cooling tubes, [L]
a_k	coefficient in Eqs. (3.61) and (3.62)
A	total skin surface area, $[L^2]$
A_1	defined by Eq. (3.69)
b	depth of tissue layer, [L]
b_k	coefficient in Eqs. (3.61) and (3.62)
c_1	defined by Eq. (E.19)
c_3	defined by Eq. (E.20)
c_b	specific heat of blood $[L^2\theta^{-2}T^{-1}]$
c_k	coefficient in Eqs. (3.61) and (3.62)
c_p	specific heat of tissue, $[L^2\theta^{-2}T^{-1}]$
$C\{\ \}$	Fourier cosine transform operator, defined by Eq. (3.28)
$E(y)$	defined by Eq. (3.13), [T]
f	heat flux, $[M\theta^{-3}]$
f_a	average heat flux, defined by Eq. (3.16), $[M\theta^{-3}]$
F, F_o	uniform heat flux, $[M\theta^{-3}]$
G	defined by Eq. (3.14), $[L^{-1}T]$
$G(y,\tau)$	defined by Eq. (3.21)
h	height, [L]
$H(\zeta)$	defined by Eq. (3.15), $[M\theta^{-3}T^{-1}]$
I_i	modified Bessel function of the first kind of order i
J_i	Bessel function of the first kind of order i
k	thermal conductivity, $[ML\theta^{-3}T^{-1}]$

†Units in brackets are: M, mass; L, length; θ, time; T, temperature.

k^*	ratio of thermal conductivities, defined by Eq. (B.8)
K_i	modified Bessel function of the second kind of order i
M	defined by Eqs. (3.40) or (3.42), $[L^{-1}T]$
q_b	rate of heat transported by blood, defined by Eq. (3.1), $[ML^{-1}\theta^{-3}]$
q_m, Q'	internal heat generation rate per unit volume, $[ML^{-1}\theta^{-3}]$
Q	defined by Eq. (3.10), $[L^{-2}T]$
Q_m	total metabolic rate, $[ML^2\theta^{-3}]$
r	radial coordinate, [L]
$\overline{R}$	defined under Eq. (D.6), [L]
R_1	radius of inner core in cylindrical model, [L]
R_{12}	radius of interface between skeletal muscle and skin layer in cylindrical model, [L]
R_2	radius of the skin surface in cylindrical model, [L]
s	defined under Eq. (D.6)
t	time, [θ]
t^*	characteristic time, [θ]
T	tissue temperature, [T]
T_a	arterial blood temperature, [T]
T_1, T_2^*	constant temperature at inner core, [T]
T_{ref}	reference temperature, [T]
$U(\zeta R)$	defined under Eq. (D.6)
V	volume, $[L^3]$
w	defined by Eq. (3.9), $[L^{-1}]$
w_b	blood perfusion rate per unit volume, $[ML^{-3}\theta^{-1}]$
W	weight $[ML\theta^{-2}]$

$W[\phi_1, \phi_2]$	Wronskian, defined by Eq. (3.24)
x	coordinate, normal to cooling tubes along the skin surface, [L]
y	coordinate, normal to skin surface, [L]
Y_i	Bessel function of the second kind of order i
$Y(y)$	defined by Eq. (3.26), [T]
z	coordinate, parallel to the axis of cooling tubes, [L]
α	thermal diffusivity, $[L^2\theta^{-1}]$
α_n	defined by Eq. (3.19), $[L^{-1}T]$
β	ratio of width of cooling tube to cooling tube spacing
γ	Euler's constant
γ_i	defined by Eq. (3.51), $[L^{-1}]$
δ_n	defined by Eq. (3.50), $[L^{-1}]$
ε_i	defined by Eq. (3.60), $[L^{-1}]$
ζ_i	defined by Eq. (3.17), $[L^{-1}]$
η	defined by Eq. (3.46)
θ	defined by Eq. (3.8), [T]
$\theta^*(y)$	variable blood supply temperature, [T]
λ_n	defined by Eq. (3.18), $[L^{-1}]$
$\Lambda(wr)$	defined by Eq. (3.38), [T]
μ_n	defined by Eq. (3.59), $[L^{-1}]$
ν_n	defined by Eq. (3.31), $[L^{-1}]$
ξ	dummy variable of integration, [L]
ρ	specific gravity of tissue, $[ML^{-3}]$
ρ^*	ratio of radii, defined by Eq. (E.8)
σ	defined by Eq. (3.55), $[L^{-1}]$

τ	dummy variable of integration, [L]
ϕ	angular coordinate in cylindrical model
Φ_1	plane angle between two adjacent tubes in cylindrical model
Φ_1, Φ_2	defined by Eq. (3.22a)
$\chi(\mu_n r)$	defined by Eq. (3.58)
$\psi(n)$	Psi or Digamma function
$\psi^j_{k\ell}(\zeta_i r)$	combination of modified Bessel functions, defined by Eq. (3.37)
$\Omega(\zeta r)$	defined by Eq. (3.39), $[M\theta^{-3}T^{-1}]$

Subscripts

1	pertaining to skin layer or initial state
2	pertaining to skeletal muscle or final state
b	blood
i	integer
j	integer
k	integer
ℓ	integer
m	integer
n	integer

LIST OF FIGURES

Page

Figure 3.1 Cross section of the normal skin. Copyright, 1967, CIBA Corporation, reproduced with permission from the Clinical Symposia by Frank H. Netter, M.D. 18

Figure 3.2 Representative section of the cylindrical model with the cooling tubes on the skin running perpendicular to the axis of the cylinder. 20

Figure 3.3 Representative section of the cylindrical model with the cooling tubes on the skin running parallel to the axis of the cylinder. 21

Figure 3.4 Representative section of the rectangular model. . 22

Figure 3.5 Geometry and boundary conditions for the rectangular model. Skin layer and skeletal muscle are considered as separate regions. 27

Figure 3.6 Temperature distribution in the separated tissue for the rectangular model. Dashed curves indicate temperature distribution obtained by Buchberg and Harrah [39] without blood flow. Q_m = 2600 Btu/hr, (760 w), β = 0.1 and constant temperature at inner core. 32

Figure 3.7 Effect of changing the specified flux function on the temperature of the skin for the rectangular model. Q_m = 2600 Btu/hr, (760 w), β = 0.1 and constant temperature at inner core. 34

Figure 3.8 Effect of increasing the contact area between the cooling tubes and the skin on the temperature distribution on the skin surface. Q_m = 290 Btu/hr (85 w), f_2/f_1 = 1.5 and constant temperature at inner core. 35

Figure 3.9 Steady state, one dimensional temperature distribution in the combined tissue with variable linear blood supply temperature for the rectangular model. Dashed line indicates locus of maxima. Q_m = 2600 Btu/hr (760 w), and constant temperature at inner core. 40

Figure 3.10 Geometry and boundary conditions for the cylindrical model with the cooling tubes on the skin running perpendicular to the axis of the cylinder. Skin layer and skeletal muscle are considered as separate regions. 42

Page

Figure 3.11 Geometry and boundary conditions for the cylindrical model with the cooling tubes on the skin running parallel to the axis of the cylinder. Skin layer and skeletal muscle are considered as a combined tissue. 48

Figure 3.12 Transient temperature distribution in the combined tissue for the one-dimensional rectangular model. Step changes:
(a) from 290 Btu/hr (85 w) to 2600 Btu/hr (760 w)
(b) from 2600 Btu/hr (760 w) to 290 Btu/hr (85 w)
Constant temperature at inner core. 53

Figure 3.13 Transient temperature distribution on the skin of the combined tissue for the two-dimensional rectangular model. Step change assumed from 290 Btu/hr (85 w) to 2600 Btu/hr (760 w), $\beta = 0.1$ and constant temperature at inner core. 56

Figure 3.14 Comparison between the steady state, two-dimensional solutions for rectangular and cylindrical models (tubes running perpendicular to the axis of the cylinder, $R_1 = 0.15$ ft, V and b are constant). $Q_m = 290$ Btu/hr (85 w), $\beta = 0.1$ and constant temperature at inner core. 62

Figure 3.15 Comparison between steady state, one-dimensional solutions obtained for the rectangular and cylindrical models (V and b are constant). Constant temperature at inner core. 63

Figure 3.16 Comparison between steady state, one-dimensional solutions obtained for the rectangular and cylindrical models (B and A are constant). Constant temperature at inner core. 64

Figure 3.17 Comparison between steady state, one-dimensional solutions obtained for the rectangular and cylindrical models (A and b are constant). Constant temperature at inner core. 65

Figure 3.18 Steady state temperature distributions in the combined tissue for the one-dimensional rectangular model. Constant temperature at inner core. . . . 67

Figure 3.19 Steady state temperature distributions in the combined tissue for the one-dimensional rectangular model. Constant flux at inner core. 68

Figure 3.20 Location of the maximum temperature in the combined tissue for the one-dimensional rectangular model. 70

Page

Figure 4.1 General view of the cooling garment. 77

Figure 4.2 Schematic diagram of the cooling garment and the control, supply and measuring systems. 81

Figure 4.3 View of the water supply system, rotameter and potentiometer recorder used for the experiments with the cooling suit. 82

Figure 4.4 View of the treadmill, Tele-Thermometer and system for collecting samples for determining metabolic rates. 84

Figure 4.5 General view of the set-up used for the experiments with the cooling suit. A test subject is shown dressed up in the cooling suit walking on the treadmill. No tennis shoes are shown in this picture and the ear canal thermistor is not connected. 86

Figure 4.6 View of one of the individual pads. 88

Figure 4.7 Activity schedules used for the experiments with the cooling suit. 91

Figure 4.8 Front view of the cooling garment. 96

Figure 4.9 Side view of the cooling garment. 97

Figure 4.10 Back view of the cooling garment. 98

Figure 4.11 Front view of a test subject dressed up in the cooling and insulating garments. 99

Figure 4.12 A test subject shown walking on the treadmill and breathing through the system for measuring metabolic rates. No tennis shoes are shown in the picture. 100

Figure 4.13 General view of the set-up used for the experiments with the individual cooling pads. A test subject is shown pedalling the bicycle ergometer. 101

Figure 5.1 Mean values of metabolic rates and of the amounts of heat removed by the cooling suit and by respiration for Schedule I. 106

Figure 5.2 Mean values of metabolic rates and of the amounts of heat removed by the cooling suit and by respiration for Schedule II. 107

Figure 5.3 Mean values of metabolic rates and of the amounts of heat removed by the cooling suit and by respiration for Schedule III. 108

Page

Figure 5.4 Mean values of metabolic rates and of the amounts of heat removed by the cooling suit and by respiration for Schedule IV. 109

Figure 5.5 Mean values of metabolic rates and of the amounts of heat removed by the cooling suit and by respiration for Schedule V. 110

Figure 5.6 Average ear canal temperatures for the various schedules. 111

Figure 5.7 Individual variations in the ear canal temperatures and heart rates for Schedule V. 119

Figure 5.8 Mean values of the amounts of heat removed by the cooling pads for Schedule I. 122

Figure 5.9 Mean values of the amounts of heat removed by the cooling pads for Schedule II. 123

Figure 5.10 Mean values of the amounts of heat removed by the cooling pads for Schedule III. 124

Figure 5.11 Mean values of the amounts of heat removed by the cooling pads for Schedule IV. 125

Figure 5.12 Mean values of the amounts of heat removed by the cooling pads for Schedule V. 126

Figure 5.13 Mean water inlet temperatures at the various regions of the body for Schedule II. 132

Figure 5.14 Comparison of measured and calculated temperature distribution on the surface of the skin for the rectangular model. Pad No. 1, w_b = 83.4 lb/hr-ft^3, Q' = 711 Btu/hr-ft^3 and constant temperature at inner core. 138

Figure 5.15 Comparison of measured and calculated temperature distribution on the surface of the skin for the rectangular model. Pad No. 2, w_b = 83.4 lb/hr-ft^3, Q' = 805 Btu/hr-ft^3 and constant temperature at inner core. 139

Figure 5.16 Comparison of measured and calculated temperature distribution on the surface of the skin for the rectangular model. Pad No. 3, w_b = 83.4 lb/hr-ft^3, Q' = 848 Btu/hr-ft^3 and constant temperature at inner core. 140

Page

Figure B.1 Comparison of steady state temperature distributions in the tissue for the two-dimensional, rectangular model without blood flow. Q_m = 2600 Btu/hr (760 w), β = 0.1, constant temperature at inner core. 153

Figure B.2 Comparison of steady state temperature distributions in the combined tissue for the two-dimensional rectangular model with and without blood flow. Q_m = 290 Btu/hr (85 w), β = 0.1, constant temperature at inner core. 154

Figure B.3 Effect of increasing the contact area between the cooling tubes and the skin on the temperature distribution on the skin surface. Blood flow effects are not included. Q_m = 290 Btu/hr (85 w), f_2/f_1 = 1.5 and constant temperature at inner core. 155

Figure C.1 Steady state temperature distribution in the combined tissue for the rectangular model. Q_m = 2600 Btu/hr, (760 w), β = 0.1 and constant temperature at inner core. 157

Figure C.2 Steady state temperature distribution in the combined tissue for the rectangular model. Q_m = 290 Btu/hr (85 w), β = 0.1, constant flux at inner core. 159

Figure D.1 The function $\psi^1_{01}(wR)$ drawn on semi-log paper. . . . 162

Figure D.2 The function $\psi^1_{00}(wR)$. 163

Figure D.3 The function $\psi^1_{12}(wR)$ drawn on semi-log paper. . . . 164

Figure E.1 Steady state temperature distribution in the combined tissue for the cylindrical model (cooling tubes on the skin running perpendicular to the axis of the cylinder). Q_m = 2600 Btu/hr (760 w), β = 0.1, constant temperature at inner core. . . . 166

Figure E.2 Steady state temperature and surface area of the skin as functions of R_1 for the one-dimensional cylindrical model. V and b are constant and constant temperature at inner core. 169

Figure E.3 Steady state temperature of the skin and depth of tissue as functions of R_1 for the one-dimensional cylindrical model. V and A are constant and constant temperature at inner core. 170

Page

Figure E.4 Steady state temperature of the skin and volume of the tissue as functions of R_1 for the one-dimensional cylindrical model. A and b are constant and constant temperature at inner core. 171

Figure E.5 Steady state temperature of the skin as function of R_1 for the one-dimensional cylindrical model. Constant temperature at inner core. 172

Figure F.1 Metabolic rates and ear canal temperatures of subject SKB for experiments with and without the cooling suit during Schedule I. 176

Figure F.2 Metabolic rates and ear canal temperatures of subject SKB for experiments with and without the cooling suit during Schedule II. 177

Figure F.3 Metabolic rates and ear canal temperatures of subject SKB for experiments with and without the cooling suit during Schedule III. 178

Figure F.4 Metabolic rates and ear canal temperatures of subject SKB for experiments with and without the cooling suit during Schedule IV. 179

Figure F.5 Metabolic rates and ear canal temperatures of subject SKB for experiments with and without the cooling suit during Schedule V. 180

Figure F.6 Heart rates of subject SKB for experiments with and without the cooling suit during Schedule V. . . 181

LIST OF TABLES

Page

TABLE 3.1 PHYSICAL AND PHYSIOLOGICAL PROPERTIES OF THE RECTANGULAR BIOTHERMAL MODEL CORRESPONDING TO A 139 LB (63 KG) ADULT MALE WITH 90 MM HG MEAN ARTERIAL BLOOD PRESSURE AND TOTAL METABOLIC RATE OF 290 BTU/HR (85 W). REPRODUCED IN PARTS FROM BUCHBERG AND HARRAH [39] AND BRAD [59]. 29

TABLE 3.2 FIRST SIX ROOTS OF EQ. (3.59) AS A FUNCTION OF THE RATIO OF THE OUTER TO INNER RADII OF THE CYLINDRICAL MODEL, R_2/R_1. THE RIGHTMOST COLUMN GIVES THE ASYMPTOTIC VALUES ($[(2n - 1)\pi]/2b$, RECTANGULAR MODEL) AS $R_1 \to \infty$ AND $R_2/R_1 \to 1$. . . . 60

TABLE 3.3 PHYSIOLOGICAL QUANTITIES AND THE CORRESPONDING DIMENSIONLESS PARAMETERS. $c_b = 1$ Btu/lb-°F (4187 J/kg-°C), $k = 0.311$ Btu/ft-hr-°F (0.540 w/m-°C), $b = 0.0731$ ft (0.0223 m), AND $A = 15.4\ ft^2$ ($1.43\ m^2$) 72

TABLE 3.4 COMPARISON OF MAGNITUDES OF THE TERMS IN EQ. (3.70). $c_b = 1$ Btu/lb-°F (4187 J/kg-°C), $k = 0.311$ Btu/hr-ft-°F (0.540 w/m-°C), AND $a = 0.032$ ft (0.00975 m) 74

TABLE 4.1a DATA ON THE COOLING GARMENT 78

TABLE 4.1b DATA ON THE COOLING GARMENT 79

TABLE 4.2 DATA ON THE INDIVIDUAL COOLING PADS 87

TABLE 4.3 CHARACTERISTICS OF THE TEST SUBJECTS 94

TABLE 4.4 CHARACTERISTICS OF SUBJECT TEK 103

TABLE 5.1 ORDER OF PREFERRED CHANGES IN WATER INLET TEMPERATURES AND THE COMFORT VOTE FOR THE VARIOUS ACTIVITIES 113

TABLE 5.2 WEIGHT LOSSES DURING TREADMILL EXPERIMENTS 128

TABLE F.1 MEAN VALUES AND RANGES OF TOTAL METABOLIC RATES, HEAT REMOVED BY SUIT AND BY RESPIRATION AT THE VARIOUS SCHEDULES OF ACTIVITY 182

TABLE F.2 MEAN VALUES AND RANGES OF WATER INLET TEMPERATURES FOR THE VARIOUS REGIONS AT DIFFERENT SCHEDULES OF ACTIVITY 188

TABLE OF CONTENTS

		Page
1.	INTRODUCTION	1
2.	REVIEW OF RELATED WORKS	4
	2.1 ANALYTICAL THERMAL MODELING	4
	2.2 WATER COOLED GARMENTS	12
	2.3 MEASUREMENT OF THERMOPHYSICAL PROPERTIES	12
3.	THEORETICAL ANALYSIS	14
	3.1 DEVELOPMENT OF THE GOVERNING PARTIAL DIFFERENTIAL EQUATION	14
	3.2 GEOMETRIES, BOUNDARY AND INITIAL CONDITIONS	17
	3.3 ANALYTICAL SOLUTIONS	23
	3.4 STEADY STATE, RECTANGULAR COORDINATES	24
	3.5 STEADY STATE, CYLINDRICAL COORDINATES	41
	3.6 TRANSIENT STATE, RECTANGULAR COORDINATES	50
	3.7 TRANSIENT STATE, CYLINDRICAL COORDINATES	57
	3.8 COMPARISON OF STEADY STATE SOLUTIONS FOR RECTANGULAR AND CYLINDRICAL COORDINATES	59
	3.9 DIMENSIONLESS PARAMETERS ASSOCIATED WITH THE THERMAL BEHAVIOR OF LIVING BIOLOGICAL TISSUE	66
4.	EXPERIMENTS	75
	4.1 OBJECTIVES	75
	4.2 DESCRIPTION OF THE EXPERIMENTAL SETUPS	75
	4.2.1 Cooling Suit	75
	4.2.2 Individual Cooling Pads	85
	4.3 EXPERIMENTS WITH THE COOLING SUIT	89
	4.3.1 Activity Schedules	89
	4.3.2 Test Subjects	92
	4.3.3 Experimental Procedure	93
	4.3.4 Measured, Recorded and Calculated Quanities	101
	4.4 EXPERIMENTS WITH THE INDIVIDUAL PADS	102
5.	DISCUSSION	105
	5.1 EXPERIMENTS WITH THE COOLING SUIT	105
	5.2 EXPERIMENTS WITH THE INDIVIDUAL COOLING PADS	135
6.	SUMMARY AND CONCLUSIONS	141

Page

APPENDIX

A. THE THERMOREGULATORY SYSTEM OF THE HOMEOTHERM 146

B. STEADY STATE, RECTANGULAR COORDINATES WITHOUT BLOOD FLOW 149

C. STEADY STATE, RECTANGULAR COORDINATES WITH THE SKIN AND MUSCLE CONSIDERED AS A SINGLE REGION 156

D. THE FUNCTION $\psi^{j}_{k\ell}(\zeta_i r)$ 160

E. STEADY STATE, CYLINDRICAL COORDINATES WITH THE SKIN AND MUSCLE CONSIDERED AS A SINGLE REGION 165

F. ADDITIONAL EXPERIMENTAL DATA 175

LIST OF REFERENCES 194

1. INTRODUCTION

The thermal system of homeotherms, and that of the human body in particular, has long been of interest to many researchers. The ability to maintain a fairly constant "deep body" temperature and to dissipate or preserve heat under widely varying environmental conditions have been among the most fascinating aspects of this system.

With the progress of scientific knowledge and methods, emphasis has shifted from mere observations of this system and its functions to more systematic studies. The efforts were directed to provide more understanding and insight into the nature and behavior of the mechanisms that govern such thermal phenomena. For completeness, a brief outline of the thermoregulatory system of homeotherms, as currently understood, is given in APPENDIX A.

In common with many branches of physiology, the study of the thermoregulatory system is approaching a stage in which work of descriptive nature will yield progressively less in the way of improved insight. Consequently, analytical approaches become more and more necessary. Analytical modeling of various aspects of the thermoregulatory system is expected to provide improved understanding of the mechanisms of thermoregulation and heat transfer. From these models new experimental directions are expected to emerge.

In our era of advanced technology, man has also been venturing into and exploring environments that are, among other things, thermally hostile to life. As a result, man's natural physiological abilities had to be augmented to render these hostile environments habitable.

The required artificial systems had to provide "micro-climates" to man that were capable of countering any adverse thermal changes in the environment.

As an example, the first such system used for pilots in the Royal Air Force was a gas-ventilated suit [1]†. Such suits proved to be of limited capacity for the removal of metabolic heat and hybrid systems emerged. These "second generation" suits were composed of two sub-systems; a water cooled garment, first suggested by Billingham in 1959 [2], fabricated from flexible tubes in contact with the skin and an overlying gas-ventilated system. In the current Apollo suits that are of this hybrid type [1], a change in body temperature and activity level is compensated by a uniform change in the cooling water inlet temperature. It would seem reasonable, however, to cool active muscles first; i.e., where heat is generated. Moreover, there are regions in the body that are more temperature sensitive, e.g., the back, that may render a uniform change in temperature less tolerable from a comfort standpoint.

Consideration of the above-mentioned points led to formulation of the specific objectives for this study:

(1) Analytical modeling of the thermal behavior of the living biological tissue. Blood flow effects were included in the model explicitly because heat transfer is an important concomitant of the circulatory system.

(2) Experiments with cooling pads directed at partially

---

†Numbers in brackets refer to entries in REFERENCES.

validating the temperature distributions obtained from the analysis.

(3) Exploration of the characteristics of regional cooling, i.e., independently cooling various regions of the body.

2. REVIEW OF RELATED WORKS

During the last few decades, three major avenues have been pursued to study and modify the thermal behavior of biological media, namely:

(1) Analytical modeling of the thermal system and partitional calorimetry relating to homeotherms.

(2) Experimental studies of man-environment interactions involving whole-body or partial cooling devices, e.g., cooling garments, hoods.

(3) Measurements of pertinent thermophysical and physiological properties, both "in vivo" and "in vitro."

The following is a brief review of works done in these three areas.

2.1 ANALYTICAL THERMAL MODELING

The fact that the body exchanges water vapor with the environment was first established by Santorio, an Italian physician living in the sixteenth and seventeenth centuries [3]. He spent a portion of the latter part of his life in a large balance; his food intake and excreta were accurately weighed. Santorio attributed the differences he found in the two weights to losses of water evaporated from the skin and carried by respiration. He termed these losses "insensible perspiration." Although not concerned with the heat transfer aspects of the processes he had observed, Santorio can still be considered as one of the founders of the "bio-heat transfer" school.

However, it was not until the second half of the eighteenth century, that Lavoisier [4] conceived the idea of the human body being a heat generator. With this concept, more rigorous studies of the man-environment heat exchanges and the heat transfer processes occurring inside the body, have become feasible.

It appears that Burton [5] in 1934 was the first to apply heat transfer equations to the human body. He assumed a uni-dimensional, steady state model with constant properties and uniform heat generation in the tissue. Solving the equation analytically, he obtained a parabolic temperature distribution.

Eichna, et al. [6] in 1945, and Machle and Hatch [7] in 1947 adopted the concept of "core and shell" and applied it to the human body. In this method, two temperatures are assigned to the body, i.e., deep body (rectal) and skin temperatures. Skin temperature was taken as a weighted average of temperatures of various regions of the skin. Heat exchange between man and his environment was then calculated as a function of conductance and core and shell temperature differences. This approach to the problem has since then been popular particularly with physiologists. However, it is not concerned with the details of temperature distribution and effects of blood flow.

In 1948 Pennes [8] introduced two new concepts into the problem of modeling the thermal behavior of the human body. First, he depicted the human body as consisting approximately of cylinders with circular cross section. Second, he realized the important role that blood flow plays in the process of heat transfer in the tissue and introduced an additional term into the heat equation, making the heating effect due to blood flow proportional to its heat capacity rate and to its temperature change within the tissue. Further, assuming the body to be homogeneous and isotropic with constant physical properties and uniform rate of heat production, he obtained a steady state solution in terms of Bessel functions for the temperature distribution in the forearm. The boundary condition satisfied at the skin was in accordance with Newton's cooling law (convective boundary condition). Pennes also commented that axial temperature gradients of the extremities can be neglected when compared to radial gradients and that the heat production in the skin and subcutaneous fat is of low order of magnitude.

As is suggested by the title of their article, Wyndham and coworkers in 1952 [9] examined the use of heat exchange equations to determine changes in body temperature.

Pursuing the concepts advanced by Pennes, Hertzman in 1953 [10] obtained correlations between skin temperature and cutaneous blood flow.

The "computer era" in thermal modeling began in 1955 when Taylor [11] advanced the idea of using an electrical analog to simulate heat transfer modes occurring inside the human body and between man and his thermal environment. He divided the body into five layers: skin, functional peripheral shell (subcutaneous tissue and part of the muscles), functional central section (skeletal muscle, heart and blood), core organs (liver, kidneys, central nervous system) and the inert tissue (skeleton and alimentary tract). He also assigned values of thermal capacity, conductance, and heat generation to these layers. Taylor proposed an electrical analog circuit composed of resistances, capacitances and potential sources to simulate the human-environment thermal system.

Herrington, in two articles in 1958 [12] and 1959 [13], discussed a full scale human body model for thermal exchanges. Using algebraic and least-square concepts, he derived a five element linear differential equation to describe extensive calorimetric data collected from seated, clothed human subjects. Rate of change of the skin temperature with respect to metabolic heat input, evaporative cooling, ambient air and ambient radiation temperature, were the result of the former work. In the latter, the data were compared with those obtained for an electrically heated body model ("copper man").

In 1958 Westland [14] followed up the ideas developed by Taylor of a biothermal analog to simulate and study interior and exterior heat transfer mechanisms related to the human body. Assuming one-dimensional heat flow and equivalent conductance to account for blood flow and the thermal conductivity, he studied the transient response of the human body to thermal exposures. Osman in 1962 [15] refined and improved on Westland's work.

A similar approach to the problem of heat transfer associated with the human body was used by Wyndham and Atkins in 1960 [16]. They approximated the body by a series of concentric cylinders corresponding to the core, muscle, and skin; and considered radial heat flow only. Using a numerical technique and utilizing an analog computer they obtained transient solutions for their model. At about the same time, Crosbie, et al., [17] employed a similar technique and applied it to a one-dimensional slab model. They assumed the slab to be divided into the same three layers and assigned constant, uniform, but different temperatures to each of the layers and compared their results with physiological data. Neither of the latter two approaches included a blood flow term explicitly.

In 1961 Wissler [18,19] initiated a study of mathematical modeling of the human thermal system. He divided the body into six cylinders corresponding to the extremities, trunk, and head. Including the blood flow term, he obtained analytical solutions for radial heat transfer for both the steady and transient states. He also introduced the concept of a central "pool," where blood from all regions is gathered, mixed, and redistributed, and the idea of lumped heat exchange between arteries and veins. Later, in 1964, he improved his model by dividing the body into fifteen circular cylinders interconnected by blood vessels [20]. These cylinders were subdivided into fifteen layers and numerical solutions were obtained on a digital computer. Just recently, Wissler increased the number of compartments into which the body is divided to include some 250 elements [21].

Perl, in 1962 [22], conceived of a method of indirect measurement of blood flow rates by employing Fick's second principle. He solved analytically the steady state and the transient problems and compared his results with experiments. Extensions of the initial work were published by him and co-workers in 1963 [23], 1965 [24], and 1966 [25].

The idea of using an analog computer for simulating temperature regulation in man was further utilized by Brown in 1963 [26]. He divided the body into four regions (central, muscle, subcutaneous region and skin) and studied interactions with the environment as well as heat distribution within the body. Further development of the biothermal analog computer was given by him in 1966 [27].

Numerical solutions for a uni-dimensional, four layer transient model were also obtained by Layne and Barker [28] in 1965 and by Stolwijk and Cunningham [29]. In 1966 Birkebak, et al., considered the application of heat transfer equations to the animal system [30].

In 1966 Soltwijk and Hardy [31] represented the human body by three cylinders corresponding to the head, trunk, and extremities and assumed the ends to be perfectly insulated. Each of the cylinders was subdivided into layers to represent the skin, muscle, viscera, brain, etc., and each sublayer was assumed to be at a constant temperature. Only radial heat flow was assumed and the effect of blood flow, as well as metabolic heat production, was included. Eight simultaneous differential equations were written for the various sublayers and three "controller" equations. These equations corresponded to evaporative heat losses, muscle blood flow changes with temperature and exercise rate, and also took into consideration the effects of shivering on heat transfer. The set of equations was solved on an analog computer yielding transient temperature distributions for various environmental and metabolic conditions. These two researchers were the first to introduce the concept of the passive system and active controller as applied to the human thermoregulatory system. According to this concept, the passive system represents a complex transfer function between the controller and the disturbance. The controller is responsible for maintaining the human body within the narrow limits of acceptable thermal conditions by activating the various thermoregulatory mechanisms, i.e., vasoconstriction or dilatation, sweating, and shivering.

A group from the University of Washington became interested, in 1967 [32], in the effects of electromagnetic heating patterns in human tissue. One year later [33], they also studied the propagation of acoustic waves and the resulting thermal effect in biological materials. In 1969, two solutions to the problem, one using an analytical method

[34] and the other a finite difference method [35], were presented by this group.

Richardson and Whitelaw in 1968 [36] studied transient heat transfer in the human skin. They constructed two probes: a cylindrical and a rectangular slab. The probes were made of nylon and methyl methacrylate (Perspex), respectively, and had thermocouples embedded in them at known locations. After being immersed in a constant temperature bath, the probes were brought into contact with the skin (enclosed areas of arm-pit and clenched hand) and the temperature of the thermocouples was recorded. Using available analytical solutions to the heat conduction equation in solids, the conductance of the human skin was evaluated. It was found that the change in conductance was independent of the surface temperature and heat flux to which the skin was exposed.

Infrared thermometry was utilized by Gros and Gautherie in 1968 [37] to study transient changes in human skin temperature as a function of ambient temperature. By means of a simplified model of heat exchange between the organism and the environment (only one-dimensional, transient conduction was considered), a mathematical law was derived. This law, obtained by using Laplace transform, was expressed by error functions and gave satisfactory representation of the experimental data.

At about the same time Mitchell and Myers [38] developed an analytical model for countercurrent heat exchange between arteries and veins. They proposed two different configurations for the countercurrent heat exchange that can be found in animals. These were: equal number of arteries and veins (arm of man, leg of bird, rete of a sloth's leg) and veins encircling a single artery (fins of whales and porpoises). Applying the principle of conservation of energy they obtained analytical solutions to the various configurations and compared their results with available experimental data.

Buchberg and Harrah [39] in 1968 tried a numerical solution of a two-dimensional, steady state model cooled by a network of tubes at the skin. They divided the slab into four layers corresponding to the core, musclature, a so-called functional periphery, and the skin. They assumed the thermal conductivity of the tissue to be a function of temperature and no heat to be generated in the skin. They did not include a blood flow term explicitly.

Chato in 1968 [40] reported on a method for measuring both local thermal diffusivity and blood perfusion rate. He modeled the tissue as an infinitely large medium with a spherical heat source (thermistor bead) embedded in it. He obtained analytical solutions and satisfactory results were obtained experimentally.

In 1968 Trezek and Jewett [41] initiated a study of the thermal field emanating from a cylindrical probe embedded in a tissue, in general, and in a brain, in particular. They were initially interested in applications to cryo-surgical probes. Other works on the subject were published later by Trezek and Cooper in 1968 [42], Trezek in 1969 [43], and Cooper in 1970 [44].

A study of the stationary heat transport from a heated spherical probe located in a tissue was made in 1969 by Priebe and Betz [45]. The tissue was assumed to be of spherical shape, too, and was considered to be isotropic and homogeneously perfused by blood. Assuming the discrete capillary heat sinks as well as the venous heat sources to be "smeared" over the whole volume of the tissue, they obtained analytical solutions to the problem. This treatment provided a method for estimating local blood flows. Also, thermal conductivity as a function of blood flow was obtained.

Just recently, Keller and Seiler [46] reported on an analysis of peripheral heat transfer in humans. In a steady state, one-dimensional continuum model, they accounted for effects of heat conduction, convection by blood flow and vascular heat exchange. They did not assume heat to be generated inside the tissue. Solving the resulting three simultaneous differential equations, they obtained general expressions for the effective conductivity of the tissue. They also discussed a method for estimating the degree of arterial precooling by the vessel spacing.

2.2 WATER COOLED GARMENTS

A most complete review on water cooled garments (WCG) was recently given by S. A. Nunneley [47]. She discussed the history of water cooled garments in the United States and in the United Kingdom. The discussion also includes variables affecting WCG design and operation, the development of automatic control and possible uses for regional cooling. Some 118 references are cited in this work and form a complete list of works pertinent to the subject.

2.3 MEASUREMENT OF THERMOPHYSICAL PROPERTIES

A large number of works describing methods and techniques for measuring the thermophysical properties of biological tissues has been published. These include both "in vitro" and, to a lesser extent, "in vivo" measurements.

Webb in 1964 [48] published a monograph entitled "Bioastronautics Data Book" in which he listed extensive data on the human body. He also included a chapter on thermophysical properties.

In 1966 Chato [49] made a rather extensive survey of thermal diffusivity and conductivity data on biological materials. This work was extended in 1968 [50]. He reported the data available at that time to include properties of internal organs, skin, biological fluids, frozen and then thawed materials and animal integuments.

Pond in 1968 [51] measured the thermal conductivity of rat brain. For the measurements he utilized a thermistor bead and used the same concepts as those suggested earlier by Chato [40].

Recently, Cooper [44] completed the development of a needle-probe for measuring thermal properties of human organs. The needle probe is essentially a copper-constantan thermocouple in the shape of a long, thin cylinder. This probe, while being at a temperature different than that of the organ, is suddenly plunged into the tissue. The changes in temperature of the probe are then recorded until it reaches the temperature of the medium. Thermal diffusivity values are calculated from the initial portion of the response curve. This method was developed to allow for blood flow effects to be taken into account and thus may be used for both "in vivo" and "in vitro" measurements. Cooper and Trezek report data obtained via the needle probe technique elsewhere [52].

Chato and co-workers further applied the thermistor bead to measure effective conductivity values of cat brain and hind leg muscle "in vivo" and "in vitro" [53].

3. THEORETICAL ANALYSIS

3.1 DEVELOPMENT OF THE GOVERNING PARTIAL DIFFERENTIAL EQUATION

Among the factors to be considered when attempting the modeling of the human thermal system are the following:

(1) Geometry of the body.

(2) Heat capacity of the body (thermal inertia).

(3) Conduction of heat due to thermal gradients.

(4) Metabolic heat production.

(5) The role of blood flow in heat transfer; i.e., transport of heat by circulating blood and countercurrent heat exchange between large blood vessels.

(6) Thermoregulatory mechanisms in the body and their functions; i.e., vasomotor activity, sweating, shivering, increased metabolism due to glandular activity, and pilo-motor activity (goose flesh). (In warm-blooded species other than humans, an additional mechanism of panting is also of importance.)

(7) Thermophysical and physiological properties of various organs and tissues; e.g., thermal conductivity, specific heat, density, blood perfusion rates, etc., and their dependence upon temperature and location.

(8) The interaction with the environment and its condition; i.e., dry and wet bulb temperatures, pressure, and air motion relative to the body.

In what follows, these factors will be considered while a heat balance on a differential element of tissue will be established.

Storage, conduction, and production of heat within the tissue will be assumed to be represented by the well-known heat equation. The additional term representing the heat transported by the blood stream will be derived using Fick's principle. This principle, when applied to biological systems, can be stated as, "the amount of a substance taken up by an organ (or by the whole body) per unit time is equal to the arterial level of the substance minus the venous level times the blood flow" [54]. When applied to the amount of heat gained (lost) by the blood perfusing an element of tissue, it yields

$$q_b = w_b c_b (T_{in} - T_{out}) \tag{3.1}$$

Equation (3.1), when combined with the heat equation, obtains

$$\rho c_p \frac{\partial T}{\partial t} = \nabla(k \ \nabla T) + w_b c_b (T_{in} - T_{out}) + q_m \tag{3.2}$$

Equation (3.2) is the mathematical statement of the first law of thermodynamics describing the "in vivo" relationship between the various modes of heat transfer, storage, and production within a biological tissue. It may be referred to as the "bio-heat" equation. Similar forms were obtained by Pennes [8], Hertzman [10], Wissler [18], Perl [22], Chato [40], Trezek [42], and Keller and Seiler [46].

In view of the complexity of the thermal behavior and structure of a living tissue and also because of the lack of accurate, detailed data of the thermophysical properties and the distribution of blood perfusion and metabolic heat production rates in the body, a number of assumptions should be made to facilitate analytical modeling.

(1) The thermophysical properties of the tissue will be assumed constant and the tissue will be assumed to be homogeneous and isotropic.

(2) The temperature of blood leaving the tissue will be assumed equal to the temperature of the tissue. This assumption can be justified by the structure of the capillary bed and the slow rate of flow of blood through the capillaries which makes them almost perfect heat exchangers.

(3) The temperature of blood entering the tissue will be assumed constant and equal to the temperature of the artery. Later, however, this assumption will be changed and an arbitrary function will be assumed to represent the inlet temperature of blood perfusing the tissue.

(4) Blood perfusion and metabolic heat production rates will be assumed uniform and constant throughout the entire layer of tissue and will be assumed to represent average values.

Accordingly, Eq. (3.2) becomes

$$\rho c_p \frac{\partial T}{\partial t} = k\nabla^2 T + w_b c_b (T_a - T) + q_m \tag{3.3}$$

Equation (3.3) will be applied to the various layers of tissue and analytical solutions will be given for different geometries and boundary conditions.

The various thermoregulatory mechanisms outlined above are included in the present model indirectly. The major role that these mechanisms play in the thermoregulation of the homeotherm [55] is expressed, among other effects, by the modification of local heat transfer characteristics, such as blood perfusion (vasomotor activity) and metabolic heat production rates (shivering and glandular activity), and the boundary conditions (sweating and pilo-motor activity). Accordingly, the effect of the thermoregulatory mechanisms on the transport of heat in the tissue can be incorporated by properly changing the values of the rate of blood flow and heat generation. The interaction with the environment will be accounted for in the following section via the boundary conditions.

3.2 GEOMETRIES, BOUNDARY AND INITIAL CONDITIONS

This study will be primarily concerned with the removal of metabolic heat produced in the body by means of a network of cooling tubes that are in direct contact with the skin. Consequently, it is possible to approximate the very involved geometry of the body by circular cylinders or even by strips of rectangular cross section.

To this end, the tissue is assumed to be divided into three layers:

(1) A skin layer composed of epidermis, dermis, and subcutaneous fat as shown in Fig. 3.1. The actual thickness of the layer varies from 1-6 mm [56]. All excess metabolic heat will be assumed to be removed at the contact areas between the epidermis and the cooling tubes.

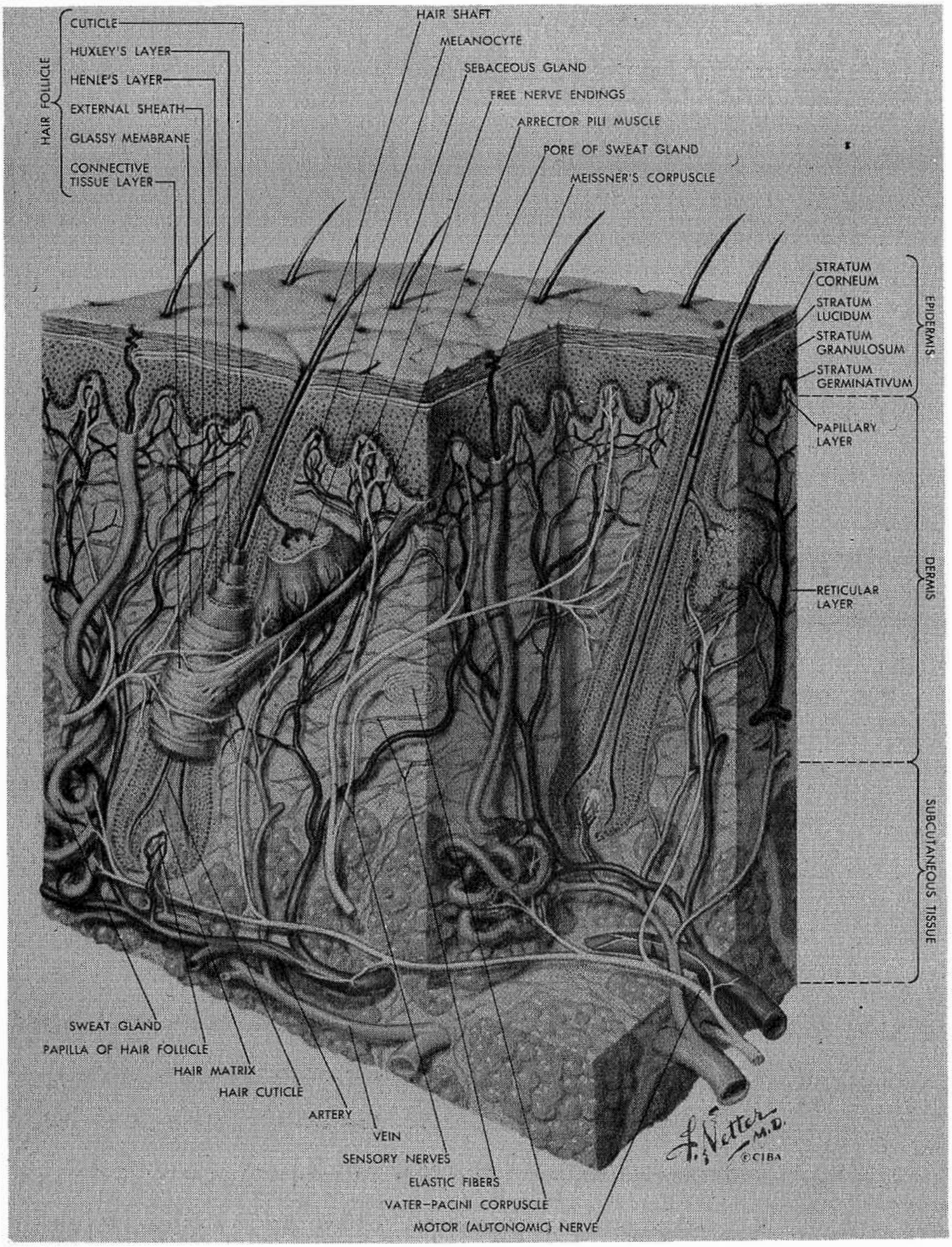

Figure 3.1 Cross section of the normal skin. Copyright, 1967, CIBA Corporation, reproduced with permission from the Clinical Symposia by Frank H. Netter, M.D.

(2) A layer called skeletal muscle composed of all the muscles.

(3) An inner core layer consisting of the skeleton and all the internal organs. At steady state, this layer will be assumed to be at a constant temperature which will vary with metabolic rates [57].

Assuming the body to be represented by cylinders of circular cross section, two configurations of cooling tubes seem conceivable:

(1) The tubes running perpendicular to the axis of the cylinder, Fig. 3.2.

(2) The tubes running parallel to the axis of the cylinder, Fig. 3.3.

Other intermediate configurations of the cooling tubes can be represented as a combination of these two. However, as the inside diameter of the cylinders becomes larger (which is the case with the trunk, thighs, and lower legs and approximately with the arms, too), the cylindrical configuration can be replaced by strips of rectangular cross section, Fig. 3.4. The calculations of the temperature distribution inside the tissue thus become simpler and easier without any significant loss of accuracy, as is demonstrated later.

As mentioned above, the temperature of the interface between the skeletal muscle and the inner core is assumed constant and uniform and equal to that of the inner core. An assumption of a constant, uniform flux at this interface is also possible and the two will be considered separately. At the skin surface, a heat flux corresponding to the amount of heat to be removed by the tubes will be assumed.

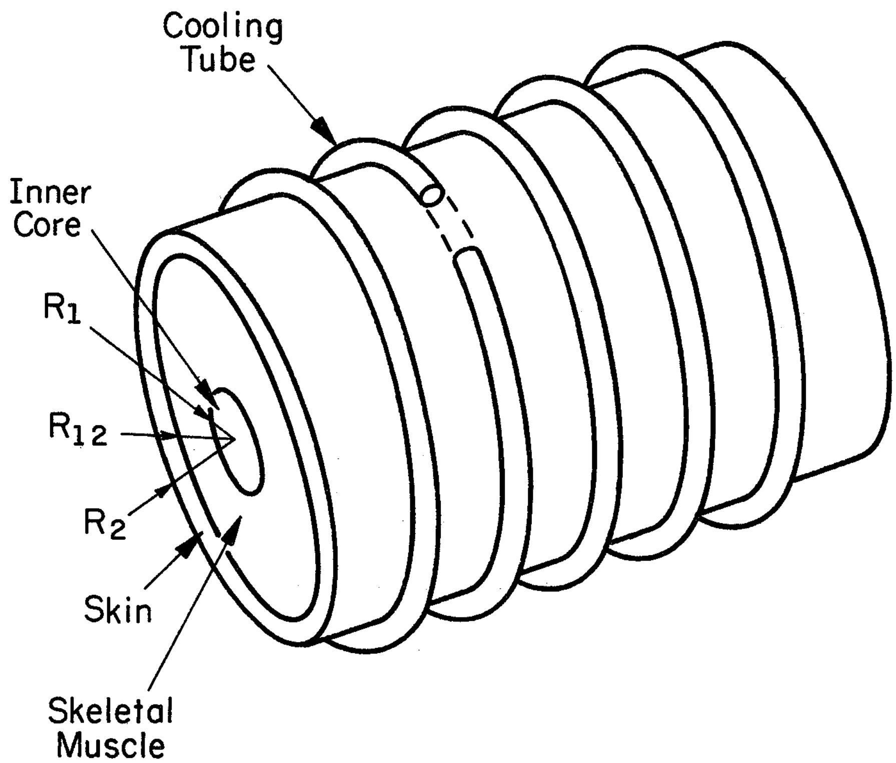

Figure 3.2 Representative section of the cylindrical model with the cooling tubes on the skin running perpendicular to the axis of the cylinder.

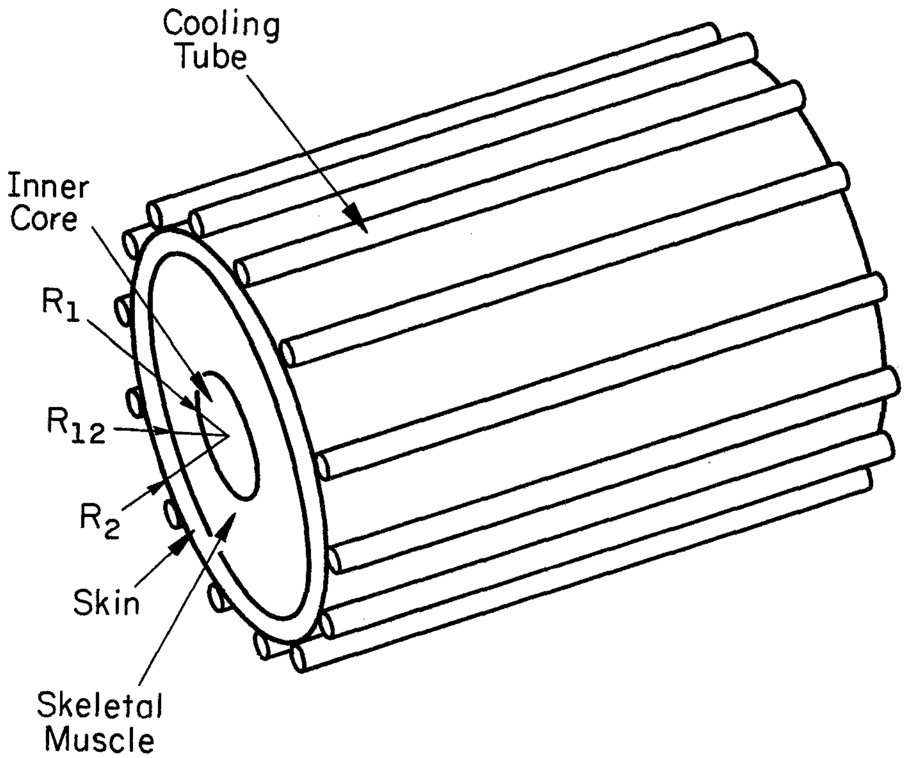

Figure 3.3 Representative section of the cylindrical model with the cooling tubes on the skin running parallel to the axis of the cylinder.

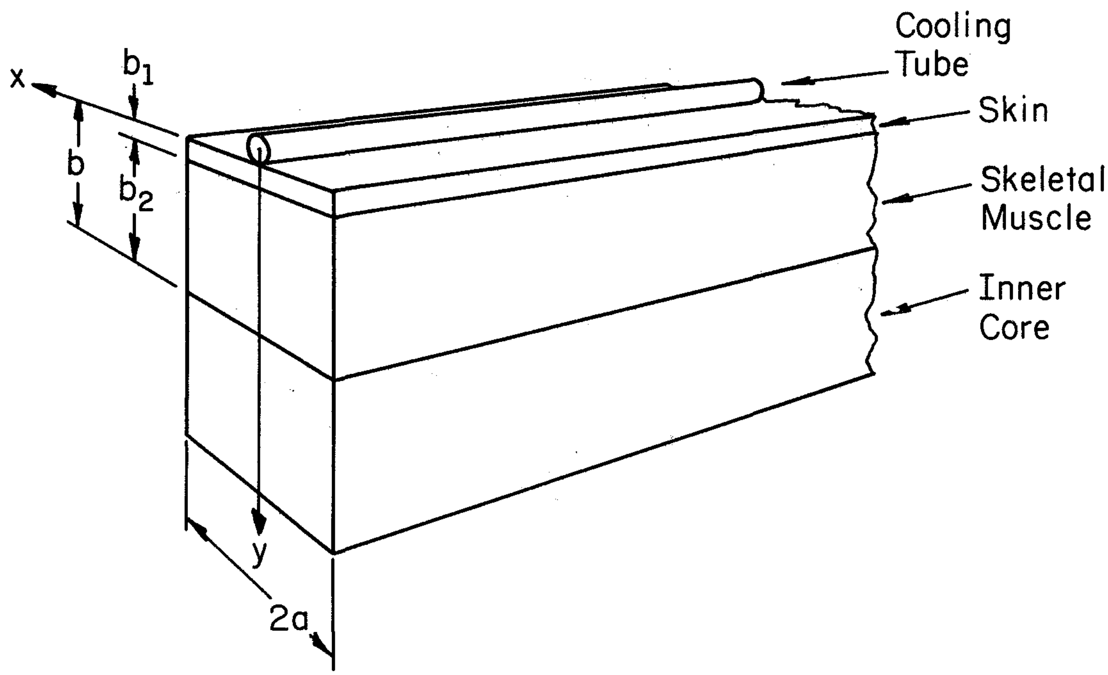

Figure 3.4 Representative section of the rectangular model.

First, an arbitrary distribution of the flux will be assumed,† but, later, it will be shown that knowledge of the actual shape of the flux function is not necessary as long as the heat is removed only by the tubes [58]. Because of the symmetry of the problem, the lines of symmetry running through the tubes and half-way between two adjacent tubes can be assumed adiabatic. At the interface between the skin layer and the skeletal muscle, two matching conditions will be satisfied: equal temperatures and equal heat fluxes.

The steady state temperature distribution in the tissue at a given metabolic rate will be assumed to be the initial condition for the transient state.

3.3 ANALYTICAL SOLUTIONS

It will be assumed that the changes along the axes of the cooling tubes are small compared to those occurring in the directions perpendicular to the tubes. In mathematical notation, this statement becomes

$$\frac{\partial}{\partial z} = 0 \tag{3.4}$$

and, consequently, the problem becomes two dimensional. Steady state solutions in the two most relevant coordinate systems, i.e., rectangular and cylindrical, will be given first. These solutions will

†By properly modifying the distribution of the specified flux function over the skin, heat removed by sweat evaporation and convection can be incorporated, too.

be used as initial conditions for the more general transient cases.

3.4 STEADY STATE, RECTANGULAR COORDINATES

The first case to be studied is the one with the skin and skeletal muscle considered as separate regions using rectangular coordinates. All metabolic heat is assumed to be removed at the skin along the portion contacted by the cooling tubes. No heat is assumed to be removed at the rest of the skin surface. At the interface between the skeletal muscle and the inner core, a constant temperature, equal to that of the inner core, is assumed. Because of the symmetry of the problem, the boundaries at $x = 0$ and $x = a$ are assumed to be adiabatic. Two matching conditions of equal temperature and equal heat flux are satisfied at the interface between the skin and the skeletal muscle. Although the problem as formulated above neglects end effects, it can still be considered general; for, the solution presented below pertains to the areas covered by the cooling pads, modeled as rectangular, symmetrical, two-dimensional strips. Temperature distributions in the tissue underneath the areas not covered by the cooling pads can be obtained by properly modifying the heat flux at the skin while using the same approach as presented below. The problem, in mathematical notation, becomes:

SKIN

$$\frac{\partial^2 \theta_1}{\partial x^2} + \frac{\partial^2 \theta_1}{\partial y_1^2} - w_1^2 \theta_1 = -Q_1 \qquad (3.5a)$$

$$0 \le x \le a \;, \quad 0 \le y_1 \le b_1$$

$$\text{at } y_1 = b_1 \,, \left\{ \begin{array}{ll} \dfrac{\partial \theta_1}{\partial y_1} = -\dfrac{f(x)}{k_1} \,, & 0 \le x < \beta a \\[2ex] \dfrac{\partial \theta_1}{\partial y_1} = 0 \,, & \beta a < x \le a \end{array} \right\} \qquad (3.5b)$$

$$\text{at } x = 0 \;, \quad \frac{\partial \theta_1}{\partial x} = 0 \qquad (3.5c)$$

$$\text{at } x = a \;, \quad \frac{\partial \theta_1}{\partial x} = 0 \qquad (3.5d)$$

SKELETAL MUSCLE

$$\frac{\partial^2 \theta_2}{\partial x^2} + \frac{\partial^2 \theta_2}{\partial y_2^2} - w_2^2 \theta_2 = -Q_2 \qquad (3.6a)$$

$$0 \le x \le a \;, \quad 0 \le y_2 \le b_2$$

$$\text{at } y_2 = b_2 \;, \quad \theta_2 = 0 \qquad (3.6b)$$

$$\text{at } x = 0 \;, \quad \frac{\partial \theta_2}{\partial x} = 0 \qquad (3.6c)$$

$$\text{at } x = a \;, \quad \frac{\partial \theta_2}{\partial x} = 0 \qquad (3.6d)$$

matching conditions at $y_1 = y_2 = 0$,

$$\partial_1 = \theta_2 \qquad (3.7a)$$

$$k_1 \frac{\partial \theta_1}{\partial y_1} = -k_2 \frac{\partial \theta_2}{\partial y_2} \qquad (3.7b)$$

where

$$\theta_i \equiv T_i(x, y_i) - T_2^* \tag{3.8}$$

$$w_i^2 \equiv \frac{W_{i\,b}\,C_b}{k_i} \tag{3.9}$$

$$Q_i \equiv \frac{Q_i'}{k_i} \tag{3.10}$$

f(x) is an arbitrary function representing the flux of heat removed by the cooling tubes at the skin. Figure 3.5 shows the two regions, the coordinate system, and the boundary conditions for this case.

The solutions to the above two simultaneous sets were obtained by using appropriate transformations and Fourier series expansions. In terms of regional temperatures, these solutions are:

For the skin layer,

$$\begin{aligned} T_1(x, y_1) = {} & T_2^* + \frac{Q_1}{w_1^2} + E(0)\cosh(w_1 y_1) - \left[\frac{\beta f_a}{k_1} + \frac{G}{\cosh(w_1 b_1)}\right] \\ & \cdot \frac{\sinh(w_1 y_1)}{w_1} - \left[\frac{Q_1 k_2 w_2}{w_1^2} + \frac{k_1 G \tanh(w_2 b_2)}{\cosh(w_1 b_1)}\right] \\ & \cdot \frac{\cosh[w_1(b_1 - y_1)]}{H(w)} + k_1 \sum_{n=1}^{\infty} \frac{\alpha_n}{\cosh(\zeta_1 b_1)} \\ & \left\{ \frac{\tanh(\zeta_2 b_2)\cosh[\zeta_1(b_1 - y_1)]}{H(\zeta)} \right. \\ & \left. + \frac{\sinh(\zeta_1 y_1)}{k_1 \zeta_1} \right\} \cos(\lambda_n x) \end{aligned} \tag{3.11}$$

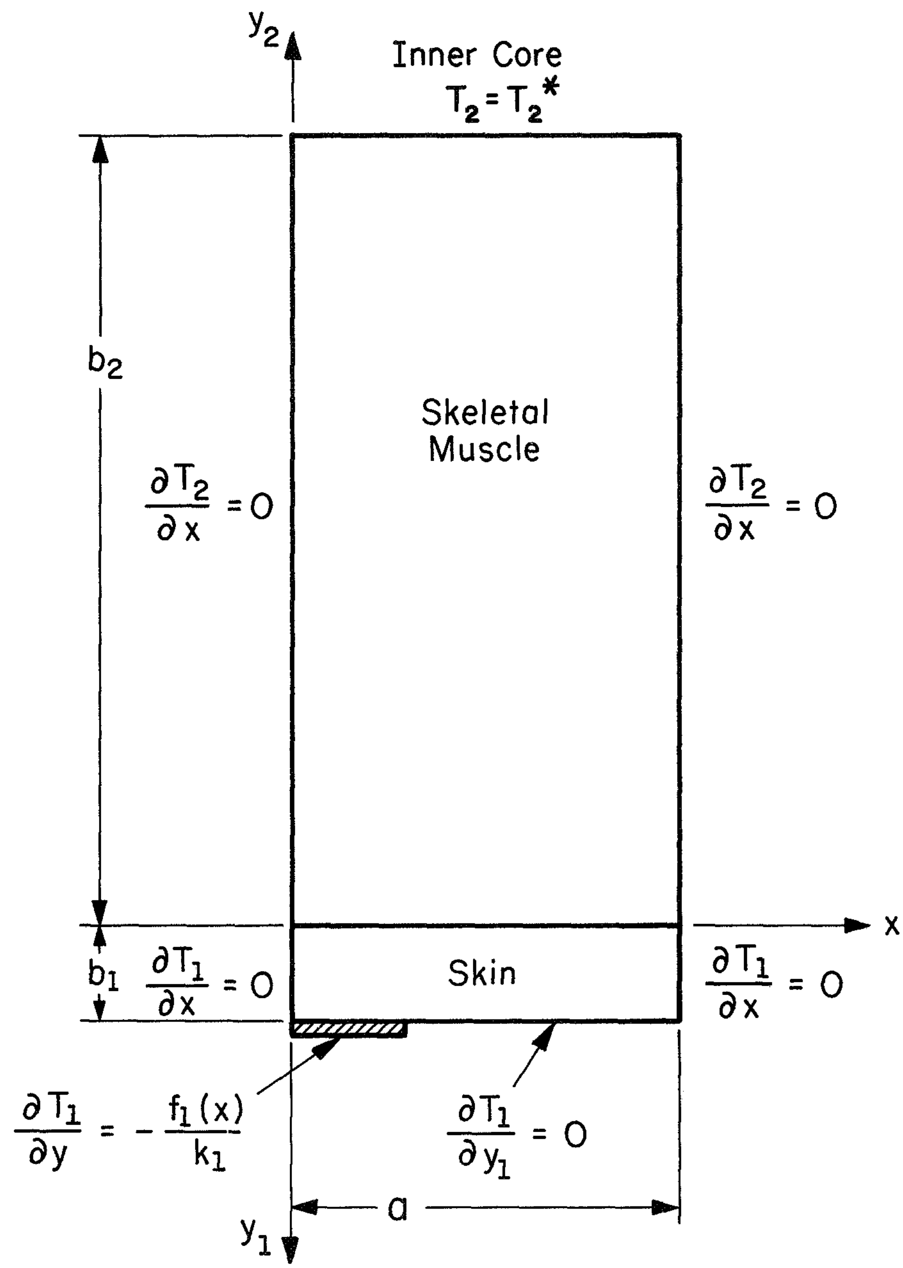

Figure 3.5 Geometry and boundary conditions for the rectangular model. Skin layer and skeletal muscle are considered as separate regions.

For the skeletal muscle layer,

$$T_2(x,y_2) = T_2^* + E(y_2) + \left[\frac{Q_1 \sinh(w_1 b_1)}{w_1} - G\right] \cdot \frac{k_1 \sinh[w_2(b_2 - y_2)]}{H(w)\cosh(w_2 b_2)} + k_1 \sum_{n=1}^{\infty} \cdot \frac{\alpha_n \sinh[\zeta_2(b_2 - y_2)]}{H(\zeta)\cosh(\zeta_2 b_2)} \cos(\lambda_n x) \tag{3.12}$$

where

$$E(y) \equiv \frac{Q_2}{w_2^2}\left[1 - \frac{\cosh(w_2 y)}{\cosh(w_2 b_2)}\right] - \frac{\beta f_a}{k_2 w_2}\,\frac{\sinh[w_2(b_2 - y)]}{\cosh(w_2 b_2)} \tag{3.13}$$

$$G \equiv w_1 E(0)\sinh(w_1 b_1) - \frac{\beta f_a}{k_1}[\cosh(w_1 b_1) - 1] \tag{3.14}$$

$$H(\zeta) \equiv k_2 \zeta_2 \cosh(\zeta_1 b_1) + k_1 \zeta_1 \sinh(\zeta_1 b_1)\tanh(\zeta_2 b_2) \tag{3.15}$$

$$f_a = \frac{1}{\beta a}\int_0^{\beta a} f(\xi)\, d\xi \tag{3.16}$$

$$\zeta_i^2 \equiv w_i^2 + \lambda_n^2 \tag{3.17}$$

$$\lambda_n \equiv \frac{n\pi}{a} \tag{3.18}$$

$$\alpha_n \equiv \frac{2}{a}\int_0^{\beta a} \frac{f(x)}{k_1}\cos(\lambda_n \xi)\, d\xi \tag{3.19}$$

Equations (3.11) through (3.19) were programmed on the digital computer and temperature distributions for various values of parameters and metabolic rates were obtained. TABLE 3.1 gives dimensions and thermophysical properties of the model used for the numerical

TABLE 3.1

PHYSICAL AND PHYSIOLOGICAL PROPERTIES OF THE RECTANGULAR BIOTHERMAL MODEL CORRESPONDING TO A 139 LB (63 KG) ADULT MALE WITH 90 MM HG MEAN ARTERIAL BLOOD PRESSURE AND TOTAL METABOLIC RATE OF 290 BTU/HR (85 W). REPRODUCED IN PARTS FROM BUCHBERG AND HARRAH [39] AND BRAD [59].†

Property		Region				
		Skin	Skeletal Muscle	Inner Core		Whole Body
				Heart Muscle	Rest of Body	
Mass	kg	3.6	31.0	0.3	28.1	63.0
	lb	7.94	68.40	0.66	62.00	139.00
Volume	m^3	0.00350	0.02800	0.00028	0.02700	0.05878
	ft^3	0.125	1.000	0.010	0.965	2.100
Depth	m	0.02475	0.019800	--	0.019350	0.041625
	ft	0.00812	0.06500	--	0.06350	0.13662
Width of Strip	m	0.01945	0.01945	--	0.01945	--
	ft	0.064	0.064	--	0.064	--
Blood Flow Rate	ml/min	462	840	250	3848	5400
	ft^3/min	0.0165	0.0300	0.1375	0.0089	0.1929

†These numerical values were used in the computations, but they do not imply accuracies corresponding to the number of digits given.

(continued)

TABLE 3.1 continued

Property		Region				
		Skin	Skeletal Muscle	Inner Core		Whole Body
				Heart Muscle	Rest of Body	
Oxygen Consumption	ml/min	12	50	29	159	250
	ft^3/min	0.000429	0.001785	0.001035	0.005675	0.008924
Percent of Total	Blood Flow Rate	8.6	15.6	4.7	71.1	100.0
	Oxygen Consumption	4.8	20.0	11.6	63.6	100.0
Thermal Conductivity	w/m-°C	0.419	0.540	--	--	--
	Btu/hr-ft-°F	0.242	0.311	--	--	--

computations. The first twenty terms of the series were used in the numerical solution. It was found that by doing so the truncation error introduced was less than 0.01; i.e., $|\alpha_{20}| - |\alpha_{21}| < 0.01$ °F/ft. A typical temperature distribution in the tissue for one set of parameters is shown in Fig. 3.6.

Three observations were made based on the preceding analysis:

(1) If $y/x > 2$ (the ratio of b/a in the present rectangular model was about 2.3), the isotherms become essentially independent of x; i.e., the isotherms become parallel and a function of depth only as illustrated in Fig. 3.6. This observation leads to the conclusion that, at the interface between the inner core and the skeletal muscle, the boundary conditions of constant, uniform flux or temperature become identical for any practical purposes. From a physiological standpoint, this conclusion is not surprising. It is known that, in a steady state, inner body temperature is maintained at a fairly constant level while, at the same time, most of the heat generated inside the body is removed at the skin. The heat to be removed at the skin is transported there by the blood stream and by conduction through the tissue, mechanisms that are included in the present mathematical model.

(2) One of the most difficult parameters to assess is the shape of the flux at the portion of the skin contacted by the cooling tubes. Fortunately, it was demonstrated [58] that the actual shape of this function is not of great importance

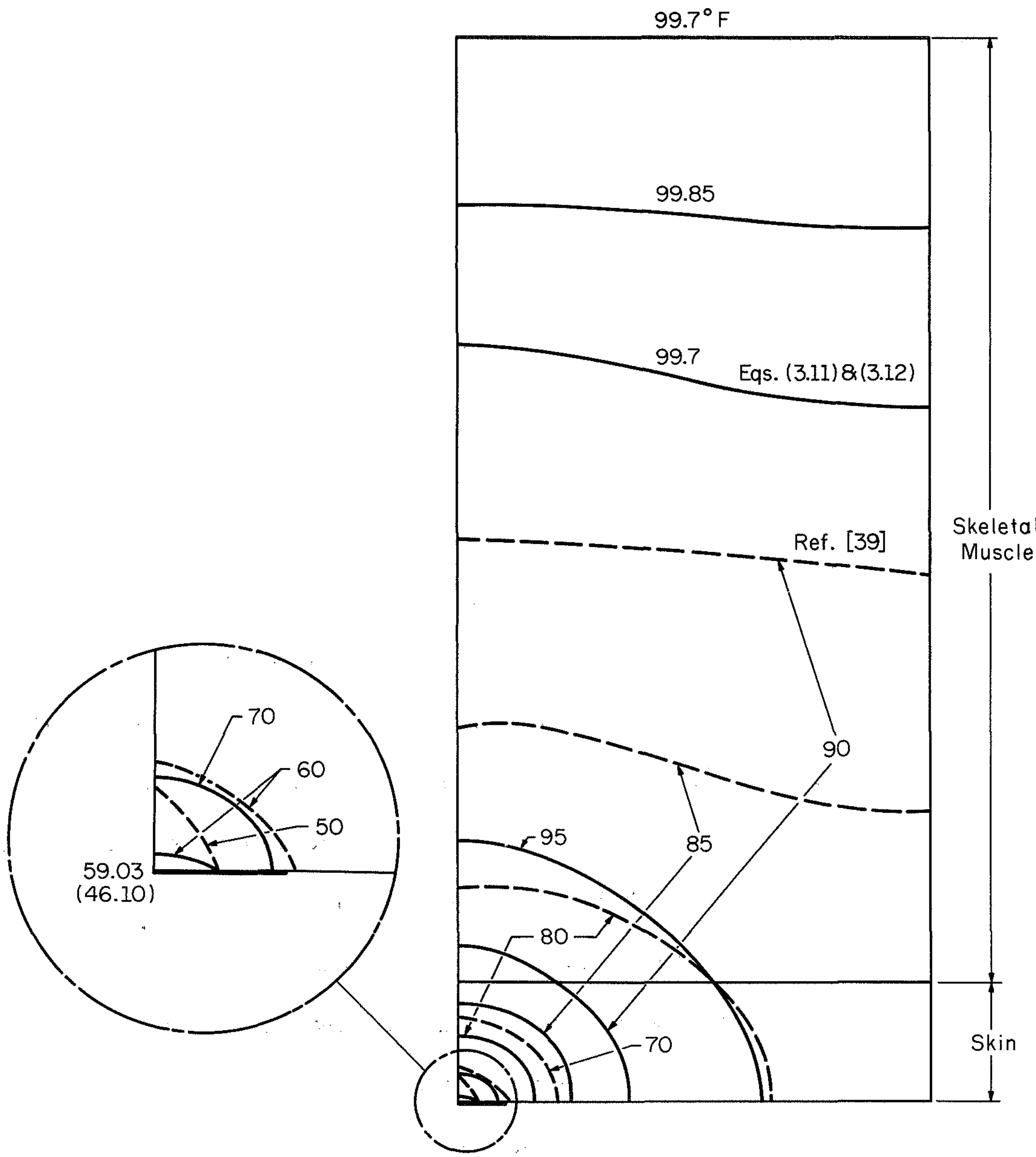

Figure 3.6 Temperature distribution in the separated tissue for the rectangular model. Dashed curves indicate temperature distribution obtained by Buchberg and Harrah [39] without blood flow. Q_m = 2600 Btu/hr, (760 w), β = 0.1 and constant temperature at inner core.

so long as it provides for the removal of all the excessive heat at the skin. This was done by assuming an arbitrary, linear heat flux function at the skin. This function varied from its maximum value at $x = 0$ (centerline of the cooling tube) to 2/3 of the maximum at $x = \beta a$ (edge of the cooling tube) or $f_2/f_1 = 1.5$. The mean value of the flux over the area covered by the cooling tube was taken to correspond to the appropriate amount of heat to be removed. As a second choice, this function was reversed; i.e., $f_2/f_1 = 1/1.5$. With these two extreme assumptions, the temperature distribution in the tissue was evaluated. The effect of selecting different flux functions at the skin was noticeable only in the vicinity of the cooling tubes and became indistinguishable at a very short distance away. Thus, knowledge of the exact shape of the flux function is not essential and the error introduced by various functions is insignificant so long as the above obvious condition is satisfied. Figure 3.7 demonstrates this finding. Figure 3.8 shows the effect of increasing the contact area between the cooling tubes and the skin (increasing β) while f_2/f_1 is maintained at 1.5.

(3) It was found that, if $b \cdot (w_b c_b/k)^{1/2} > 2.3$, the maximum temperature of the body occurs in the skeletal muscle rather than in the inner core. This observation demonstrates, among other things, the important role that the blood stream plays in the transport of heat in the body; for, without

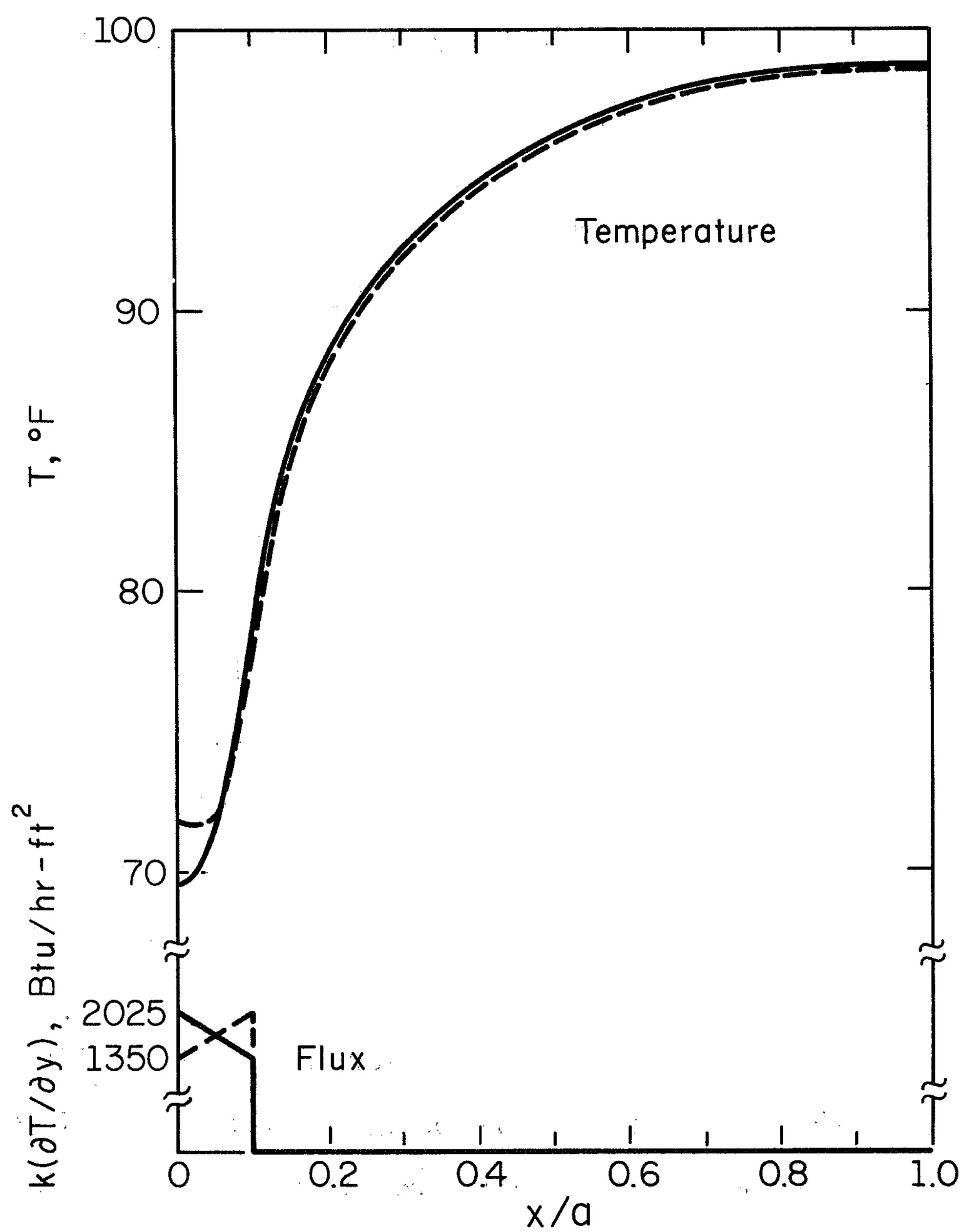

Figure 3.7 Effect of changing the specified flux function on the temperature of the skin for the rectangular model. Q_m = 2600 Btu/hr, (760 w), β = 0.1 and constant temperature at inner core.

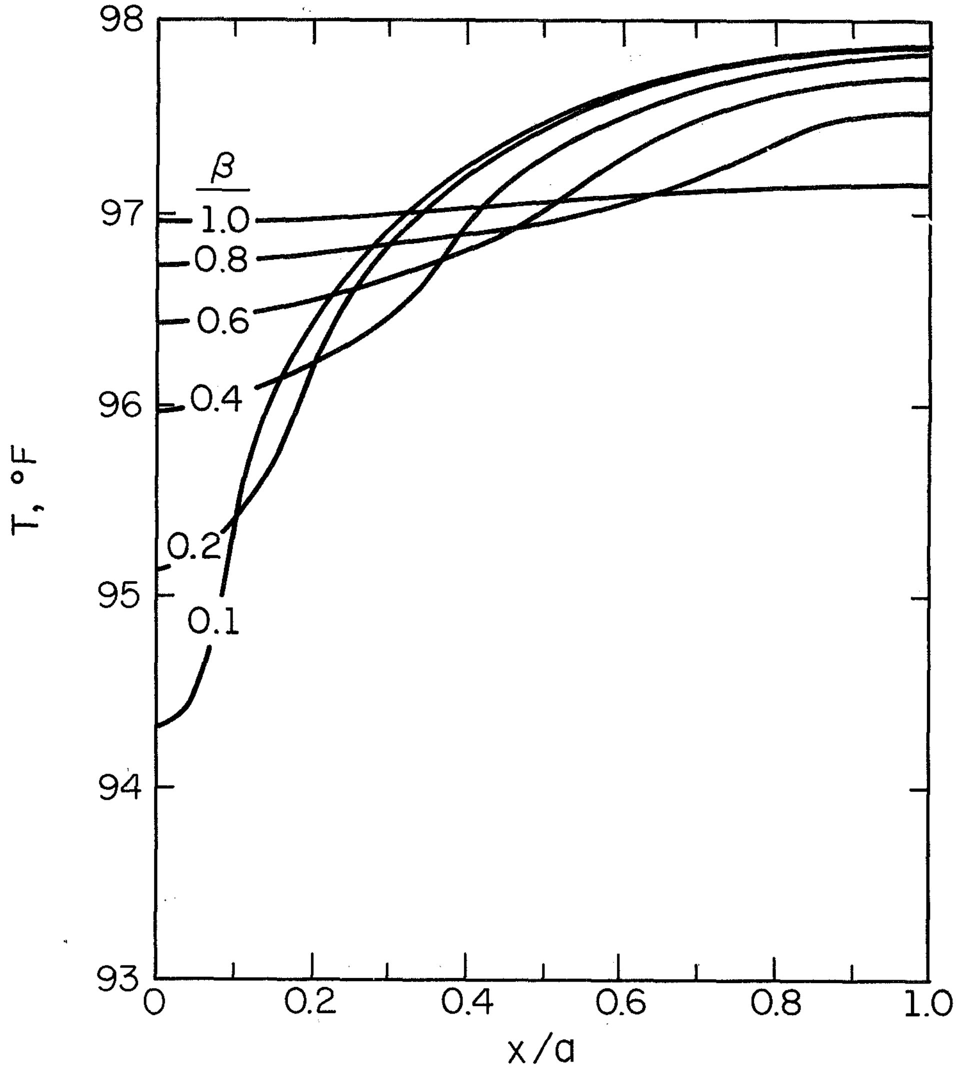

Figure 3.8 Effect of increasing the contact area between the cooling tubes and the skin on the temperature distribution on the skin surface. Q_m = 290 Btu/hr (85 w), f_2/f_1 = 1.5 and constant temperature at inner core.

this mode of heat transfer, the occurrence of a maximum temperature inside the tissue will mean inability to adequately dissipate heat with all the acute physiological consequences. Only heat transported by the blood stream can by-pass this "barrier" and reach the skin where it will eventually be removed. From a mathematical standpoint, when the term representing blood flow is not included in Eq. (3.3), as was done by Buchberg and Harrah [39], the above-mentioned phenomenon does not occur (Fig. 3.6, dashed lines). However, there are cases when blood flow reduces significantly or even vanishes; e.g., vasoconstriction. Therefore, a solution for this limiting case, $w_b \to 0$, is presented and compared in APPENDIX B with the more general result that includes blood flow and the results of Ref. [39].

As was mentioned before, very little accurate and reliable data are available pertaining to the thermophysical properties of the tissue, local blood perfusion and metabolic heat production rates. The most comprehensive source of thermophysical properties was given by Chato [50]. Scant physiological data can be found in medical or physiological textbooks, such as the one by Brad [59]. Consequently, any attempt to improve on the preceding analysis will have to be delayed until such data become available.

Nevertheless, two additional sets of solutions will be given. The first additional solution is less detailed than the previous one. It is obtained when the skin and skeletal muscle zones are combined to form a single zone.† The result is of gross nature, but, in view of the inadequacy of the available data, it is almost as good as the more complete one with the two zones separated and is easier for computation. This case is presented and discussed in APPENDIX C.

The second additional solution assumes a variable, arbitrary blood supply temperature rather than a constant one. Since this solution is more detailed and requires more information on the actual changes that the temperature of the blood perfusing the tissue undergoes, it seemed sufficient to assume a one-dimensional model with uniform flux at the skin. It is believed that the extension of this solution to two dimensions should not present any major difficulties.

In mathematical notation,

$$\frac{d^2T}{dy^2} + w^2[\theta^*(y) - T] = -Q \tag{3.20a}$$

and the boundary conditions are

$$\text{at } y = 0 \text{ , } \quad \frac{dT}{dy} = \frac{F}{k} \tag{3.20b}$$

$$\text{at } y = b \text{ , } \quad T = T_1 \tag{3.20c}$$

where F is the uniform flux at the skin.

This set was integrated using a Green function [60],

---

†This procedure amounts to carrying the above solution to the limit $b_1 \to 0$ and $b_2 \to b$, or $b_2 \to 0$ and $b_1 \to b$, while assuming $k_1 = k_2$, $w_1 = w_2$, and $Q_1 = Q_2$ and reversing the sign of the flux at the skin.

$$G(y,\tau) = \begin{cases} \dfrac{\Phi_1(\tau)\Phi_2(y)}{W[\Phi_1,\Phi_2]}, & y < \tau \\ \dfrac{\Phi_1(y)\Phi_2(\tau)}{W[\Phi_1,\Phi_2]}, & y > \tau \end{cases} \tag{3.21}$$

where $\Phi_1(y)$ and $\Phi_2(y)$ are two independent solutions of the homogeneous differential equation,

$$\Phi''(y) - w^2\Phi(y) = 0 \tag{3.22a}$$

satisfying,

$$\Phi_1'(0) = 0 \tag{3.22b}$$

$$\Phi_2(b) = 0 \tag{3.22c}$$

namely,

$$\Phi_1(y) = \cosh(wy) \tag{3.23a}$$

$$\Phi_2(y) = \sinh[w(b - y)] \tag{3.23b}$$

and $W[\Phi_1,\Phi_2]$ is the Wronskian defined

$$W[\Phi_1,\Phi_2] = \begin{vmatrix} \Phi_1 & \Phi_2 \\ \Phi_1' & \Phi_2' \end{vmatrix} \tag{3.24}$$

The solution obtained is

$$T(y) = T_1 + \frac{Q}{w^2}\left[1 - \frac{\cosh (wy)}{\cosh (wb)}\right] - \frac{F}{kw}\,\frac{\sinh [w(b - y)]}{\cosh (wb)}$$

$$- \frac{w}{\cosh (wb)}\left\{\sinh [w(b - y)] \int_0^y Y(\tau) \cosh (w\tau)\, d\tau\right.$$

$$\left. + \cosh (wy) \int_y^b Y(\tau) \sinh [w(b - \tau)]\, d\tau\right\} \qquad (3.25)$$

where, with the dummy variable τ replaced by y,

$$Y(y) = T_1 - \theta^*(y) \qquad (3.26)$$

and $\theta^*(y)$ is an arbitrary function describing the variations of the blood supply temperature. Figure 3.9 shows typical results obtained for assumed linear temperature variations of the blood supply. It can be seen that, as the slope of blood supply temperature increases, skin temperature decreases and the maximum temperature of the tissue is shifted toward the inner core.

If the boundary condition at the inner core, Eq. (3.20c) is changed

$$\text{at } y = b\ , \quad \frac{dT}{dy} = \frac{F_o}{k} \qquad (3.27)$$

(uniform flux instead of uniform temperature), a solution for the temperature inside the tissue can be obtained by employing the finite cosine Fourier transform

$$C\{\Phi(y)\} = \int_0^b \Phi(\tau) \cos (\nu_n \tau)\, d\tau \qquad (3.28)$$

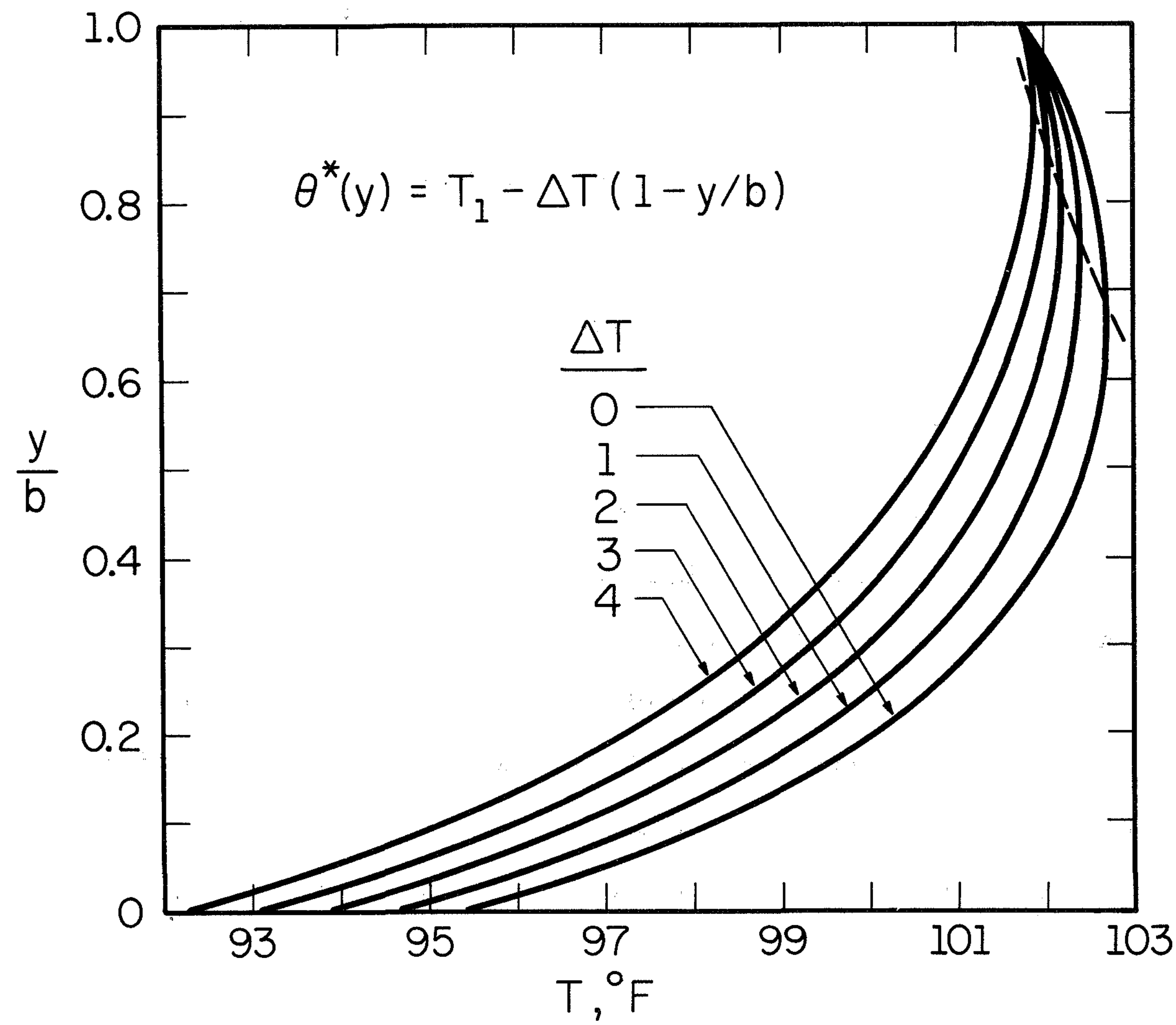

Figure 3.9 Steady state, one dimensional temperature distribution in the combined tissue with variable, linear blood supply temperature for the rectangular model. Dashed line indicates locus of maxima. Q_m = 2600 Btu/hr (760 w), and constant temperature at inner core.

$$C\{\Phi''(y)\} = -\nu_n^2 C\{\Phi(y)\} + (-1)^n \Phi'(b) - \Phi'(0) \tag{3.29}$$

to obtain

$$T(y) = T_{ref} + \frac{Q}{w^2} + \frac{1}{kw} \frac{F_o \cosh(wy) - F \cosh[w(b-y)]}{\sinh(wb)}$$

$$+ \frac{1}{b}\left\{ \int_0^b \theta^*(\tau)\, d\tau + 2w^2 \sum_{n=1}^{\infty} \frac{\int_0^b \theta^*(\tau) \cos(\nu_n \tau)\, d\tau}{w^2 + \nu_n^2} \right\} \tag{3.30}$$

where

$$\nu_n = \frac{n\pi}{b} \tag{3.31}$$

and $\theta^*(y)$ is the arbitrary function defined above.

3.5 STEADY STATE, CYLINDRICAL COORDINATES

In many cases, a closer approximation of the geometry of the human body is achieved by representing it as a set of cylinders. This is particularly true for the extremities and was used by many investigators [8,16,18,31,33].

Two general cases were studied: the cooling tubes running on the skin perpendicular to the cylinder (limb) axis, Fig. 3.2, and the tubes running parallel to the axis, Fig. 3.3. The first case was studied with the two zones separated, whereas only a solution for the combined tissue was obtained for the second.

The geometry of the first case (assuming the gradients along the axis of the cylinder to be negligible compared to those in the plane perpendicular to it) is essentially rectangular and similar to the one shown in Fig. 3.5. For completeness, the exact geometry and boundary conditions are shown in Fig. 3.10.

The mathematical formulation for this case is

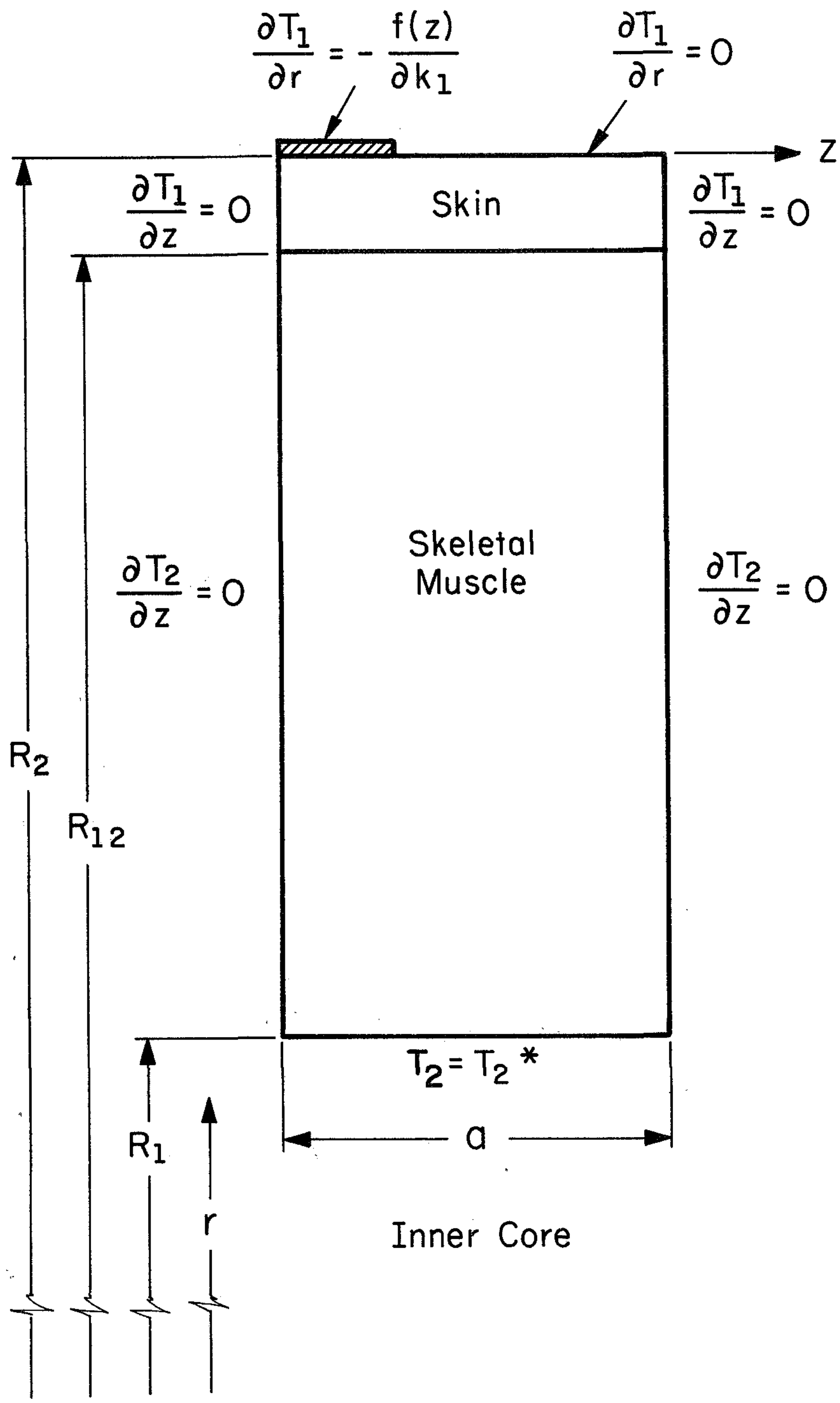

Figure 3.10 Geometry and boundary conditions for the cylindrical model with the cooling tubes on the skin running perpendicular to the axis of the cylinder. Skin layer and skeletal muscle are considered as separate regions.

SKIN

$$\frac{1}{r}\frac{\partial}{\partial r}\left(r\,\frac{\partial \theta_1}{\partial r}\right) + \frac{\partial^2 \theta_1}{\partial z^2} - w_1^2\theta_1 = -Q_1 \tag{3.32a}$$

$$R_{12} < r \leq R_2 \; ; \quad 0 \leq z \leq a$$

$$\text{at } r = R_2 \,, \quad \left\{ \begin{array}{ll} \dfrac{\partial \theta_1}{\partial r} = -\dfrac{f(z)}{k_1} \,, & 0 \leq z < \beta a \\[2ex] \dfrac{\partial \theta_1}{\partial r} = 0 \,, & \beta a < z \leq a \end{array} \right\} \tag{3.32b}$$

$$\text{at } z = 0 \,, \quad \frac{\partial \theta_1}{\partial z} = 0 \tag{3.32c}$$

$$\text{at } z = a \,, \quad \frac{\partial \theta_1}{\partial z} = 0 \tag{3.32d}$$

SKELETAL MUSCLE

$$\frac{1}{r}\frac{\partial}{\partial r}\left(r\,\frac{\partial \theta_2}{\partial r}\right) + \frac{\partial^2 \theta_2}{\partial z^2} - w_2^2\theta_2 = -Q_2 \tag{3.33a}$$

$$R_1 \leq r < R_{12} \; ; \quad 0 \leq z \leq a$$

$$\text{at } r = R_1 \,, \quad \theta_2 = 0 \tag{3.33b}$$

$$\text{at } z = 0 \,, \quad \frac{\partial \theta_2}{\partial z} = 0 \tag{3.33c}$$

$$\text{at } z = a \,, \quad \frac{\partial \theta_2}{\partial z} = 0 \tag{3.33d}$$

matching conditions at $r = R_{12}$,

$$\theta_1 = \theta_2 \tag{3.34a}$$

$$k_1 \frac{\partial \theta_1}{\partial r} = k_2 \frac{\partial \theta_2}{\partial r} \tag{3.34b}$$

where all the parameters are defined by Eqs. (3.8), (3.9), and (3.10). The solution obtained is:

For the skin layer ($R_{12} < r \leq R_2$),

$$
\begin{aligned}
T_1(r,z) = T_2^* &+ \Lambda(w_2 R_{12}) \frac{\psi_{01}^{12}(w_1 r)}{\psi_{01}^{12}(w_1 R_{12})} + \frac{\beta f_a}{k_1 w_1} \frac{\psi_{00}^{12}(w_1 r)}{\psi_{10}^{12}(w_1 R_{12})} \\
&- \frac{M}{w_1 K_1(w_1 R_2)} \\
&\cdot \Bigg[\frac{k_2 w_2 K_o(w_1 R_{12}) \psi_{10}^{1}(w_2 R_{12}) - k_1 w_1 K_1(w_1 R_{12}) \psi_{00}^{1}(w_2 R_{12})}{\Omega(w R_{12})} \\
&\cdot \psi_{01}^{2}(w_1 r) - K_o(w_1 r) \Bigg] \\
&+ \frac{Q_1}{w_1^2} \left[1 + \frac{w_2 k_2 \psi_{10}^{1}(w_2 R_{12}) \psi_{01}^{2}(w_1 r)}{\Omega(w R_{12})} \right] - \sum_{n=1}^{\infty} \frac{\alpha_n}{\zeta_1 K_1(\zeta_1 R_2)} \\
&\cdot \Bigg\{ \frac{k_2 \zeta_2 K_o(\zeta_1 R_{12}) \psi_{10}^{1}(\zeta_2 R_{12}) + k_1 \zeta_1 K_1(\zeta_1 R_{12}) \psi_{00}^{1}(\zeta_2 R_{12})}{\Omega(\zeta R_{12})} \\
&\cdot \psi_{01}^{2}(\zeta_1 r) - K_o(\zeta_1 r) \Bigg\} \cos(\lambda_n z) \qquad (3.35)
\end{aligned}
$$

For the skeletal muscle ($R_1 \leq r < R_{12}$),

$$T_2(r,z) = T_2^* + \Lambda(w_2 r) + \frac{Q_1}{w_1^2} \frac{w_1 k_1 \psi_{11}^2(w_1 R_{12})\psi_{00}^1(w_2 r)}{\Omega(wR_{12})}$$

$$+ \frac{k_1 M}{K_1(w_1 R_2)}$$

$$\cdot \frac{K_1(w_1 R_{12})\psi_{01}^2(w_1 R_{12}) + K_o(w_1 R_{12})\psi_{11}^2(w_1 R_{12})}{\Omega(wR_{12})} \psi_{00}^1(w_2 r)$$

$$- k_1 \sum_{n=1}^{\infty} \frac{\alpha_n}{K_1(\zeta_1 R_2)}$$

$$\cdot \frac{K_1(\zeta_1 R_{12})\psi_{01}^2(\zeta_1 R_{12}) + K_o(\zeta_1 R_{12})\psi_{11}^2(\zeta_1 R_{12})}{\Omega(\zeta R_{12})}$$

$$\cdot \psi_{00}^1(\zeta_2 r) \cos(\lambda_n z) \tag{3.36}$$

where

$$\psi_{k\ell}^j(\zeta_i r) \equiv I_k(\zeta_i r) K_\ell(\zeta_i R_j) + (-1)^{k+\ell+1} I_\ell(\zeta_i R_j) K_k(\zeta_i r) \tag{3.37}$$

$$\Lambda(wr) \equiv \frac{Q_2}{w^2}\left[1 - \frac{\psi_{01}^{12}(wr)}{\psi_{01}^{12}(wR_{12})}\right] - \frac{\beta f_a}{k_2 w} \frac{\psi_{00}^1(wr)}{\psi_{10}^1(wR_{12})} \tag{3.38}$$

$$\Omega(\zeta R_{12}) \equiv k_1 \zeta_1 \psi_{11}^2(\zeta_1 R_{12})\psi_{00}^1(\zeta_2 R_{12}) - k_2 \zeta_2 \psi_{01}^2(\zeta_1 R_{12})\psi_{10}^1(\zeta_2 R_{12}) \tag{3.39}$$

$$M \equiv -\frac{\beta f_a}{k_1}\left\{1 - \frac{\psi_{10}^{12}(w_1 R_2)}{\psi_{10}^{12}(w_1 R_{12})} + \frac{k_1 w_1}{k_2 w_2} \frac{\psi_{00}^1(w_2 R_{12})\psi_{11}^{12}(w_1 R_2)}{\psi_{10}^1(w_2 R_{12})\psi_{10}^{12}(w_1 R_{12})}\right\} \tag{3.40}$$

Observing that [61]

$$\psi_{k,\,k+1}^j(wR_j) = \frac{1}{wR_j} \tag{3.41}$$

Equation (3.40) can be rewritten

$$M \equiv -\frac{\beta f_a}{k_1}\left\{1-(w_1R_{12})\psi_{10}^{12}(w_1R_2)+\frac{k_1w_1^2R_{12}}{k_2w_2}\cdot\frac{\psi_{00}^{1}(w_2R_{12})\psi_{11}^{12}(w_1R_2)}{\psi_{10}^{1}(w_2R_{12})}\right\} \tag{3.42}$$

I_i and K_i are the modified Bessel functions of the first and second kind of order i and w_i, f_a, ζ_i, λ_n, and α_n are defined by Eqs. (3.9), (3.16), (3.17), (3.18), and (3.19), respectively.

The solution to the cylindrical case exhibits the same characteristics as the one for the rectangular case. However, it is more difficult to obtain numerical results because of the presence of the Bessel functions in the series part of the solution. Still, temperature distribution of limited accuracy for this case for the skin layer and skeletal muscle considered as one combined tissue is shown in Fig. E.1. Fortunately, it was found that, without any significant loss in accuracy, the rectangular case yields results that are remarkably close to the cylindrical ones, as will be demonstrated in a separate chapter.

A special function, $\psi_{k\ell}^{j}(\zeta_i r)$, was defined to simplify the mathematical derivation, Eq. (3.37). It is a combination of modified Bessel functions of the first and second kind which was found to recur in the solution many times. This function is further discussed in some detail in APPENDIX D.

As was done for the rectangular model, additional solutions for the combined tissue, including the limiting ones for no blood flow, are presented in APPENDIX E.

The second steady state case in cylindrical coordinates is the one with the cooling tubes running parallel to the cylinder axis. Figure 3.11 shows the geometry and boundary conditions for this case.

The mathematical formulation for this case is

$$\frac{1}{r}\frac{\partial}{\partial r}\left(r\frac{\partial\theta}{\partial r}\right)+\frac{1}{r^2}\frac{\partial^2\theta}{\partial\phi^2}-w^2\theta=-Q \tag{3.43a}$$

$$R_1 \leq r \leq R_2 \;,\quad 0 \leq \phi \leq \Phi_1$$

with the boundary conditions,

$$\text{at } r = R_1 \;,\quad \theta = 0 \tag{3.43b}$$

$$\text{at } r = R_2 \;,\left\{\begin{array}{ll} \dfrac{\partial\theta}{\partial r} = -\dfrac{f(\phi)}{k} \;, & 0 \leq \phi < \beta\Phi_1 \\ \dfrac{\partial\theta}{\partial r} = 0 \;, & \beta\Phi_1 < \phi \leq \Phi_1 \end{array}\right\} \tag{3.43c}$$

$$\text{at } \phi = 0 \;,\quad \frac{\partial\theta}{\partial\phi} = 0 \tag{3.43d}$$

$$\text{at } \phi = \Phi_1 \;,\quad \frac{\partial\theta}{\partial\phi} = 0 \tag{3.43e}$$

Solution for this set was obtained by using the same technique as before to yield

$$T(r,\phi) = T_1 + \frac{Q}{w^2}\left[1 - \frac{\psi^2_{01}(wr)}{\psi^2_{01}(wR_2)}\right] - \frac{\beta f_a}{kw}\,\frac{\psi^1_{00}(wr)}{\psi^2_{01}(wR_1)}$$

$$- R_2 \sum_{n=1}^{\infty} \frac{\alpha_n \psi^1_{\eta\eta}(wr)}{\eta\psi^1_{\eta\eta}(wR_2) + wR_2\psi^1_{\eta(\eta+1)}(wR_2)} \cos(\eta\phi) \tag{3.44}$$

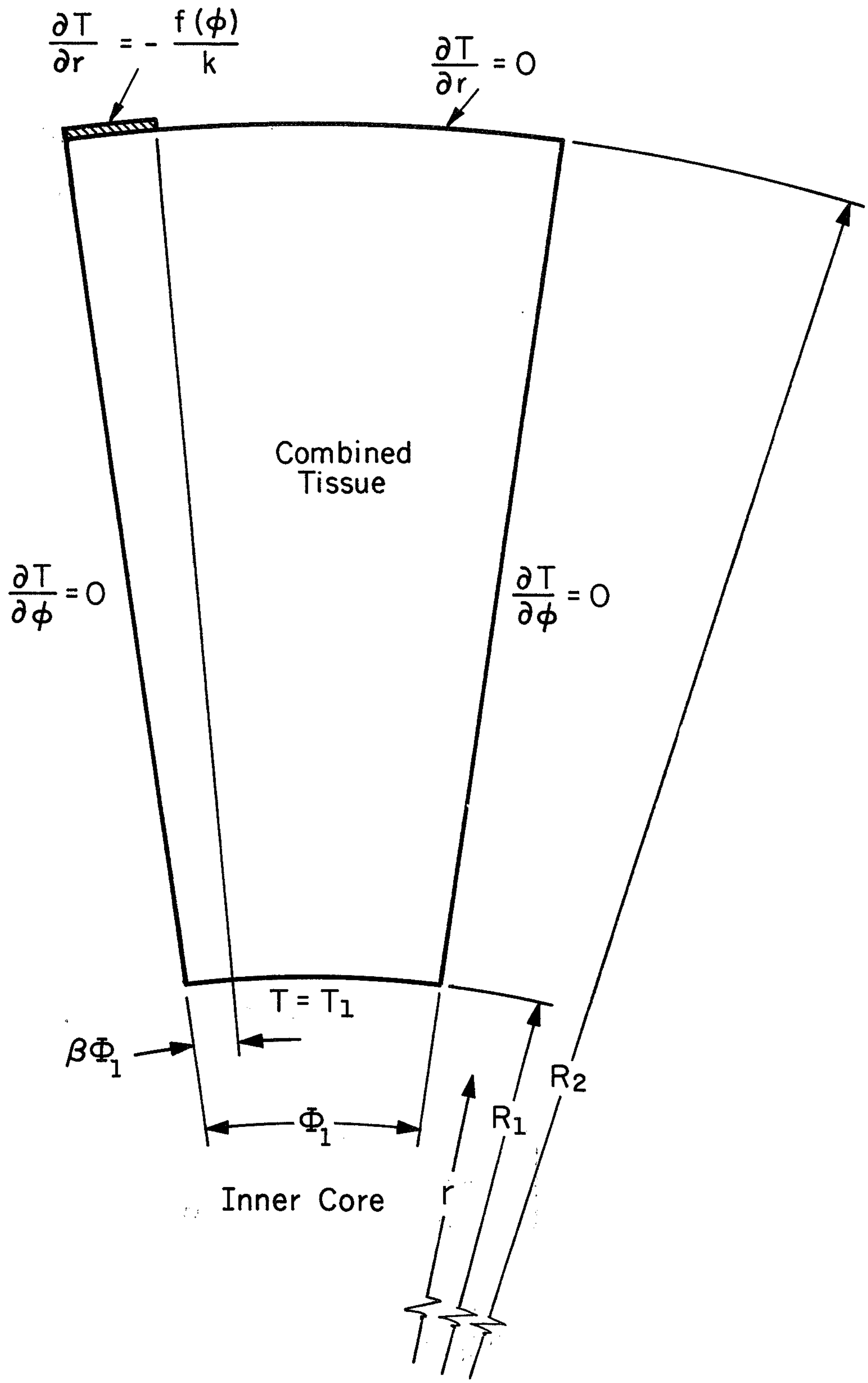

Figure 3.11 Geometry and boundary conditions for the cylindrical model with the cooling tubes on the skin running parallel to the axis of the cylinder. Skin layer and skeletal muscle are considered as a combined tissue.

where

$$\alpha_n = \frac{2}{\Phi_1} \int_0^{\beta\Phi_1} \frac{f(\xi)}{k} \cos\ (\eta\xi)\ d\xi \tag{3.45}$$

$$\eta = nm \tag{3.46}$$

m is the number of equally spaced tubes on the circumference.

The presence of the function $\psi^i_{\eta\eta}(wr)$ in the series of Eq. (3.44) hindered accurate computation of the temperature distributions in the tissue. This was true particularly in the vicinity of the cooling tubes. For example, if one assumes m = 20, the capacity of the computer is exceeded after the first two terms of the series for a low metabolic rate. Also, when R_1 increases (while still being meaningful physiologically), the accuracy of the computation is further limited. Consequently, the temperature distribution obtained for this case was considered of limited value and is not presented here. This computational limitation was also one of the reasons why this case was not studied with the zones separated.

Solutions for cases where the tubes run diagonally on the skin, i.e., not parallel or perpendicular to the cylinder axis, can be obtained as linear combinations of the above two extreme cases. This can be done by resolving the flux function at the skin into two components corresponding to the above two cases. Because of the linearity of the equation, a linear combination of solutions constitutes a solution to this more general case.

3.6 TRANSIENT STATE, RECTANGULAR COORDINATES

Available experimental evidence shows that the thermal transients in the human body are of the order of a half hour [62]. Consequently, the steady state solutions become of limited importance and transient solutions should be sought.

The lack of accurate and detailed thermophysical and physiological data hinders any detailed analysis. This is even more noticeable in the transient cases. Therefore, the analysis presented below, although successful in obtaining solutions to the problem, should be considered approximate only. In view of these limitations, the following assumptions will be made:

(1) The two outer zones, i.e., skin and skeletal muscle, will be considered to constitute one combined tissue.

(2) All properties will be assumed to be constant and independent of time, temperature, and location.

(3) The temperature at the interface between the inner core and the combined tissue will be assumed uniform and constant and will correspond to the final condition.

(4) Step-like functions will be assumed to represent changes in blood perfusion and metabolic heat generation rates; that is, at $t \geq 0$, values of blood perfusion and heat generation rates correspond to the final ones. This assumption can be justified on the grounds that the transient time for changes in these quantities is much shorter than the thermal transients.

(5) The initial temperature in the tissue will be taken as the steady state distribution. The final temperature distribution, as $t \to \infty$, was expected to correspond to the steady state at the new metabolic activity level.

Two cases will be studied: one with a uniform heat flux at the skin, i.e., one-dimensional, and the other with variable flux over the skin, similar to the steady state case presented in APPENDIX C.

CASE 1:

$$\frac{1}{\alpha}\frac{\partial\theta}{\partial t} = \frac{\partial^2\theta}{\partial y^2} - w_2^2\theta + Q_2 \tag{3.47a}$$

$$0 \leq y \leq b \ ; \quad 0 \leq t$$

with the boundary and initial conditions,

$$\text{at } y = 0 \ , \quad \frac{\partial\theta}{\partial y} = \frac{F_2}{k} \tag{3.47b}$$

$$\text{at } y = b \ , \quad \theta = 0 \tag{3.47c}$$

$$\text{at } t \leq 0 \ , \quad \theta = \frac{Q_1}{w_i^2}\left[1 - \frac{\cosh\ (w_1 y)}{\cosh\ (w_1 b)}\right] - \frac{F_1}{k w_1} \cdot \frac{\sinh\ [w_1(b - y)]}{\cosh\ (w_1 b)} \tag{3.47d}$$

where

$$\theta \equiv T(y,t) - T_1 \tag{3.48}$$

and all the other parameters were defined before. Index 1 indicates values prior to the step, $t \leq 0$, and index 2 values after the step, $t > 0$.

The solution to this case is

$$T(y,t) = T_1 + \frac{Q_2}{w_2^2}\left[1 - \frac{\cosh(w_2 y)}{\cosh(w_2 b)}\right] - \frac{F_2}{kw_2}\frac{\sinh[w_2(b - y)]}{\cosh(w_2 b)}$$
$$+ \frac{2}{ak}\sum_{n=1}^{\infty}\left\{\frac{F_2}{\gamma_2^2} - \frac{F_1}{\gamma_1^2} + \frac{(-1)^n}{\delta_n}\left[\frac{Q_2'}{\gamma_2^2} - \frac{Q_1'}{\gamma_1^2}\right]\right\}\cos(\delta_n y)$$
$$\cdot \exp(-\alpha\gamma_2^2 t) \tag{3.49}$$

where

$$\delta_n \equiv \frac{(2n - 1)\pi}{2b} \tag{3.50}$$

$$\gamma_i^2 \equiv w_i^2 + \delta_n^2 \tag{3.51}$$

Figure 3.12 shows results obtained for step changes in metabolic rates. It is clearly seen that most of the changes in temperature occur during the first five minutes when the step is from the low to the high rate, and during the first twenty minutes when the step is from the high to the low rate. After these periods, the temperature of the tissue is essentially equal to the steady state temperature. It should be noted that the temperature at the interface between the inner core and the combined tissue was assumed constant. This assumption, however, does not conform to the actual situation. Deep body temperature is known to change almost linearly with changes in metabolic rates [57]. However, the transient times of these changes are much longer than those obtained for the temperature profile inside the tissue. Consequently, the final configuration of the temperature distribution inside the tissue will be reached after about 5-20 minutes from the onset of a change in metabolic rate. From then on, only a shift of the "fully developed" temperature profile will occur.

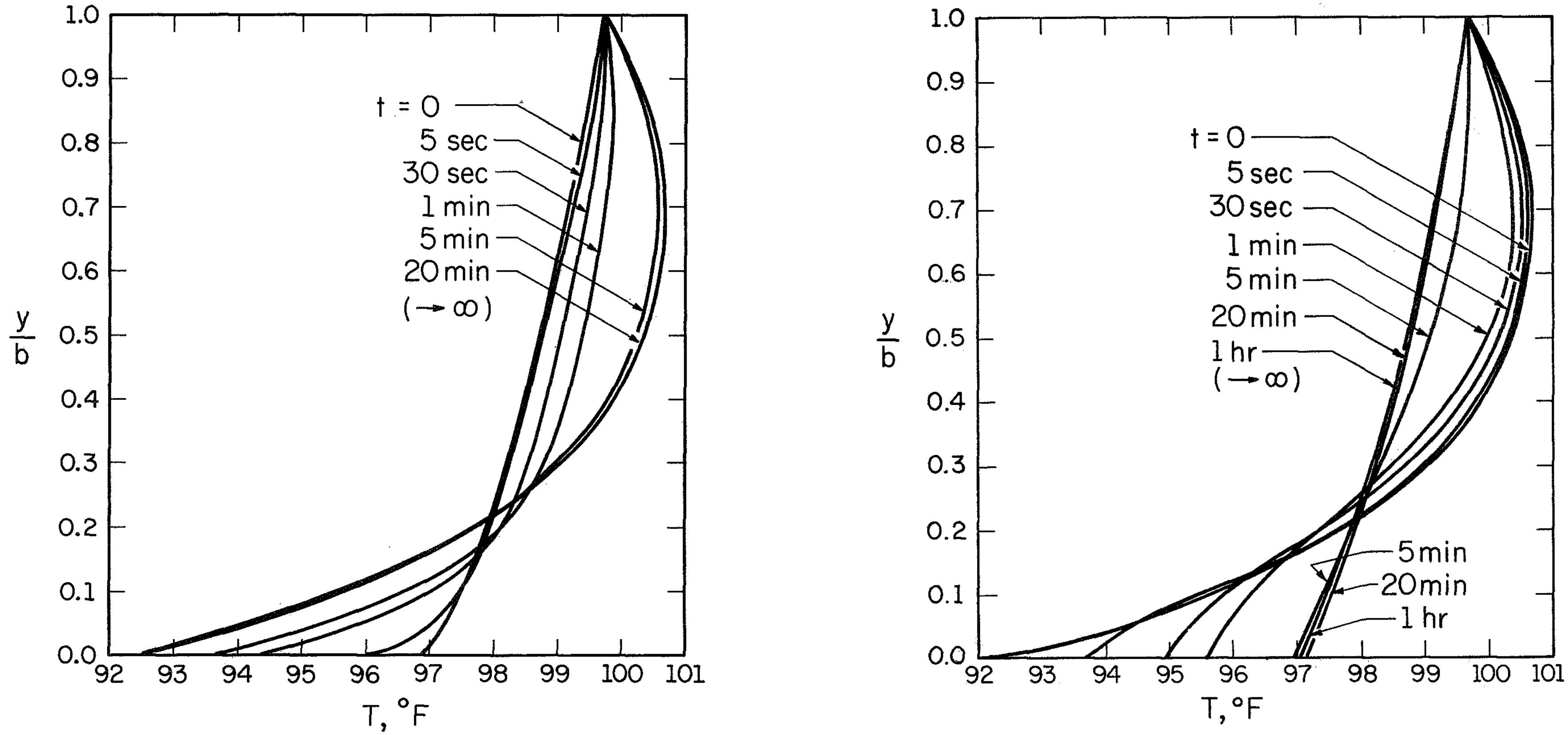

Figure 3.12 Transient temperature distribution in the combined tissue for the one-dimensional rectangular model. Step changes:
(a) from 290 Btu/hr (85 w) to 2600 Btu/hr (760 w)
(b) from 2600 Btu/hr (760 w) to 290 Btu/hr (85 w)
Constant temperature at inner core.

When a variable flux is assumed at the skin, the problem becomes

CASE 2:

$$\frac{1}{\alpha}\frac{\partial\theta}{\partial t} = \nabla^2\theta - w_2\theta + Q_2 \tag{3.52a}$$

$$0 \le x \le a \ , \quad 0 \le y \le b \ , \quad 0 \le t$$

with the boundary and initial conditions,

$$\text{at } y = 0 \ , \ \left\{ \begin{array}{ll} \dfrac{\partial\theta}{\partial y} = \dfrac{f_2(x)}{k} \ , & 0 \le x < \beta a \\ \dfrac{\partial\theta}{\partial y} = 0 \ , & \beta a < x \le a \end{array} \right\} \tag{3.52b}$$

$$\text{at } y = b \ , \quad \theta = 0 \tag{3.52c}$$

$$\text{at } x = 0 \ , \quad \frac{\partial\theta}{\partial x} = 0 \tag{3.52d}$$

$$\text{at } x = a \ , \quad \frac{\partial\theta}{\partial x} = 0 \tag{3.52e}$$

$$\text{at } t \le 0 \ , \quad \theta = \frac{Q_1}{w_1^2}\left[1 - \frac{\cosh(w_1 y)}{\cosh(w_1 b)}\right] - \frac{\beta f_{a1}}{k w_1} \cdot \frac{\sinh[w_1(b-y)]}{\cosh(w_1 b)} + \sum_{n=1}^{\infty} \cdot \frac{\alpha_{n,1}\sinh[\zeta_1(b-y)]}{\zeta_1 \cosh(\zeta_1 b)}\cos(\lambda_{n,1}x) \tag{3.52f}$$

The solution to this set was obtained by using transformations and a double Fourier series expansion to yield

$$T(x,y,t) = T_1 + \frac{Q_2}{w_2^2}\left[1 - \frac{\cosh(w_2 y)}{\cosh(w_2 b)}\right] - \frac{\beta f_{a2}}{k w_2}\,\frac{\sinh[w_2(b-y)]}{\cosh(w_2 b)}$$

$$- \frac{2}{ak}\sum_{j=1}^{\infty} \frac{\alpha_{j,2}\sinh[\zeta_{j,2}(b-y)]}{\zeta_{j,2}\cosh(\zeta_{j,2}b)}\cos(\lambda_j x)$$

$$+ \frac{2}{bk}\sum_{i=1}^{\infty}\left\{\frac{\beta f_{a2}}{\gamma_2^2} - \frac{\beta f_{a1}}{\gamma_1^2} + \frac{(-1)^i}{\delta_i}\right.$$

$$\left.\cdot\left[\frac{Q_2'}{\gamma_2^2} - \frac{Q_1'}{\gamma_1^2}\right]\right\}\cos(\delta_i x)\exp(-\alpha\gamma_2^2 t) + \frac{4}{abk}$$

$$\cdot\sum_{n=1}^{\infty}\sum_{m=1}^{\infty}\left\{\frac{\alpha_{n,1}}{\zeta_{n,1}^2 + \delta_m^2} - \frac{\alpha_{n,2}}{\zeta_{n,2}^2 + \delta_m^2}\right\}$$

$$\cdot\cos(\lambda_n x)\cos(\delta_m y)\exp(-\alpha\sigma_2^2 t) \tag{3.53}$$

where

$$\alpha_{i,j} \equiv \int_0^{\beta a} f_j(\xi)\cos(\lambda_i \xi)\, d\xi \tag{3.54}$$

$$\sigma_2^2 \equiv w_2^2 + \lambda_n^2 + \delta_m^2 = w_2^2 + \pi^2\left[\left(\frac{n}{a}\right)^2 + \frac{(2m-1)^2}{4b^2}\right] \tag{3.55}$$

and w_i, f_a, ζ_i, λ_i, δ_i, and γ_i are defined by Eqs. (3.9), (3.16), (3.17), (3.18), (3.50), and (3.51), respectively.

Temperature variations on the skin are shown for this case in Fig. 3.13. These results exhibit the same basic characteristics as do those for the one-dimensional case; i.e., most of the changes in temperature occur during the first 5-20 minutes from the onset of a change in level of activity.

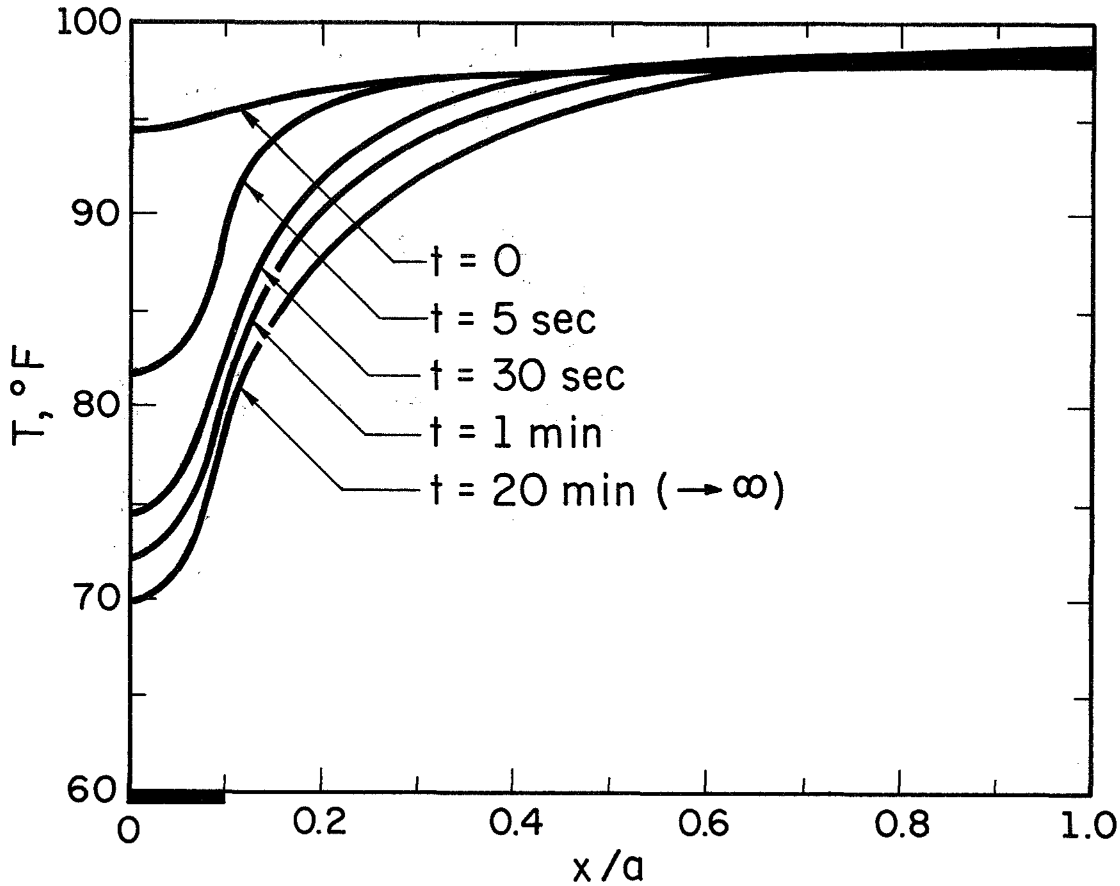

Figure 3.13 Transient temperature distribution on the skin of the combined tissue for the two-dimensional rectangular model. Step change assumed from 290 Btu/hr (85 w) to 2600 Btu/hr (760 w), β = 0.1 and constant temperature at inner core.

Examination of the time dependent exponent in Eq. (3.49) leads to the following two conclusions:

(1) The exponent is strongly dominated by the separation coefficient λ_n rather than by the blood flow term. This becomes even more noticeable for low blood flow rates. The effect of the blood can, in any case, be neglected for $n > 2$.

(2) Time constants (transients) appear to be in the range of 5-20 minutes. This observation is supported by experimental evidence and partially validates the analysis.

Extension of the transient solutions outlined in this section to account for the actual changes occurring in the tissue will have to be delayed until more reliable experimental data become available. This extension, however, appears to be possible by using Duhamel's method [63].

3.7 TRANSIENT STATE, CYLINDRICAL COORDINATES

As a result of the preceding analysis, it was felt that an extensive solution of the transient problem in cylindrical coordinates, i.e., variable flux at the skin, could be neglected at present; for, the small amount of additional information obtained from such a solution would not justify the effort required. Consequently, only the case with uniform flux at the skin was studied as presented below.

$$\frac{1}{\alpha}\frac{\partial\theta}{\partial t} = \frac{1}{r}\frac{\partial}{\partial r}\left(r\frac{\partial\theta}{\partial r}\right) - w_2^2\theta + Q_2 \tag{3.56a}$$

$$R_1 \leq r \leq R_2 \;, \quad 0 \leq t$$

with the boundary and initial conditions,

$$\text{at } r = R_1 \ , \ \theta = 0 \tag{3.56b}$$

$$\text{at } r = R_2 \ , \ \frac{\partial\theta}{\partial r} = -\frac{F_2}{k} \tag{3.56c}$$

$$\text{at } t \le 0 \ , \ \theta = \frac{Q_1}{w_1^2}\left[1 - \frac{\psi_{01}^2(w_1 r)}{\psi_{01}^2(w_1 R_1)}\right] - \frac{F_1}{kw_1}\frac{\psi_{00}^1(w_1 r)}{\psi_{01}^2(w_1 R_1)} \tag{3.56d}$$

Using the same technique as for the rectangular case, the following solution was obtained

$$\begin{aligned} T(r,t) = {} & \frac{Q_2}{w_2^2}\left[1 - \frac{\psi_{01}^2(w_2 r)}{\psi_{01}^2(w_2 R_1)}\right] - \frac{F_2}{kw_2}\frac{\psi_{00}^1(w_2 r)}{\psi_{01}^2(w_2 R_1)} + T_1 \\ & + \frac{\pi}{k}\sum_{n=1}^{\infty} \frac{\left[\frac{Q_2'}{\varepsilon_2^2} - \frac{Q_1'}{\varepsilon_1^2}\right] Y_1(\mu_n R_2) - \mu_n\left[\frac{F_2}{\varepsilon_2^2} - \frac{F_1}{\varepsilon_1^2}\right] Y_o(\mu_n R_1)}{Y_o^2(\mu_n R_1) - Y_1^2(\mu_n R_2)} \\ & \cdot Y_1(\mu_n R_2)\chi_n(\mu_n r)\exp(-\alpha\varepsilon_2^2 t) \end{aligned} \tag{3.57}$$

where

$$\chi_n(\mu_n r) = J_o(\mu_n r)Y_o(\mu_n R_1) - J_o(\mu_n R_1)Y_o(\mu_n r) \tag{3.58}$$

and μ_n are the roots of

$$J_o(\mu_n R_1)Y_1(\mu_n R_2) - J_1(\mu_n R_2)Y_o(\mu_n R_1) = 0 \tag{3.59}$$

$$\varepsilon_i^2 \equiv \mu_n^2 + w_i^2 \tag{3.60}$$

J_i and Y_i are Bessel functions of the first and second kind, respectively, of order i.

No numerical solutions were obtained for this case because of the appearance of the combination of Bessel functions in the time dependent series in Eq. (3.57). These functions reach high numerical values at relatively small arguments and, therefore, exceed the calculating capacity of the computer. However, the first six roots of Eq. (3.59) were computed using Newton-Raphson's method as a function of the ratio R_2/R_1 and are presented in TABLE 3.2. As this ratio approaches unity (rectangular model), the roots approach the limiting value for the rectangular case; i.e., $\mu_n \to \delta_n$, as was to be expected.

3.8 COMPARISON OF STEADY STATE SOLUTIONS FOR RECTANGULAR AND CYLINDRICAL COORDINATES

As was noted above, the human body can be more closely approximated by cylinders rather than by rectangular slabs. According to Wissler [18], the outside radii of these cylinders vary from 0.15 ft for the arm to about 0.43 ft for the trunk. Unfortunately, the expressions obtained for the cylindrical coordinates are more difficult for numerical evaluation because of the presence of the combination of modified Bessel function in the solution for the cylindrical case, Eqs. (3.35) and (3.36). This combination, when programmed on a digital computer, caused an overflow after the first few terms of the series and rendered the numerical results inaccurate.

A comparison of the simpler, rectangular and the cylindrical cases revealed that the temperature distributions obtained for the two cases do not differ significantly. This fact became even more apparent as R_1 increased. For $R_1 \geq 0.20$ ft, the results obtained

TABLE 3.2

FIRST SIX ROOTS OF EQ. (3.59) AS A FUNCTION OF THE RATIO OF THE OUTER TO INNER RADII OF THE CYLINDRICAL MODEL, R_2/R_1. THE RIGHTMOST COLUMN GIVES THE ASYMPTOTIC VALUES ($[(2n - 1)\pi]/2b$, RECTANGULAR MODEL) AS $R_1 \to \infty$ AND $R_2/R_1 \to 1$.

R_2/R_1	2.46	1.73	1.37	1.24	1.18	1.15	1
n \ R_1 (ft)	0.05	0.10	0.20	0.30	0.40	0.50	∞
1	17.83	19.18	20.16	20.55	20.76	20.90	21.49
2	63.29	63.74	64.04	64.16	64.23	64.27	64.46
3	106.74	107.01	107.19	107.26	107.30	107.33	107.44
4	149.91	150.11	150.24	150.29	150.32	150.34	150.42
5	193.00	193.15	193.24	193.30	193.32	193.33	193.39
6	236.05	236.17	236.25	236.29	236.30	236.32	236.37

for the rectangular model were adequate for any practical purpose. Figures 3.14, 3.15, 3.16, and 3.17 demonstrate this finding for uniform and variable heat fluxes at the skin (see APPENDIX E).

A partial explanation to this similarity of the solutions can be given as follows. If the argument of the modified Bessel function is greater than 10, which is mostly the case here ($wR_1 > 10$), the following expressions can be used to approximate the modified Bessel functions of the first and second kind [64],

$$I_k(z) \simeq \frac{0.3989 \exp(z)}{z^{1/2}} \left\{ 1 + (-1)^k \left[\frac{a_k}{8z} + \frac{b_k}{128z^2} + \frac{c_k}{1024z^3} \right] \right\} \tag{3.61}$$

$$K_k(z) \simeq \frac{1.2533 \exp(z)}{z^{1/2}} \left\{ 1 + (-1)^{k+1} \left[\frac{a_k}{8z} + \frac{b_k}{128z^2} + \frac{c_k}{1024z^3} \right] \right\} \tag{3.62}$$

where a_k, b_k, and c_k are constants and $k = 0$ or 1. When these expressions are substituted into Eq. (3.37), an essentially exponential expression results. This expression corresponds to the hyperbolic functions that appear in the solution for the rectangular case.

It should be noted that the above comparison is valid for the cylindrical case with the cooling tubes running perpendicular to the axis of the cylinder, Fig. 3.2. The reason is the similarity of the resulting rectangular geometry.

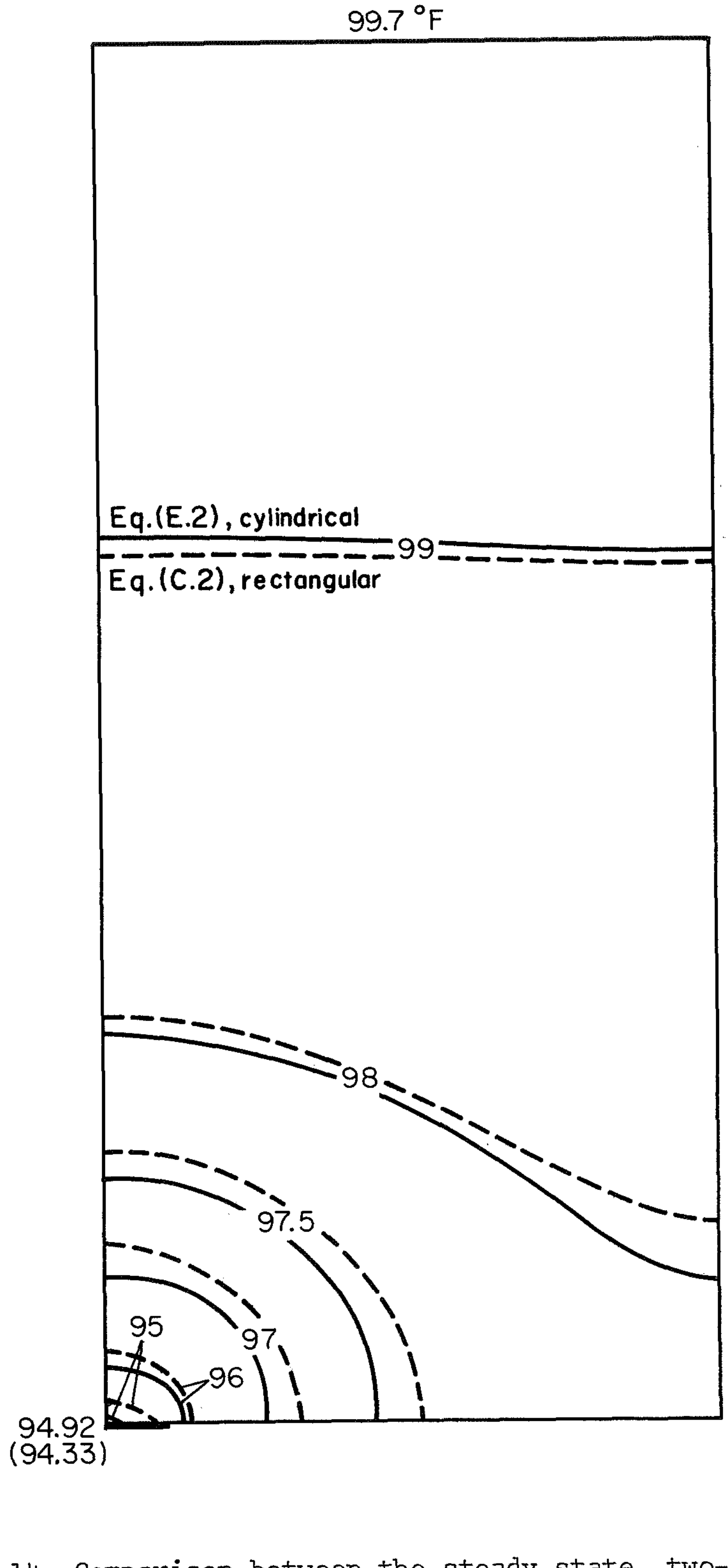

Figure 3.14 Comparison between the steady state, two-dimensional solutions for rectangular and cylindrical models (tubes running perpendicular to the axis of the cylinder, R_1 = 0.15 ft, V and b are constant). Q_m = 290 Btu/hr (85), β = 0.1 and constant temperature at inner core.

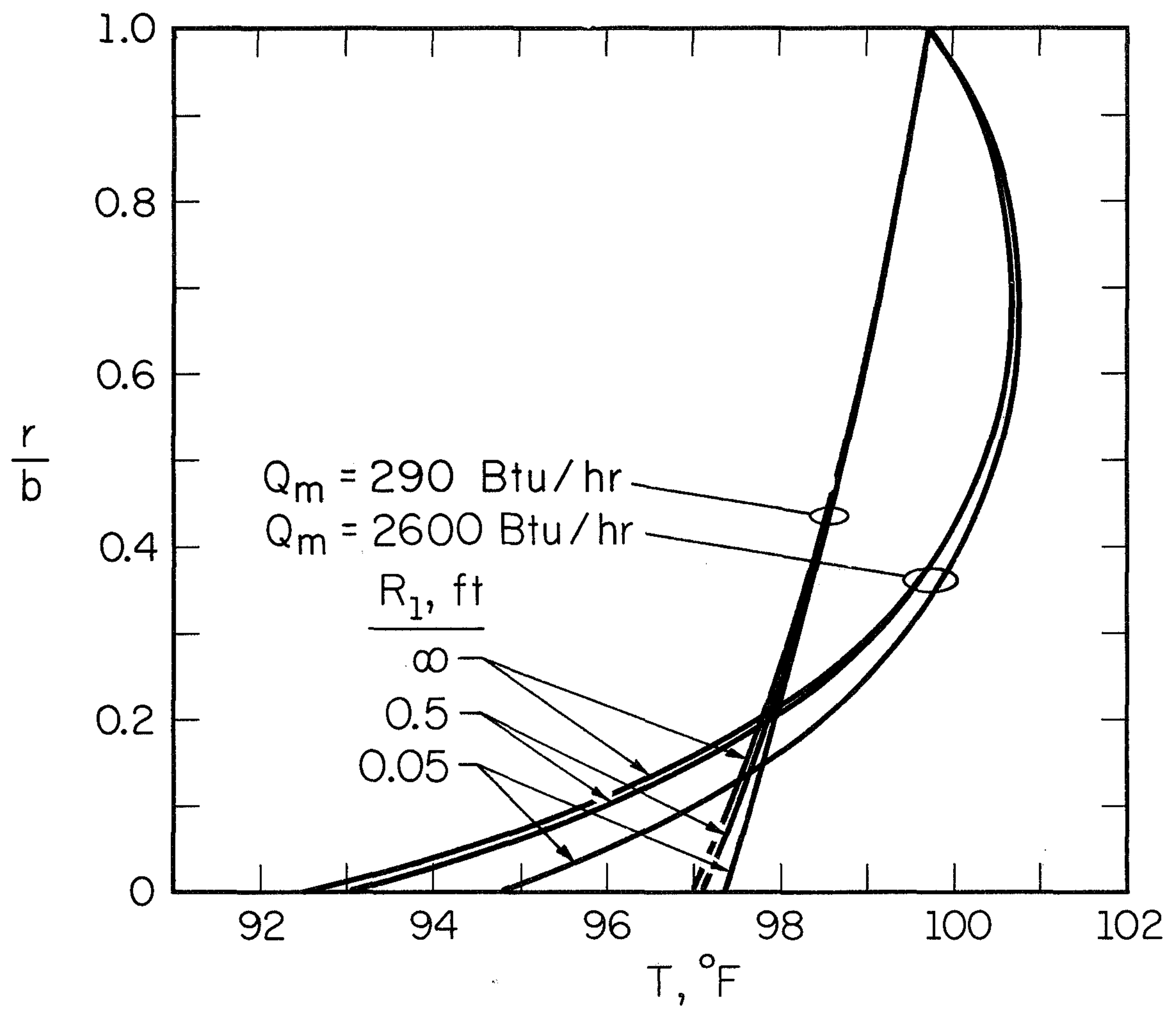

Figure 3.15 Comparison between steady state, one-dimensional solutions obtained for the rectangular and cylindrical models (V and b are constant). Constant temperature at inner core.

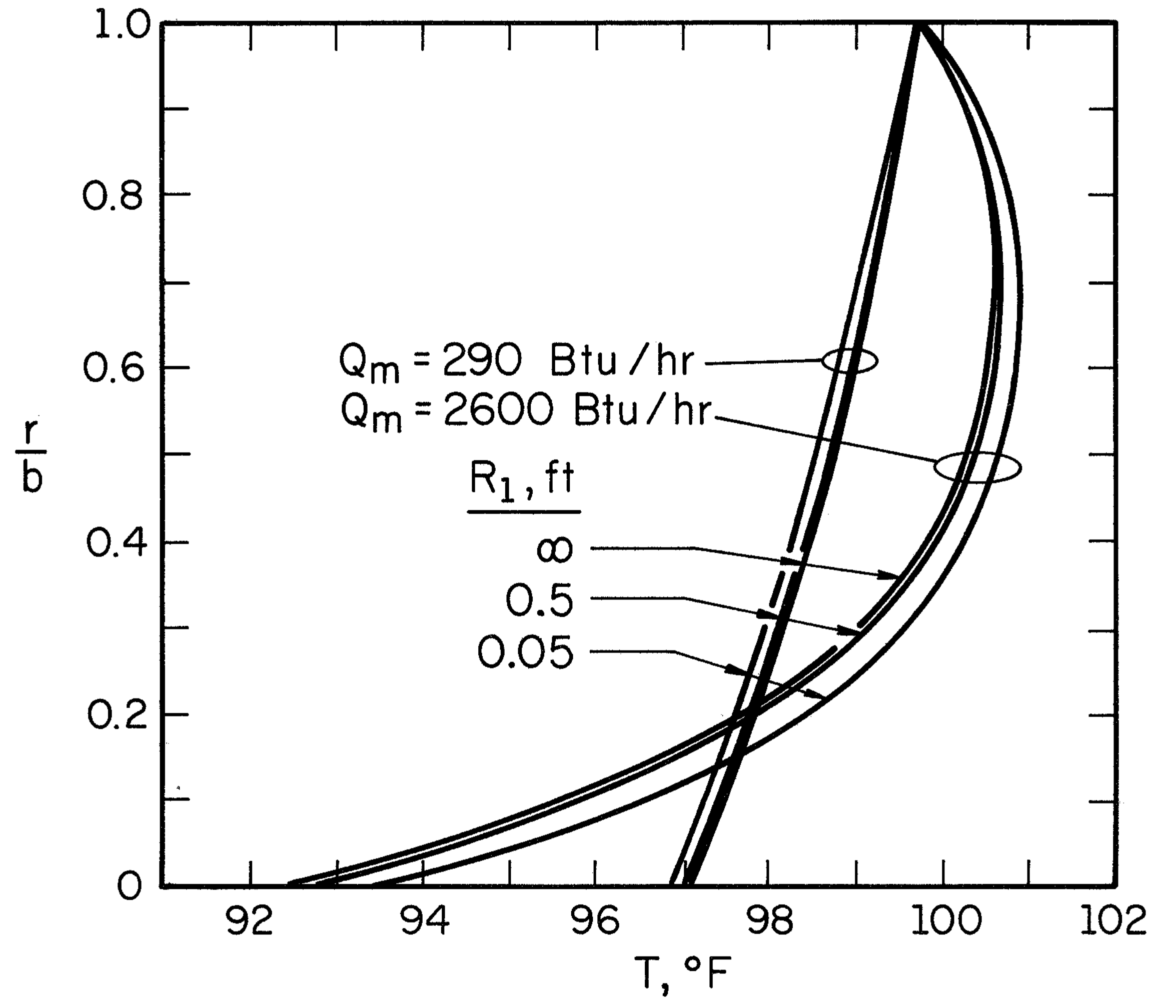

Figure 3.16 Comparison between steady state, one-dimensional solutions obtained for the rectangular and cylindrical models (V and A are constant). Constant temperature at inner core.

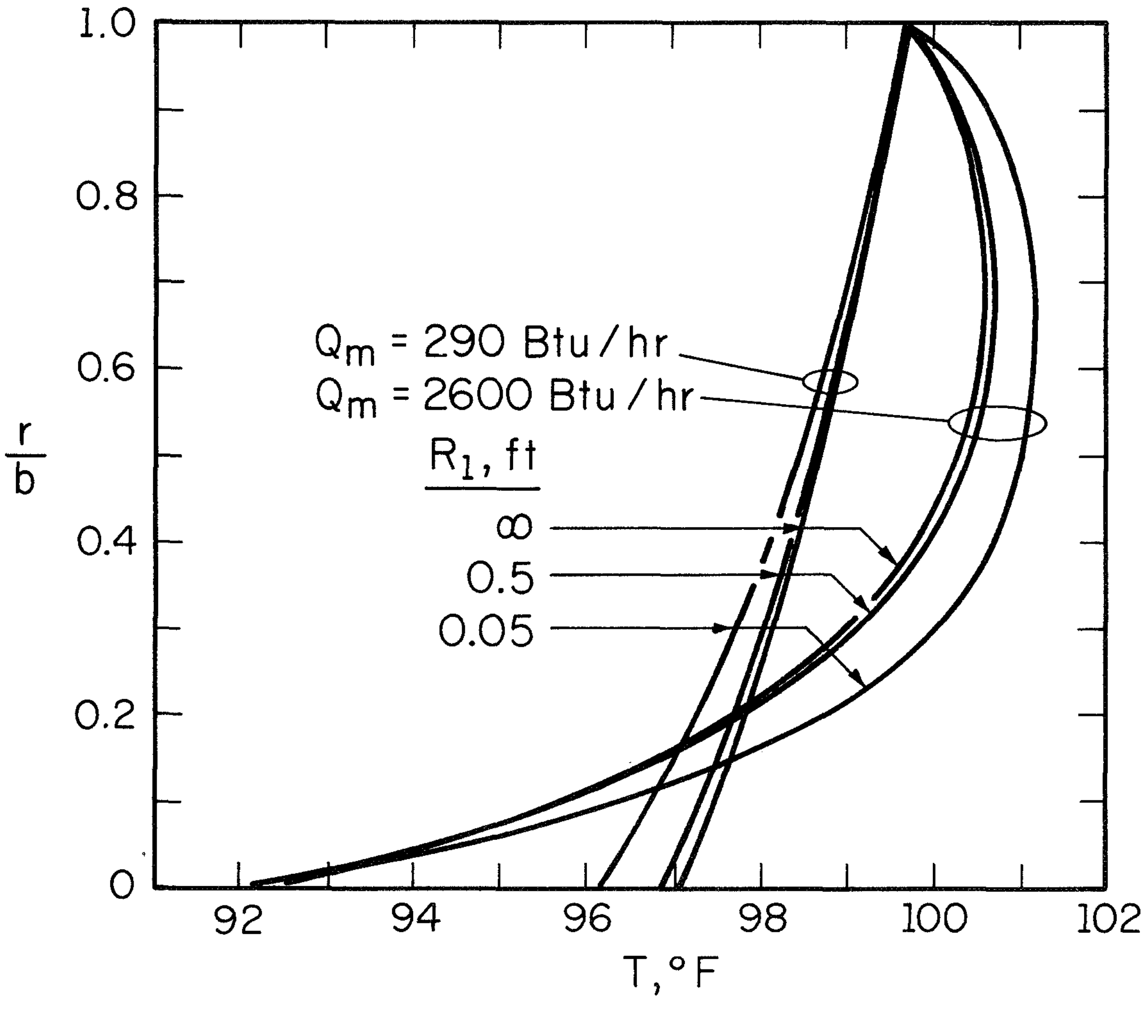

Figure 3.17 Comparison between steady state, one-dimensional solutions obtained for the rectangular and cylindrical models (A and b are constant). Constant temperature at inner core.

3.9 DIMENSIONLESS PARAMETERS ASSOCIATED WITH THE THERMAL BEHAVIOR OF LIVING BIOLOGICAL TISSUE

It is always desirable, from an engineering viewpoint, to have appropriate dimensionless parameters for the description of any physical phenomena. The best method for obtaining these parameters is via an analytical model.

Consider a one-dimensional, steady state case in rectangular coordinates. The analytical expressions for the temperature distributions in the tissue can be obtained from Eqs. (C.2) and (C.4) to yield, for constant temperature at the inner core,

$$T(y) = T_1 + \frac{Q}{w^2}\left[1 - \frac{\cosh (wy)}{\cosh (wb)}\right] - \frac{F}{kw}\,\frac{\sinh [w(b - y)]}{\cosh (wb)} \tag{3.63}$$

and, for a constant heat flux at the inner core,

$$T(y) = T_1 + \frac{Q}{w^2} + \frac{1}{kw \sinh (wb)}\left\{ F \cosh (wy) - F_o \cosh [w(b - y)]\right\} \tag{3.64}$$

Figures 3.18 and 3.19 show results obtained for Eqs. (3.63) and (3.64), respectively, for both low (290 Btu/hr, 85 W) and high (2600 Btu/hr, 760 W) metabolic rates.

As was noted above, a maximum temperature was found to occur in the combined tissue rather than in the inner core (Fig. 3.18). In order to obtain the location of these maxima, Eqs. (3.63) and (3.64) were differentiated and equated with zero to obtain [65],

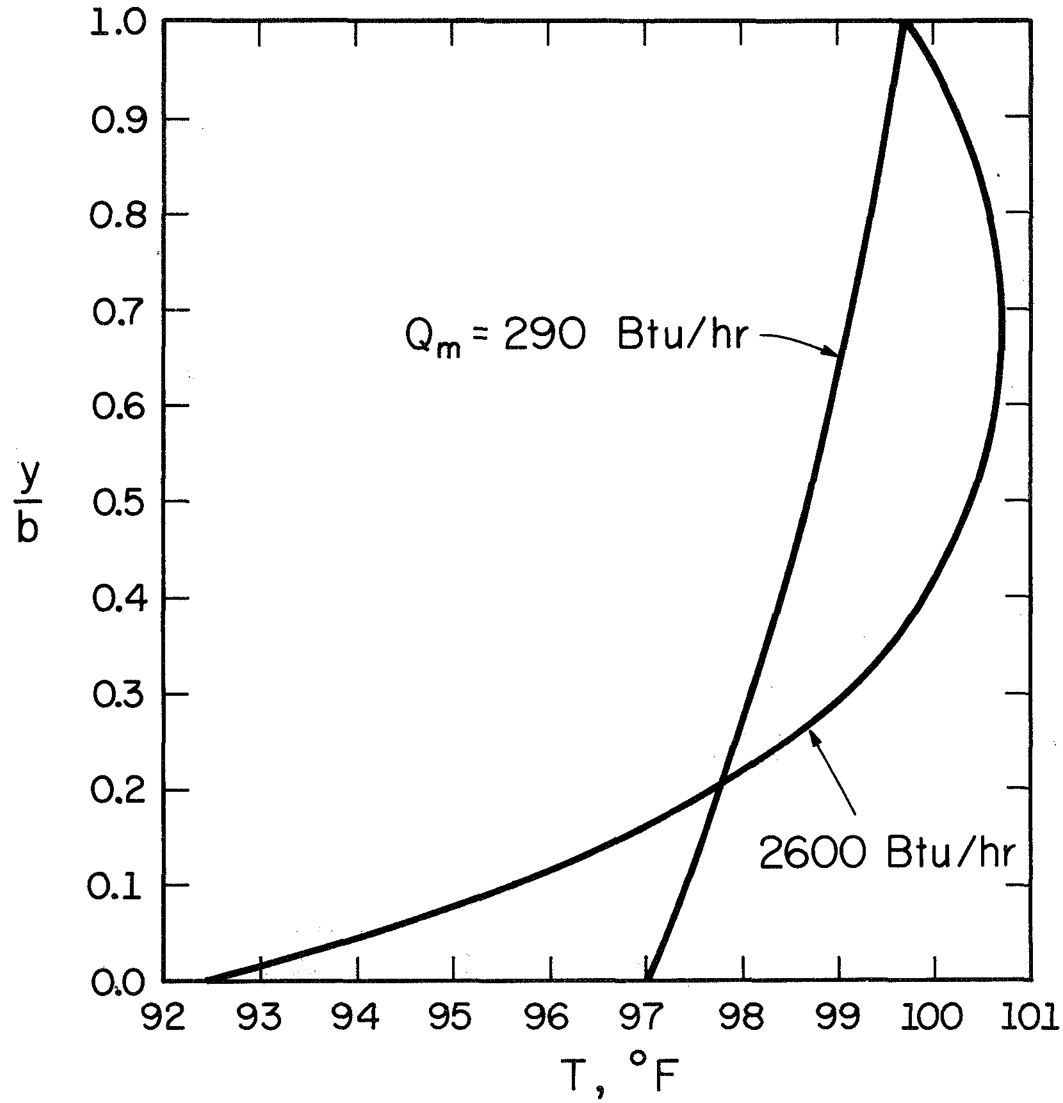

Figure 3.18 Steady state temperature distributions in the combined tissue for the one-dimensional rectangular model. Constant temperature at inner core.

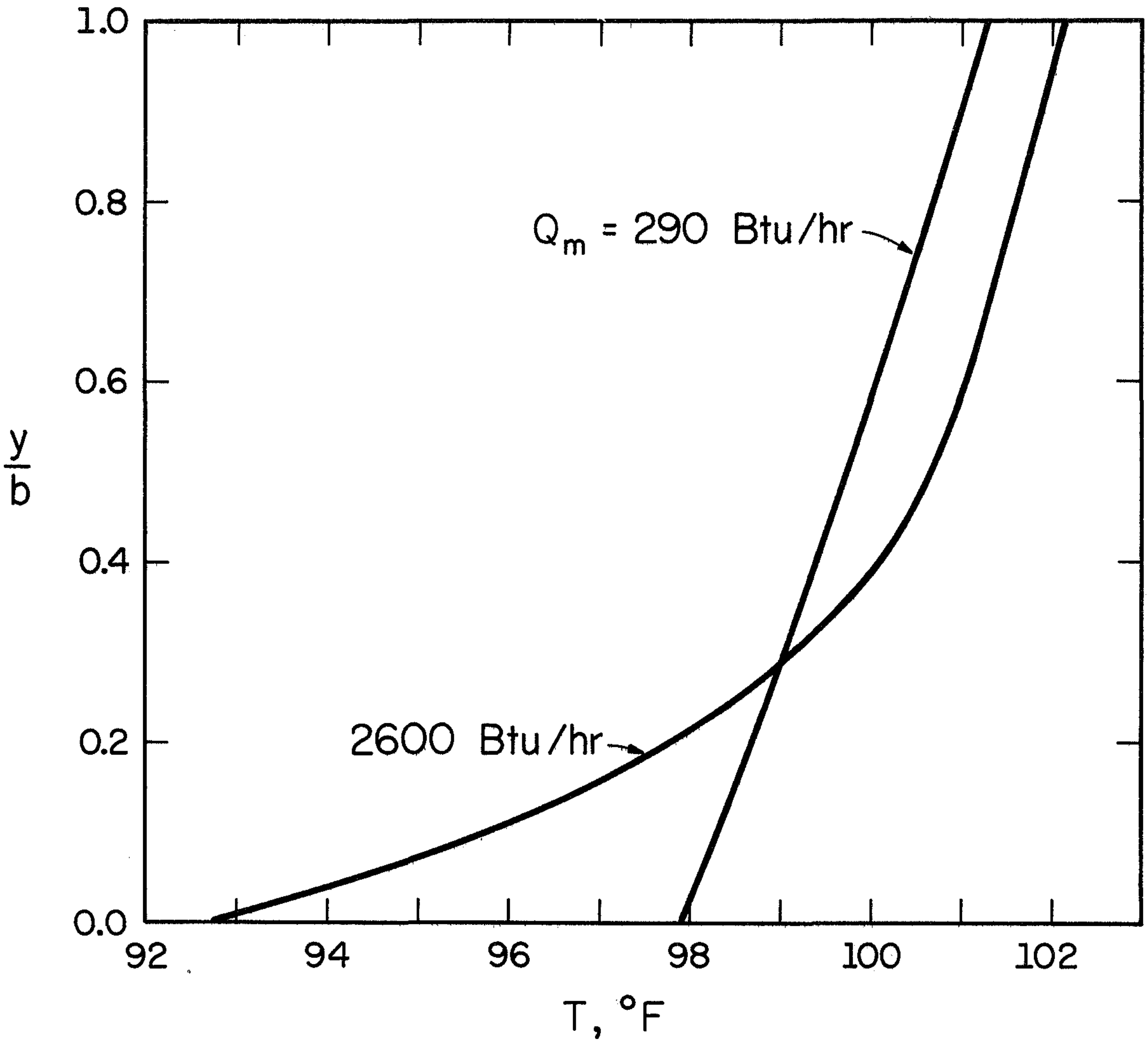

Figure 3.19 Steady state temperature distributions in the combined tissue for the one-dimensional rectangular model. Constant flux at inner core.

$$\tanh\left[(wb)\frac{y}{b}\right] = \frac{\cosh(wb)}{\frac{Q'Ab}{Q_m}\frac{1}{wb} + \sinh(wb)} \tag{3.65}$$

$$\tanh\left[(wb)\frac{y}{b}\right] = \frac{\sinh(wb)}{\frac{Q'Ab}{Q_m} - 1 + \cosh(wb)} \tag{3.66}$$

No maximum temperature was found to occur inside the tissue for the case with a specified flux at the inner core, Eqs. (3.64) and (3.66). This result is to be expected since, by imposing a heat flux from the inner core into the combined tissue, the temperature gradients must sustain heat flow toward the skin only. Equation (3.65), however, was solved for the y/b values for which the maximum temperature occurs as a function of the parameters present in it. The location of the maximum was found to be independent of inner body temperature. Results are shown in Fig. 3.20.

Based on the preceding analysis, three dimensionless parameters, which have significant effects on the steady state heat transfer in the living tissue, emerged. These are:

(1) $wb = (w_b c_b/k)^{1/2} b$--ratio of heat transported by the blood stream to the heat transferred by conduction through the tissue.

(2) $Q'Ab/Q_m$--ratio of rate of heat generated in the tissue to the total metabolic heat generation rate.

(3) $(Q'Ab/Q_m)[(w_b c_b/k)^{-1/2} b^{-1}]$--the quotient of the first and second groups which contains most of the physical and physiological properties describing the thermal condition of the human body. From the scant physiological data available [59], this third group appeared to be almost constant at 0.2 for a wide range of metabolic rates. If this value

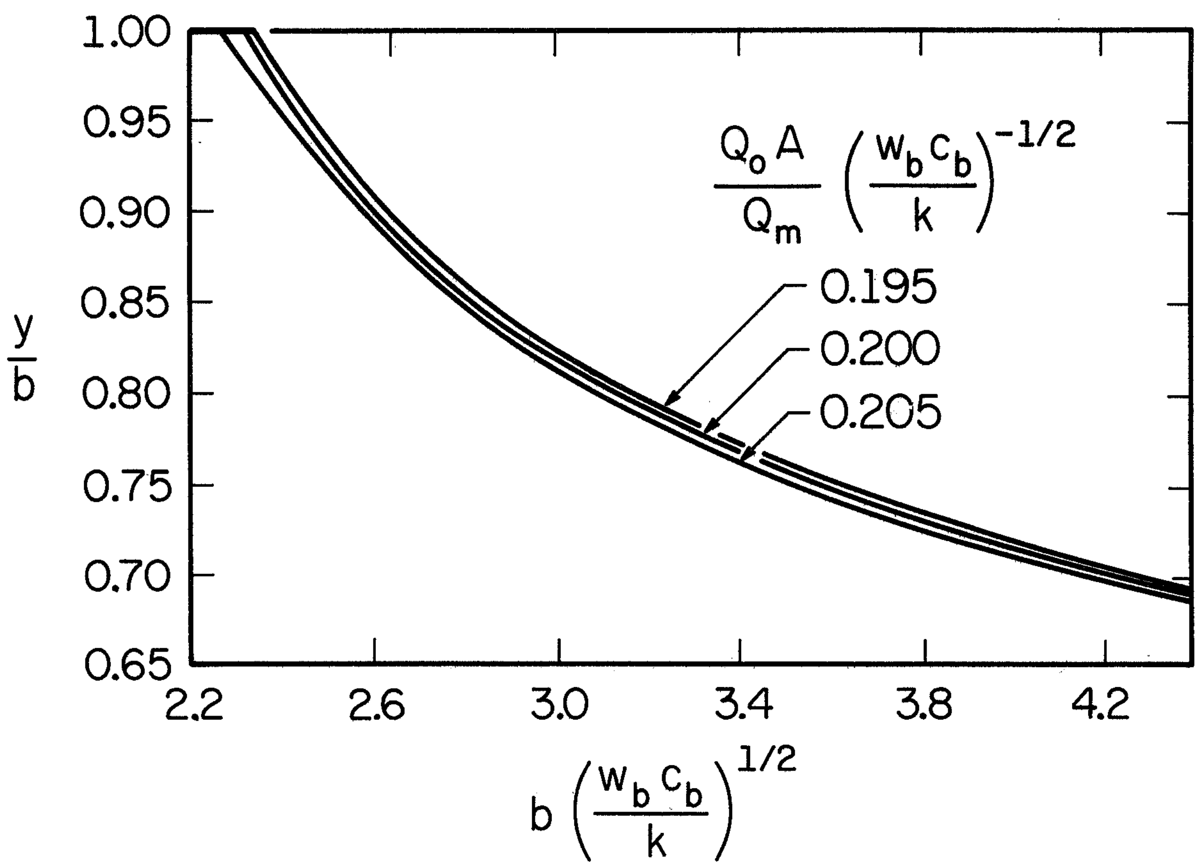

Figure 3.20 Location of the maximum temperature in the combined tissue for the one-dimensional rectangular model.

could be verified experimentally, which is beyond the scope of this work, a very strong physiological tool would become available, which would facilitate the calculation of quantities such as blood perfusion or heat generation rates that are very difficult to measure.

TABLE 3.3 summarizes the physiological quantities and the corresponding values of the above parameters.

No additional information was obtained from studying the corresponding cylindrical case. It is, however, presented below for completeness.

The temperature distribution in the cylindrical shell, which is uniformly cooled at the skin and has a constant temperature at the inner core, is

$$T(r) = T_1 + \frac{Q}{w^2}\left[1 - \frac{\psi^2_{01}(wr)}{\psi^2_{01}(wR_1)}\right] - \frac{F}{kw}\frac{\psi^1_{00}(wr)}{\psi^2_{01}(wR_1)} \tag{3.67}$$

with the resulting expression for the location of the maximum temperatures

$$\frac{I_1\left[(wR_1)\frac{r}{R_1}\right]}{K_1\left[(wR_1)\frac{r}{R_1}\right]} = \frac{A_1 I_1(wR_2) - I_o(wR_1)}{A_1 K_1(wR_2) + K_o(wR_1)} \tag{3.68}$$

where

$$A_1 = \frac{Q'AR_1}{Q_m}\frac{1}{wR_1} \tag{3.69}$$

TABLE 3.3

PHYSIOLOGICAL QUANTITIES AND THE CORRESPONDING DIMENSIONLESS PARAMETERS.

c_b = 1, Btu/lb-°F (4187 J/kg-°C), k = 0.311 Btu/ft-hr-°F (0.540 w/m-°C), b = 0.0731 ft (0.0223 m), AND A = 15.4 ft^2 (1.43 m^2)

Q_m		Q'		w_b		$(w_b c_b/k)^{1/2} b$	$Q' Ab/Q_m$	$(Q' Ab/Q_m)(1/wb)$
Btu/hr	w	Btu/hr-ft^3	w/m^3	lb/hr-ft^3	kg/hr-m^3			
290	85	64	660	94	1,510	1.273	2.484	0.195
2,600	760	2,090	21,600	1,120	18,000	4.394	9.049	0.206

In the cylindrical model, two groups appear, wR_1 and wR_2, representing ratios of heat transported by blood to that conducted through the tissue.

For the transient case, an additional dimensionless parameter appears [from Eq. (3.49)],

$$\alpha[w^2 + \delta_n^2]t \equiv \frac{k}{\rho c_p}\left\{\frac{w_b c_b}{k} + \left[\frac{(2n - 1)\pi}{2b}\right]^2\right\}t \tag{3.70}$$

Equation (3.70) may be resolved into two expressions after multiplying and dividing it by the temperature of the inner core, T_1. The results are the following two dimensionless groups:

(1) $(w_b c_b T_1)/(\rho c_p T_1/t^*)$--ratio of rate of heat transported by the blood stream to rate of energy stored in the tissue.

(2) $(kT_1/b^2)/(\rho c_p T_1/t^*)$--ratio of rate of heat conducted through the tissue to rate of energy stored in it.

In the above two expressions, t^* is some characteristic time.

TABLE 3.4 gives values of the two expressions in the brackets of Eq. (3.70). It clearly demonstrates the dominance of the geometrical separation coefficient relative to the term containing blood flow for $n \geq 2$.

TABLE 3.4

COMPARISON OF MAGNITUDES OF THE TERMS IN EQ. (3.70).
c_b = 1 Btu/lb-°F (4187 J/kg-°C), k = 0.311 Btu/hr-ft-°F
(0.540 w/m-°C), and b = 0.073 ft (0.0223 m)

Q_m	w	85	760
	Btu/hr	290	2,600
$w_b c_p/k$	$1/m^2$	3,230	38,750
	$1/ft^2$	300	3,600
n		1	2
$\left[\frac{(2n-1)\pi}{2b}\right]^2$	$1/m^2$	4,950	44,720
	$1/ft^2$	460	4,160

4. EXPERIMENTS

4.1 OBJECTIVES

The experimental phase of this work was undertaken with the following objectives:

(1) Exploration of the feasibility and operating characteristics of independently cooling separate regions of the body regional cooling). This part was to determine preferable water inlet temperatures, amount of heat removed at each region and the order of cooling or warming preferences at different metabolic rates. The subjects' own sense of comfort was the criterion for determining these data.

(2) Partial validation of the analytical predictions. This was planned to be achieved by measuring skin temperatures between two adjacent cooling tubes. No penetration of the skin was contemplated.

4.2 DESCRIPTION OF THE EXPERIMENTAL SETUPS

4.2.1 Cooling Suit

A water cooled suit was constructed for the purpose of testing the characteristics of the proposed differential scheme of cooling the body. The suit consisted of sixteen individual pads made of 3/32 in. I.D. by 5/32 in. O.D. Tygon tubes running parallel 5/8 in. apart. The spacings between the tubes were maintained by the use of Mylar strips and heavy cotton thread. This assembly was stitched onto cotton fabric pieces, cut to fit the dimensions of the various parts of the body. "Velcro" strips were glued to the fabric to facilitate quick fastening and to accommodate subjects of different sizes (Fig. 4.1).

The cooling pads covered the head (2)†, front and back, upper and lower torso (4), upper and lower, right and left arms (4), right and left thighs (4), and right and left lower legs (2). The face, neck, hands and feet were not covered with cooling tubes. TABLE 4.1 gives pertinent dimensions of the cooling pads and the whole suit.

All the pads, excluding the one for the head, were stitched onto the inside of a No. 44 long sleeve, Towncraft, Raschel knit, men's thermal union underwear garment. The cooling hood was made of a snow suit hood with the cooling tubes stitched onto the inside. The 3/8 in. O.D. main supply Tygon tubes were stitched on the outside of the garment.

The body was divided into six separate regions:

(1) Head,

(2) Upper torso,

(3) Lower torso,

(4) Arms,

(5) Thighs, and

(6) Lower legs.

These regions were supplied with water from cold and hot headers. Inlet pressure of the water was maintained at 20 psig by pressure regulators. Before entering the cooling pads, the two streams were mixed, thus allowing for continuous regulation of water inlet temperature. Water inlet temperatures were measured by means of No. 30 gage copper-

†Numbers in parentheses here represent number of pads in region.

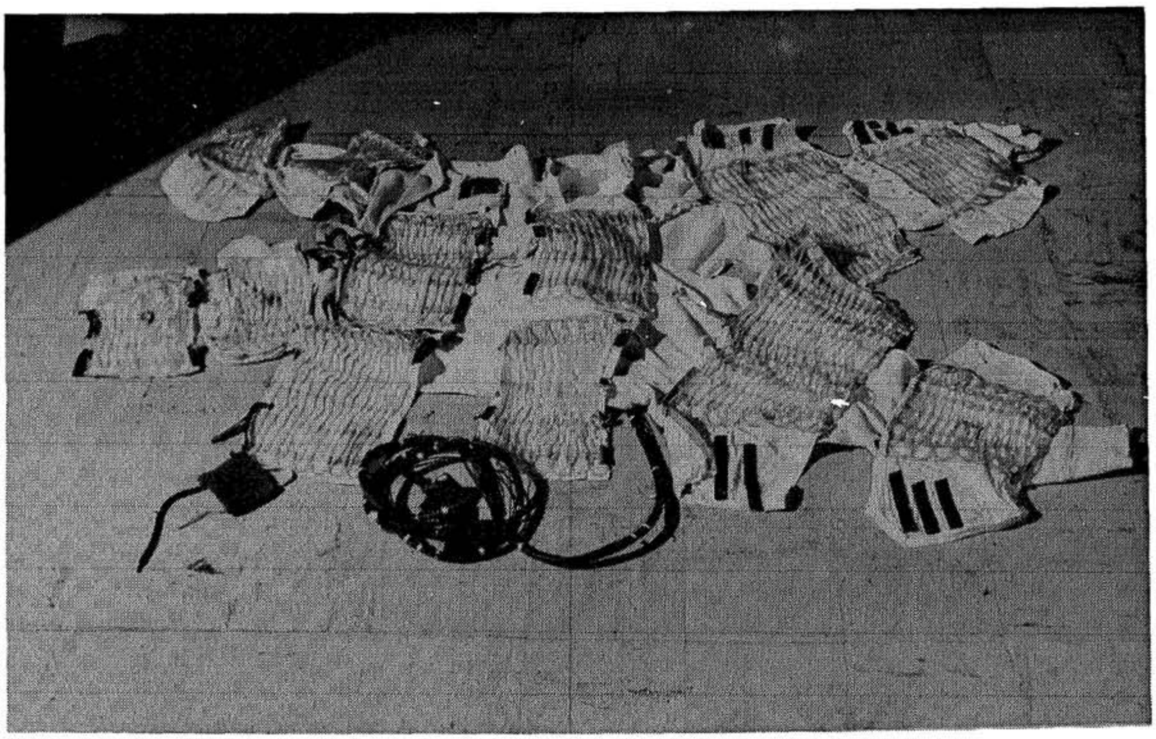

Figure 4.1 General view of the cooling garment.

TABLE 4.1a

DATA ON THE COOLING GARMENT

Pad	Number of Pads	Number of Tube Rows in Pad	Area Covered by Pad		Total Area Covered by Pads		Percent Area Covered
			$in.^2$	cm^2	$in.^2$	cm^2	
Head	2	12	65	419	130	838	9.6
Front and Back, Upper and Lower Torso	4	14	111	716	444	2864	33.0
Upper Arms	2	11	62	400	124	800	9.2
Lower Arms	2	12	60	387	120	774	8.9
Upper Thighs	2	7	83	535	166	1070	12.3
Lower Thighs	2	10	96	619	192	1238	14.2
Lower Legs	2	16	86	555	172	1110	12.8
Total	16	--	--	--	1348	8694	100

TABLE 4.1b

DATA ON THE COOLING GARMENT

	Cooling Garment		Insulating Suit		Cooling Hood		Insulating Hood		Total	
	kg	lb	kg	lb	kg	lb	kg	lb	kg	lb
Weight, dry	4.41	9.72	0.80	1.61	0.25	0.55	0.31	0.68	5.77	12.56
Weight, wet	4.88	10.77	--	--	0.30	0.66	--	--	6.29	19.33

constantan thermocouples using a Leeds and Northrup millivolt potentiometer. At a later stage, the thermocouples were replaced by interchangeable, multipurpose No. 401 thermistors using a Yellow Springs Instrument Co. Tele-Thermometer.

The difference between outlet and inlet temperature of each individual pad was measured by thermopiles consisting of five No. 30 gage copper-constantan thermocouples. These were connected in series to increase the sensitivity of the measurement. The thermopiles were glued to special Plexiglas connectors using 910 Eastman adhesive. The temperatures were continuously recorded on a Leeds and Northrup Speedomax Type G recording potentiometer. Water flow rates of each of the regions were measured by a Fisher and Porter rotameter. All the thermocouple assemblies and thermistors were precalibrated in a constant temperature bath against a precision platinum resistance thermometer. Figure 4.2 shows a schematic of the cooling pads and the control, supply, and measuring systems. Figure 4.3 shows the water supply system, the rotameter, and the potentiometer recorder.

On top of the underwear garment, the subjects donned an insulating suit which thermally isolated them from the environment. A heavily furred hood was used for the same purpose on the head. On the feet, all test subjects wore tennis shoes.

An A. R. Young treadmill was used for the walking sessions. The speed of the treadmill belt was controlled to correspond to the desired level of activity and was timed by a stop watch.

For metabolic measurements, expired air samples were taken with metalized Douglass bags [66]. The bags were placed inside a tightly

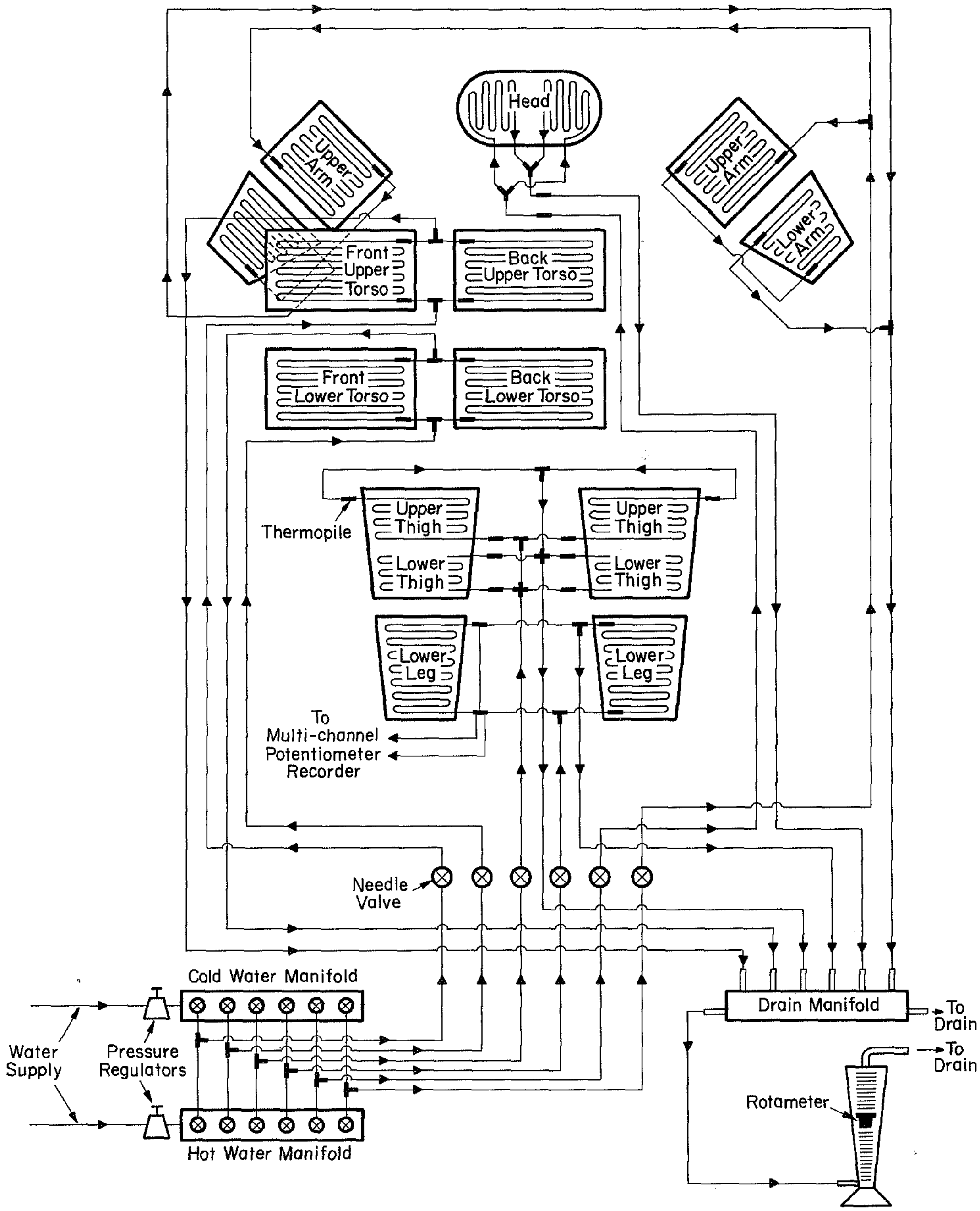

Figure 4.2 Schematic diagram of the cooling garment and the control, supply and measuring systems.

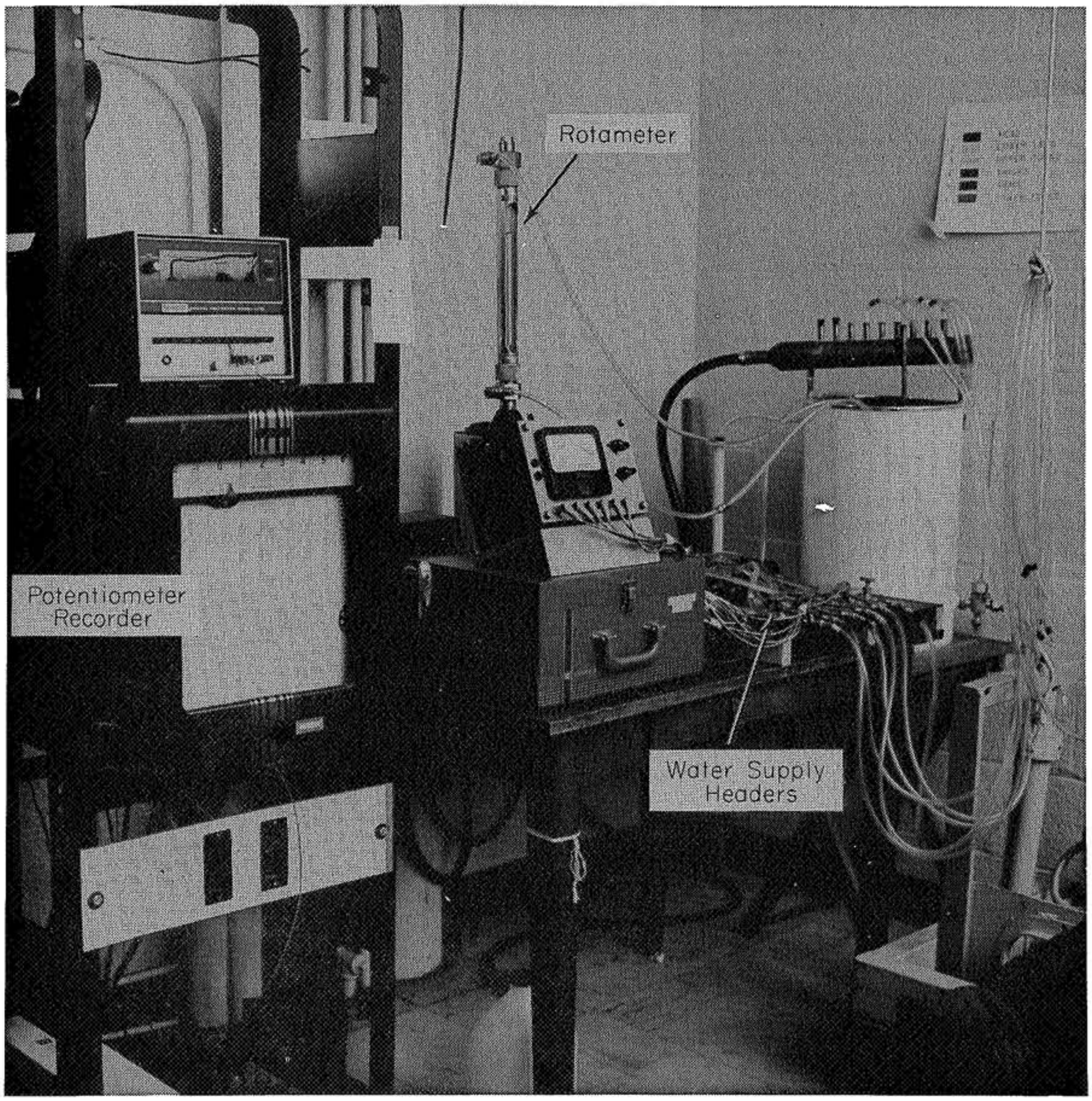

Figure 4.3 View of the water suppy system, rotameter and potentiometer recorder used for the experiments with the cooling suit.

sealed Plexiglas chamber that was under vacuum of about 5 mm Hg [67]. Air was inhaled and exhaled through a mouth piece while the nostrils were blocked with a noseclip. Two sets of one-way rubber valves insured the separation of the two streams. The expired air was then directed through a 1 in. I.D. rubber hose into a mixing chamber. One minute sampling was achieved by opening a one-way stopcock valve thus exposing a previously evacuated metalized bag to the exhaled air.

Air volumetric flow rates were measured by means of a Parkinson-Cowan dry gas meter. Inlet and outlet air temperatures were measured by two interchangeable, multipurpose, No. 401 Yellow Springs thermistors using the company's Tele-Thermometer. Figure 4.4 shows part of the treadmill and the system used for collecting air samples. Air samples were analyzed for CO_2 and O_2 content. A Godart-Mijnhardt CO_2 thermal conductivity meter, Pulmo Analysor Type 44-A-2 and a Beckmann Paramagnetic O_2 analyzer, Model C2, were used. The results of this analysis together with the corresponding air flow rates were then used to evaluate the energy expenditure [68].

The temperature of the ear canal was taken as a measure of deep body temperature. This was done by an ear thermistor No. 510 and a Yellow Springs Instrument Co. Tele-Thermometer. The thermistor was inserted approximately one-half inch into the ear canal and was held in place by a specially prepared ear plug made of medical grade silicone rubber. The outside ear was covered by a piece of polyurethane foam to exclude possible effects of the cooling tubes. The reasons for measuring the temperature of the ear canal rather than the more commonly used rectal temperature were twofold: first, it was more convenient for walking; and second, it gave a closer indication to the

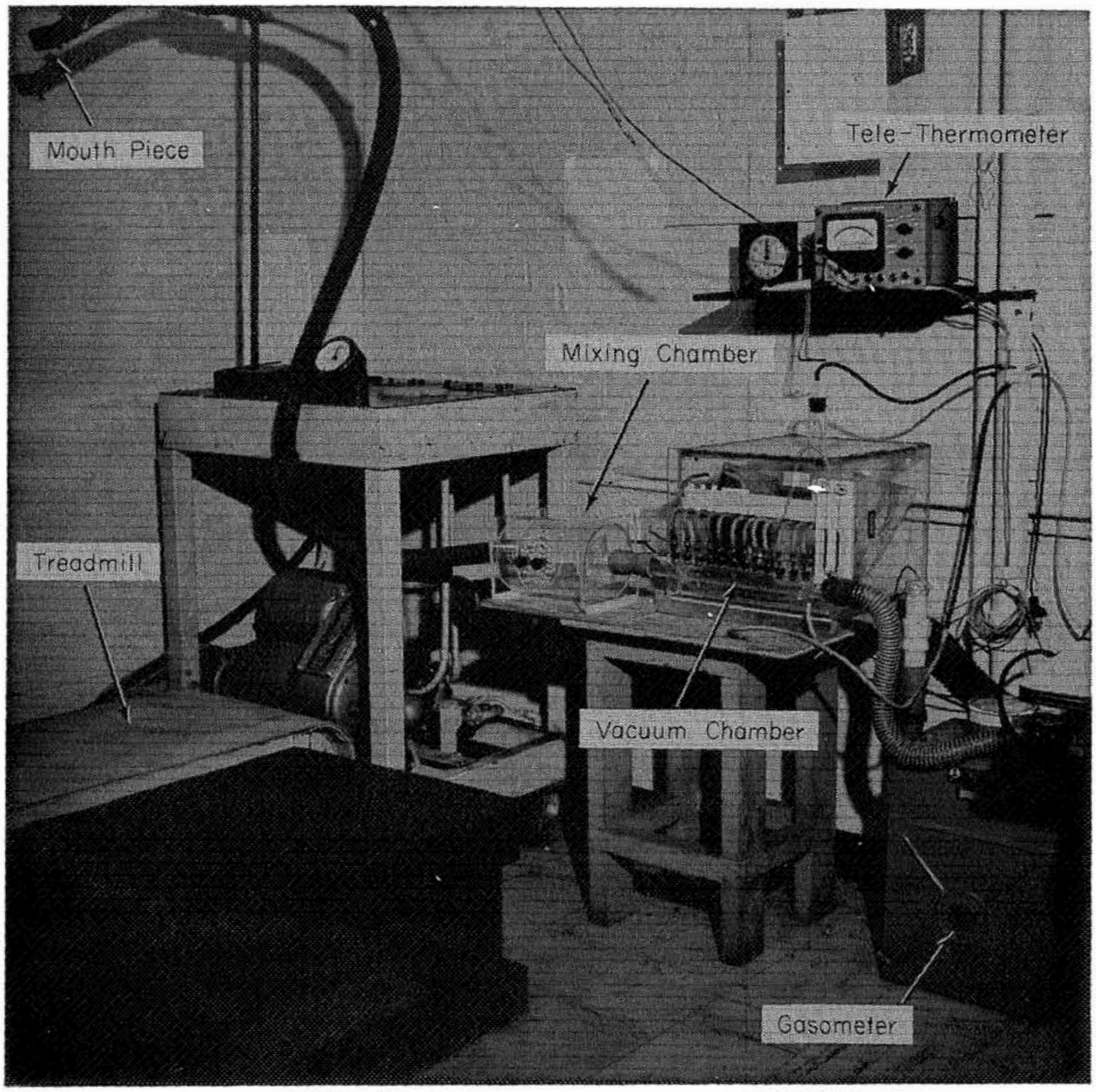

Figure 4.4 View of the treadmill, Tele-Thermometer and system for collecting samples for determining metabolic rates.

temperature regulated by the body, i.e., the temperature of the hypothalamus. Figure 4.5 shows a general view of the experimental set-up with a test subject dressed up with the cooling and insulating suits walking on the treadmill. Ear canal thermistor is not shown connected in this picture.

A Buffalo special physiological beam scale was used to weigh the subjects before and after the experiments. The capacity of this scale is 125 kg and the sensitivity is ± 0.25 gr.

4.2.2 Individual Cooling Pads†

Three different individual cooling pads were constructed for the purpose of partially validating the analytical predictions. These pads were designed to fit over the thigh of a test subject. They were all made of gum rubber with parallel Tygon tubing glued onto one side using RTV glue. TABLE 4.2 gives pertinent data on the individual pads.

Number 30 gage copper-constantan thermocouples were used to measure cooling water temperatures and skin temperatures between two adjacent tubes. The thermocouples were equally spaced along a diagonal between the tubes and were pressed against the skin to insure good thermal contact. Figure 4.6 illustrates one of the cooling pads and the thermocouples.

The cooling pads were supplied with water by the same system as described in the preceding section. Water supply temperature and the difference between water outlet and inlet temperatures were

†This set-up was built and these experiments were performed by Mr. R. J. Leo under the supervision of the author.

Figure 4.5 General view of the set-up used for the experiments with the cooling suit. A test subject is shown dressed up in the cooling suit walking on the treadmill. No tennis shoes are shown in this picture and the ear canal thermistor is not connected.

TABLE 4.2

DATA ON THE INDIVIDUAL COOLING PADS

	Outside Diameter of Tubes		Spacing of Tubes		Number of Rows of Tubes	Total Length of Tubes		Area Covered by Pad		Approximate Contact Area with the Skin		Percent of Area in Contact with Tubes
	in.	cm	in.	cm		in.	cm	$in.^2$	cm^2	$in.^2$	cm^2	
Pad No. 1	5/32	0.397	1	2.54	10	163	414	140	910	22.9	148	16.4
Pad No. 2	5/32	0.397	5/8	1.59	14	228	580	132	852	32.1	207	24.3
Pad No. 3	7/32	0.556	1	2.54	10	163	414	145	937	28.5	184	19.7

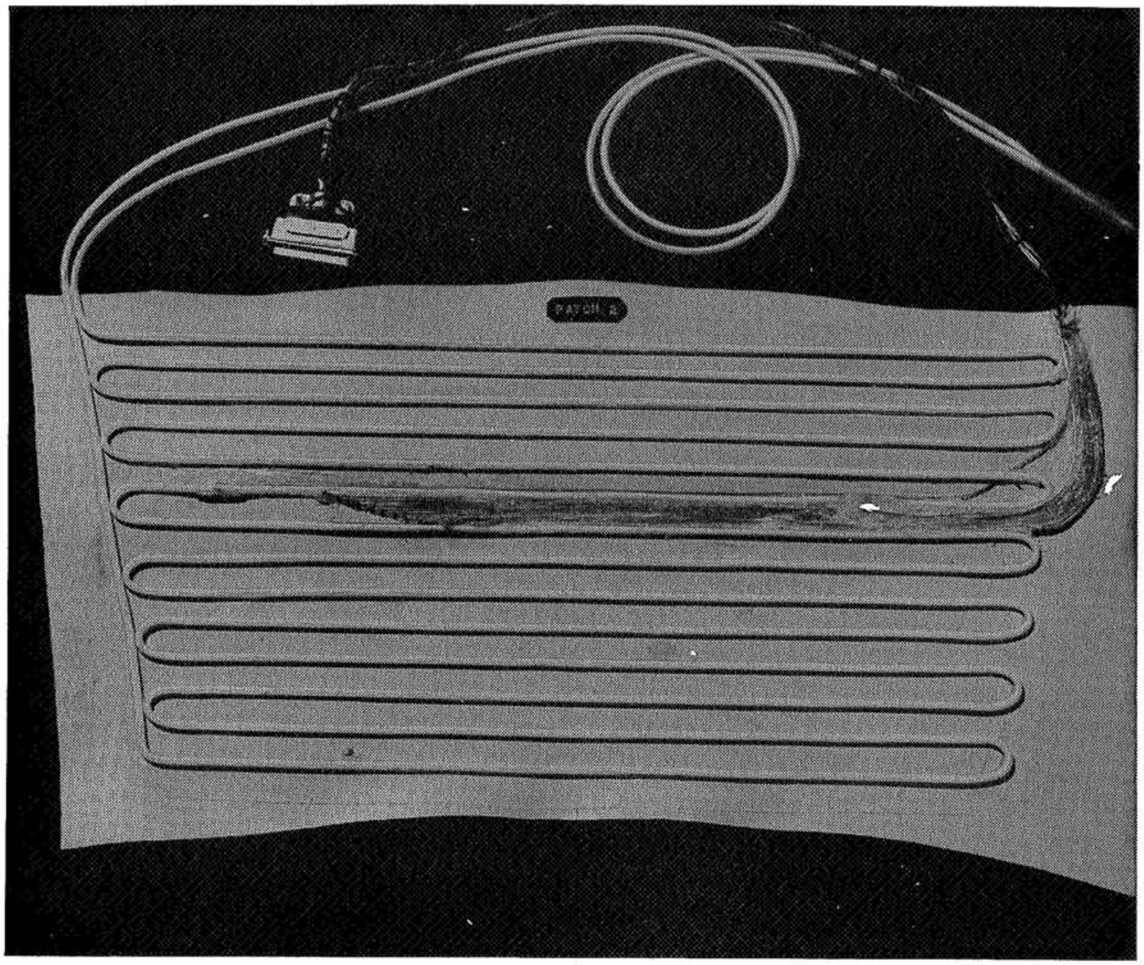

Figure 4.6 View of one of the individual pads.

continuously recorded by a Brush Mark 280 Recorder. Thermopiles consisting of five copper-constantan thermocouples connected in series and a Brush pre-amplifier were used to increase the sensitivity of the reading of the difference between outlet and inlet water temperatures.

For metabolic measurements, the same system as described in the preceding section was used. Ear canal temperatures were taken using the same technique as was used for the experiments with the cooling suit.

A Leeds and Northrup Speedomax W, 12-point potentiometer-recorder was used for continuously monitoring and recording the temperature of the cooling water and the skin temperatures between the adjacent tubes.

During the experiments the subject pedalled a Monark bicycle ergometer at a constant preset speed and load.

4.3 EXPERIMENTS WITH THE COOLING SUIT

4.3.1 Activity Schedules

Five different schedules of activity were used for all the test subjects. The schedules consisted of alternate periods of standing and level walking on the treadmill with or without the cooling suit. The various levels of activity were chosen to cover a variety of different activity loads. The steady state and, to some extent, transient state characteristics of the cooling suit were studied under those conditions. Each of the schedules started with the subject standing still for at least 45 minutes. During this period water inlet temperatures were adjusted to correspond to the subject's own sense of comfort. The duration of each of the standing and walking sessions (except the second part of Schedule V) was 45 minutes. It was assumed that after 45 minutes from the onset of a change in activity level the subjects reached a thermal quasi-steady state. Figure 4.7 illustrates schematically the details of the five activity schedules.

Schedule I, with the lowest activity levels, consisted of four step changes: standing; walking at 2 mph; standing; walking at 2.5 mph; and standing. Two mph was the slowest speed that could be obtained from the treadmill with the subject on it. Once the subject's comfort was achieved while standing, no deliberate changes in water inlet temperatures were made. The small changes in water inlet temperatures were due to the instability of the water supply system. The purpose for maintaining constant temperature was to test the cooling capacity of the suit at higher metabolic rates while operating at the same temperature levels which were considered comfortable at the lower metabolic rate.

Schedule II was designed to compare the effect of changing the water inlet temperature at the same activity level. It consisted of two identical, periodic step changes: standing; walking at 3 mph; standing; and again walking at 3 mph and standing. During the first walking session, no adjustments in water inlet temperatures were permitted. During the second cycle, however, the water temperatures were adjusted to correspond to the subject's comfort.

Schedule III consisted of four step changes: standing; walking at 2 mph; walking at 4 mph; walking at 2 mph; and standing. The purpose of this schedule of activities was to study the characteristics of the suit at a moderately high activity level. (Approximately 1650 Btu/hr, 482 w) The intermediate 2 mph walking sessions were used for two

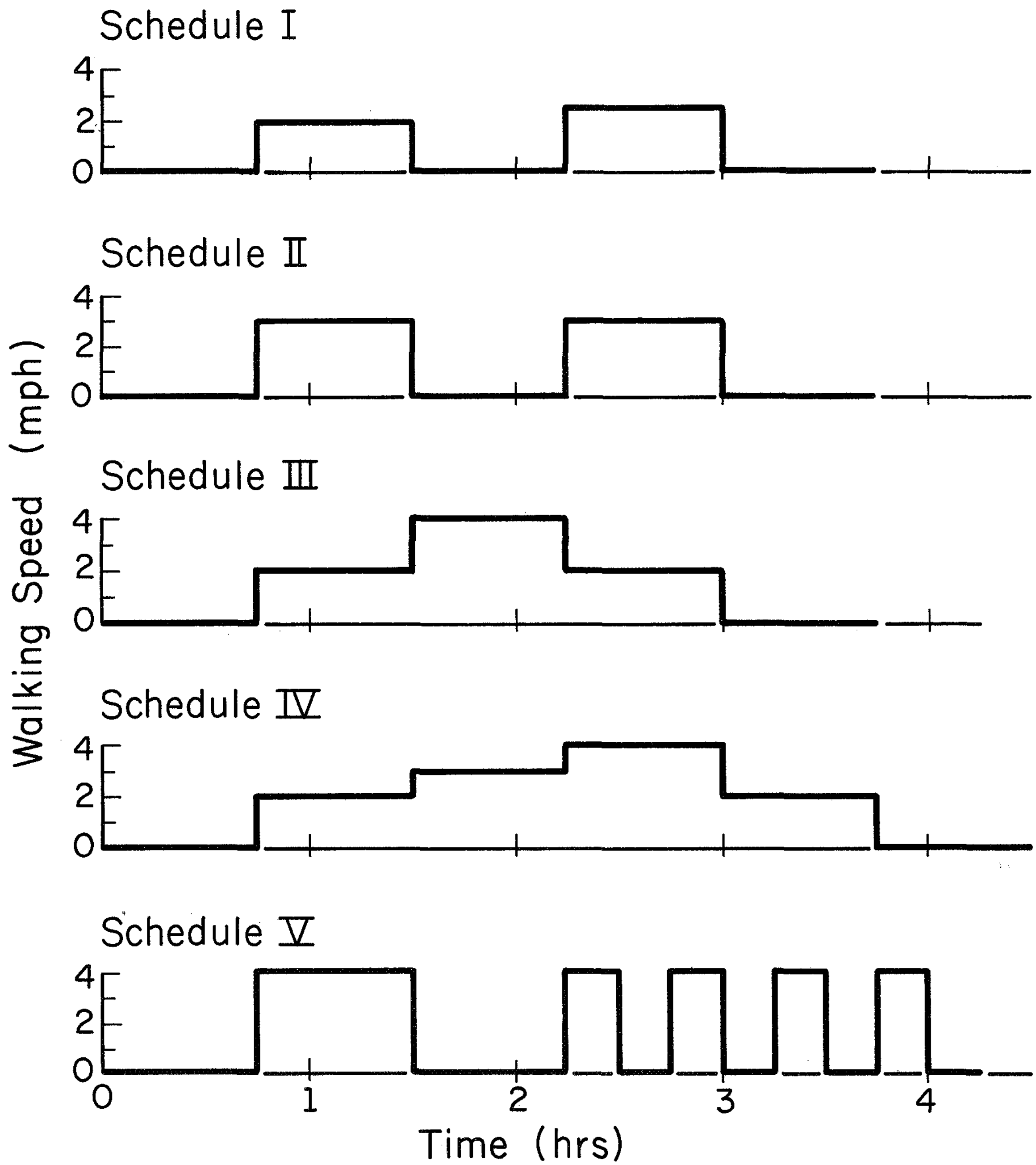

Figure 4.7 Activity schedules used for the experiments with the cooling suit.

reasons: first, to allow a gradual change to the high activity level and, second, to some extent, to acquaint the subjects with the relatively high speed that was also included in the last two schedules. Adjustments of water inlet temperatures were permitted throughout the entire duration of the experiment.

Schedule IV was almost identical to Schedule III, but it included an additional walking session at 3 mph immediately preceding the 4 mph walking period. This was done to study the effect of a more gradual change in activity level.

Schedule V was used to study two features: first, to examine the performance of the suit at a step from standing to the moderately high activity level without any intermediate changes and, second, to determine the characteristics of the suit with thermal transient changes at the same activity levels. This schedule consisted of the following step changes: standing; walking at 4 mph and standing followed by four short identical periodic sessions of walking at 4 mph and standing. The duration of each of the short walking and standing sessions was 15 minutes. Readjustments in water inlet temperatures were permitted throughout this entire schedule.

4.3.2 Test Subjects

Five male students, ranging in age from 18 to 29 years, volunteered to serve as test subjects. They were all required to pass a thorough physical examination. They represented a variety of physical fitnesses ranging from poor to athletic. There were limits on the height and weight of the subjects dictated by the size of the cooling suit. The physical characteristics of the test subjects are summarized in TABLE 4.3. Surface areas were determined from the Dubois height/weight formula [69]†. All but one subject completed all five experiments. Subject PF did not complete Schedule V due to a stiff thigh muscle.

4.3.3 Experimental Procedure

All the experiments were performed at the Laboratory for Ergonomics Research, University of Illinois at Urbana-Champaign. This laboratory is permanently air conditioned at about 23°C and 60 percent relative humidity. The experiments were all run during July and August 1970 and were scheduled at the subject's convenience. The subjects performed at least once a week and usually more often.

A total of 29 experiments were run. Of these, 24 were performed with the cooling suit. Five pilot runs were performed by subject SKB repeating the regular activity schedules without the suit. During the pilot runs subject SKB wore tennis shoes, shorts and a light T shirt. All subjects started with Schedule I and, in order, completed the other schedules sequentially. The subjects were permitted to listen to the radio, and read while standing, but no eating, drinking or smoking was allowed during the experiments.

At the beginning and end of each experiment the subjects were weighed, and their oral temperature and blood pressure were taken. The last two measurements were taken only as precautionary measures against any acute effects of the experiment on the subject. Also the barometric

†Surface area $[cm^2] = 71.84\ W[kg]^{0.425} \cdot h[cm]^{0.725}$.

TABLE 4.3

CHARACTERISTICS OF THE TEST SUBJECTS

Subject	Age	Height		Weight		Surface Area		Percent Area Covered by Cooling Pads
		cm	in.	kg	lb	m^2	ft^2	
A. SGP	20	173	68	65.7	144.8	1.78	19.2	48.8
B. SKB	22	170	67	61.1	134.7	1.71	18.4	50.8
C. HNT	27	170	67	64.2	141.5	1.74	18.7	50.0
D. RET	18	169	66.5	64.2	141.5	1.74	18.7	50.0
E. PF	29	161	63.5	55.8	123.0	1.58	17.0	55.0
Means	23.2	169	66.4	62.2	137.1	1.71	18.4	50.9

pressure was measured. During the experiments the following data were collected: ear canal temperatures, water inlet temperatures, differences between water inlet and outlet temperatures at each of the six regions of the body, water flow rates, respiratory volumetric rates and temperatures of expired air. During the runs of Schedule V and during the pilot runs without the suit, pulse rates were also taken. All measurements were taken at the end of each activity in the schedule and were assumed to represent the quasi-steady state values.

After the preliminary measurements, the subjects donned the cooling garment. Each of the cooling pads was fastened in place to insure good thermal contact. The thermally insulated suit was then put over the cooling garment. Next, the ear thermistor was inserted into the ear and the ear was covered to exclude possible thermal effects of the cooling hood. Finally, the water inlet and outlet tubes were connected, flow was started and the leads of the thermopiles were connected to the potentiometer recorder. Figures 4.8 through 4.11 show one of the subjects at various stages of dressing.

The subjects stood on a bench and water inlet temperatures were adjusted to conform to their sense of comfort. When a thermal quasi-steady state† was reached, as indicated by the potentiometer recorder, the treadmill was started. With the support of the supervisor of the experiment, the subjects stepped on the moving belt and started to walk. The speed of the treadmill was then quickly adjusted to the desired level. Step changes from walking to standing were done in the same manner. Figure 4.12 shows one of the subjects while walking and breathing through the system

†Quasi-steady state was defined as that state wherein no significant changes in the difference in outlet and inlet water temperatures was noticeable.

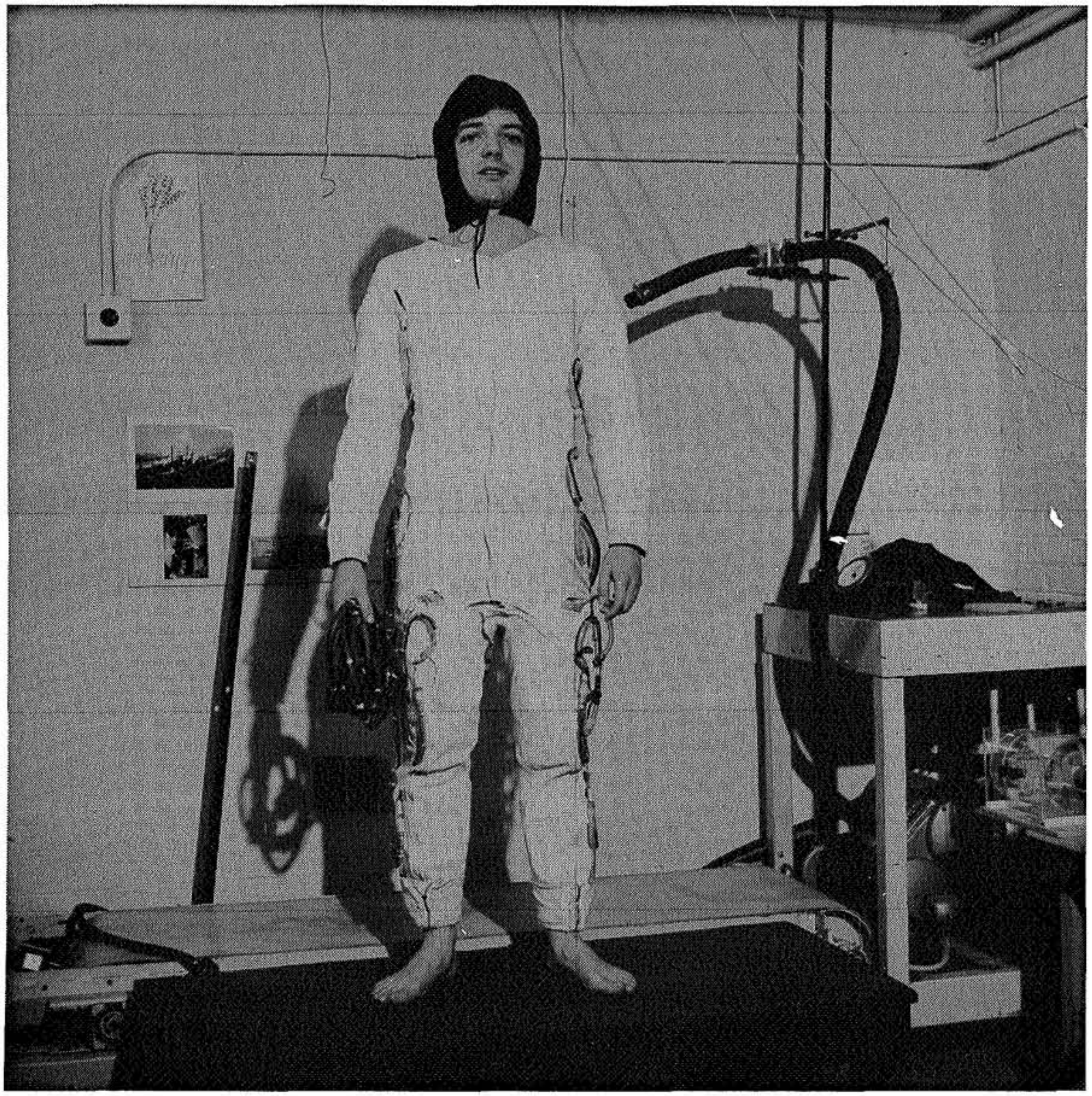

Figure 4.8 Front view of the cooling garment.

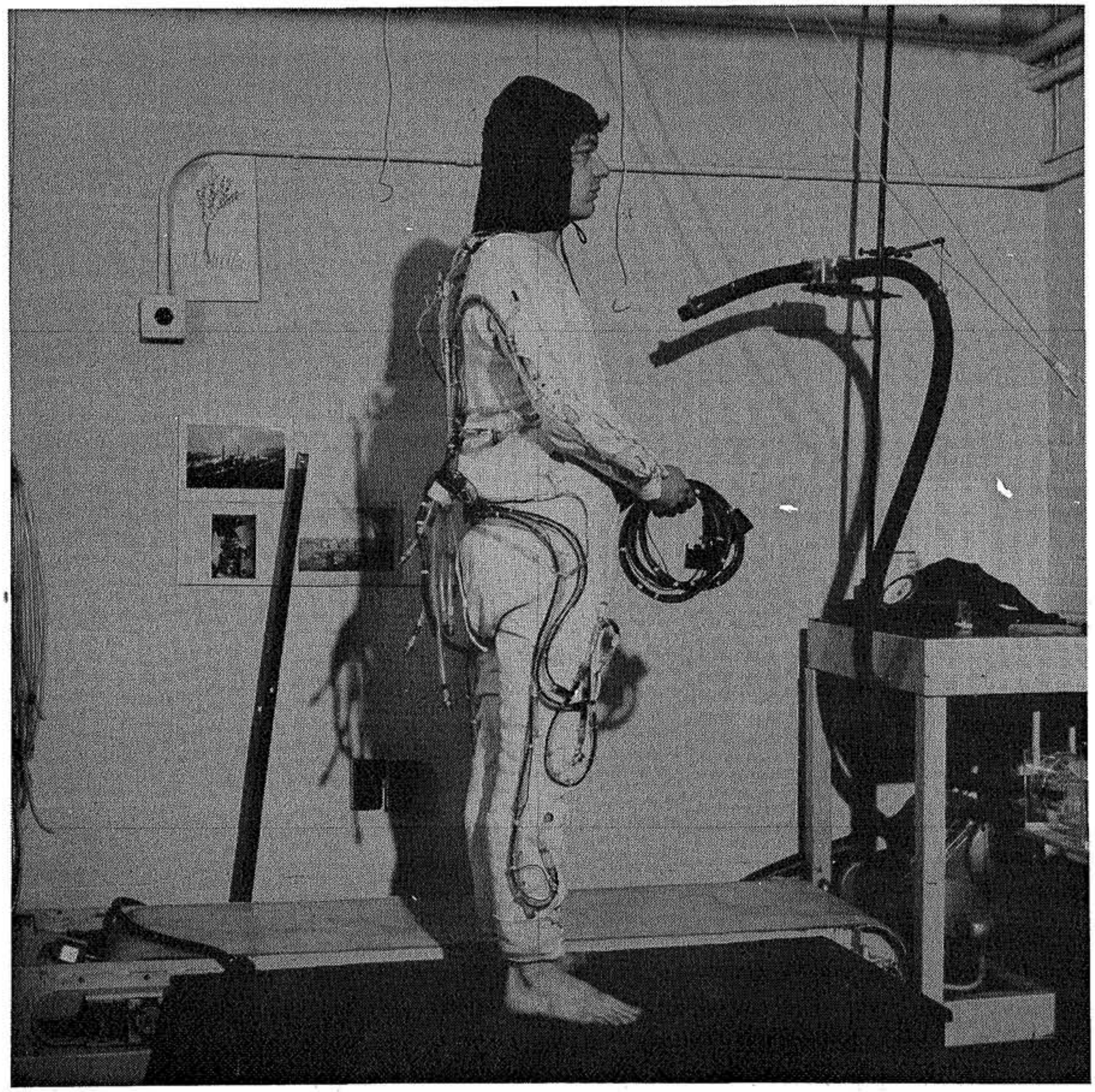

Figure 4.9 Side view of the cooling garment.

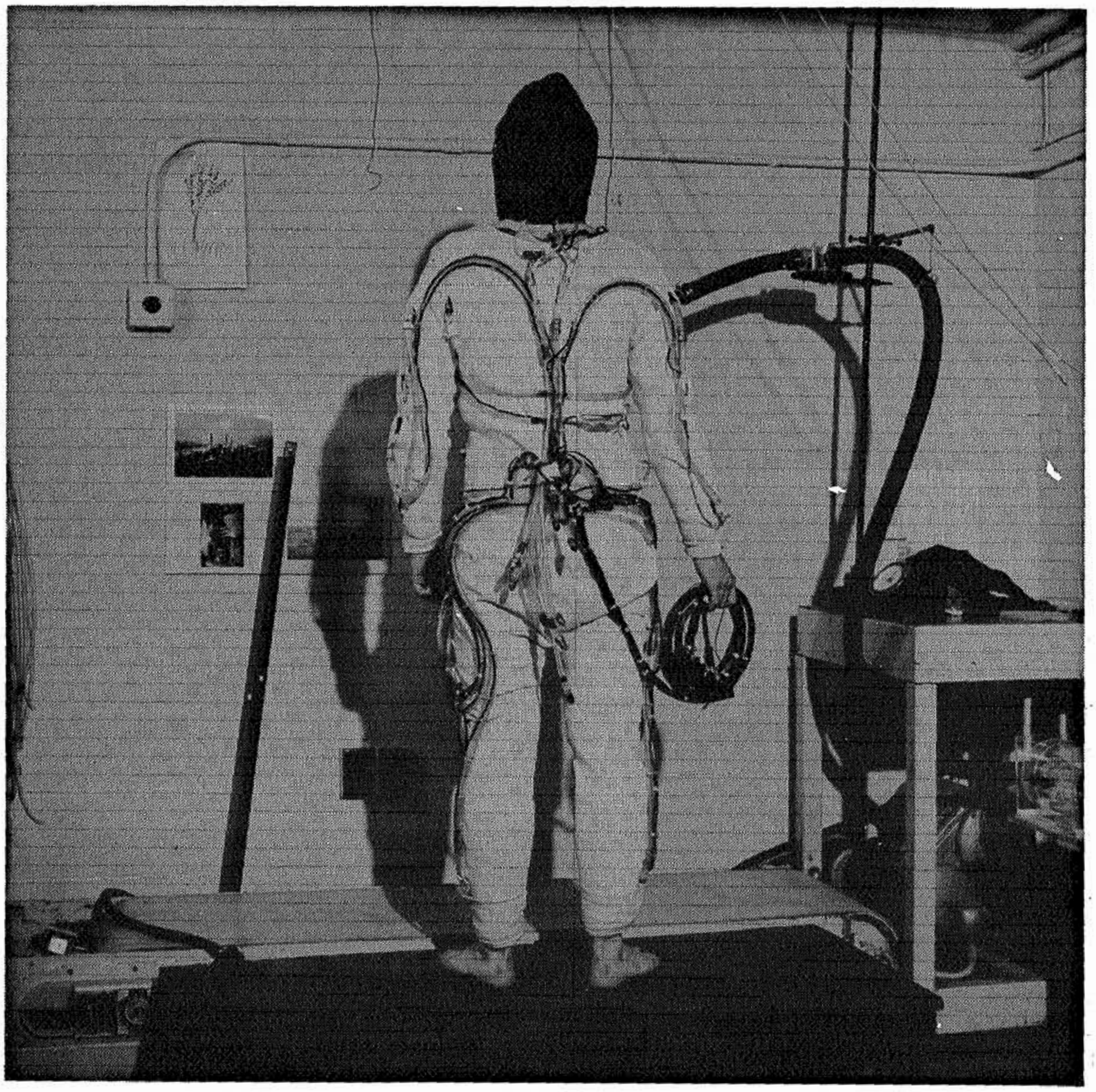

Figure 4.10 Back view of the cooling garment.

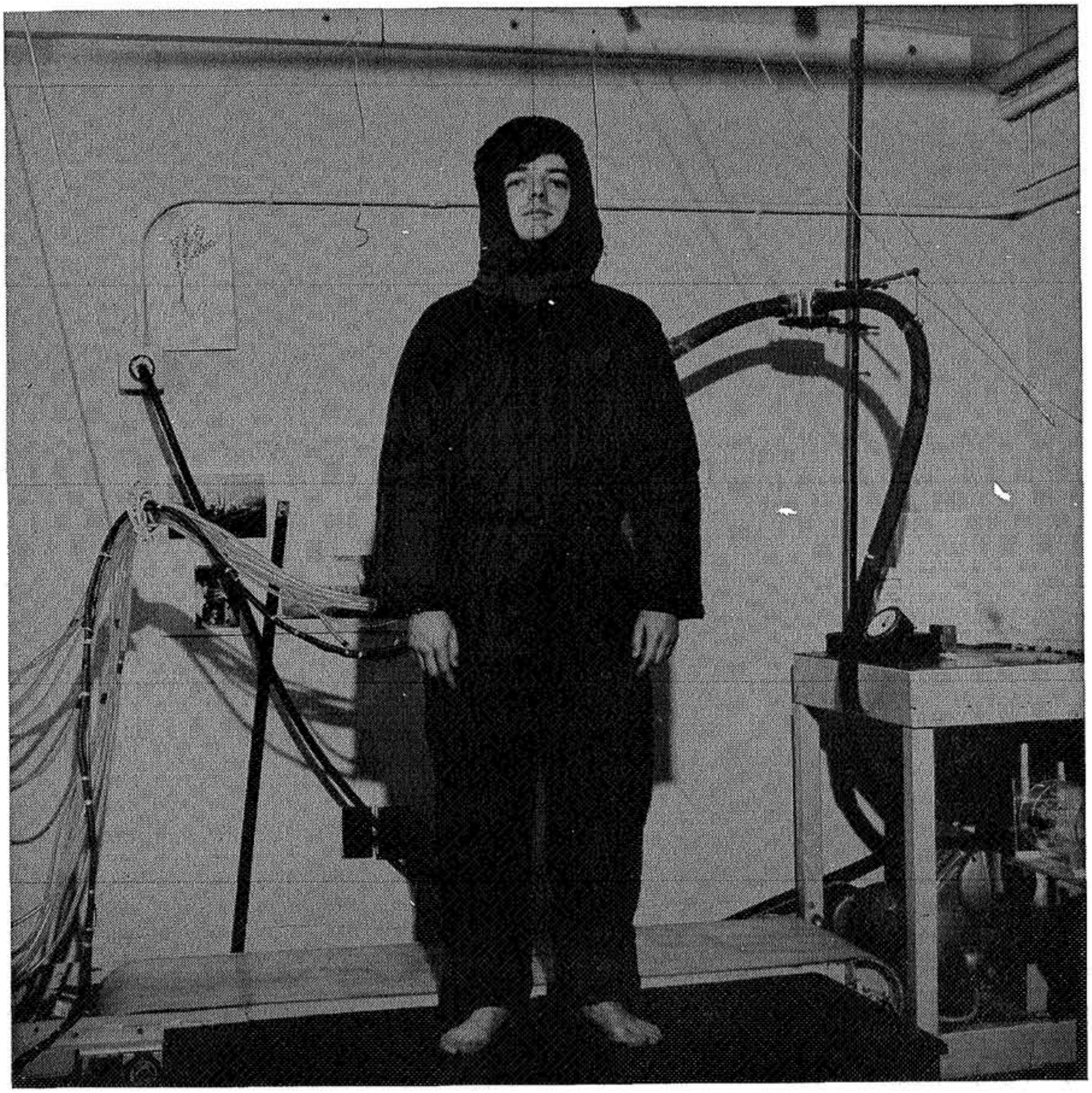

Figure 4.11 Front view of a test subject dressed up in the cooling and insulating garments.

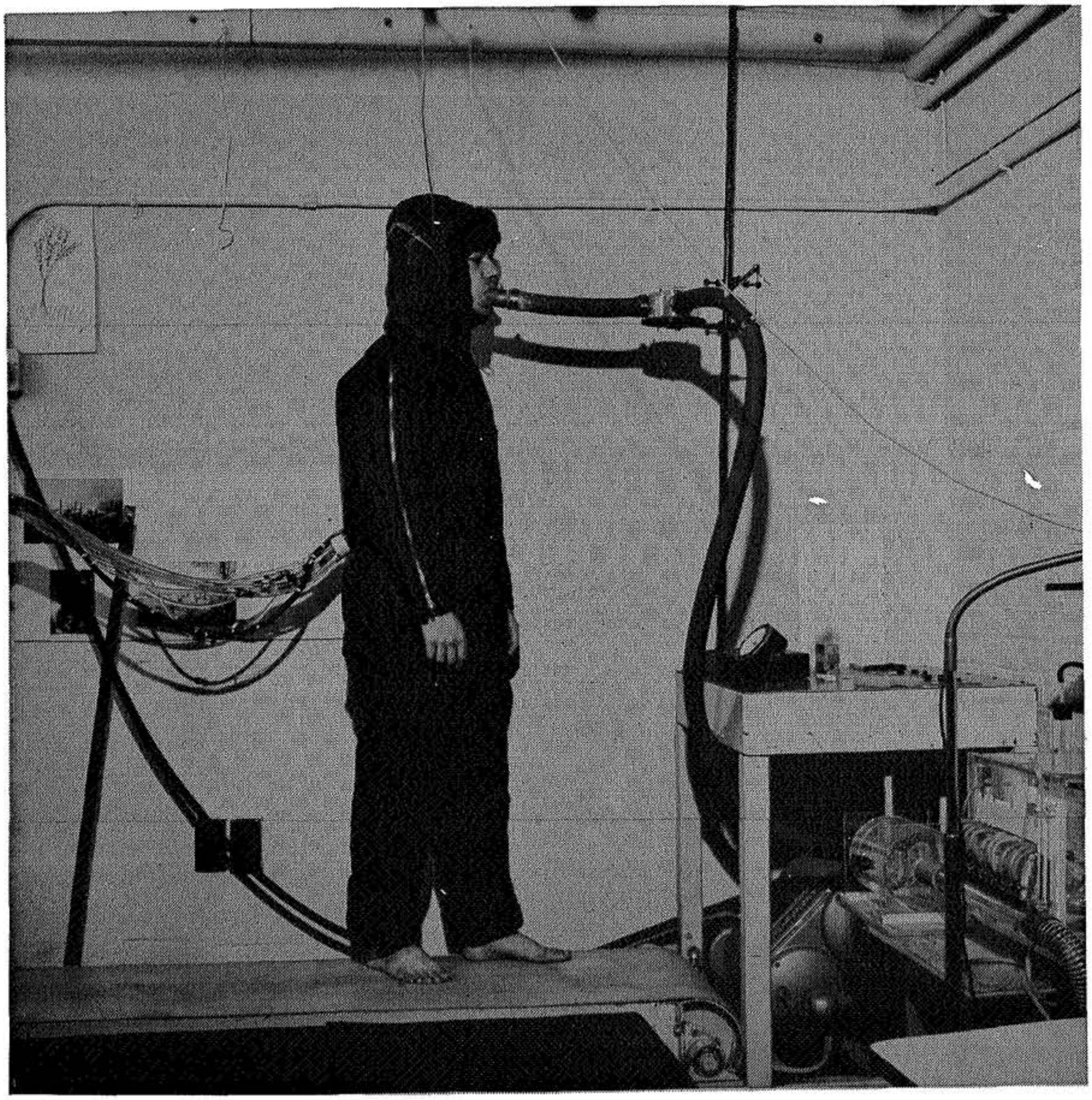

Figure 4.12 A test subject shown walking on the treadmill and breathing through the system for measuring metabolic rates. No tennis shoes are shown in the picture.

for measuring the metabolic rate.

4.3.4 Measured, Recorded and Calculated Quantities

The following quantities were measured, recorded, or calculated from other measured data:

(1) Total metabolic rate. This was calculated from volumetric flow rate of the expired air and the oxygen content obtained from the gas analysis. The caloric value of oxygen was assumed at 5.0 kcal/lit [70]. This value, although slightly high, conformed well with the respiratory quotients found in most of the runs. Maximum deviation from the actual caloric value was assumed to be about 4 percent.

(2) Rate of heat removed by the suit at each region. This was taken as the product of the difference between water inlet and outlet temperatures and water flow rate. Specific heat of water was assumed to be unity.

(3) Rate of heat lost by respiration. Flow rate, temperature and enthalpy of the expired air, assuming it to be saturated, were used for calculating this quantity.

(4) Weight loss during the experiment. Taken as the difference between the initial and final weights of the subject.

(5) Ear canal temperature. Measured by an ear thermistor and was assumed to simulate closely the temperature of the body that is regulated by the central temperature control mechanism.

(6) Water inlet temperatures to each of the regions at the various activity levels. These were measured by thermistors that were

inserted into the water streams.

(7) Order of preferred changes in water inlet temperatures to the different regions. This was recorded for the purpose of identifying those regions of the body that require changes in water temperature and the preferred order of the changes as a function of activity level.

(8) Comfort vote. Based on the subject's own evaluation of his state of comfort. Only three choices were suggested: slightly cold, thermally comfortable, too warm.

(9) Pulse rate. This was measured only during the experiments of Schedule V and the pilot runs without the suit. The pulse rate was assumed to be an index of the metabolic and cardiac costs of the physical work. Pulse rate was not taken during the experiments of the other schedules because these schedules were considered to represent quasi-steady states.

4.4 EXPERIMENTS WITH THE INDIVIDUAL PADS

Three identical tests were conducted with the individual cooling pads. These tests were designed to compare the steady state temperature distribution on the skin for different cooling pads at the same level of activity. All experiments consisted of riding the bicycle ergometer at a constant speed and load for about two hours, corresponding to a total metabolic rate of about 1200 Btu/hr (352 w).

One male student volunteered to serve as a test subject for the experiments with the individual cooling pads. The physical characteristics of this subject are summarized in TABLE 4.4. At the beginning and end of

TABLE 4.4 CHARACTERISTICS OF SUBJECT TEK

Subject	Age	Height		Weight		Surface Area	
		cm	in.	kg.	lb.	m^2	ft^2
TEK	19	189	74.5	79.7	175.5	2.02	21.7

each of the experiments, the same procedure as was used for the experiments with the cooling suit was repeated (weighing, measuring blood pressure, etc.). Then the cooling pad was put in place on the thigh of the right leg. The water supply tubes were then connected, flow was started and the leads of the various measuring devices were connected to the appropriate recording instruments.

The subject started to bicycle at the preset speed and load and continued to do so until a steady state was reached. The steady state was obtained when no changes could be noticed in any of the measured parameters.

Figure 4.13 gives a general view of the set-up used for the experiments with the individual cooling pads with a test subject shown pedalling the bicycle ergometer.

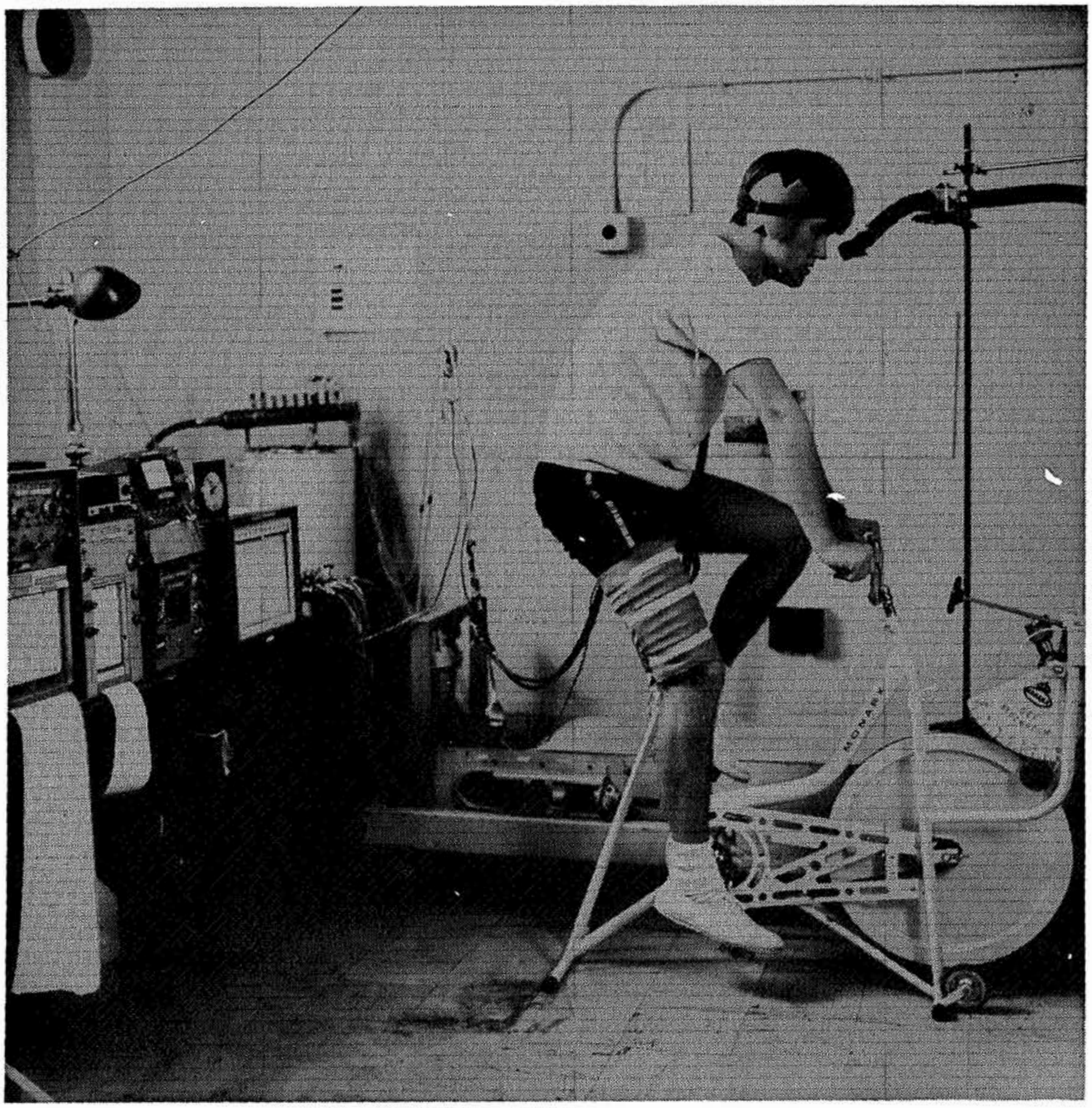

Figure 4.13 General view of the set-up used for the experiments with the individual cooling pads. A test subject is shown pedalling the bicycle ergometer.

5. DISCUSSION

5.1 EXPERIMENTS WITH THE COOLING SUIT

In order to present the large amount of data that was gathered during the experiments, most of the results of each schedule were averaged and are presented in this form. Wherever it was feasible, entire ranges of individual variations were also shown. All the data, excluding the weight losses, were measured or calculated at the end of each of the step changes in activity level.

Figures 5.1 through 5.5 show mean values of metabolic rates and of heat removed by the suit and by respiration during the various schedules of activity. Also shown are the ranges of metabolic rates included in the mean values. It is seen that during the standing sessions of Schedules I through IV and the first part of Schedule V, most of the heat produced in the body was removed by the cooling suit. In many cases the amount of heat removed by the suit even exceeded slightly the total metabolic rate. This phenomenon is believed to be due to possible thermal transients indicated by a decrease in "deep body" temperature following a change in activity from walking to standing (Fig. 5.6) and cumulative measurement errors.

During all of the walking sessions the relative amount of heat removed by the suit dropped significantly. At best, only about 70 percent of the total metabolic rate was removed by the suit during the walking sessions; this value was usually closer to 50 percent. Possible explanations to account for the portion of the total metabolic rate that was not removed by the cooling suit are the following:

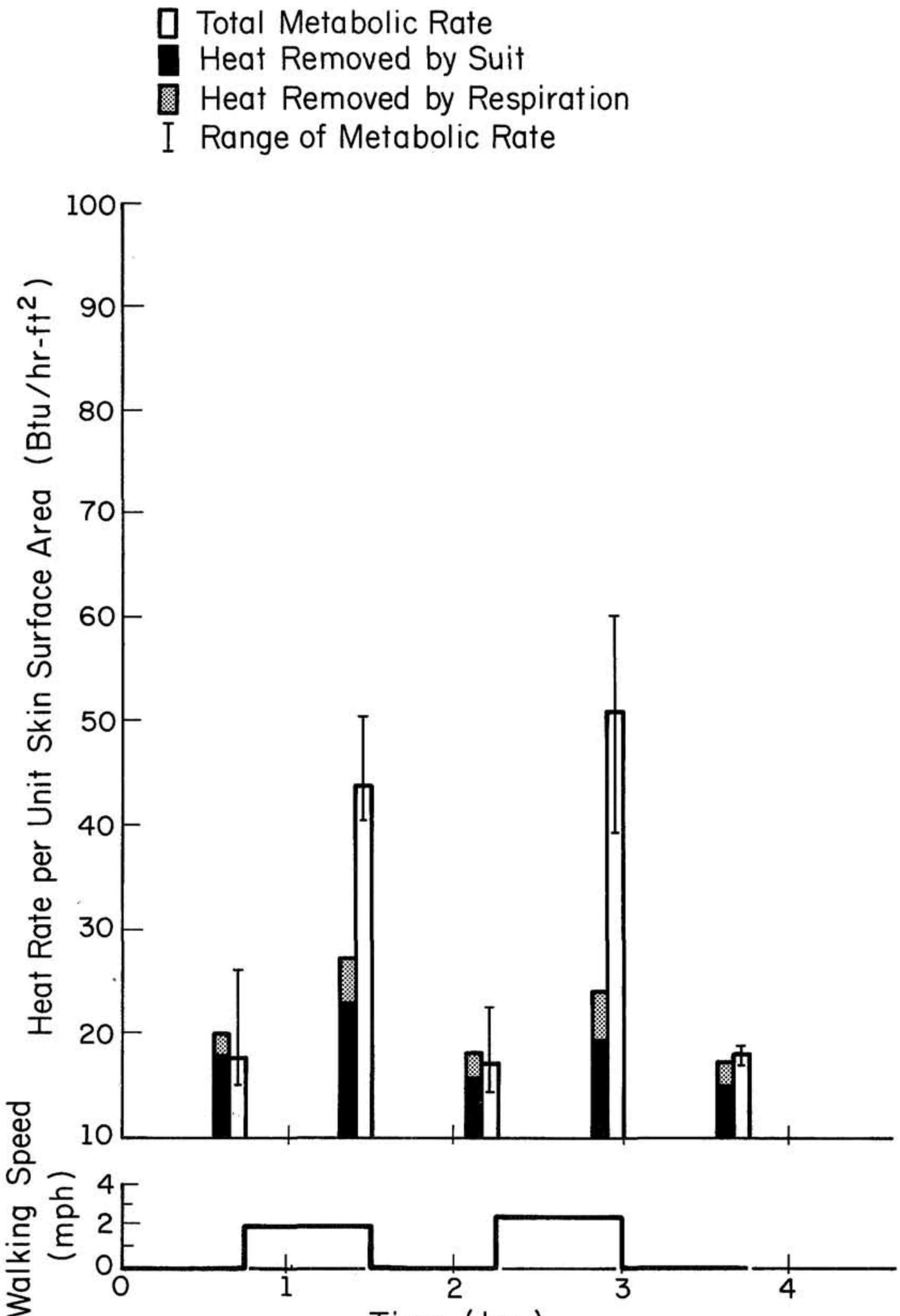

Figure 5.1 Mean values of metabolic rates and of the amounts of heat removed by the cooling suit and by respiration for Schedule I.

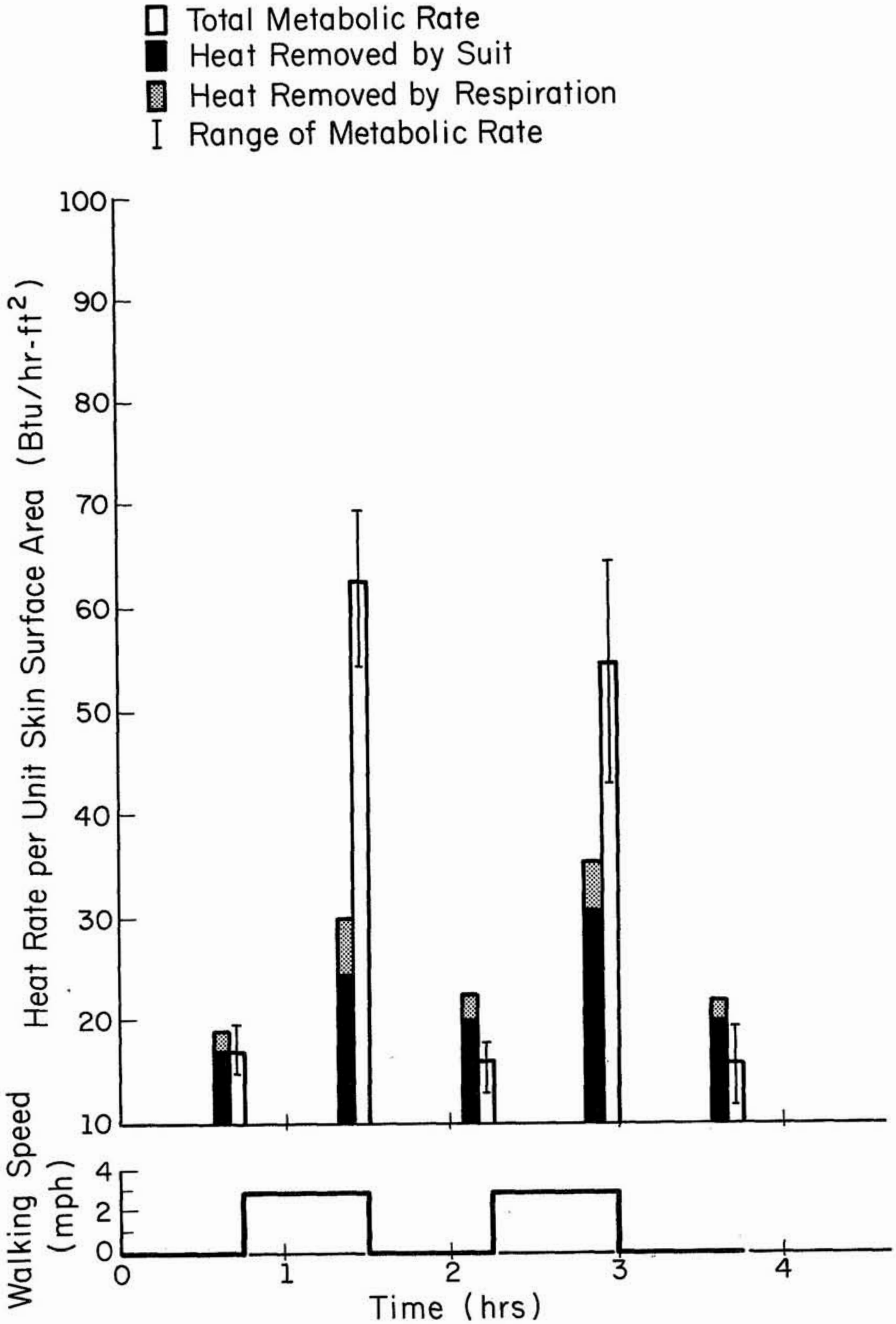

Figure 5.2 Mean values of metabolic rates and of the amounts of heat removed by the cooling suit and by respiration for Schedule II.

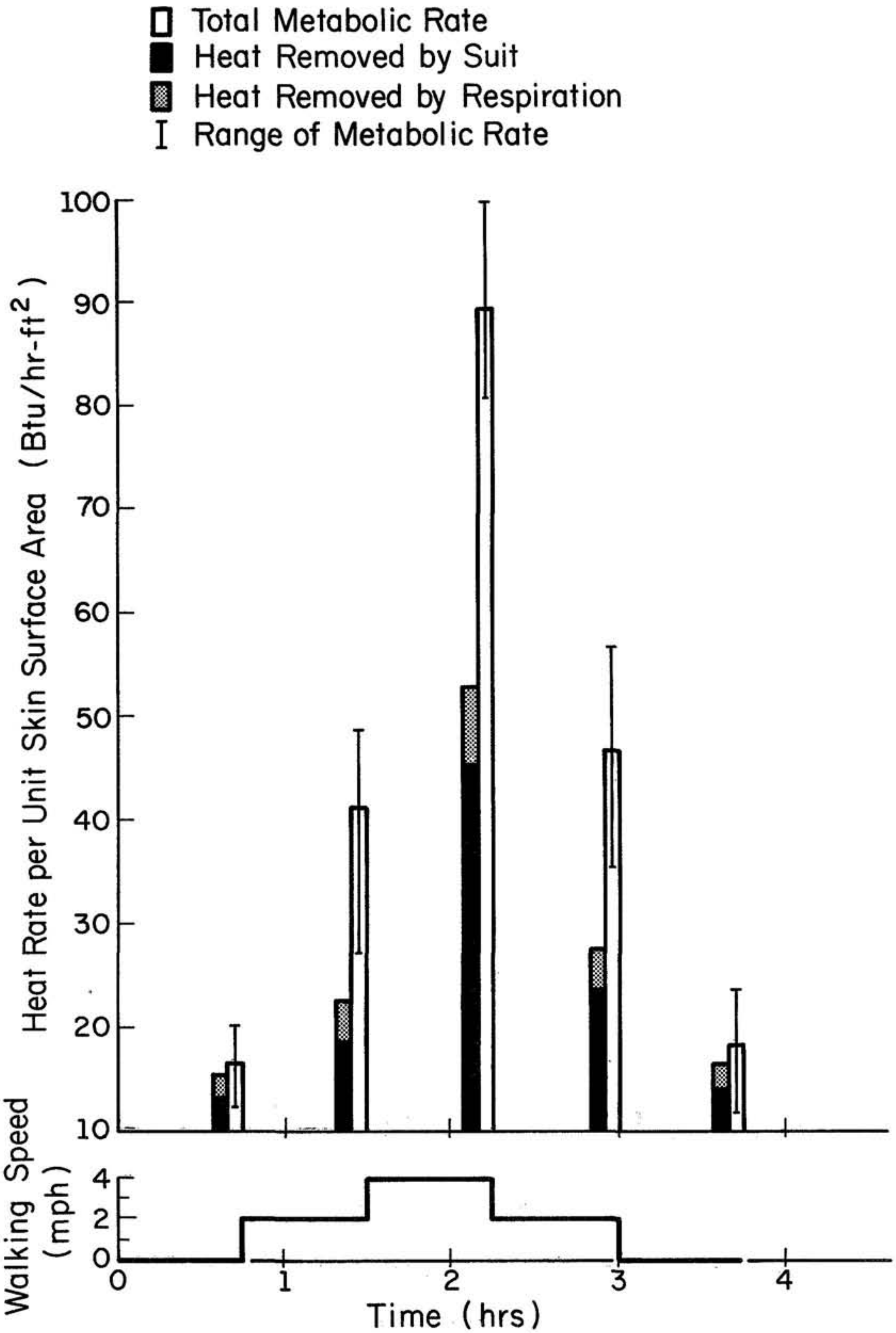

Figure 5.3 Mean values of metabolic rates and of the amounts of heat removed by the cooling suit and by respiration for Schedule III.

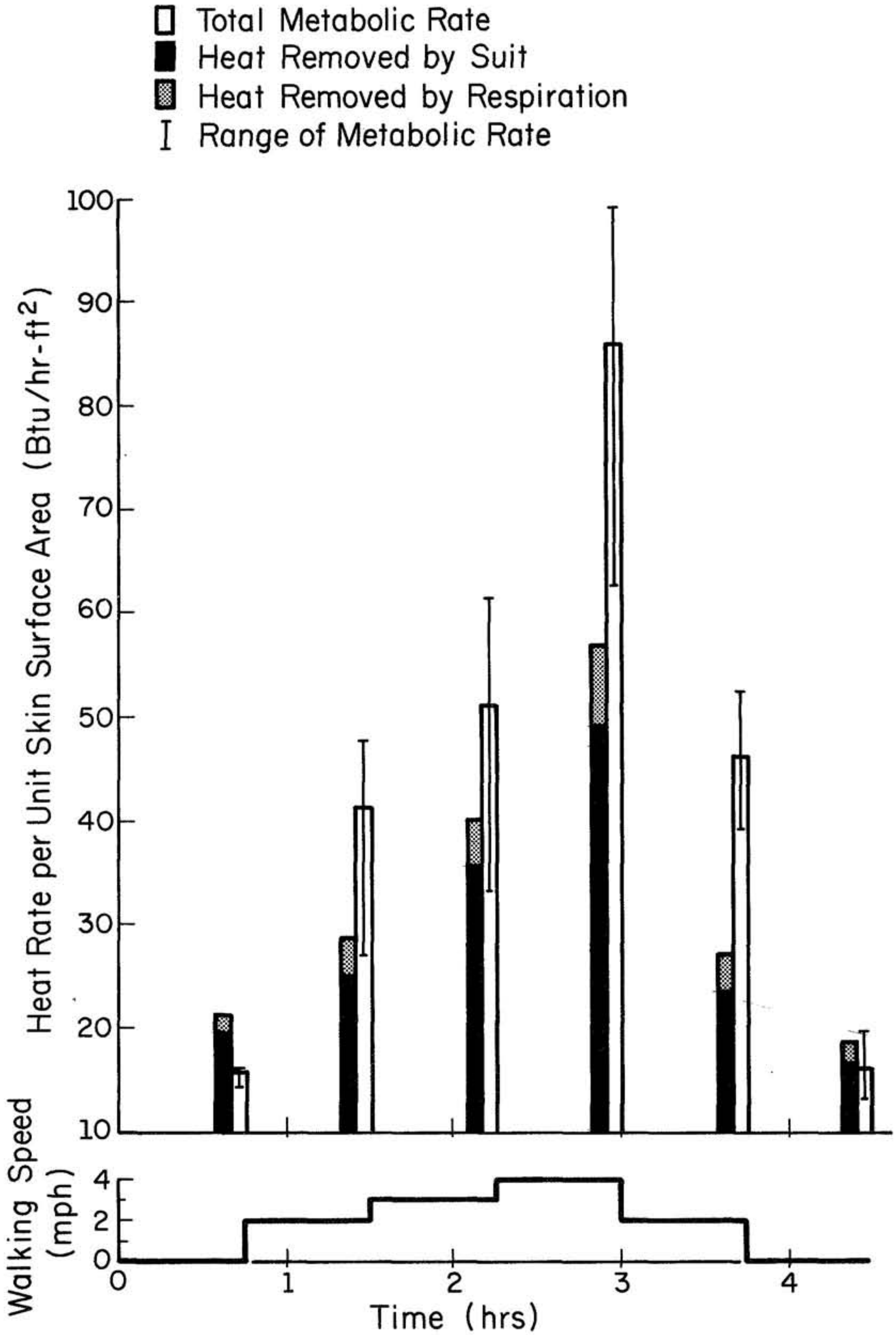

Figure 5.4 Mean values of metabolic rates and of the amounts of heat removed by the cooling suit and by respiration for Schedule IV.

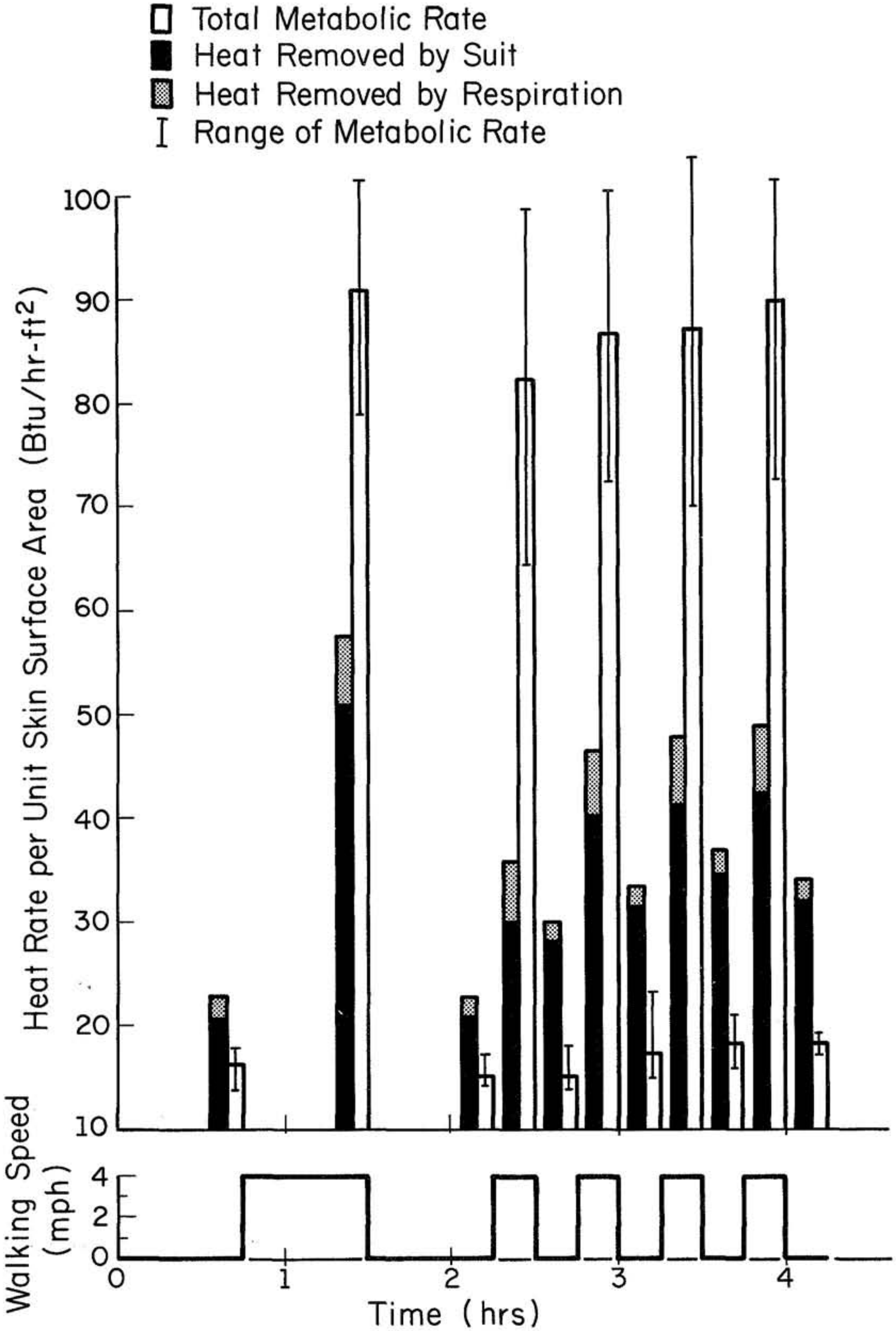

Figure 5.5 Mean values of metabolic rates and of the amounts of heat removed by the cooling suit and by respiration for Schedule V.

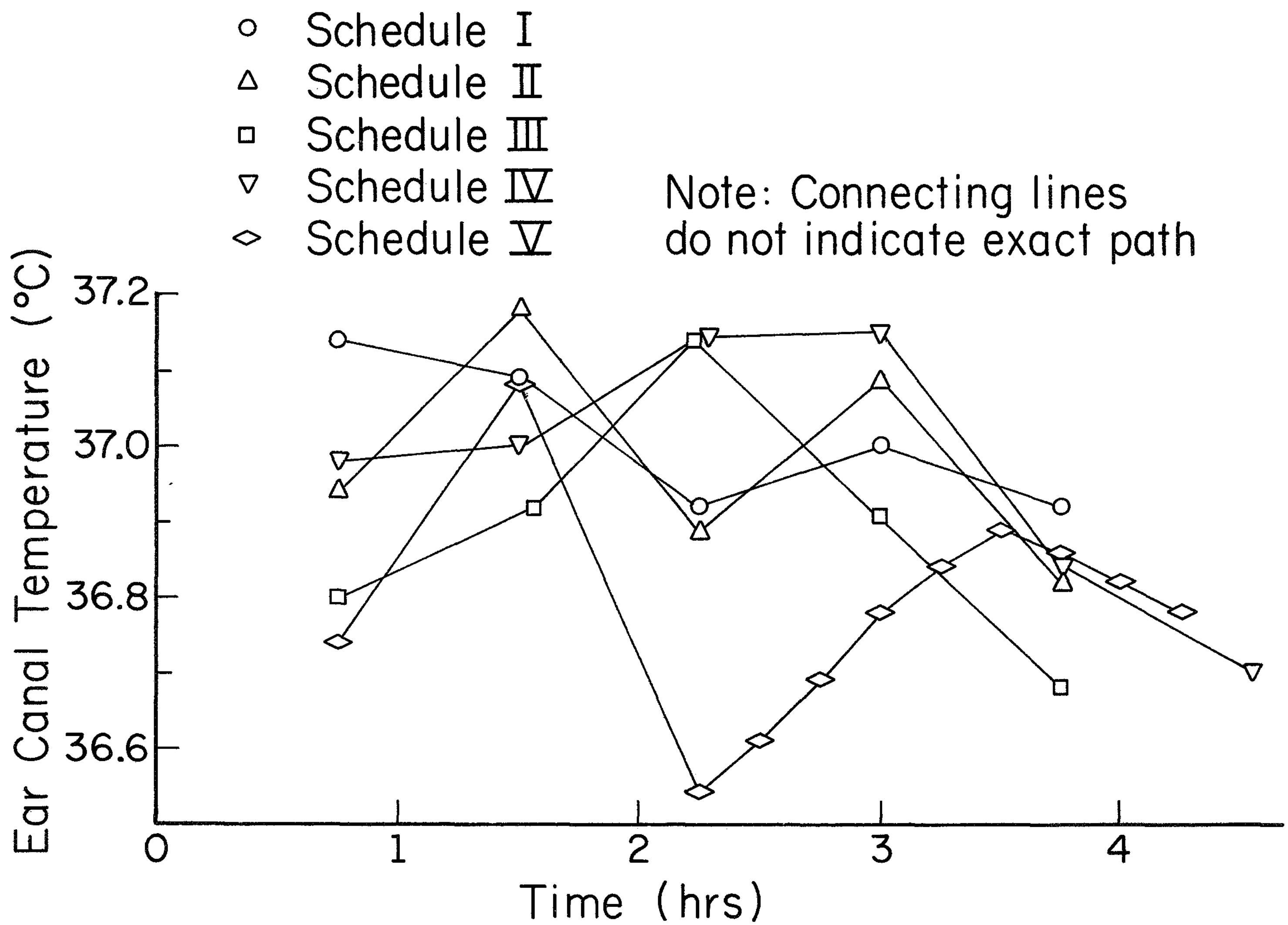

Figure 5.6 Average ear canal temperatures for the various schedules.

(1) Thermal transient states with heat still being stored inside the body. (Increase in "deep body" temperatures, Fig. 5.6.)

(2) Heat dissipated to the environment from the uncovered surfaces, e.g., face, forehead and hands.

(3) Heat removed by the respiratory system.

(4) Heat removed by perspiration aided by air that was pumped under the somewhat loose thermal insulating suit.

(5) Work done by the muscles.

(6) Measurement errors and inaccuracies.

(7) Heat lost to the environment through the clothing assembly.

From these, only the contribution of item 3, i.e., respiration, was estimated. It was calculated that the amount of heat dissipated by the respiratory system ranged from 7.3 percent to 14.8 percent of the total metabolic rate. These values are consistent with values reported by Bazett [55]. With the increase in metabolic rate the amount of heat carried away by respiration also increased. However, the relative amount of heat removed by the exhaled air decreased. The remaining unaccounted-for portion of the metabolic rate is assumed to have been removed by the other channels that were mentioned above.

It was found that, from the comfort standpoint, the present cooling system was not sufficient to accommodate for metabolic rates in excess of about 1200 Btu/hr (352 w). This finding was manifested by the consistent comfort votes of "too warm" at the moderately high activity levels (TABLE 5.1). It is assumed that the insufficieny of the cooling system was due to two reasons: too small a contact area

TABLE 5.1

ORDER OF PREFERRED CHANGES IN WATER INLET
TEMPERATURES AND THE COMFORT VOTE FOR THE VARIOUS ACTIVITIES

	Change in Water Inlet Temperature	Subjects				
		SGP	SKB	HNT	RET	PF
SCHEDULE II						
Standing to 3 mph	Decrease	All over the body	Not Recorded	Not Recorded	1. Upper Torso 2. Lower Legs 3. Thighs 4. Lower Torso	All over the body
Comfort Vote		Comfortable	Comfortable	Comfortable	Comfortable	Comfortable
3 mph to Standing	Increase	No Changes	Not Recorded	Not Recorded	All over the body <u>but</u> the lower legs	No Changes
Comfort Vote		Comfortable	Comfortable	Comfortable	Comfortable	Comfortable

(continued)

TABLE 5.1 continued

	Change in Water Inlet Temperature	Subjects				
		SGP	SKB	HNT	RET	PF
SCHEDULE III						
Standing to 2 mph	Decrease	Not Recorded	No Changes	1. Legs 2. Arms	All over the body	1. Head 2. Upper Torso
Comfort Vote		Comfortable	Comfortable	Comfortable	Comfortable	Comfortable
2 mph to 4 mph	Decrease	Not Recorded	1. Legs 2. Lower Torso 3. Head 4. Arms 5. Upper Torso	All over the body	1. Lower Torso 2. Lower Legs 3. Upper Torso	1. Head 2. Upper Torso
Comfort Vote		Too Warm	Too Warm	Too Warm	Too Warm	Too Warm
4 mph to 2 mph	Increase	Not Recorded	1. Upper Torso 2. Arms	No Changes	1. Head 2. Arms 3. Upper Torso	No Changes
Comfort Vote		Comfortable	Comfortable	Comfortable	Comfortable	Comfortable
2 mph to Standing	Increase	Not Recorded	No Changes	1. All over the body 2. Lower Torso	1. Arms 2. Upper Torso 3. Thighs	No Changes
Comfort Vote		Comfortable	Comfortable	Comfortable	Comfortable	Comfortable

(continued)

TABLE 5.1 continued

	Change in Water Inlet Temperature	Subjects				
		SGP	SKB	HNT	RET	PF
SCHEDULE IV						
Standing to 2 mph	Decrease	1. Thighs 2. Arms 3. Upper Torso	No Changes	1. Lower Torso 2. Lower Legs 3. Upper Torso 4. Arms	No Changes	No Changes
Comfort Vote		Comfortable	Comfortable	Comfortable	Comfortable	Comfortable
2 mph to 3 mph	Decrease	1. Thighs 2. Upper Torso 3. Arms 4. Lower Torso	1. Lower Legs 2. Upper Torso	1. Lower Torso 2. Lower Legs 3. Head	1. Lower Legs 2. Lower Torso 3. Thighs 4. Upper Thighs	No Changes
Comfort Vote		Comfortable	Comfortable	Comfortable	Comfortable	Comfortable
3 mph to 4 mph	Decrease	All over the body	All over the body	1. Lower Torso 2. Lower Legs 3. Head 4. All over the body	1. Lower Torso 2. Thighs 3. Lower Legs 4. Head 5. Lower Legs	Head
Comfort Vote		Too Warm	Too Warm	Too Warm	Too Warm	Too Warm

(continued)

TABLE 5.1 continued

	Change in Water Inlet Temperature	Subjects				
		SGP	SKB	HNT	RET	PF
SCHEDULE IV cont.						
4 mph to 2 mph	Increase	All over the body	1. Upper Torso 2. Lower Torso 3. Arms	No Changes	All over the body	No Changes
Comfort Vote		Comfortable	Comfortable	Comfortable	Comfortable	Comfortable
2 mph to Standing	Increase	No Changes	1. Upper Torso 2. Lower Torso 3. Arms 4. Head 5. Lower Legs	1. All over the body 2. Lower Torso 3. Lower Legs	All over the body	No Changes
Comfort Vote		Slightly Cool	Comfortable	Comfortable	Comfortable	Comfortable

(continued)

TABLE 5.1 continued

	Change in Water Inlet Temperature	Subjects			
		SGP	SKB	HNT	RET
SCHEDULE V					
Standing to 4 mph (45 min run)	Decrease	1. Upper Torso 2. Lower Torso 3. Thighs 4. Upper Torso 5. Head	1. Lower Legs 2. All over the body 3. Head	All over the body	All over the body
Comfort Vote		Too Warm	Too Warm	Too Warm	Too Warm
4 mph to Standing (45 min run)	Increase	1. Upper Torso 2. Arms 3. Thighs	1. Thighs 2. Upper Torso 3. Arms 4. Upper Torso	1. Lower Torso 2. Lower Legs	All over the body
Comfort Vote		Comfortable	Comfortable	Comfortable	Comfortable
Standing to 4 mph (15 min run)	Decrease	No Changes	No Changes	All over the body	No Changes
Comfort Vote		Comfortable	Comfortable	Comfortable	Comfortable
Rest of Experiment (4 mph and standing alternately)		No Changes	No Changes	No Changes	Alternate Changes All over the Body
Comfort Vote		Comfortable	Comfortable	Comfortable	Comfortable

between the skin and the cooling tubes and too high water inlet temperatures. The actual contact area between the skin and the cooling tubes was estimated to be about 10 percent of the total skin surface area. The lowest water inlet temperature that was obtained in most of the experiments was about 16°C. Increasing the contact area between the skin and the cooling tubes and/or lowering water inlet temperatures should improve the cooling capacity of the suit. This conclusion was suggested by the results obtained by Webb and Annis [71], who also reported experiments with a cooling suit. They estimated that 22 percent of the total skin surface area was in contact with the cooling tubes in their experiments. All of their subjects were reported to have been comfortable with the lowest water inlet temperature of 16°C and high metabolic rates of 2400 Btu/hr (700 w) for two hours.

It is evident that during the second part of the experiments of Schedule V, a quasi-steady state was never reached. This finding was true for the metabolic rates and amounts of heat removed by the cooling suit (Fig. 5.5) and also for the heart rates and ear canal temperatures (Fig. 5.7). These quantities show a clear trend of increase with time at least during the two hours of the short (15 minutes each) alternate changes in levels of activity. The amount of heat removed by respiration, however, seems to have reached a quasi-steady state after 15 minutes or less from the onset of a change in the exercise level (Fig. 5.5 and TABLE F.1). This result indicates that the transient time of the respiratory system is much shorter than that of the thermal system of the human body within the investigated range.

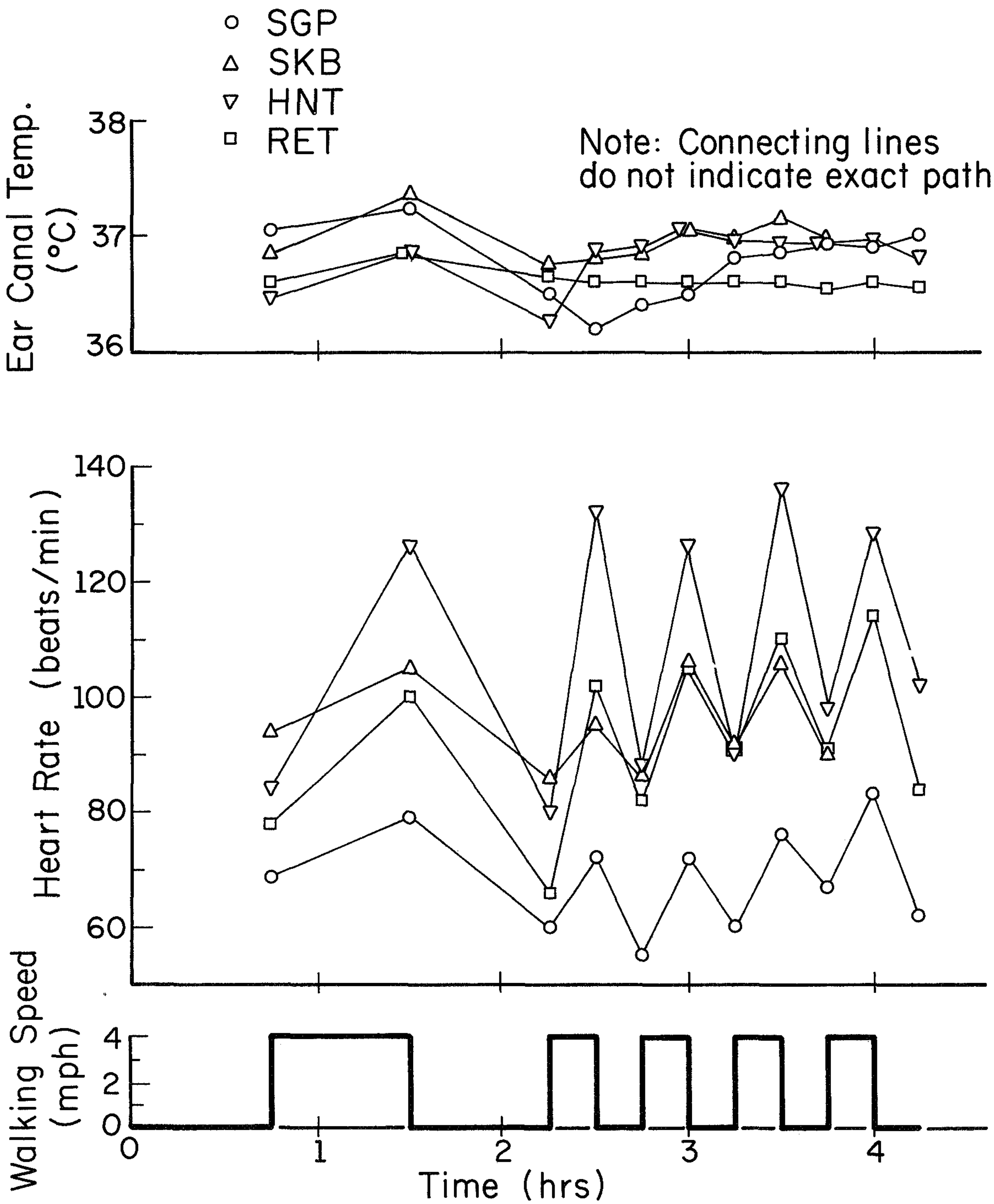

Figure 5.7 Individual variations in the ear canal temperatures and heart rates for Schedule V.

During the second part of the experiments of Schedule V, heart rates not only showed a trend to increase with time but also exceeded the values found in the first part. This observation is a possible indication of a fatigue effect that was supported by the feeling of all the subjects. It is also indicative of a lack of steady state.

During the experiments of Schedules III, IV, and V, the effects of gradual and abrupt step changes from standing to walking at 4 mph, were considered. No significant differences were found in total metabolic rates and amounts of heat removed by the cooling suit (Figs. 5.3, 5.4, and 5.5). Of those two quantities, only the cooling effectiveness† of the cooling suit seemed to have changed during the experiments of that schedule which included two intermediate steps (Schedule IV). This result may mean that during the experiments of Schedule IV the thermal steady state of the moderately high activity level was more nearly attained because of the two intermediate step changes preceding it. However, there were differences in the temperature of the ear canal. It was found to be lower by about 0.5°C when a step change from standing to walking at 4 mph was introduced without any intermediate changes (Fig. 5.6). There were no major differences between the temperatures of the ear canal measured during both experiments that involved gradual changes (Schedules III and IV). This observation probably indicates that the transient time for a thermal steady state in the human body is longer than 45 minutes and is more likely of the order of two hours.

TABLE F.1 in APPENDIX F summarizes the mean values and the ranges of the total metabolic rates and of the amounts of heat removed by the

---

†Cooling effectiveness of the cooling suit was defined as the ratio of the rate of heat removed by the suit to the total metabolic rate.

suit and by respiration at the various schedules of activity.

Figures 5.8 through 5.12 show the relative amounts of heat removed by the suit at the various regions of the body as functions of the different schedules of activity. Based on these data, the following observations were made:

(1) The relative amount of heat removed from the arms by the arm pads was the lowest in most cases. It ranged from 1.7 percent to 7.2 percent of the total removed by the suit and was usually around 3 to 4 percent. This was despite the fact that the arm pads covered about 18 percent of the total skin surface area covered by the suit. It is assumed that this finding should be attributed to the nature of the schedules of activity used in this study; these were composed primarily of work of the leg muscles and did not involve much arm work. This assumption is supported by the fact that the relative value of the heat removed at the arms increased during the walking sessions with the subjects swinging their arms.

(2) The largest amount of heat removed by the suit from a single region came from the thighs. It ranged from a low of 25.8 percent (while standing) to a high of 41.7 percent (while walking at 3 mph) of the total removed by the suit. As the metabolic rate exceeded the upper limit that could be accommodated by the suit, the relative amount of heat removed from the thighs decreased. This is probably due to the too high water inlet temperatures and the too small contact areas between the skin overlying the thighs and the cooling tubes. As a result, heat

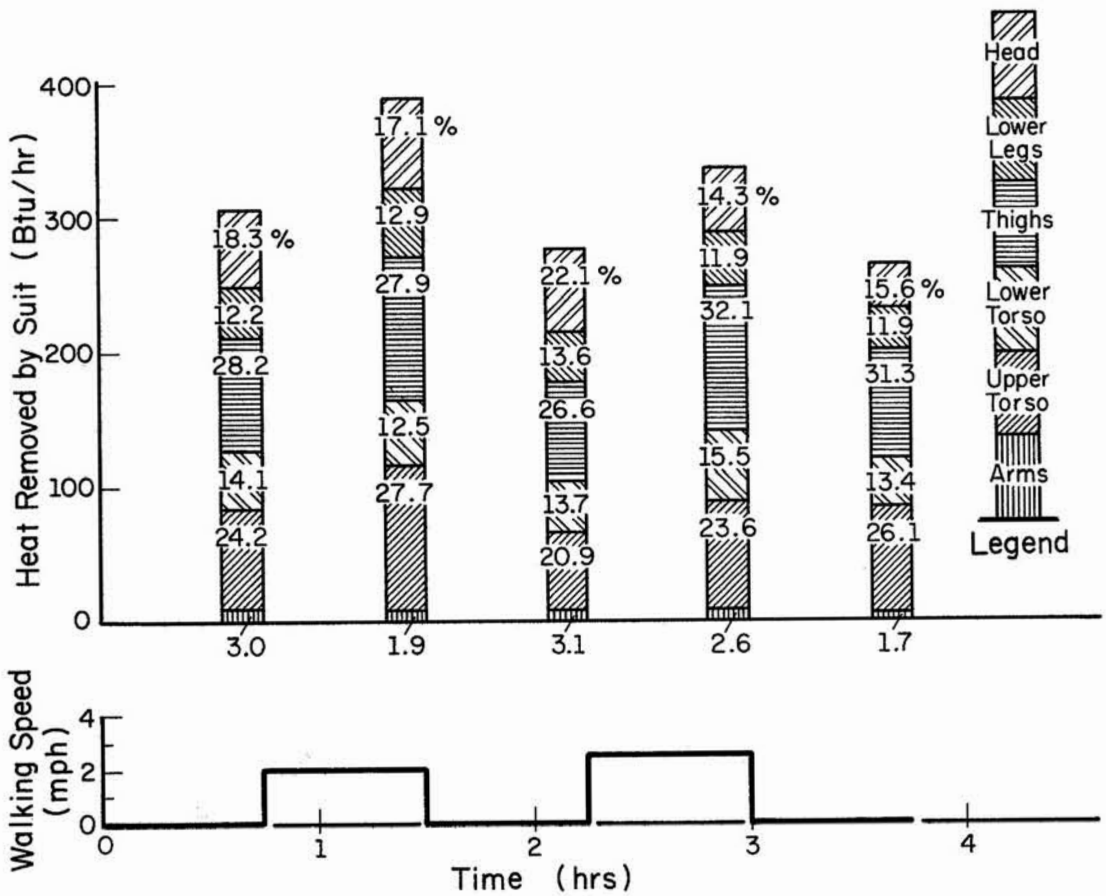

Figure 5.8 Mean values of the amounts of heat removed by the cooling pads for Schedule I.

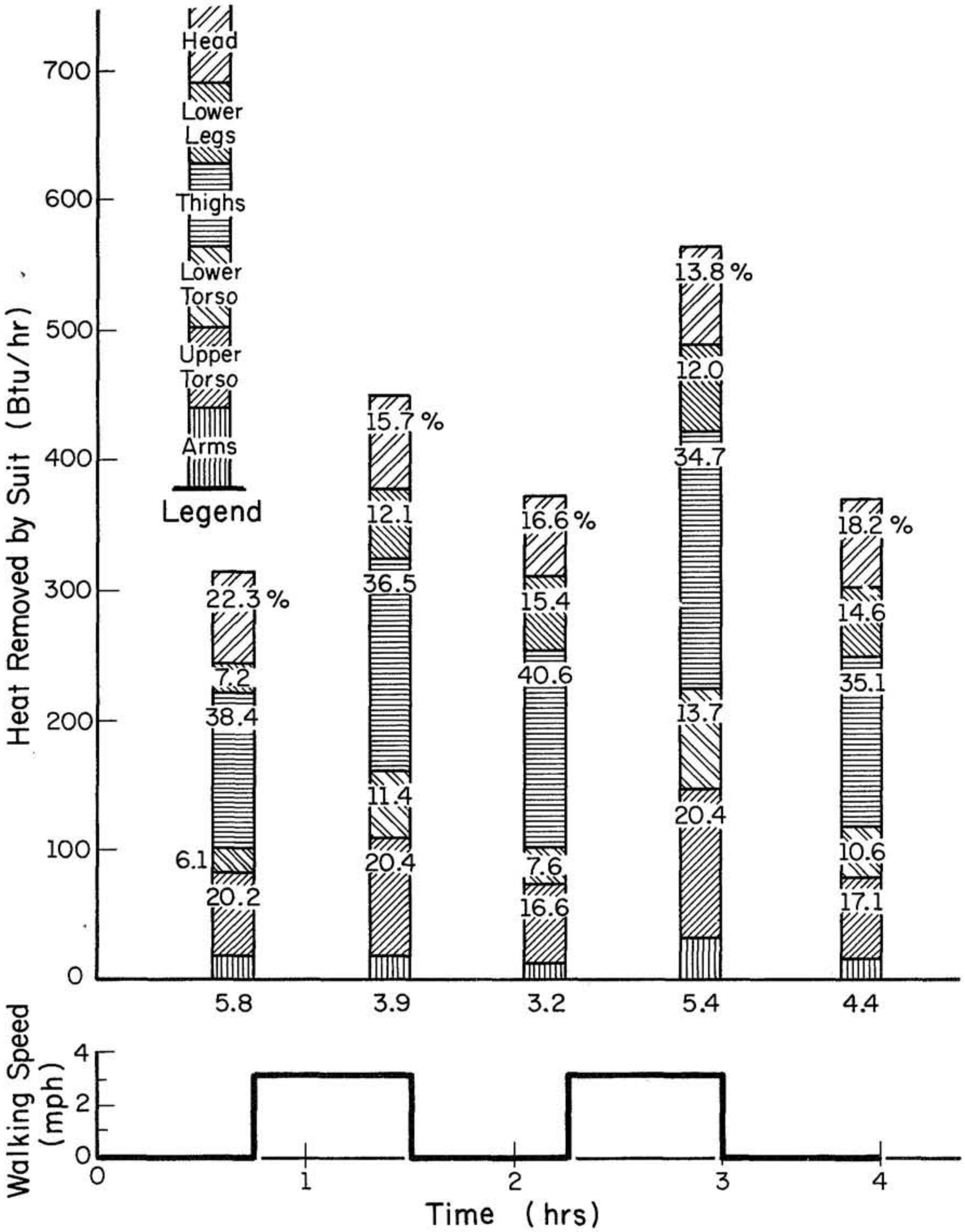

Figure 5.9 Mean values of the amounts of heat removed by the cooling pads for Schedule II.

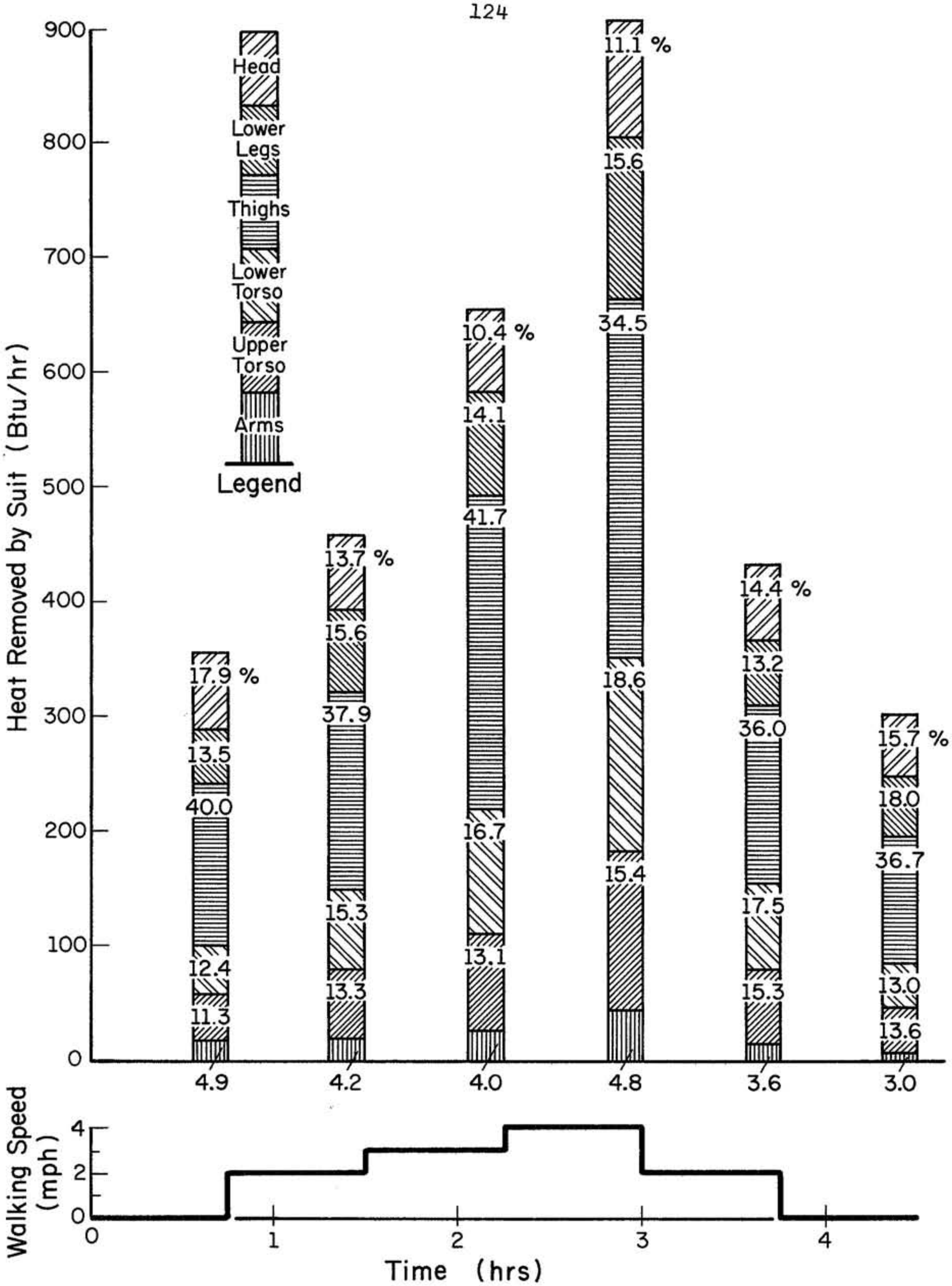

Figure 5.10 Mean values of the amounts of heat removed by the cooling pads for Schedule III.

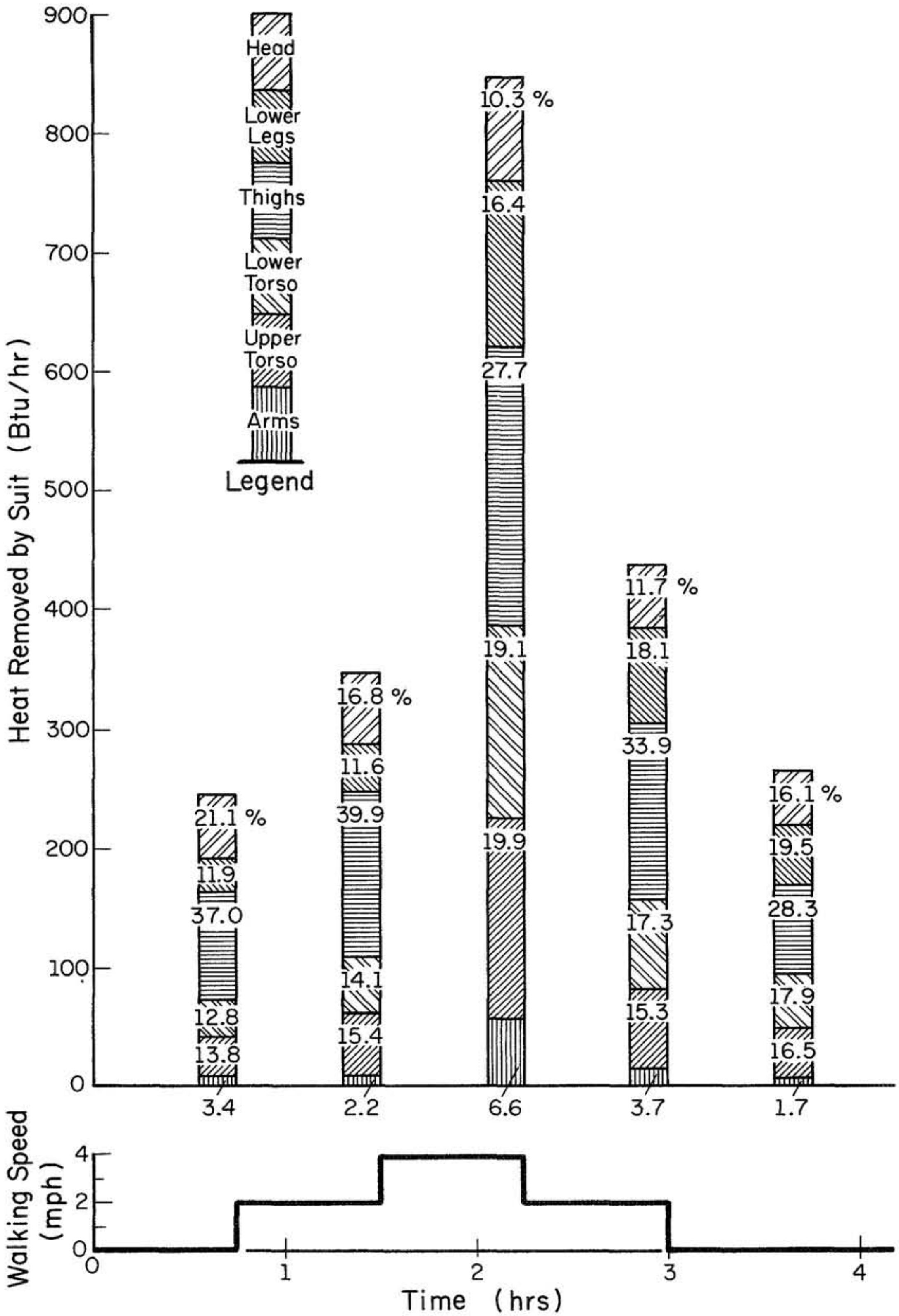

Figure 5.11 Mean values of the amounts of heat removed by the cooling pads for Schedule IV.

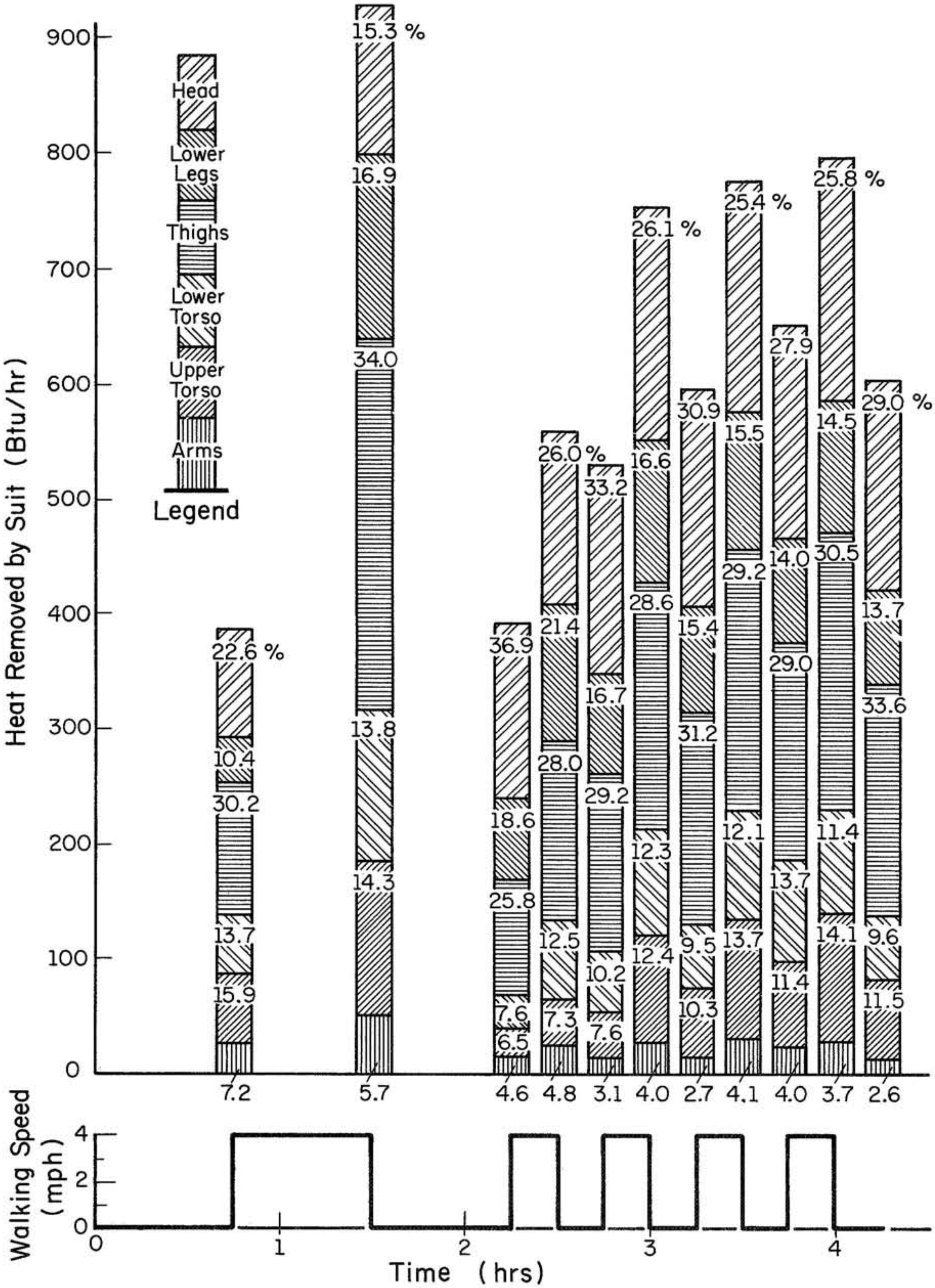

Figure 5.12 Mean values of the amounts of heat removed by the cooling pads for Schedule V.

was probably carried away from the thighs by the blood stream to be dissipated elsewhere where conditions were more favorable. Also, the "deep body" temperature increased and sweating was enhanced, as indicated by higher weight losses (TABLE 5.2).

(3) A relatively high percentage of the total heat removed by the suit came from the head which constitutes about 7 percent of the total surface area. It ranged from 10.3 percent to 36.9 percent. The highest values were obtained during the second part of the experiments of Schedule V (Fig. 5.12). This result seems to indicate that during the thermal transient period from the onset of a change in activity level, relatively high amounts of heat are removed from the head. According to Nunneley [72], up to 40 percent of the total metabolic rate was removed from the head during resting and steady states by a cap consisting of cooling tubes. In her study, however, she did not use a cooling suit along with the hood. Another study with a cooling suit that included a cooling hood was reported by Shvartz [73]. He found that during steady states, the hood removed about 40 percent of the total removed by the cooling suit assembly. However, 12 percent of the total surface area was covered by the hood in his studies as compared to only about 5 percent that was covered by the hood in the present study.

(4) During the experiments of Schedule I more heat was removed

TABLE 5.2

WEIGHT LOSSES DURING TREADMILL EXPERIMENTS

Subject		Schedule				
		I	II	III	IV	V
SGP	Weight loss-Δw (gr)	--†	450	875††	738	472
	Δw/w (gr/kg)	--	6.89	13.02	11.16	7.25
	Δw/t (gr/hr)	--	94.7	145.8	118.1	75.5
	Δw/w/t (gr/kg,hr)	--	1.45	2.17	1.79	1.16
SKB	Weight loss-Δw (gr)	390	346	516	478	412†††
	Δw/w	6.46	5.74	8.44	7.78	6.75
	Δw/t	78	65.9	114.7	95.8	91.6
	Δw/w/t	1.29	1.09	1.88	1.56	1.50
HNT	Weight loss-Δw (gr)	262	370	758	718	930
	Δw/w	4.01	5.81	11.92	11.04	14.49
	Δw/t	61.6	70.5	126.3	131.7	169.1
	Δw/w/t	0.94	1.11	2.00	2.03	2.63
RET	Weight loss-Δw (gr)	232	456	468	506	636
	Δw/w	3.61	7.05	7.31	7.96	9.87
	Δw/t	48.8	96.0	98.5	113.7	127.2
	Δw/w/t	0.76	1.48	1.54	1.79	1.97
PF	Weight loss-Δw (gr)	382	424	590	662	--†
	Δw/w	6.88	7.64	10.47	11.82	--
	Δw/t	63.7	84.8	131.1	132.4	--
	Δw/w/t	1.15	1.53	2.33	2.36	--

†Did not complete the schedule.

††Irregular schedule.

†††Shorter activity schedule.

(continued)

TABLE 5.2 continued

Subject		Schedule I	II	III	IV	V
MEAN	Weight loss-Δw (gr)	317†	409	583†	620	679††
	Δw/w	5.62	6.63	9.53	9.95	9.59
	Δw/t	64.4	82.4	117.7	118.3	115.8
	Δw/w/t	1.05	1.33	1.94	1.91	1.82
SKB WITHOUT SUIT	Weight loss-Δw (gr)	414	382	382	654	646
	Δw/w	6.72	6.19	6.15	10.60	10.52
	Δw/t	82.8	84.9	89.9	124.6	143.6
	Δw/w/t	1.34	1.38	1.45	2.02	2.34

†Average of 4 runs.

††Average of 3 runs.

by the cooling suit during the first walking session at two mph than that removed during the second at 2.5 mph (Fig. 5.8). The reason was the unexpected drop in "deep body" temperature as indicated by the temperature of the ear canal (Fig. 5.6). It should be noted that no readjustments in water inlet temperatures were permitted during these experiments. All changes were due to the instability of the cooling system. Therefore, this phenomenon of less heat removed by the suit at a higher metabolic rate is not considered to have any physiological meaning.

(5) During the experiments of Schedule II readjustments of the water inlet temperatures at the same level of activity resulted in the following changes:

   (a) The total metabolic rate decreased, (Fig. 5.2),

   (b) The amount of heat removed by the cooling suit increased, (Fig. 5.9), and

   (c) The temperature of the ear canal dropped, (Fig. 5.6).

   Consequently, the cooling effectiveness of the suit increased from 0.39 to 0.56, (TABLE F.1). Also, it is clear that adjustments of water inlet temperature actually did diminish the subjects' heat strain.† This reduction of heat strain was in spite of the consistent comfort vote of

---

†Heat strain is often referred to as the physiological response in consequence of a heat load [74]. This should be distinguished from the heat stress which is used to denote the heat load imposed on man [74]. A commonly used index to assess physiological strain was developed by Craig [75] and modified by others [76]. It is a linear combination of heart rate, rise in rectal temperature and sweat production rate.

"comfortable" obtained throughout the experiments of Schedule II (TABLE 5.1). The findings of this section indicate that additional cooling provided by some artificial means, e.g., a cooling suit, may reduce heat strain beyond that which is considered "comfortable" by human subjects. A similar conclusion was reached by Gold and Zornitzer [77].

Figure 5.13 shows the average values of water inlet temperatures at the various regions of the body for Schedule II. This schedule was selected for comparative presentation for two reasons:

(1) The effect of additional cooling at the same level of activity was studied during the experiments of this schedule and

(2) The metabolic rates encountered during the experiments of this schedule did not exceed the cooling capacity of the suit.

It can be seen that during the initial standing session, most of the subjects preferred an almost uniform temperature all over the body (Fig. 5.13a). This situation did not change during the first walking session where no additional cooling was permitted (Fig. 5.13b). Immediately following the first walking session, the restriction on the additional cooling was removed. A decrease in most water inlet temperatures was then requested by all of the subjects (Fig. 5.13c). The average changes requested for the arms and thighs were about 1.2 to 1.3°C, the head and upper and lower torso 0.2 to 0.6°C; and the highest decrease in water inlet temperature, 2.3°C, was requested for the lower

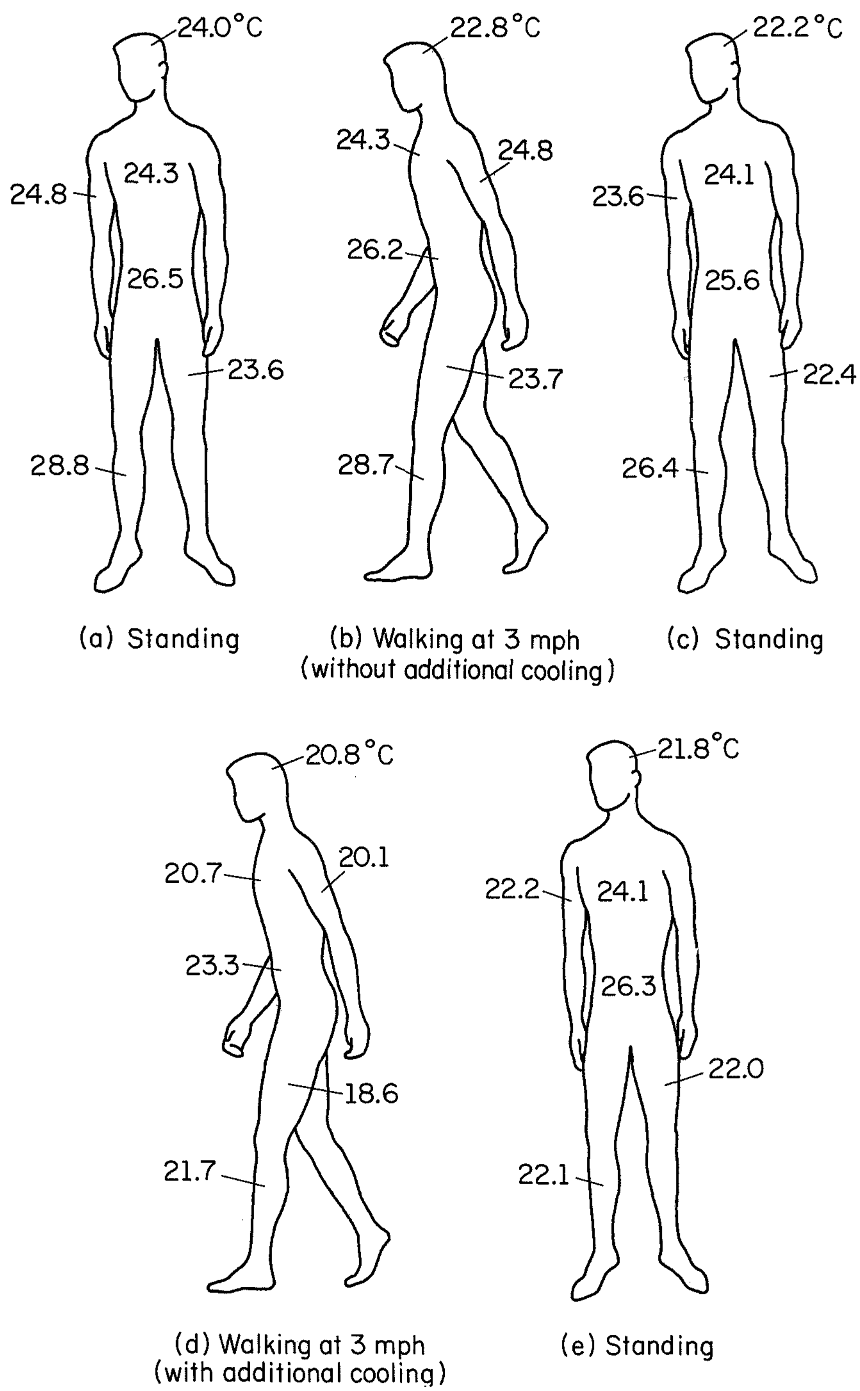

Figure 5.13 Mean water inlet temperatures at the various regions of the body for Schedule II.

legs. During the second walking session at 3 mph (Fig. 5.13d) the requests for decreases in water inlet temperatures were as follows: arms, upper torso, and thighs, 3.4 to 3.8°C; head, 1.4°C; lower torso, 2.5°C; and, again, the highest decrease in water inlet temperature, 4.7°C, was requested for the lower legs. During the last standing period, requested changes in water inlet temperatures to the various regions of the body were essentially such that they retraced the situation that prevailed during the second standing session. Only minor changes were noticeable, (Fig. 5.13e).

As a consequence of the results presented in the preceding section, the following observations were made:

(1) The working muscles, i.e., thighs and lower legs, exhibited the highest variability in water inlet temperatures. This was expected and does not seem to require any further discussion.

(2) The changes in water inlet temperatures to the head were the smallest. At the same time, the temperature of the water entering the cooling hood was, on the average, the lowest water inlet temperature of all. This indicates that cooling the head may have a profound effect on the sensation of comfort, as noted by Nunneley [72] and Shvartz [73].

A complete listing of the water inlet temperatures and their ranges at the various schedules of activity is given in TABLE F.2. It should, however, be kept in mind that the values shown there for the moderately high activity levels (walking at 4 mph) are of limited meaning. This is because the limited cooling capacity of the present cooling system was definitely exceeded during these schedules of activity.

In TABLE 5.1, the orders of preferred changes in water inlet temperatures, from the onset of a change in the level of activity, are shown. There does not seem to be any consistency in the order of changes requested by different subjects. Many more experiments with more subjects are needed to identify those regions in the body which require faster cooling or warming as a result of a change in the level of activity.

Weight losses during treadmill experiments are shown in TABLE 5.2. The mean values of weight losses range from about 65 gr/hr (Schedule I) to about 118 gr/hr (Schedules III and IV). These values, although slightly higher, are consistent with values reported by Webb and Annis [71]. In four out of five cases, the sweat rates were higher during the runs without the suit as compared to the runs with the suit. No fundamental explanation was found for the one run (Schedule III) that exhibited a higher weight loss with the suit. The reason for that may have been due to a measurement error.

Total metabolic rates for subject SKB with and without the cooling suit are compared in Figs. F.1 through F.5. Also compared in these figures are the temperatures of the ear canal. In most cases, the total metabolic rate was higher during the experiments with the cooling suit. This finding is probably due to the fact that there is a certain energy cost for wearing the suit (higher heat stress). At the same time, the temperature of the ear canal seemed to have been slightly lower during the experiments without the cooling suit.

Also, as shown in Fig. F.6, the heart rate was usually lower during at least the comparative experiments of Schedule V with the cooling suit. Heart rate was not measured during the other experiments with the suit. These two, i.e., slightly higher "deep body" temperatures and lower heart rates, indicate that the heat strain probably was reduced during the experiments with the cooling suit.

5.2 EXPERIMENTS WITH THE INDIVIDUAL COOLING PADS

Temperature distributions on the skin between two adjacent tubes were measured for the three individual cooling pads. The measurements were taken after the test subject had been pedalling for two hours on the bicycle ergometer at a constant load and speed [corresponding to a total metabolic rate of about 1200 Btu/hr (352 W)]. The measured values were assumed to represent steady state data.

The theoretical steady state temperature distribution on the skin for the rectangular model with the skin layer and skeletal muscle considered as one combined tissue was obtained from Eq. (C.2) to yield

$$T(x,0) = T_o + \frac{Q'}{w_b c_b}\left[1 - \frac{1}{\cosh (wb)}\right] - \frac{\beta f_a}{\sqrt{w_b c_b k}} \tanh (wb) - \sum_{n=1}^{\infty} \frac{\alpha_n \tanh (\zeta b)}{\zeta} \cos (\lambda_n x) \qquad (5.1)$$

As can be seen from Eq. (5.1), the parameters affecting the steady state temperature of the skin are:

(1) Temperature of the inner core, T_o.

(2) Specific heat of blood, c_b.

(3) Thermal conductivity of the combined tissue, k.

(4) Ratio of cooling tube width to cooling tube spacing, β.

(5) Cooling tube spacing, a.

(6) Average heat flux at the skin surface, f_a.

(7) Number of terms in the series used for computation.

(8) Shape of the specified flux function, f(x).

(9) Average heat generation rate per unit volume of tissue, Q'.

(10) Average blood perfusion rate per unit volume of tissue, w_b.

(11) Depth of tissue, b.

From these parameters, the first seven could either be measured or estimated. The remaining four, i.e., f(x), Q', w_b, and b, were left to be estimated by the method of fitting a theoretical curve to the experimental data. Curve fitting was done with the aid of a digital computer. A program was written for evaluating Eq. (5.1) for various combinations of the unknown parameters. The computer output was then analyzed to determine that combination of parameters which yielded a curve fitting closely with the experimental data while the parameters met a set of predetermined criteria. These criteria were:

(1) The lowest temperature of the skin should not be below 60°F. This assumption was based on the cooling water temperature which was measured at 55°F.

(2) The depth of tissue should not exceed 0.2 ft or be less than 0.05 ft.

(3) Only measurements taken away from the cooling tubes were considered accurate. Measurements underneath the cooling tube were assumed questionable because of the interference of the thermocouple with the contact between the cooling tube and the skin.

(4) The blood perfusion and heat generation rates per unit volume of tissue should not exceed values found in the literature.

The results obtained for the three individual pads are shown in Figs. 5.14, 5.15, and 5.16. In view of the complexity of the problem, the agreement between the measured and calculated values is remarkably good. It should, however, be noted that the set of parameters that yielded a good fit to the measured data is not unique. Improved techniques for measuring the unknown parameters are required to render the analysis presented in this chapter physiologically more meaningful.

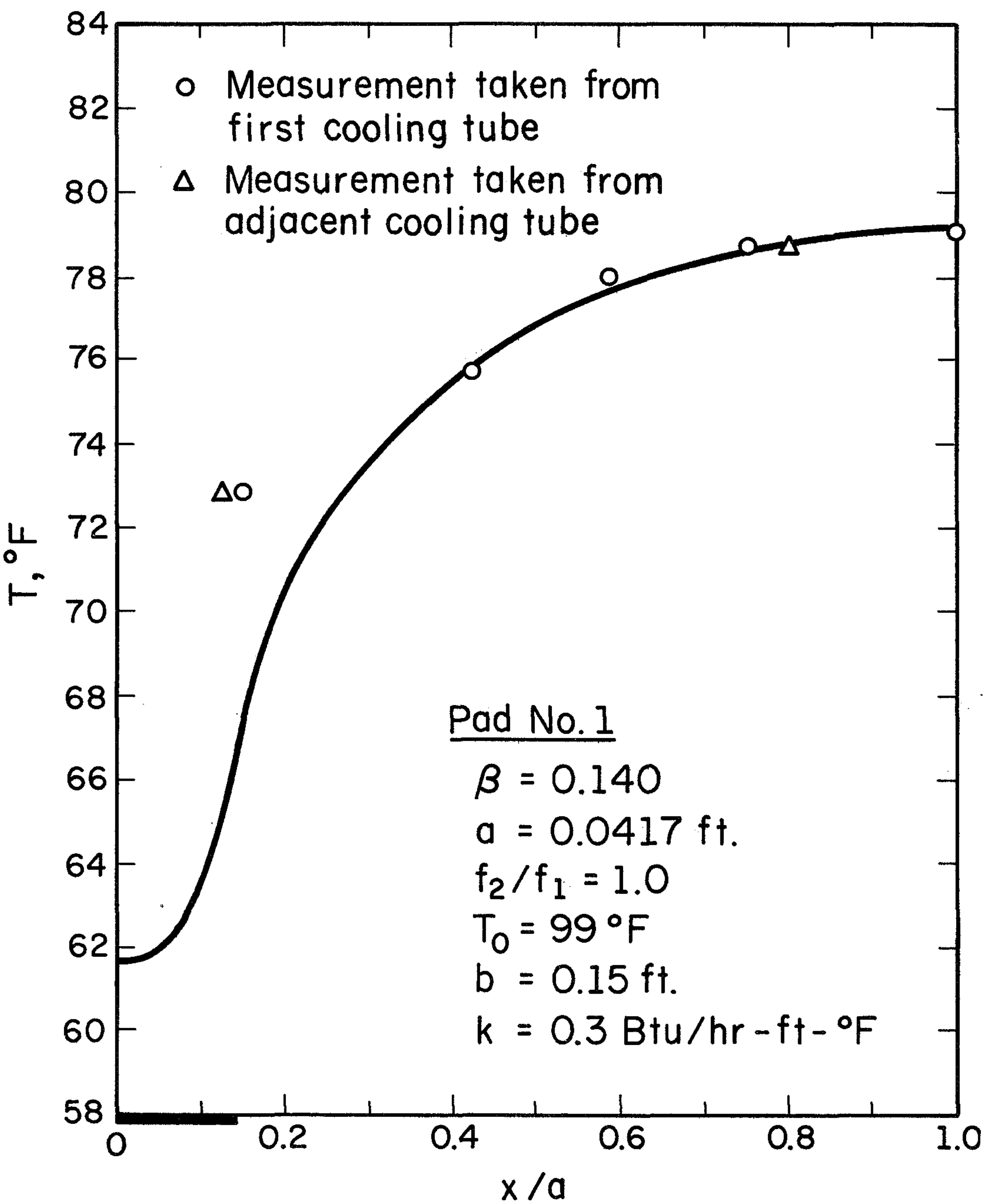

Figure 5.14 Comparison of measured and calculated temperature distribution on the surface of the skin for the rectangular model. Pad No. 1, w_b = 83.4 lb/hr-ft^3, Q' = 711 Btu/hr-ft^3 and constant temperature at inner core.

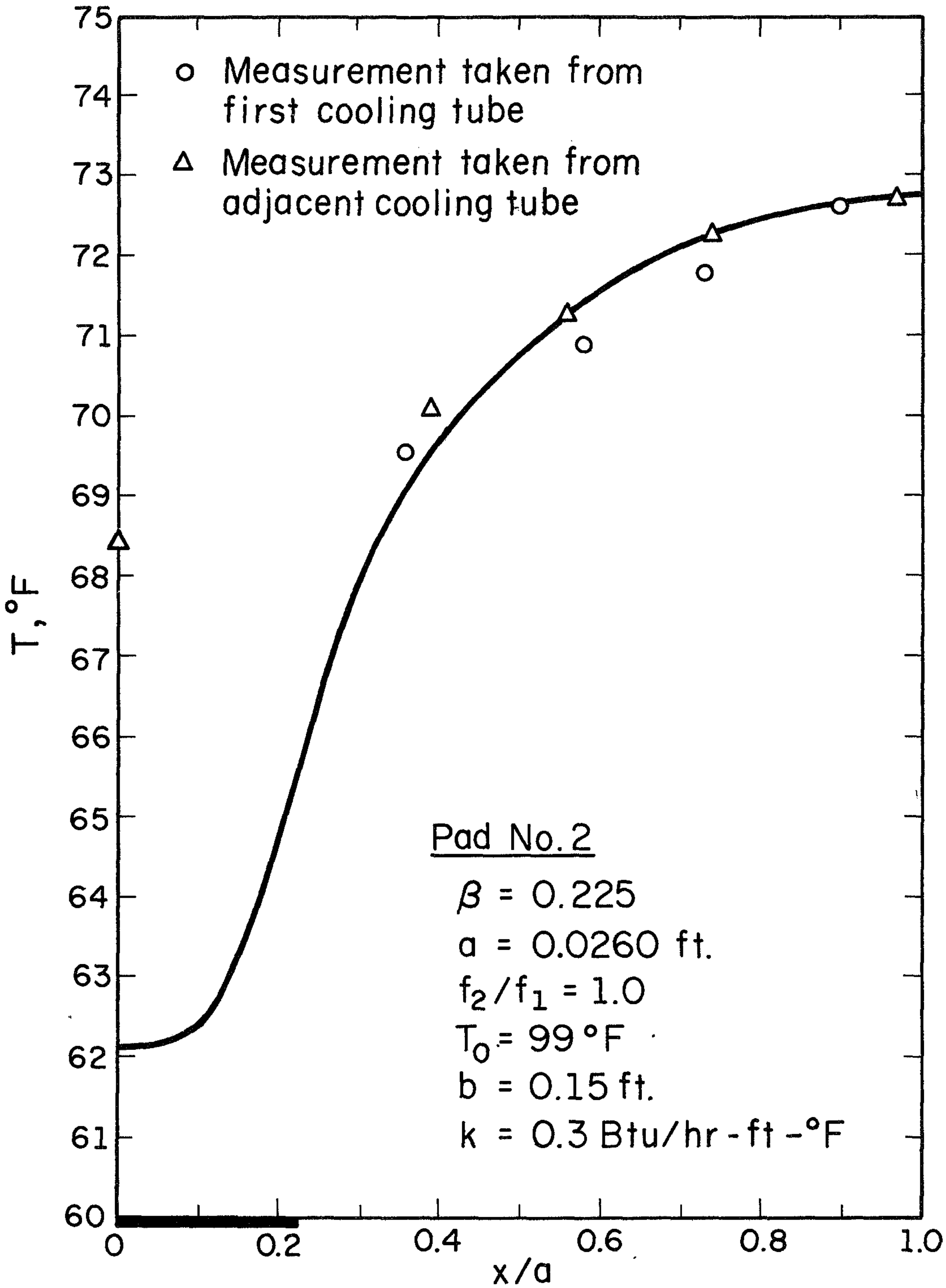

Figure 5.15 Comparison of measured and calculated temperature distribution on the surface of the skin for the rectangular model. Pad No. 2, w_b = 83.4 lb/hr-ft^3, Q' = 805 Btu/hr-ft^3 and constant temperature at inner core.

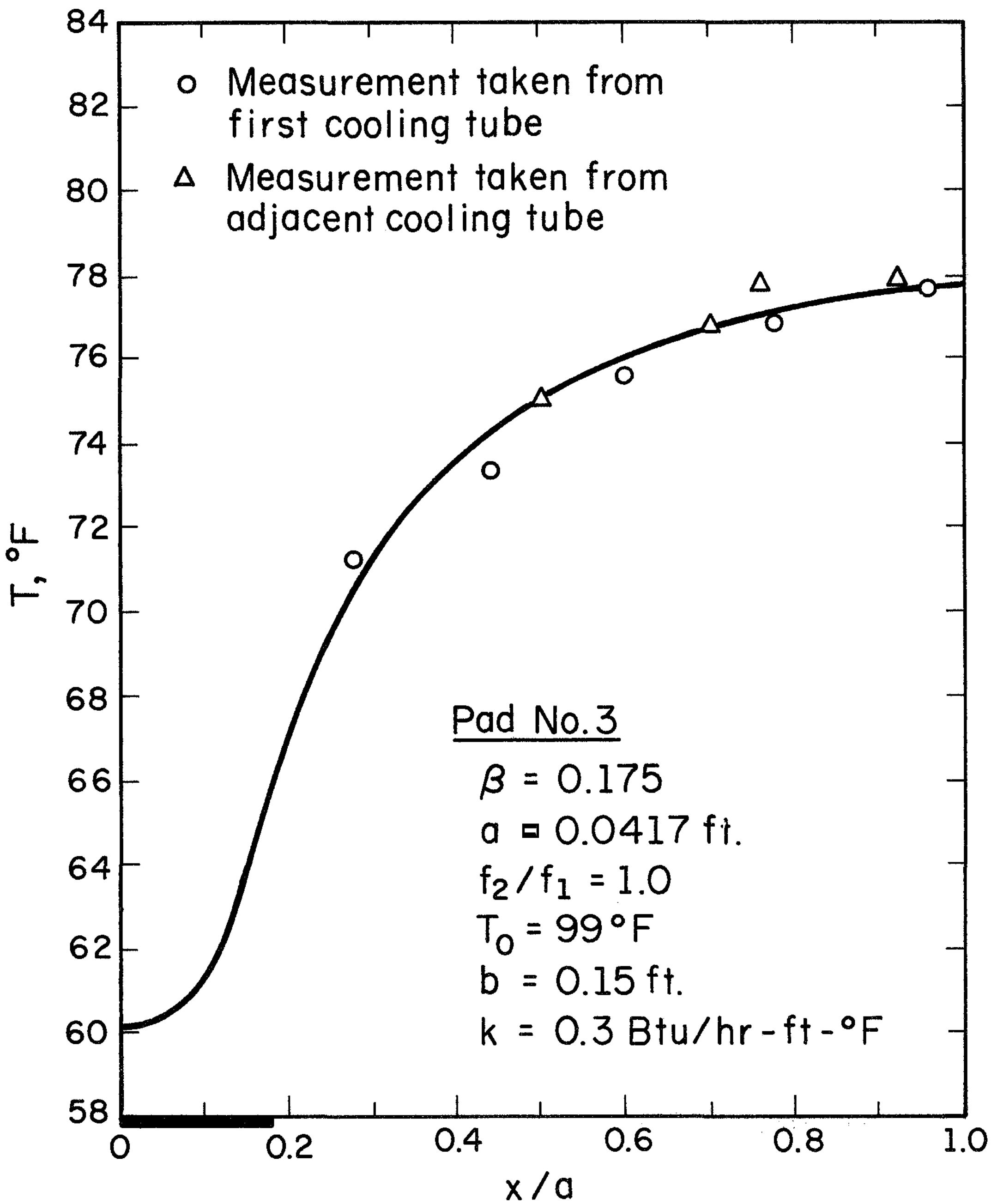

Figure 5.16 Comparison of measured and calculated temperature distribution on the surface of the skin for the rectangular model. Pad No. 3, w_b = 83.4 lb/hr-ft^3, Q' = 848 Btu/hr-ft^3 and constant temperature at inner core.

6. SUMMARY AND CONCLUSIONS

This study was directed to the exploration of two aspects related to thermal comfort of man:

(1) The analytical modeling of the thermal behavior of living biological tissue and partial experimental validation of the analytical predictions.

(2) The exploration of the characteristics of independent regional cooling of the body by means of a water-cooled garment (thermal protective suit).

A biothermal model of living biological tissue has been proposed and studied. This model includes the effects of blood flow, local heat generation rates, conduction and storage of heat on the heat transfer processes occuring in the living tissue. A second order, partial differential equation (referred to as the "bio-heat" equation) was obtained and analyzed. Closed form, steady and transient state analytical solutions were obtained for two relevant geometries (cylindrical and rectangular). Good agreement was obtained between the measured and predicted temperature profiles on the skin surface.

Based on the analysis, the following conclusions were reached:

(1) Blood flow plays a significant role in the transfer of heat in the living tissue and, therefore, should be explicitly included in any analytical model of the thermal behavior of the tissue.

(2) Much more detailed and accurate data of the thermophysical and physiological properties of the body, e.g., thermal conductivities and local blood flow rates, are required

before any extension of the present model should be attempted.

(3) Transient times for reaching a so-called "fully developed" temperature profile in the tissue are of the order of 5 to 20 minutes.

(4) Transient changes in tissue temperature are strongly dominated by a geometrical parameter (separation coefficient).

(5) Under certain conditions, maximum temperature may occur in the tissue rather than in the inner core ($wb > 2.3$). The location of the maximum temperature was found to be independent of "deep body" temperature.

(6) For $y/b > 2$, isotherms in the tissue become parallel. This observation renders assumptions of constant temperature or constant flux at the interface between the skeletal muscle and the inner core equivalent.

(7) The exact shape of the heat flux on the skin has an insignificant effect on the temperature distribution inside the tissue at a short distance away from the skin surface. It does have, however, a noticeable effect on the temperature on the skin surface.

(8) For $R_1 > 0.15$ ft (radius of inner core in the cylindrical model) the results obtained from the cylindrical and rectangular models are so close that the simpler, rectangular model can be used without loss of accuracy.

A water cooled garment was constructed and used to study the characteristics of independent regional cooling of the body in contrast to the current practice of uniform cooling. The cooling garment consisted of sixteen individual cooling pads made of 5/32 in. O.D. Tygon tubes. The pads were grouped to provide independent control of water inlet temperatures and flow rates to six regions: head, upper torso, lower torso, arms, thighs and lower legs. Experiments with and without the cooling suit assembly were conducted with the five test subjects standing and walking on a treadmill on selected schedules. Steady and, to a lesser extent, transient state characteristics of the cooling suit were obtained.

Based on the experiments with the cooling suit the following conclusions were reached:

(1) There are regions in the body that require more cooling during walking than others, e.g., thighs, head and lower legs.

(2) During standing, an almost uniform water inlet temperature was requested for all regions of the body by the test subjects. This situation changed significantly during exercise. Conclusions 1 and 2 indicate that independent regional cooling may be more efficient than the present scheme of uniform cooling.

(3) Cooling of the head during exercise has a profound effect on comfort.

(4) Transient times for reaching a thermal steady state from the onset of exercise are of the order of two hours. This transient time, however, includes a relatively slow active response of the human thermoregulatory system to changes in exercise rates, e.g., the shifting of the deep body temperature.

(5) During exercise the thermal effectiveness of the cooling suit decreased as compared to the values obtained for standing.

(6) Intermediate changes in the level of activity between an initial and a final level do not have a noticeable effect on the thermal state so long as sufficient time is allowed for reaching a steady state corresponding to the final level of activity.

(7) The cooling suit did actually diminish the heat strain of the test subjects beyond what was considered comfortable by them.

(8) The regional order of preferred changes in water inlet temperatures from the onset of a change in the level of activity could not be determined. More experiments are required to identify the regions of the body that require faster cooling (or warming) than others.

Based on the comparative experiments with and without the cooling suit, the following observations were made:

(1) Metabolic rates were, in most cases, higher during the experiments with the cooling suit, indicating that a certain energy cost was associated with wearing the suit, i.e., the subject was under higher heat stress.

(2) Ear canal temperatures were usually lower during the experiments without the cooling suit.

(3) Heart rates seem to have been lower during the experiments with the cooling suit.

(4) Weight losses were usually lower during the experiments with the cooling suit.

Thus, the cooling suit seems to have reduced the heat strain even though the heat stress was increased slightly.

Recommendations for future work are the following:

(1) Application of optimization techniques to obtain design guidelines for the construction of more efficient cooling suits.

(2) Extension of the model to include the local and temperature dependent variations of the physiological properties. This phase, however, should be delayed until more detailed physiological data become available.

(3) Experimentation with various combinations of individual cooling pads, e.g., hood and thigh pad, to determine the local effects of cooling at various heat stresses and activities.

(4) Experimentation with cooling suits while exercising other parts of the body, e.g., arms, in order to determine preferred temperature patterns for the coolant.

APPENDIX A

THE THERMOREGULATORY SYSTEM OF THE HOMEOTHERM

A homeotherm, or warm-blooded animal, exhibits a tendency to stability in the normal body states (fixed internal environment). The objective of the thermoregulatory system is counter any external or internal changes in heat stress while maintaining the temperature and metabolism (the transformation by which energy is made available for the uses of the organism) at the levels essential to life. This thermoregulatory system is composed of three interconnected elements: control, sensory, and regulatory mechanisms.

It is generally accepted that the center of thermal control is located in the hypothalamus, a structure in the brain which forms the floor and part of the lateral wall of the third ventricle [78, 79]. There appear to be two centers in the hypothalamus that are concerned with temperature control; the more posterior one, concerned with protection against cold, and the anterior one, concerned with protection against heat. These two centers are mutually inhibitory. The temperature which is being regulated, usually referred to as "deep body" temperature, is, however, not constant. It changes, within a narrow range above and below the "normal" temperature, with the metabolic rate. This concept of a "set point" rather than a fixed one was postulated by Hardy [80].

Thermal receptors in the skin are the major components of the sensory system [81]. In addition, there are indications that temperature-sensitive structures exist in the spinal cord [82], in the voluntary muscles [81], in the hypothalamus [55], and in the respiratory tract [83], which play a subsidiary role in thermoregulation. Changes in skin temperature and probably also in heat flux at the skin [55] trigger a signal which is received by the thermal receptors and which is sent through the afferent pathways to the hypothalamus.

There exist regulatory mechanisms in the human body that make up the third element of the thermal system. These mechanisms are activated in response to need and, in turn, by the control through the nervous system. Adjustment to cold stress follows the sequence:

(1) Superficial vasoconstriction that diminishes the amount of heat transported by the blood stream to the skin. This is balanced by splanchnic dilatation; i.e., dilatation of blood vessels in the internal cavities of the body.

(2) Pilo-motor activity ("goose flesh") that reduces air movement at the skin and thereby diminishes heat convection.

(3) Increased heat production that can take either (or both) of two forms: mechanical and glandular. The mechanical part is achieved by the muscles and is manifested as shivering; the glandular part involves secretion of adrenalin by the suprarenal gland. The function of the circulating adrenalin is to cause modifications in the circulation which favor blood supply to active muscles and liberation of glucose from liver glycogen and, consequently, a considerable increase in heat production (20-30 percent increase in resting metabolism [55]).

(4) Long-term adaptation--decreased blood volume and accumulation of fat in the outer layers to increase thermal insulation.

Conversely, the sequence of adjustment to heat stress is as follows:

(1) Superficial vasodilatation that increases blood flow and, consequently, the amount of heat transported to the skin.

(2) Sweating which enhances the removal of heat by evaporation of water vapor from the surface of the skin. Sweating will follow an increase in deep body temperature caused by heat storage in the body.

(3) Increased respiration that promotes more heat removal by expired air. In mammals other than humans, e.g., dogs, this mechanism, known as panting, is of great importance. This mechanism, as well as sweating, loses its effectiveness in saturated or very humid environments.

(4) Long-term adaptation--increased blood volume and decreased basal metabolism (the minimal energy expended for maintenance of life) due to reduced activity of the thyroid.

An extensive and detailed description of the thermoregulatory system and its functions was given by Bazett [55].

APPENDIX B

STEADY STATE, RECTANGULAR COORDINATES WITHOUT BLOOD FLOW

If the term representing blood flow is eliminated from Eq. (3.3), the following heat equation is obtained

$$\rho c_p \frac{\partial T}{\partial t} = k\nabla^2 T + q_m \tag{B.1}$$

or, assuming a steady state,

$$k\nabla^2 T = -q_m \tag{B.2}$$

which is often referred to as the Poisson equation.

Solution to Eq. (B.2) for the geometry shown in Fig. (3.4) is desirable for two reasons:

(1) There are cases when blood flow diminishes or even vanishes, e.g., vasoconstriction, and conduction remains as almost the sole mechanism for heat transfer in the tissue.

(2) From a more general engineering viewpoint, Eq. (B.2) describes the energy balance in a material wherein heat is conducted and generated. Such cases occur frequently in engineering and a solution may be useful.

Examination of Eqs. (3.11) through (3.15) reveals that obtaining the solution for this limiting case, i.e., $w_i \to 0$, is not straightforward, but involves fairly complicated limit operations. Therefore, the complete problem will be formulated and presented below.

SKIN

$$\frac{\partial^2 \theta_1}{\partial x^2} + \frac{\partial^2 \theta_1}{\partial y_1^2} = -Q_1 \qquad \text{(B.3a)}$$

$$0 \leq x \leq a \; ; \quad 0 \leq y_1 \leq b_1$$

$$\text{at } y_1 = b_1 \, , \begin{cases} \dfrac{\partial \theta_1}{\partial y_1} = -\dfrac{f(x)}{k_1} \, , & 0 \leq x < \beta a \\[2ex] \dfrac{\partial \theta_1}{\partial y_1} = 0 & \beta a < x \leq a \end{cases} \qquad \text{(B.3b)}$$

$$\text{at } x = 0 \, , \quad \frac{\partial \theta_1}{\partial x} = 0 \qquad \text{(B.3c)}$$

$$\text{at } x = a \, , \quad \frac{\partial \theta_1}{\partial x} = 0 \qquad \text{(B.3d)}$$

SKELETAL MUSCLE

$$\frac{\partial^2 \theta_2}{\partial x^2} + \frac{\partial^2 \theta_2}{\partial y_2^2} = -Q_2 \qquad \text{(B.4a)}$$

$$0 \leq x \leq a \; ; \quad 0 \leq y_2 \leq b_2$$

$$\text{at } y_2 = b_2 \, , \; \theta_2 = 0 \qquad \text{(3.4b)}$$

$$\text{at } x = 0 \, , \quad \frac{\partial \theta_2}{\partial x} = 0 \qquad \text{(B.4c)}$$

$$\text{at } x = a \, , \quad \frac{\partial \theta_2}{\partial x} = 0 \qquad \text{(B.4d)}$$

matching conditions at $y_1 = y_2 = 0$,

$$\theta_1 = \theta_2 \qquad \text{(B.5a)}$$

$$k_1 \frac{\partial \theta_1}{\partial y_1} = -k_2 \frac{\partial \theta_2}{\partial y_2} \qquad \text{(B.5b)}$$

where θ_i and Q_i are defined by Eqs. (3.8) and (3.10), respectively.

The solutions for the two zones are: for the skin layer,

$$T_1(x,y_1) = T_2^* + \frac{Q_2}{2} b_2^2 + \frac{Q_1}{2k^*}[2b_1 b_2 + k^* y_1(2b_1 - y_1)]$$
$$- \frac{\beta f_a}{k_2}(k^* y_1 + b_2) + k_1 \sum_{n=1}^{\infty} \frac{\alpha_n}{\cosh(\lambda_n b_1)}$$
$$\cdot \left[\frac{\tanh(\lambda_n b_2) \cosh[\lambda_n (b_1 - y_1)]}{H(\lambda)} + \frac{\sinh(\lambda_n y_1)}{k_1 \lambda_n} \right] \cos(\lambda_n x) \tag{B.6}$$

and, for the skeletal muscle layer,

$$T_2(x,y_2) = T_2^* + \frac{Q_2}{2}(b_2^2 - y_2^2) + \frac{Q_1}{k^*} b_1 (b_2 - y_2)$$
$$- \frac{\beta f_a}{k_2}(b_2 - y_2)$$
$$+ k_1 \sum_{n=1}^{\infty} \frac{\alpha_n \sinh[\lambda_n (b_2 - y_2)]}{H(\lambda) \cosh(\lambda_n b_2)} \cos(\lambda_n x) \tag{B.7}$$

where

$$k^* \equiv \frac{k_2}{k_1} \tag{B.8}$$

and $H(\lambda)$, f_a, and α_n are defined by Eqs. (3.15), (3.16), and (3.19), respectively.

As was noted in the text (Chapter 3), no maximum temperature is found in the tissue. However, in order for all the excess heat to be removed at the skin, the temperature gradients become steeper. As one result, the temperatures on the skin become lower since deep body temperature is maintained at about the same level as in the case with blood flow. In the vicinity of the cooling tube, the temperatures may become intolerably low or even dangerous, particularly if the cooling strip is relatively narrow (small β) [84].

Buchberg and Harrah studied a similar case [39]. They assumed no heat to be generated in the skin layer ($Q_1 = 0$), but assumed the thermal conductivity to be a function of temperature. By such means, they have tried to account for blood flow effects. Employing a numerical method, they obtained the temperature distribution in the separated layers for a total metabolic rate of 2600 Btu/hr (760 w). Their results are compared with those obtained here for $Q_1 = 0$ in Fig. B.1 [85]. Considering the major differences in the calculation procedures, the results are remarkably close. The numerical results obtained for Eq. (B.6) and (B.7) without blood flow (combined tissue, $b_1 \to b_2$, $k_1 \to k_2$) and Eq. (C.2) with blood flow are compared in Fig. B.2. The effect of the blood stream on the temperature distribution is clearly seen.

Figure B.3 shows the effect of increasing the contact area between the cooling tubes and the skin on the temperature distribution on the skin surface. When this figure is compared to Fig. 3.8, it is evident that one of the effects of blood flow is a higher temperature at the skin surface.

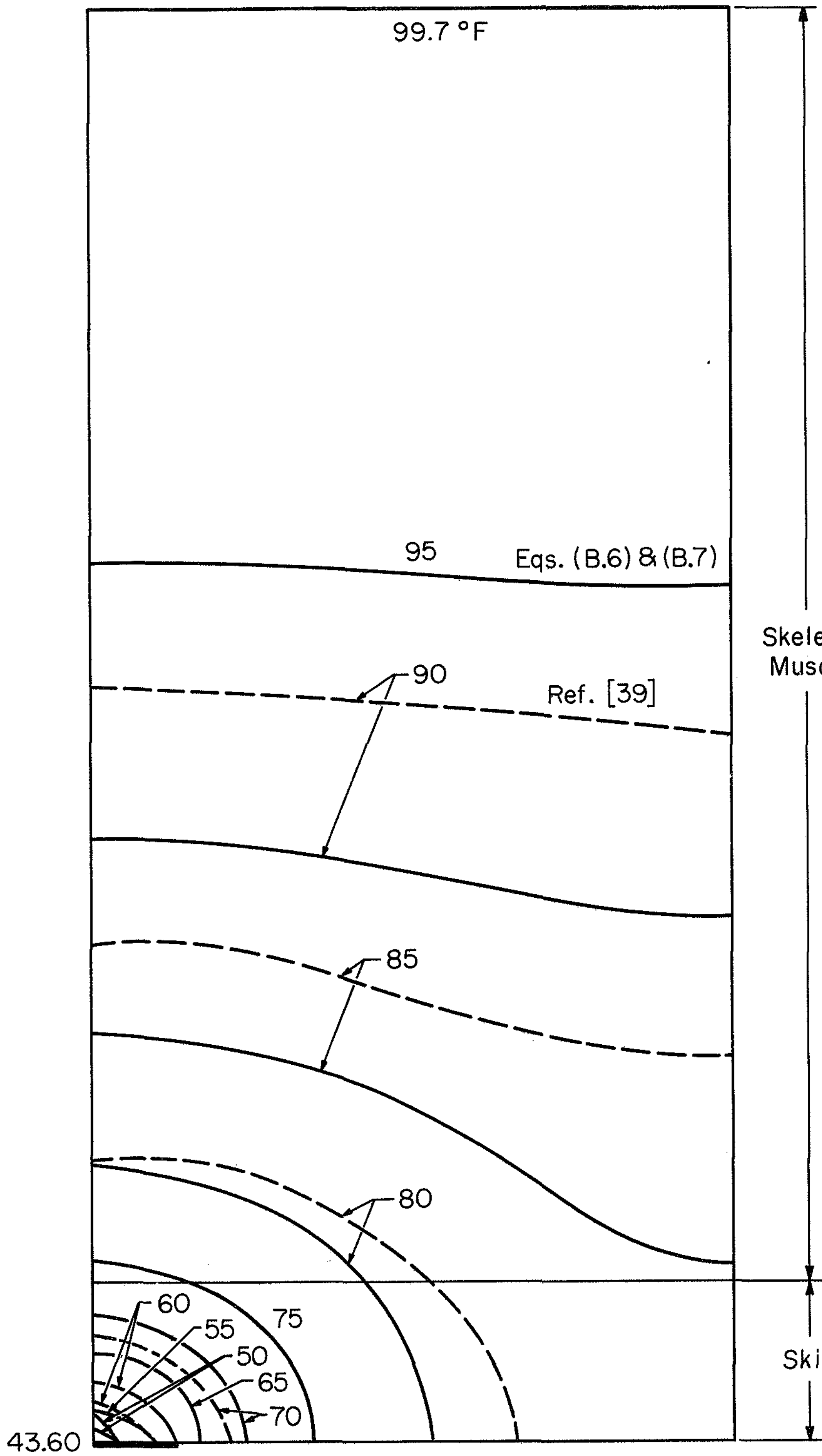

Figure B.1 Comparison of steady state temperature distributions in the tissue for the two-dimensional, rectangular model without blood flow. Q_m = 2600 Btu/hr (760 w), β = 0.1, constant temperature at inner core.

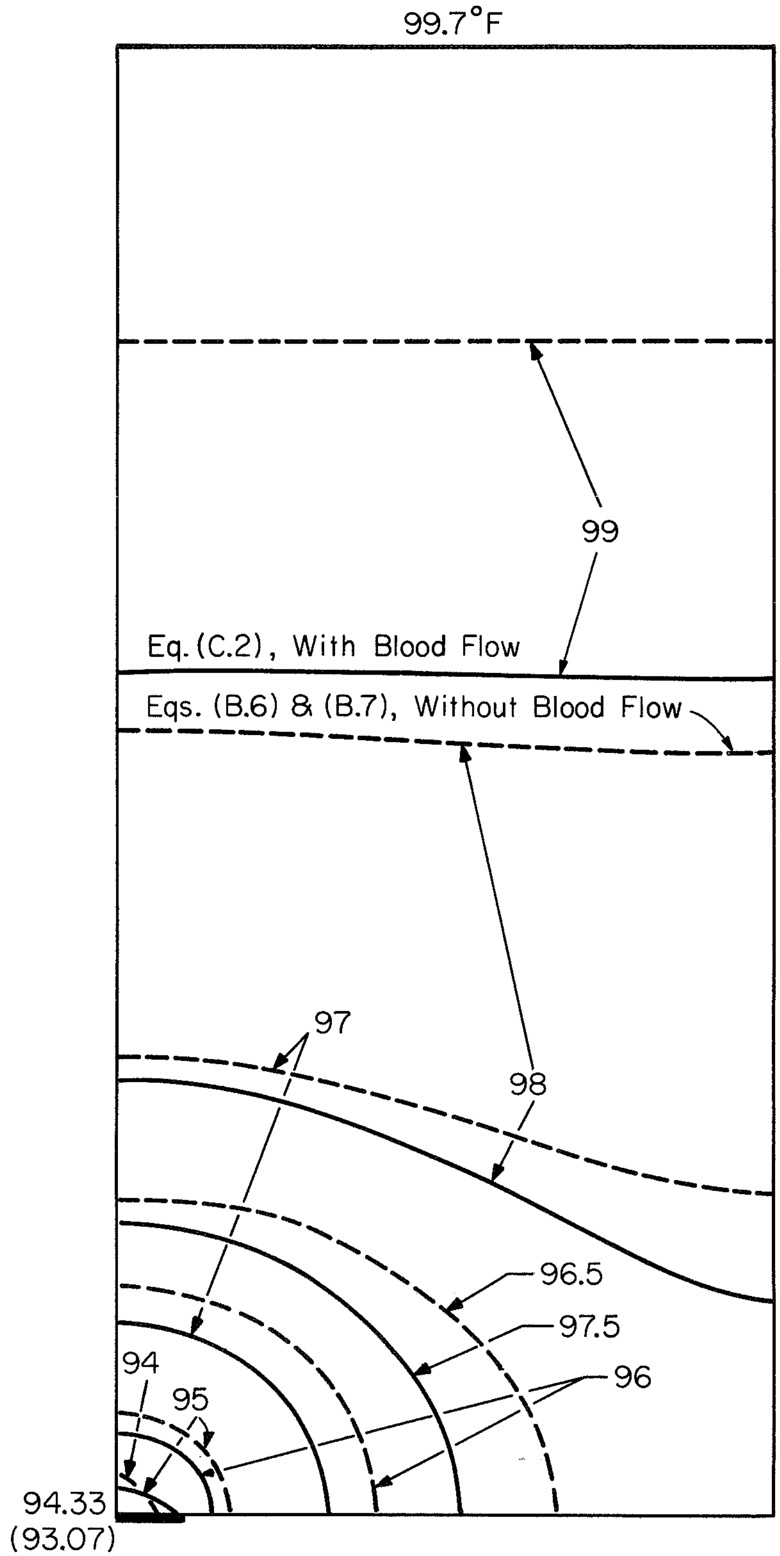

Figure B.2 Comparison of steady state temperature distributions in the combined tissue for the two-dimensional rectangular model with and without blood flow. Q_m = 290 Btu/hr (85 w), β = 0.1, constant temperature at inner core.

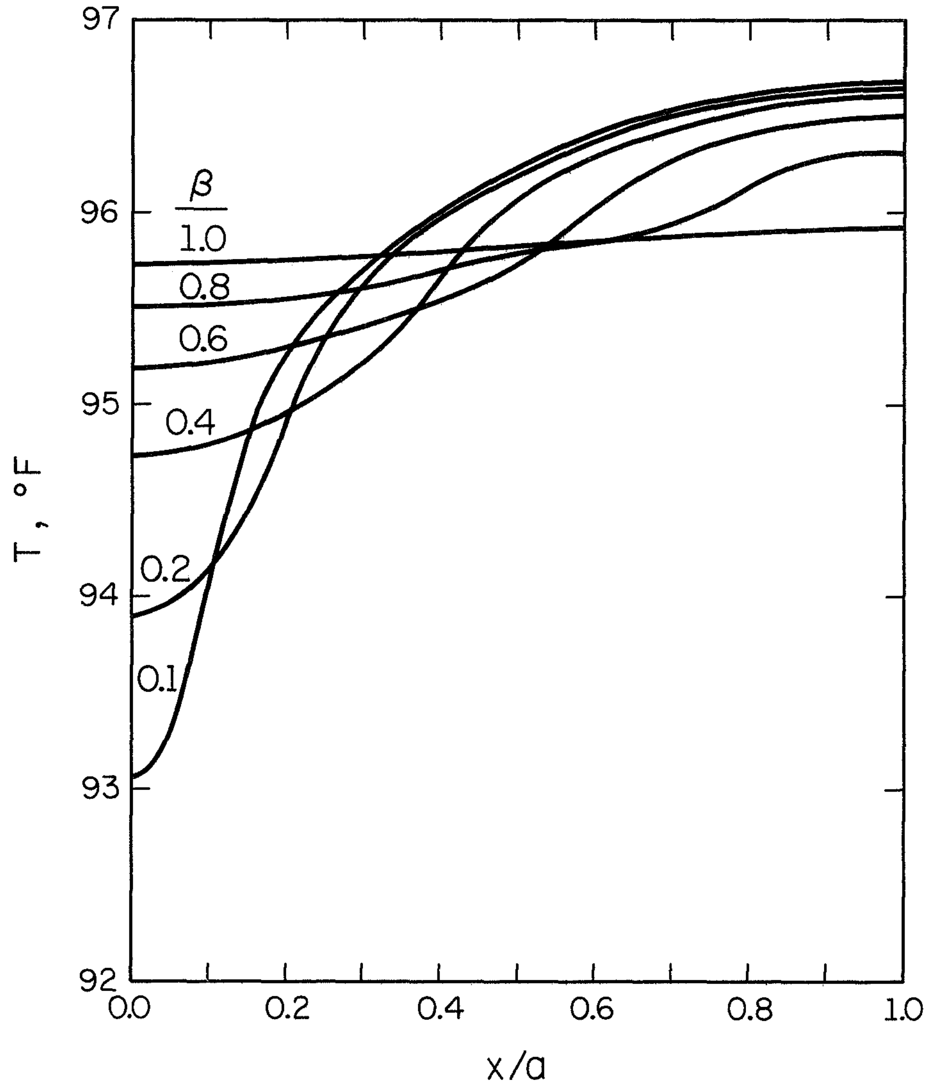

Figure B.3 Effect of increasing the contact area between the cooling tubes and the skin on the temperature distribution on the skin surface. Blood flow effects are not included. Q_m = 290 Btu/hr (85 w), f_2/f_1 = 1.5 and constant temperature at inner core.

APPENDIX C

STEADY STATE, RECTANGULAR COORDINATES WITH THE SKIN AND MUSCLE CONSIDERED AS A SINGLE REGION

If the skin and skeletal muscle layers are combined to form one layer and if both the thermophysical and the physiological properties are averaged, the problem becomes

$$\nabla^2\theta - w^2\theta = -Q \tag{C.1a}$$

$$0 \le x \le a \; ; \quad 0 \le y \le b$$

with the boundary conditions,

$$\text{at } x = 0 \;, \quad \frac{\partial\theta}{\partial x} = 0 \tag{C.1b}$$

$$\text{at } x = a \;, \quad \frac{\partial\theta}{\partial x} = 0 \tag{C.1c}$$

$$\text{at } y = 0 \;, \quad \left\{ \begin{array}{ll} \dfrac{\partial\theta}{\partial y} = \dfrac{f(x)}{k} \;, & 0 \le x < \beta a \\[2ex] \dfrac{\partial\theta}{\partial y} = 0 \;, & \beta a < x \le a \end{array} \right\} \tag{C.1d}$$

$$\text{at } y = b \;, \quad \theta = 0 \tag{C.1e}$$

The solution to this set is [58]

$$T(x,y) = T_1 + \frac{Q}{w^2}\left[1 - \frac{\cosh\,(wy)}{\cosh\,(wb)}\right] - \frac{\beta f_a}{kw}\,\frac{\sinh\,[w(b - y)]}{\cosh\,(wb)}$$

$$- \sum_{n=1}^{\infty} \frac{\alpha_n \sinh\,[\zeta(b - y)]}{\zeta \cosh\,(\zeta b)} \cos\,(\lambda_n x) \tag{C.2}$$

Figure C.1 shows results that were obtained for Eq. (C.2).

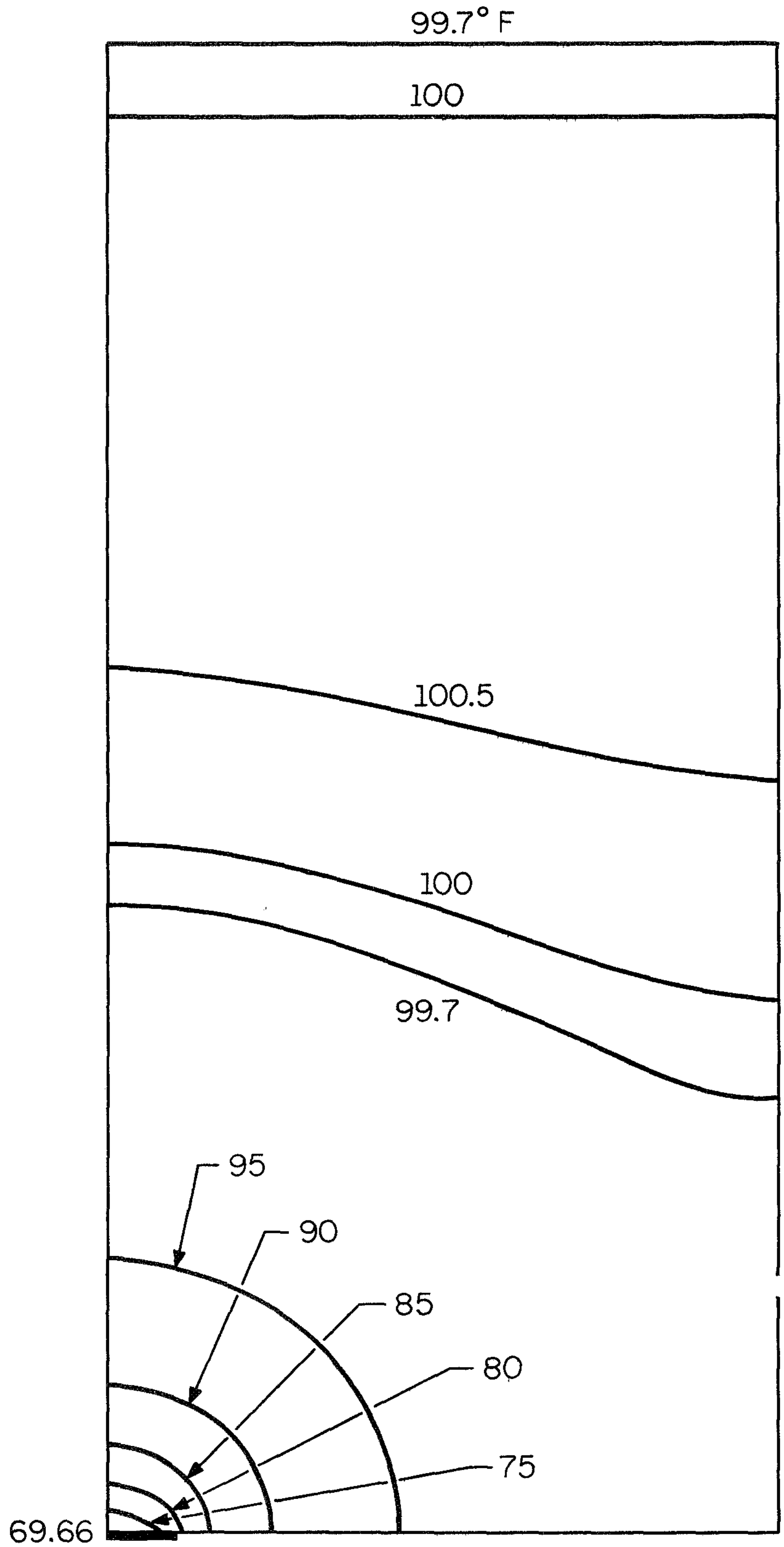

Figure C.1 Steady state temperature distribution in the combined tissue for the rectangular model. Q_m = 2600 Btu/hr, (760 w), β = 0.1 and constant temperature at inner core.

If the fourth boundary condition, Eq. (C.1e), is changed to uniform flux at the interface between the combined tissue and the inner core, that is,

$$\text{at } y = b \ , \quad \frac{\partial \theta}{\partial y} = \frac{F_o}{k} \tag{C.3}$$

a solution is obtained [58],

$$T(x,y) = T_1 + \frac{Q}{w^2} - \frac{\beta f_a}{kw} \frac{\cosh [w(b - y)]}{\sinh (wb)} + \frac{F_o}{kw} \frac{\cosh (wy)}{\sinh (wb)}$$

$$- \sum_{n=1}^{\infty} \frac{\alpha_n \cosh [\zeta(b - y)]}{\zeta \sinh (wb)} \cos (\lambda_n x) \tag{C.4}$$

Figure C.2 shows results that were obtained for Eq. (C.4).

Solutions for the corresponding one-dimensional cases, i.e., uniform cooling at the skin, may be readily obtained from Eqs. (C.3) and (C.4) by eliminating the x-dependent series and replacing the term βf_a by F.

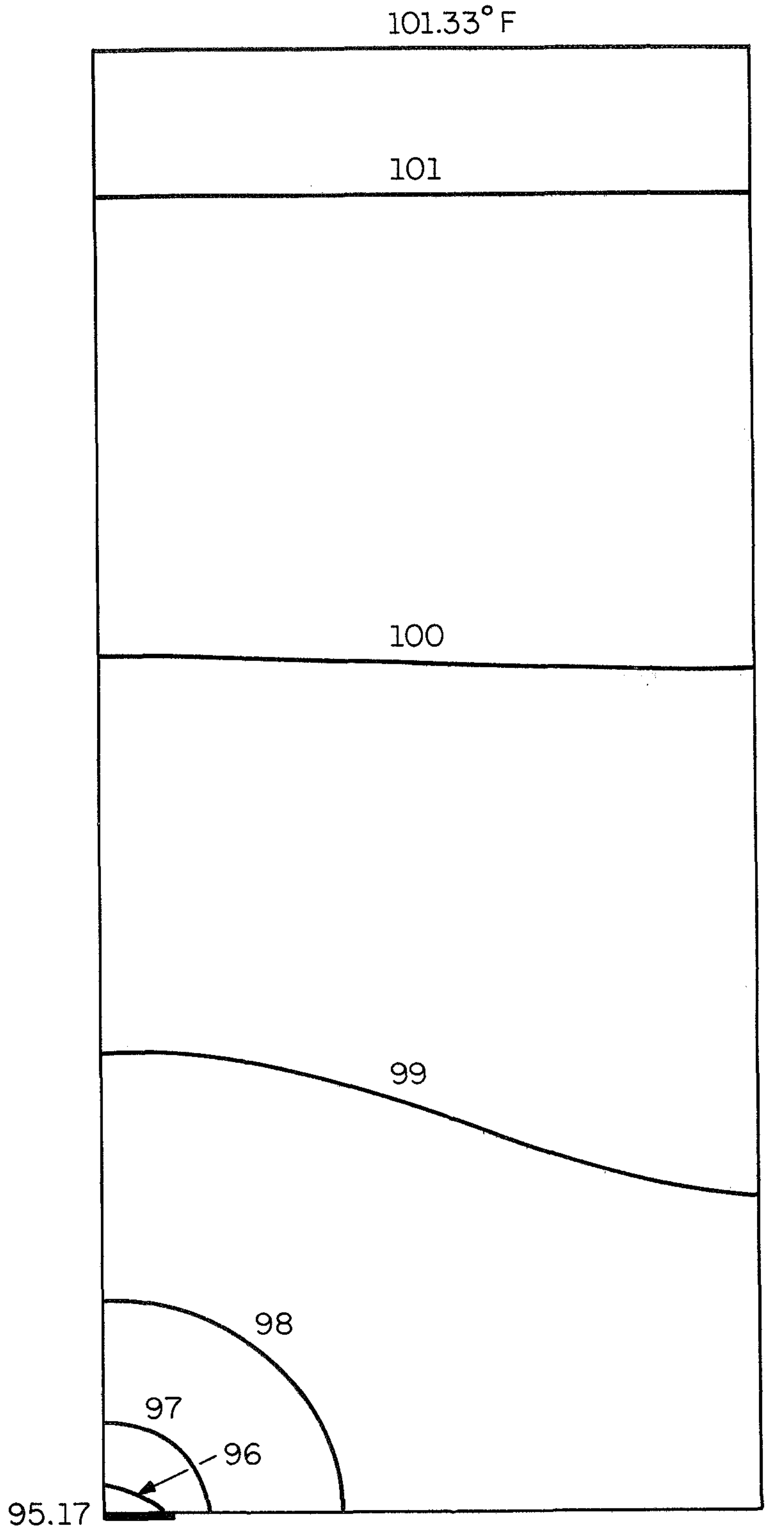

Figure C.2 Steady state temperature distribution in the combined tissue for the rectangular model. Q_m = 290 Btu/hr (85 w), β = 0.1, constant flux at inner core.

APPENDIX D

THE FUNCTION $\psi^{j}_{k\ell}(\zeta_i r)$

During the mathematical derivation of the cylindrical model, a combination of modified Bessel function was found to recur; namely,

$$\psi^{j}_{k\ell}(\zeta_i r) \equiv I_k(\zeta_i r)K_\ell(\zeta_i R_j) + (-1)^{k+\ell+1} I_\ell(\zeta_i R_j)K_k(\zeta_i r) \qquad (3.37)$$

This shorthand definition simplified the derivation considerably.

A few characteristics of this function are given below.

(1) The function $\psi^{j}_{k\ell}(\zeta_i r)$ satisfies the modified Bessel equation of order k,

$$\frac{1}{r}\frac{d}{dr}\left[r\,\frac{d\psi^{j}_{k\ell}(\zeta_i r)}{dr}\right] - \left(\zeta_i^2 + \frac{k^2}{r^2}\right)\psi^{j}_{k\ell}(\zeta_i r) = 0 \qquad (D.1)$$

(2) This function obeys the same differentiation rule as does the modified Bessel function of the first kind [64]

$$r\,\frac{d}{dr}\left[\psi^{j}_{k\ell}(\zeta_i r)\right] = k\psi^{j}_{k\ell}(\zeta_i r) + \zeta_i r\psi^{j}_{(k+1)\ell}(\zeta_i r) \qquad (D.2)$$

Therefore, it is not a so-called cylinder function [64].

(3) For two consecutive indices, it satisfies [61]

$$\psi^{j}_{k(k+1)}(\zeta_i R_j) = \frac{1}{\zeta_i R_j} \qquad (D.3)$$

(4) If the indices of the function are reversed in order, the following expression is obtained

$$\psi^{i}_{k\ell}(\zeta_j r) = (-1)^{k+\ell+1}\psi^{j}_{\ell k}(\zeta_i r) \qquad (D.4)$$

(5) For identical indices the following identity is obtained

$$\psi^{j}_{kk}(\zeta_i R_j) \equiv 0 \tag{D.5}$$

When drawn on a semi-log paper, the function $\psi^{j}_{k\ell}(wR)$ appears to behave as a straight line away from the minima (Fig. D.1, $k = 0$, $\ell = 1$, $j = 1$). Also the slopes of these straight lines appear to be identical. This phenomenon suggests approximation of the function by using exponential expressions of the kind,

$$\psi^{j}_{k,\,k+1}(\zeta_i r) = U(\zeta_i R_j) \exp(s\zeta_i r) \tag{D.6}$$

$$r \lessgtr \overline{R}$$

where U is the function describing the dependency on the parameter $\zeta_i R_j$, s is the common slope, and $\overline{R}$ is the value of the variable beyond which this approximation is valid.

Figures D.2 and D.3 show the functions $\psi^{1}_{00}(wR)$ and $\psi^{1}_{12}(wR)$. As can be seen, these two functions exhibit the same characteristics as noted above, i.e., linearity on a semi-log paper, and, therefore, can also be approximated by expressions such as Eq. (D.6).

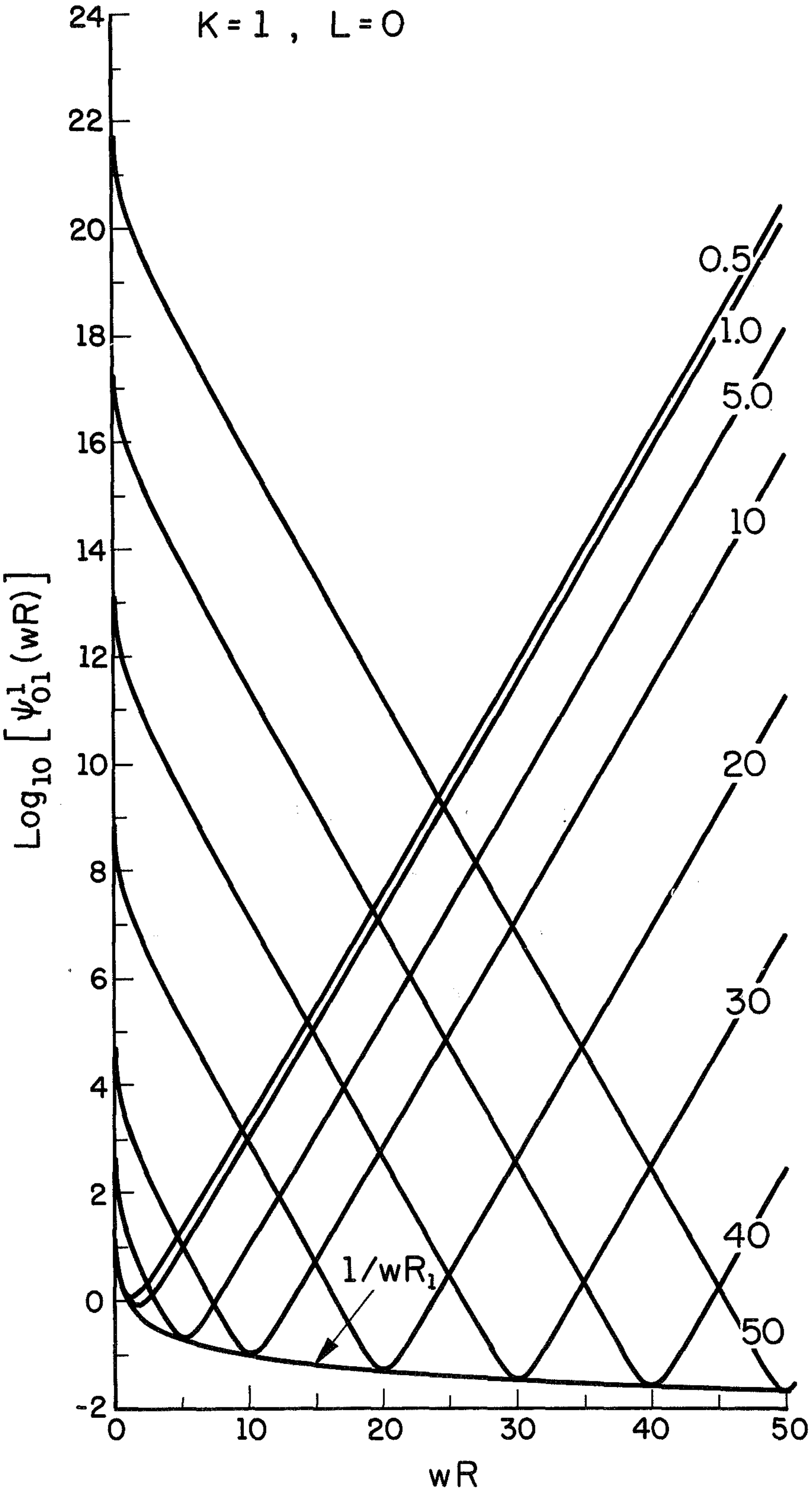

Figure D.1 The function $\psi_{01}^{1}(wR)$ drawn on semi-log paper.

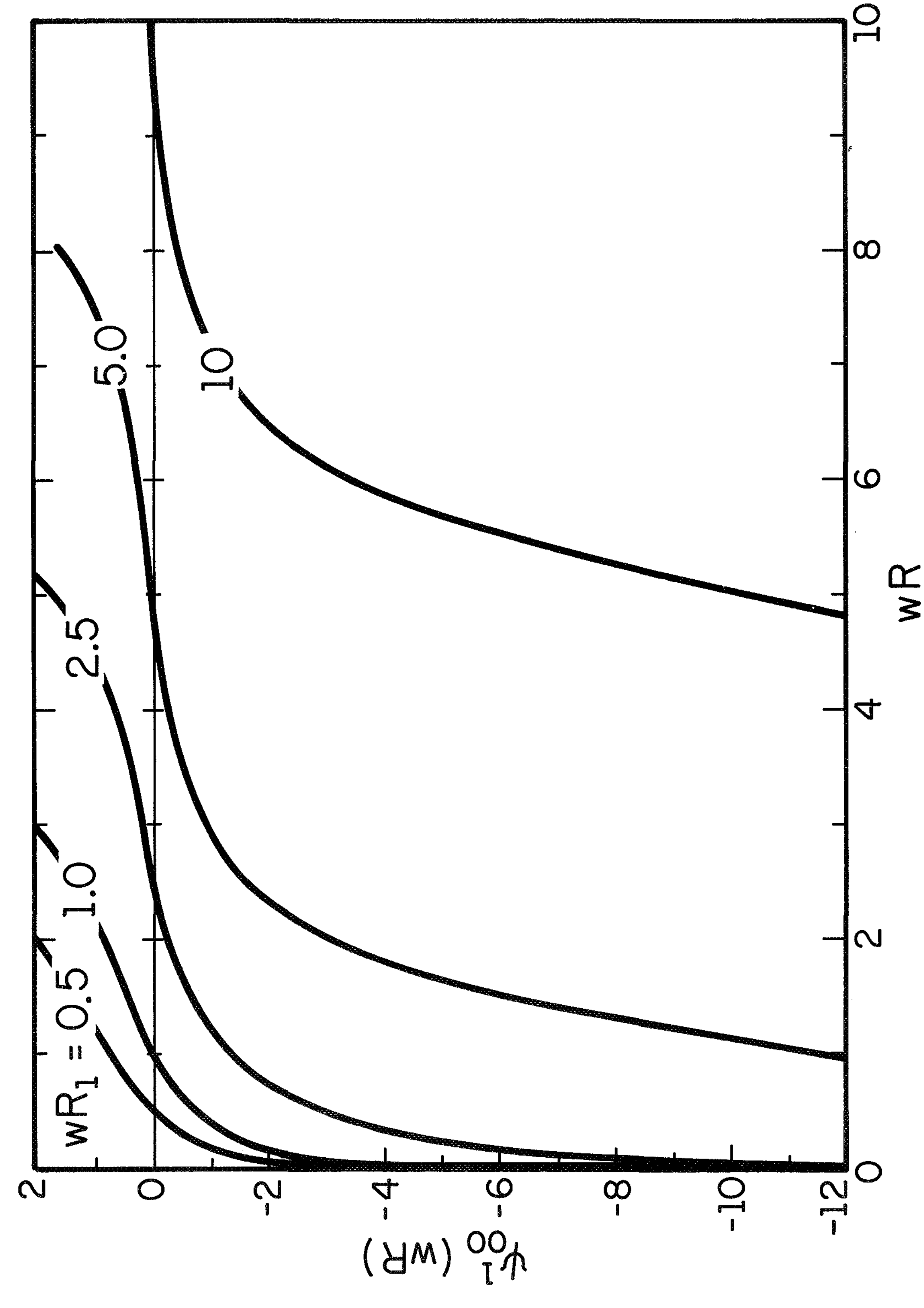

Figure D.2 The function $\psi_{00}^{1}(wR)$.

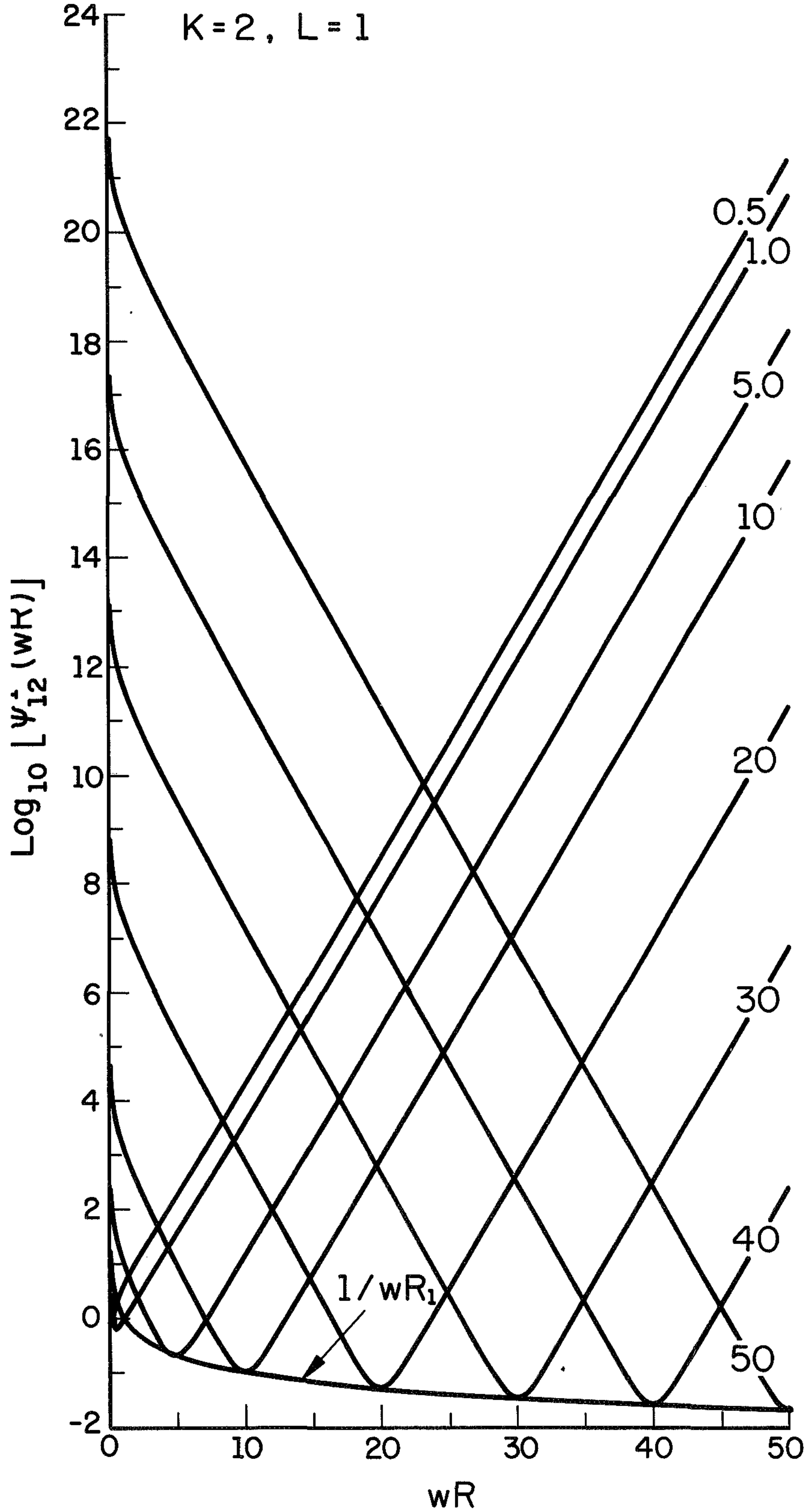

Figure D.3 The function $\psi^{1}_{12}(wR)$ drawn on semi-log paper.

APPENDIX E

STEADY STATE, CYLINDRICAL COORDINATES WITH THE SKIN AND MUSCLE CONSIDERED AS A SINGLE REGION

Combining the two layers into a single, averaged layer yields

$$\frac{1}{r}\frac{\partial}{\partial r}\left(r\,\frac{\partial\theta}{\partial r}\right) + \frac{\partial^2\theta}{\partial z^2} - w^2\theta = -Q \tag{E.1a}$$

$$R_1 \leq r \leq R_2 \ , \quad 0 \leq z \leq a$$

with the boundary conditions,

$$\text{at } r = R_1 \ , \qquad \theta = 0 \tag{E.1b}$$

$$\text{at } r = R_2 \ , \quad \left\{\begin{array}{ll} \dfrac{\partial\theta}{\partial r} = -\dfrac{f(z)}{k} \ , & 0 \leq z < \beta a \\[2ex] \dfrac{\partial\theta}{\partial r} = 0 \ , & \beta a < z \leq a \end{array}\right\} \tag{E.1c}$$

$$\text{at } z = 0 \ , \qquad \frac{\partial\theta}{\partial z} = 0 \tag{E.1d}$$

$$\text{at } z = a \ , \qquad \frac{\partial\theta}{\partial z} = 0 \tag{E.1e}$$

The solution is

$$T(r,z) = T_1 + \frac{Q}{w^2}\left[1 - \frac{\psi^2_{01}(wr)}{\psi^2_{01}(wR_1)}\right] - \frac{\beta f_a}{kw}\,\frac{\psi^1_{00}(wr)}{\psi^2_{01}(wR_1)}$$

$$- \sum_{n=1}^{\infty} \frac{\alpha_n \psi^1_{00}(\zeta r)}{\zeta\psi^2_{01}(\zeta R_1)} \cos\,(\lambda_n z) \tag{E.2}$$

Figure E.1 shows results that were obtained for this case.

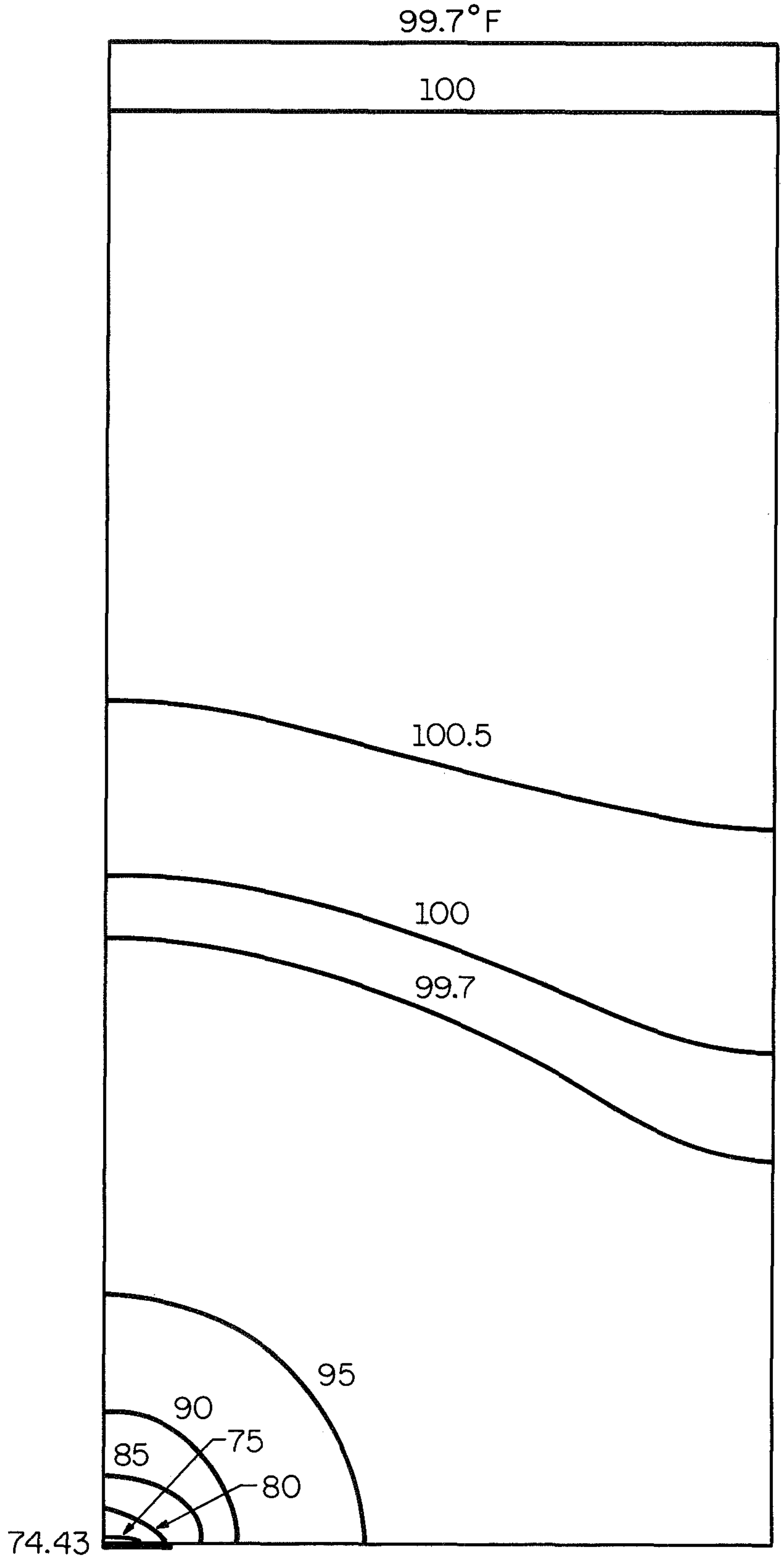

Figure E.1 Steady state temperature distribution in the combined tissue for the cylindrical model (cooling tubes on the skin running perpendicular to the axis of the cylinder). Q_m = 2600 Btu/hr (760 w), β = 0.1, constant temperature at inner core.

Modifying the first boundary condition, Eq. (E.1b), to the constant flux case, that is,

$$\text{at } r = R_1 \text{ , } \frac{\partial\theta}{\partial r} = -\frac{F_o}{k} \tag{E.3}$$

yields

$$T(r,z) = T_1 + \frac{Q}{w^2} - \frac{\beta f_a}{kw}\frac{\psi_{01}^1(wr)}{\psi_{11}^2(wR_1)} - \frac{F_o}{kw}\frac{\psi_{01}^2(wr)}{\psi_{11}^2(wR_1)}$$
$$- \sum_{n=1}^{\infty} \frac{\alpha_n \psi_{01}^1(\zeta r)}{\zeta\psi_{11}^2(\zeta R_1)} \cos(\lambda_n z) \tag{E.4}$$

Because of the cylindrical geometry, an additional parameter appeared; namely, wR_2. If the body is assumed to be represented by one cylinder, an assumption which is equivalent to the rectangular case, three independent combinations arise as R_1 is changed:

(1) The volume and thickness of the cylindrical shell are constant while the skin surface area changes,

$$A = \frac{2V}{b(1 + \rho^*)} \tag{E.5}$$

(2) The volume and surface area of the cylindrical shell are constant while the thickness changes,

$$b = \frac{V}{A} - R_1 + \sqrt{R_1^2 + \left(\frac{V}{A}\right)^2} \tag{E.6}$$

(3) The surface area and the thickness of the cylindrical shell are constant while the volume changes,

$$V = \frac{Ab}{2}[1 + \rho^*] \tag{E.7}$$

where

$$\rho^* \equiv \frac{R_1}{R_2} \tag{E.8}$$

Assuming a uniform flux at the skin, the above three cases were evaluated, as functions of R_1, and are compared to the limiting case as $R_1 \to \infty$ (rectangular case). The results are presented in Figs. E.2, E.3, E.4, and E.5.

For completeness, the limiting cases for no blood flow, $w_b \to 0$, are presented below.

Using limit calculation techniques, it can be shown

$$\lim_{w \to 0} \frac{\psi_{01}^2(wr)}{\psi_{01}^2(wR_1)} = 1 \tag{E.9}$$

$$\lim_{w \to 0} \frac{1}{w^2}\left[1 - \frac{\psi_{01}^2(wr)}{\psi_{01}^2(wR_1)}\right] = \frac{1}{4}(R_1^2 - r^2) + \frac{1}{2}R_2^2 \,\ell n\, \frac{r}{R_1} \tag{E.10}$$

$$\lim_{w \to 0} \frac{1}{w}\frac{\psi_{00}^1(wr)}{\psi_{10}^1(wR_2)} = R_2 \,\ell n\, \frac{r}{R_2} \tag{E.11}$$

and

$$\lim_{w \to 0} \frac{1}{\zeta}\frac{\psi_{00}^1(\zeta r)}{\psi_{10}^1(\zeta R_2)} = \frac{1}{\lambda_n}\frac{\psi_{00}^1(\lambda_n r)}{\psi_{10}^1(\lambda_n R_2)} \tag{E.12}$$

Then, the solution for the cylindrical case with constant temperature at the interface between the combined tissue and the inner core, Eqs. (E.1a) through (E.1e), but w = 0, can be obtained from Eq. (E.2),

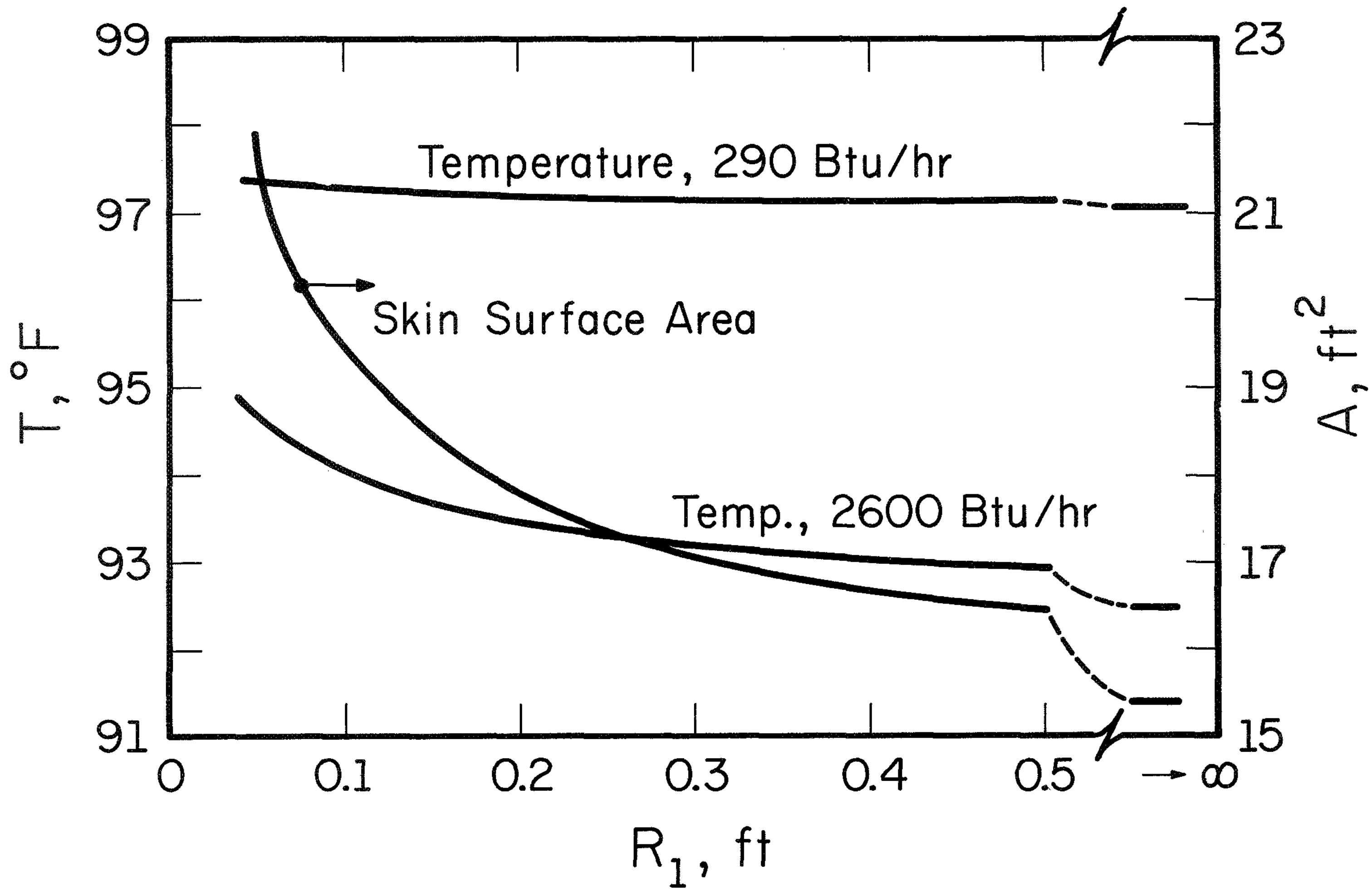

Figure E.2 Steady state temperature and surface area of the skin as functions of R_1 for the one-dimensional cylindrical model. V and b are constant and constant temperature at inner core.

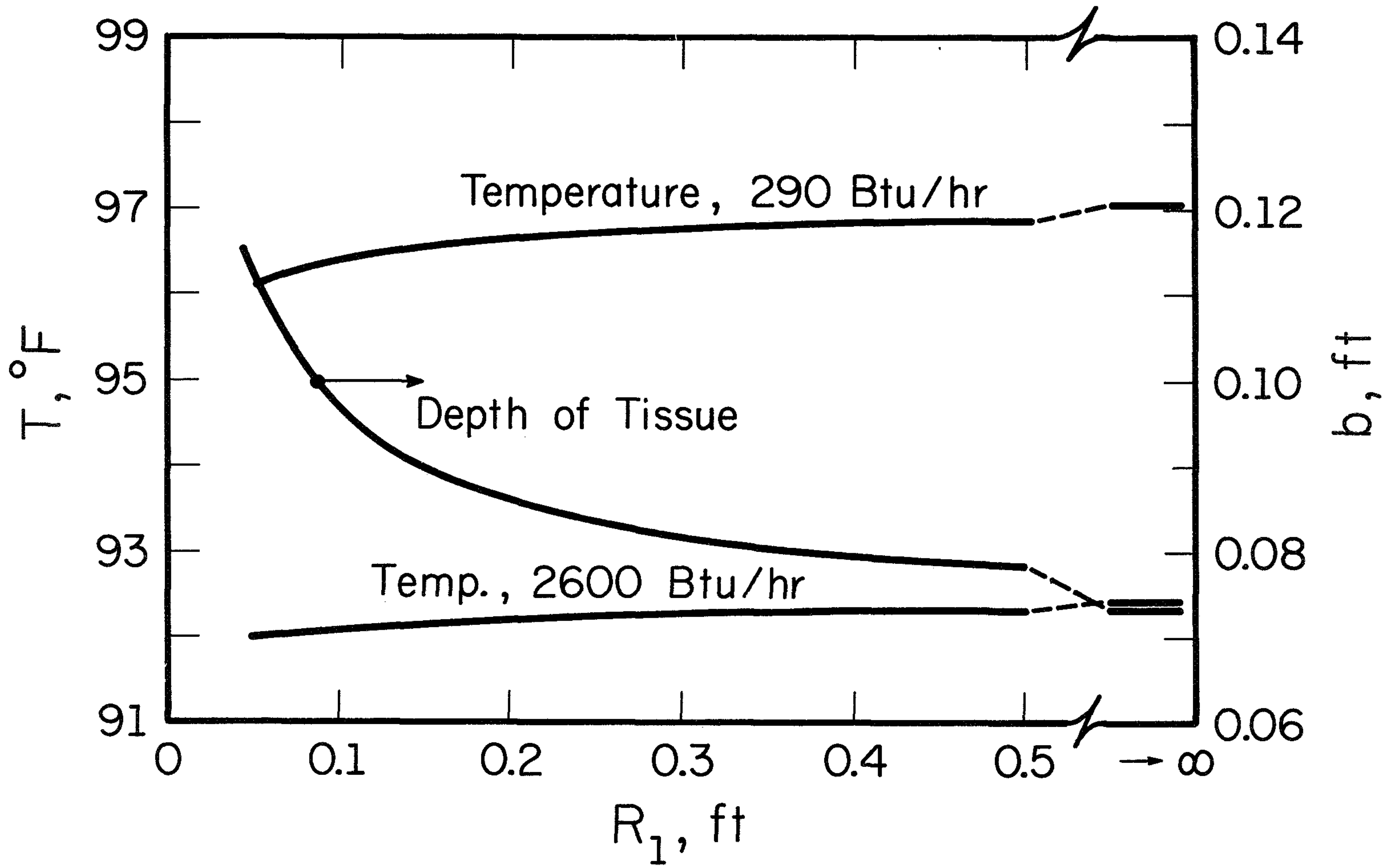

Figure E.3 Steady state temperature of the skin and depth of tissue as functions of R_1 for the one-dimensional cylindrical model. V and A are constant and constant temperature at inner core.

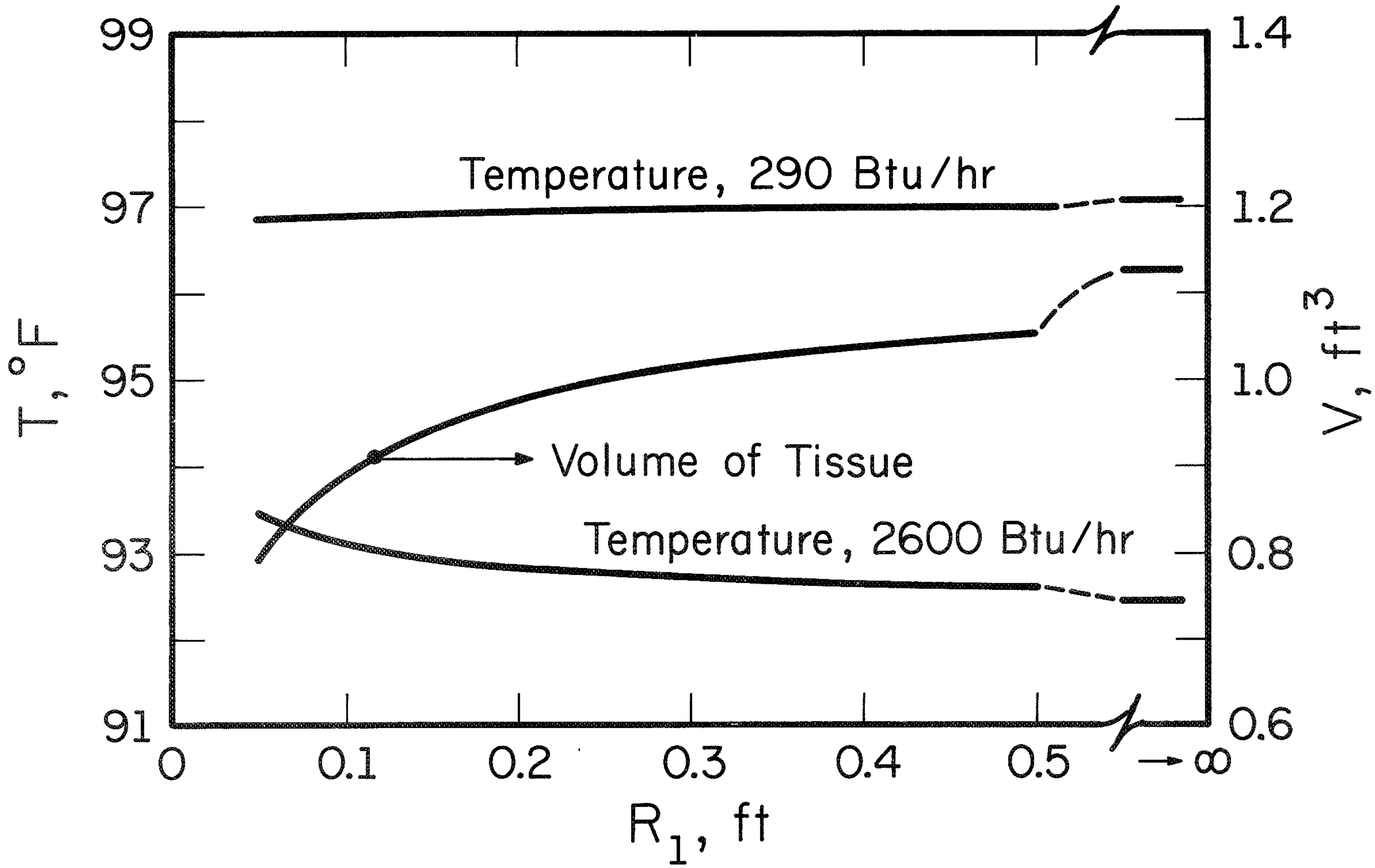

Figure E.4 Steady state temperature of the skin and volume of the tissue as functions of R_1 for the one-dimensional cylindrical model. A and b are constant and constant temperature at inner core.

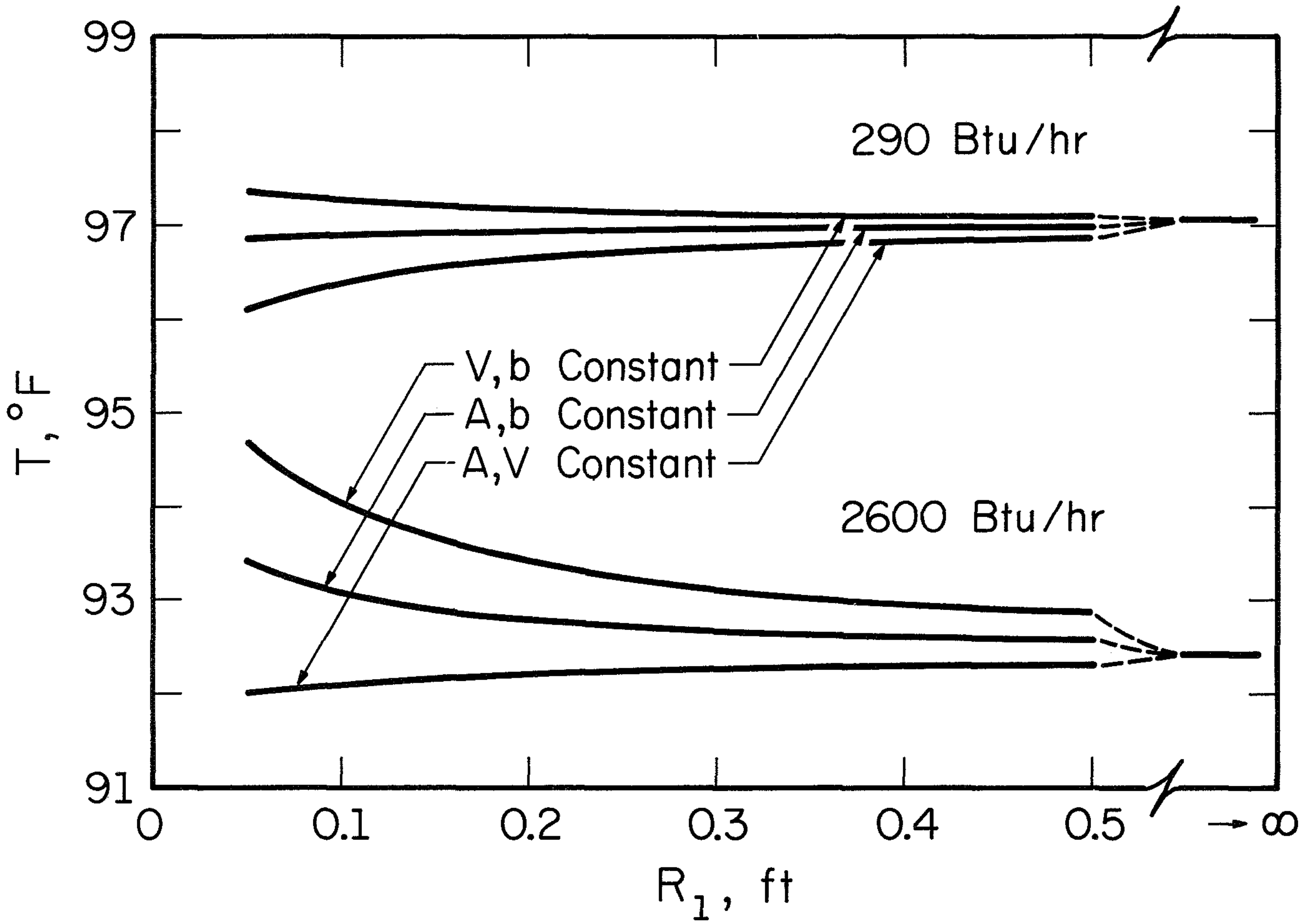

Figure E.5 Steady state temperature of the skin as function of R_1 for the one-dimensional cylindrical model. Constant temperature at inner core.

$$T(r,z) = T_1 + \frac{Q}{4}(R_1^2 - r^2) + \left[\frac{\beta f_a}{k} + \frac{QR_2}{2}\right] R_2 \ \ell n \frac{r}{R_1}$$

$$- \sum_{n=1}^{\infty} \frac{\alpha_n}{\lambda_n} \frac{\psi_{00}^1(\lambda_n r)}{\psi_{10}^1(\lambda_n R_2)} \cos(\lambda_n z) \tag{E.13}$$

Similarly, using the energy balance equation

$$R_2 \beta f_a = R_1 F_o + \frac{Q'}{2}(R_2^2 - R_1^2) \tag{E.14}$$

Eq. (E.4) can be rewritten

$$T(r,z) = T_1 + \frac{Q'}{2R_2 k} \frac{2R_2 \psi_{11}^1(wR_2) - w(R_2^2 - R_1^2)\psi_{01}^1(wr)}{w^2 \psi_{11}^1(wR_2)}$$

$$- \frac{F_o}{R_2} \frac{R_1 \psi_{01}^1(wr) - R_2 \psi_{01}^2(wr)}{w\psi_{11}^1(wR_2)}$$

$$+ \sum_{n=1}^{\infty} \frac{\alpha_n \psi_{01}^1(\zeta r)}{\zeta \psi_{11}^1(\zeta R_2)} \cos(\lambda_n z) \tag{E.15}$$

and, by using limit calculation techniques, it can be shown

$$\lim_{w \to 0} \frac{2R_2 \psi_{11}^1(wR_2) - w(R_2^2 - R_1^2)\psi_{01}^1(wr)}{w^2 \psi_{11}^1(wR_2)} = R_1 R_2 \left[R_1 \ \ell n \ r - \frac{r^2}{2R_1} \right]$$

$$+ R_1 R_2 \left\{ \frac{R_1}{R_2^2 - R_1^2} [R_1^2 \ \ell n \ R_1 - R_2^2 \ \ell n \ R_2] + \frac{R_2^2 + R_1^2}{4R_1} \right\}$$

$$+ R_1(2c_1 - c_3) \tag{E.16}$$

$$\lim_{w \to 0} \frac{R_1 \psi^1_{01}(wr) - R_2 \psi^2_{01}(wr)}{w\psi^1_{11}(wR_2)} = R_1 R_2 \; \ell n \; r$$

$$+ R_1 R_2 \left\{ \frac{R_1^2 \; \ell n \; R_1 - R_2^2 \; \ell n \; R_2}{R_2^2 - R_1^2} + 2c_1 - c_3 \right\} \qquad (E.17)$$

and

$$\lim_{w \to 0} \frac{1}{\zeta} \frac{\psi^1_{01}(\zeta r)}{\psi^1_{11}(\zeta R_2)} = \frac{1}{\lambda_n} \frac{\psi^1_{01}(wr)}{\psi^1_{11}(wR_2)} \qquad (E.18)$$

where

$$c_1 = \frac{\psi(1) + \psi(2) + 2 \; \ell n \; 2}{4} \qquad (E.19)$$

$$c_3 = \ell n \; 2 - \gamma \qquad (E.20)$$

$\psi(n)$ is the Psi or Digamma function and γ is Euler's constant.

Using the above results, the solution for the cylindrical case with constant flux at the interface between the combined tissue and the inner core, Eqs. (E.1a), (E.1c), (E.1d), (E.1e), and (E.3), but $w = 0$, can be obtained from Eq. (E.15),

$$T(r,z) = T_1 + \frac{Q'}{2k} \left[R_1^2 \; \ell n \; r - \frac{r^2}{2} \right] - \frac{F_o R_1}{k} \; \ell n \; r$$

$$+ \frac{R_1}{k} \left[\frac{Q' R_1}{2} - F_o \right] \cdot \left\{ \frac{1}{R_2^2 - R_1^2} [R_1^2 \; \ell n \; R_1 - R_2^2 \; \ell n \; R_2] \right.$$

$$\left. + \frac{1}{2} \right\} + \frac{Q'}{8k} (R_2^2 + R_1^2) + \sum_{n=1}^{\infty} \frac{\alpha_n \psi^1_{01}(wr)}{\lambda_n \psi^1_{11}(wR_2)}$$

$$\cdot \cos(\lambda_n z) \qquad (E.21)$$

APPENDIX F

ADDITIONAL EXPERIMENTAL DATA

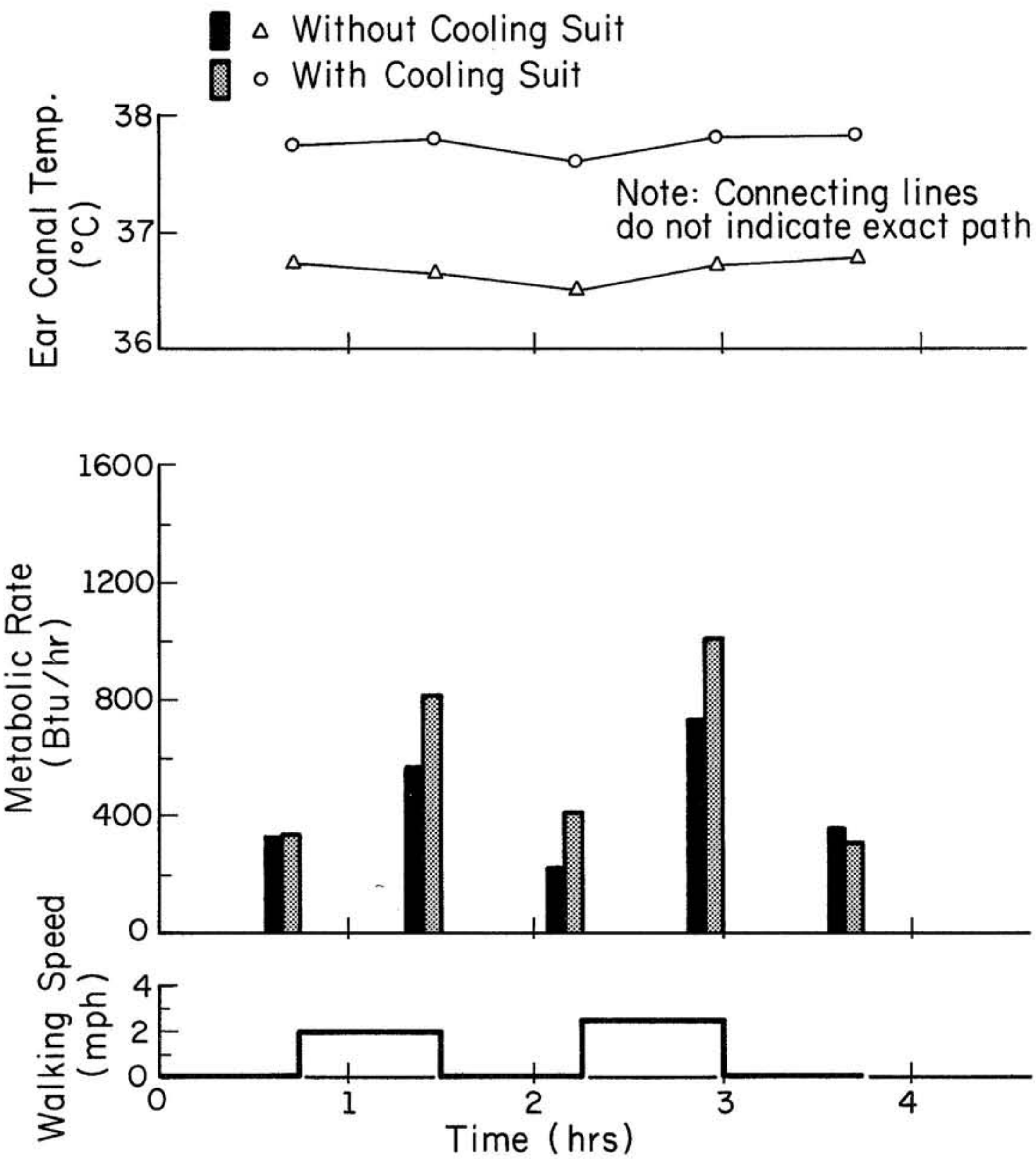

Figure F.1 Metabolic rates and ear canal temperatures of subject SKB for experiments with and without the cooling suit during Schedule I.

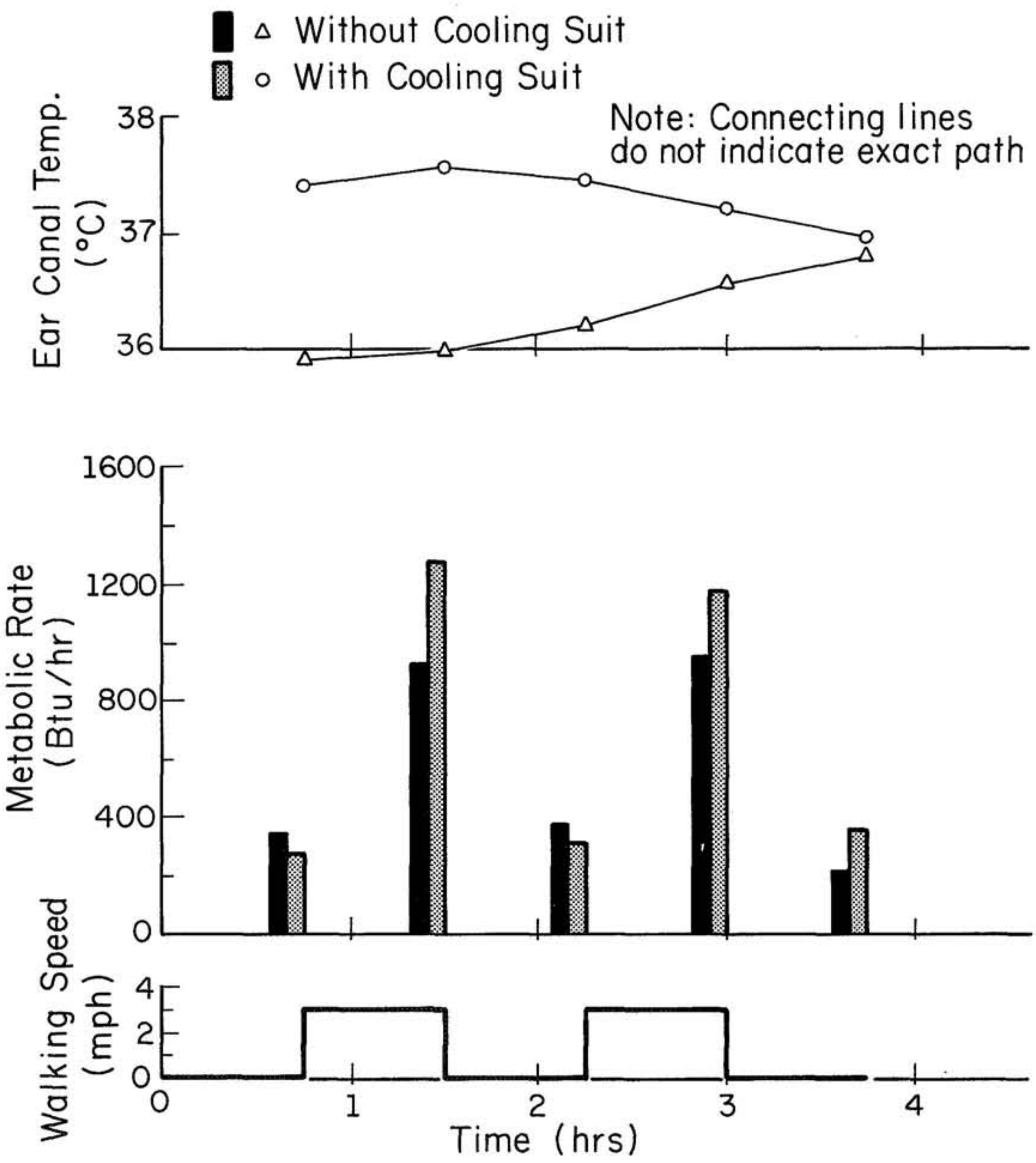

Figure F.2 Metabolic rates and ear canal temperatures of subject SKB for experiments with and without the cooling suit during Schedule II.

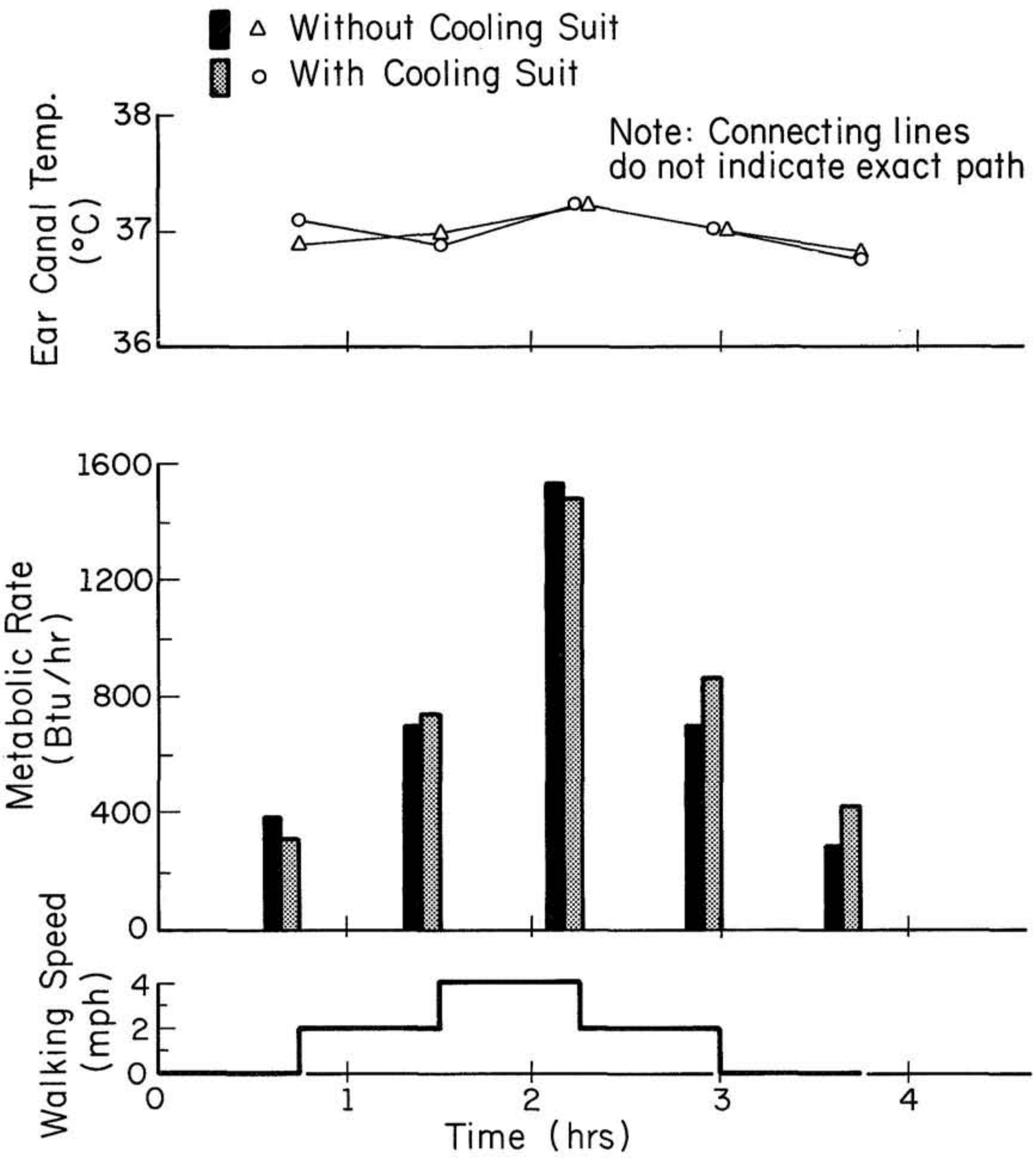

Figure F.3 Metabolic rates and ear canal temperatures of subject SKB for experiments with and without the cooling suit during Schedule III.

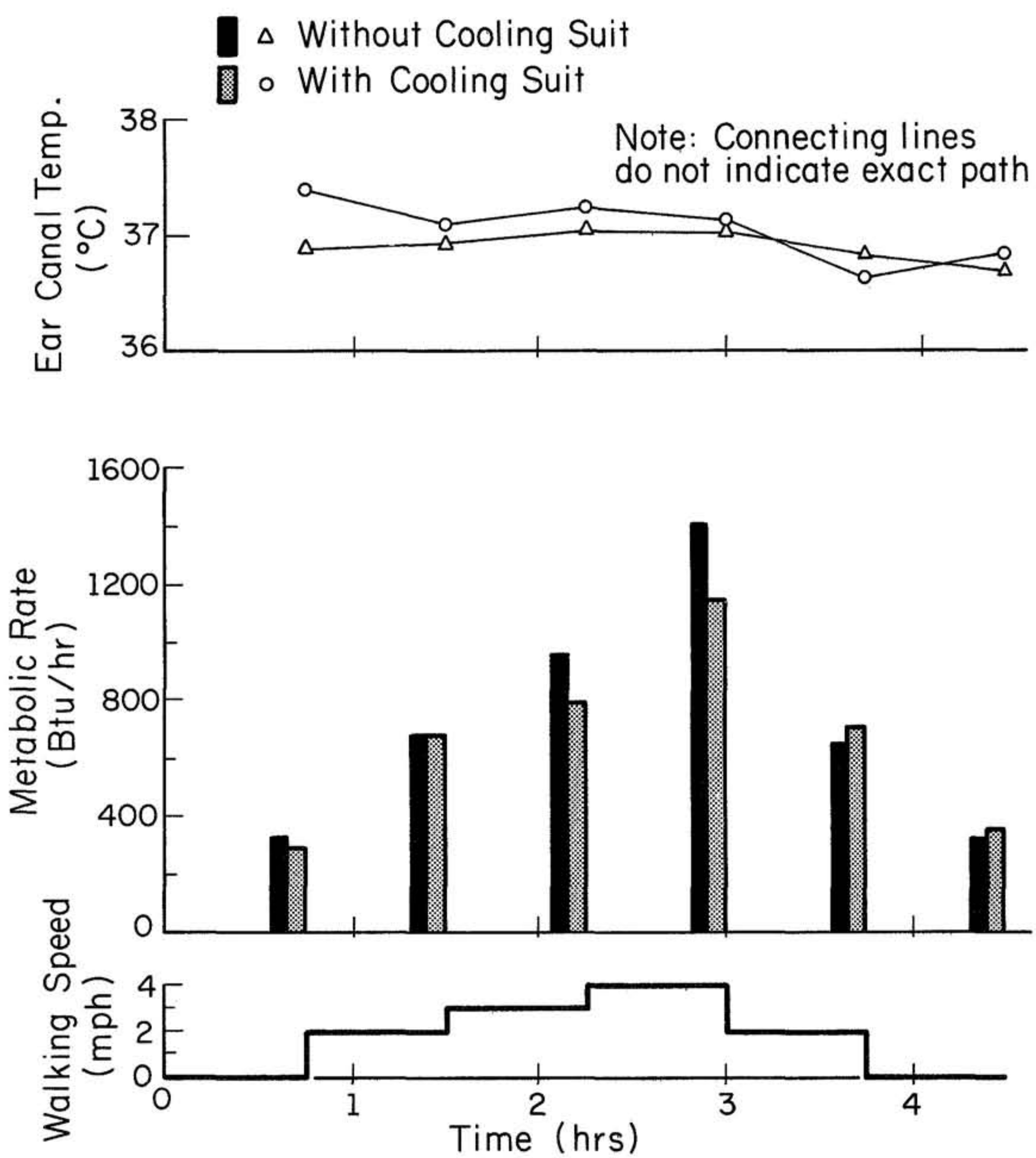

Figure F.4 Metabolic rates and ear canal temperatures of subject SKB for experiments with and without the cooling suit during Schedule IV.

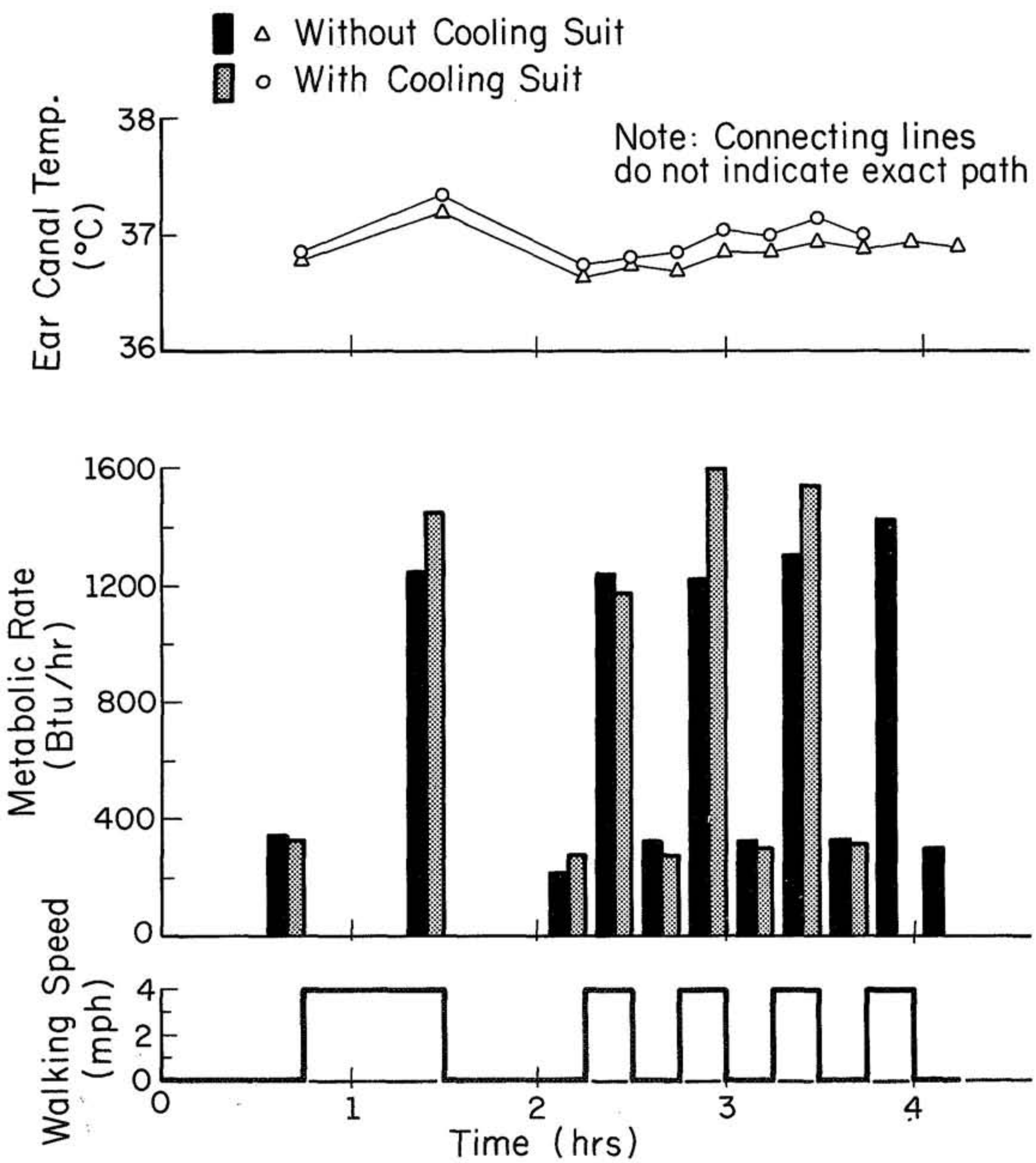

Figure F.5 Metabolic rates and ear canal temperatures of subject SKB for experiments with and without the cooling suit during Schedule V.

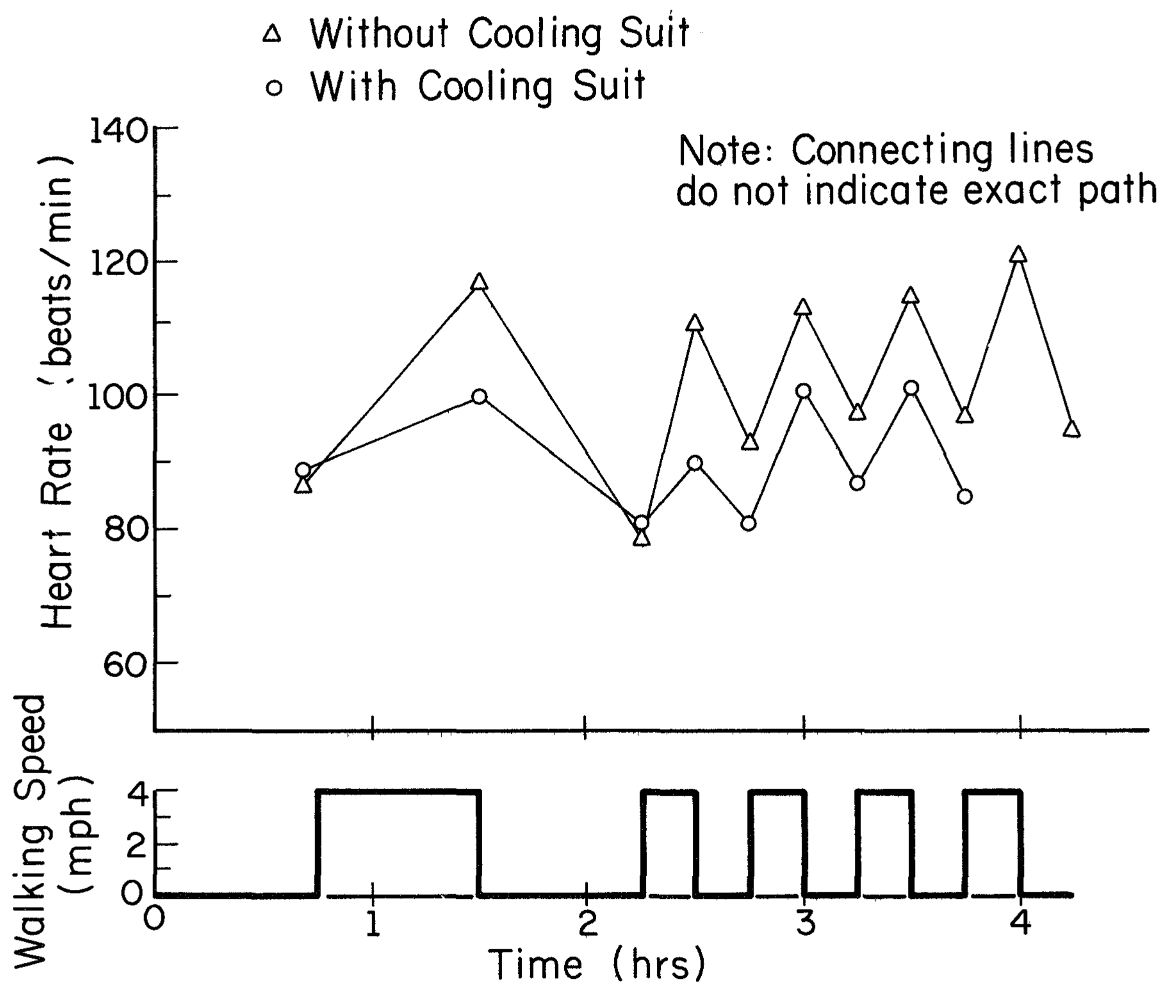

Figure F.6 Heart rates of subject SKB for experiments with and without the cooling suit during Schedule V.

TABLE F.1

MEAN VALUES AND RANGES OF TOTAL METABOLIC RATES, HEAT REMOVED BY SUIT AND BY RESPIRATION AT THE VARIOUS SCHEDULES OF ACTIVITY

Activity		Metabolic Rate Btu/hr-ft^2	Heat Removed by Suit Btu/hr-ft^2	Heat Removed by Respiration Btu/hr-ft^2	Mean Percent Heat Removed	
					Suit	Respiration
SCHEDULE I						
Standing	Mean	17.7	17.9	2.2	--	12.5
	Range	15.0-26.1	12.9-22.4	2.0-3.1		
2 mph	Mean	43.9	22.9	4.2	52.2	9.7
	Range	40.5-50.5	18.3-28.2	3.9-4.9		
Standing	Mean	17.1	15.8	2.3	92.1	13.6
	Range	14.4-22.6	11.6-23.5	1.7-3.3		
2.5 mph	Mean	50.7	19.4	4.7	38.4	9.3
	Range	39.5-60.1	15.8-25.5	4.1-7.3		
Standing	Mean	18.0	15.1	2.3	83.8	12.6
	Range	17.0-18.8	12.8-18.3	2.0-3.3		

(continued)

TABLE F.1 continued

Activity		Metabolic Rate Btu/hr-ft^2	Heat Removed by Suit Btu/hr-ft^2	Heat Removed by Respiration Btu/hr-ft^2	Mean Percent Heat Removed	
					Suit	Respiration
SCHEDULE II						
Standing	Mean	17.0	17.0	1.9	100.0	11.3
	Range	14.8-19.6	14.5-23.4	1.3-2.5		
3 mph (w/o additional cooling)	Mean	62.6	24.5	5.4	39.1	8.7
	Range	54.3-69.5	21.1-26.4	3.0-8.7		
Standing	Mean	16.1	20.2	2.4	--	14.8
	Range	12.9-17.9	15.0-23.3	1.3-4.2		
3 mph (with additional cooling)	Mean	54.8	30.7	4.9	56.0	9.0
	Range	42.9-64.6	24.9-37.9	2.3-7.1		
Standing	Mean	16.0	20.1	2.1	--	12.9
	Range	11.8-19.6	15.6-28.2	1.2-3.5		

(continued)

TABLE F.1 continued

Activity		Metabolic Rate Btu/hr-ft^2	Heat Removed by Suit Btu/hr-ft^2	Heat Removed by Respiration Btu/hr-ft^2	Mean Percent Heat Removed	
					Suit	Respiration
SCHEDULE III						
Standing	Mean	16.6	13.3	2.3	80.0	13.9
	Range	12.3-20.3	11.2-15.3	1.2-3.1		
2 mph	Mean	41.2	18.8	3.9	45.6	9.4
	Range	27.2-48.8	14.7-28.7	2.8-4.8		
4 mph	Mean	89.4	45.5	7.4	50.9	8.3
	Range	80.7-100.3	30.0-60.5	5.2-9.6		
2 mph	Mean	46.8	23.6	4.0	50.5	8.5
	Range	35.5-56.7	21.3-26.0	2.6-6.4		
Standing	Mean	18.4	14.2	2.4	77.2	13.2
	Range	11.8-23.8	6.6-21.9	1.3-4.6		

(continued)

TABLE F.1 continued

Activity		Metabolic Rate Btu/hr-ft^2	Heat Removed by Suit Btu/hr-ft^2	Heat Removed by Respiration Btu/hr-ft^2	Mean Percent Heat Removed	
					Suit	Respiration
SCHEDULE IV						
Standing	Mean	15.7	19.5	1.8	--	11.6
	Range	14.2-15.9	11.5-23.3	1.3-2.3		
2 mph	Mean	41.1	24.9	3.6	60.6	8.9
	Range	27.0-47.7	16.7-31.7	2.4-5.0		
3 mph	Mean	51.0	35.5	4.4	69.5	8.6
	Range	33.0-61.2	31.1-41.4	3.0-5.9		
4 mph	Mean	85.7	49.0	7.7	57.1	9.0
	Range	62.5-98.8	35.7-60.7	4.2-10.0		
2 mph	Mean	46.1	23.4	3.6	50.8	7.7
	Range	38.9-52.2	17.5-30.5	3.1-4.6		
Standing	Mean	16.0	16.4	2.1	--	13.4
	Range	12.9-19.6	9.1-23.5	1.2-3.9		

(continued)

TABLE F.1 continued

Activity		Metabolic Rate Btu/hr-ft^2	Heat Removed by Suit Btu/hr-ft^2	Heat Removed by Respiration Btu/hr-ft^2	Mean Percent Heat Removed	
					Suit	Respiration
SCHEDULE V						
Standing	Mean	16.1	20.6	2.1	--	13.0
	Range	13.7-17.9	12.9-31.6	1.2-3.1		
4 mph	Mean	91.1	50.9	6.6	55.8	7.3
	Range	78.8-101.4	37.6-61.5	3.5-8.9		
Standing	Mean	15.1	20.9	1.9	--	12.6
	Range	14.1-17.2	10.0-29.0	1.4-2.4		
4 mph	Mean	82.4	29.8	6.1	36.1	7.4
	Range	64.3-98.7	26.1-36.8	3.4-8.9		
Standing	Mean	15.2	28.2	1.9	--	12.2
	Range	13.8-18.0	27.0-31.3	1.3-2.3		
4 mph	Mean	86.8	40.3	6.4	46.4	7.4
	Range	72.4-100.6	28.1-59.3	3.5-8.8		

(continued)

TABLE F.1 continued

Activity		Metabolic Rate Btu/hr-ft^2	Heat Removed by Suit Btu/hr-ft^2	Heat Removed by Respiration Btu/hr-ft^2	Mean Percent Heat Removed	
					Suit	Respiration
SCHEDULE V cont.						
Standing	Mean	17.4	31.8	1.9	--	10.8
	Range	14.9-23.3	22.5-37.3	1.3-3.0		
4 mph	Mean	87.3	41.4	6.6	47.4	7.5
	Range	69.8-103.8	34.4-44.8	3.2-9.0		
Standing	Mean	18.3	34.8	2.3	--	12.3
	Range	15.9-21.2	22.8-42.8	1.6-2.9		
4 mph	Mean	90.1	42.5	6.6	47.1	7.3
	Range	72.7-101.6	34.6-50.9	4.0-9.2		
Standing	Mean	18.3	32.2	2.0	--	10.9
	Range	17.1-19.3	27.4-35.9	1.6-2.6		

TABLE F.2

MEAN VALUES AND RANGES OF WATER INLET TEMPERATURES FOR THE VARIOUS REGIONS AT DIFFERENT SCHEDULES OF ACTIVITY

Activity		Water Inlet Temperature, deg C					
		Region					
		Head	Arms	Upper Torso	Lower Torso	Thighs	Lower Legs
SCHEDULE I†							
Standing	Mean	19.6	24.9	22.7	23.1	24.5	23.8
	Range	12.6-22.9	22.1-29.4	12.7-28.9	12.8-28.5	22.6-28.2	20.2-27.6
2 mph	Mean	19.3	24.8	25.5	23.4	24.2	24.4
	Range	14.5-23.3	22.3-28.2	20.8-31.1	14.3-31.4	22.1-29.6	19.7-29.6
Standing	Mean	19.5	25.6	26.5	23.8	26.0	25.3
	Range	15.2-24.1	22.1-29.0	21.2-32.9	15.1-33.2	22.0-31.7	19.5-31.0
2.5 mph	Mean	19.6	25.5	26.3	24.2	25.7	25.2
	Range	15.7-24.6	21.5-28.7	21.0-32.6	15.5-33.6	20.9-31.7	19.0-30.9
Standing	Mean	20.3	25.0	25.8	24.3	25.3	24.7
	Range	15.9-24.6	21.3-27.6	20.5-32.1	15.8-34.1	21.2-31.0	19.0-30.3

†Averages of 5 runs.

(continued)

TABLE F.2 continued

Activity		Water Inlet Temperature, deg C					
		Region					
		Head	Arms	Upper Torso	Lower Torso	Thighs	Lower Legs
SCHEDULE II†							
Standing	Mean	24.0	24.8	24.3	26.5	23.6	28.8
	Range	15.5-33.1	21.7-27.6	20.2-28.6	21.4-30.1	21.5-25.7	26.3-31.1
3 mph (w/o additional cooling)	Mean	22.8	24.8	24.3	26.2	23.7	28.7
	Range	15.5-29.1	21.7-28.5	20.6-29.2	21.8-29.8	21.2-26.0	26.4-31.8
Standing	Mean	22.2	23.6	24.1	25.8	22.4	26.4
	Range	15.2-29.7	22.3-26.2	20.6-27.2	21.8-28.6	19.1-25.3	18.2-31.4
3 mph (with additional cooling)	Mean	20.8	20.1	20.7	23.3	18.6	21.7
	Range	14.9-26.1	14.8-23.0	14.8-22.6	17.5-29.1	17.0-19.3	16.9-29.5
Standing	Mean	21.8	22.2	24.1	26.3	22.0	22.1
	Range	15.0-34.4	19.8-25.8	22.0-28.8	24.4-28.5	19.0-26.6	17.4-28.6

†Averages of 5 runs.

(continued)

TABLE F.2 continued

Activity		Water Inlet Temperature, deg C					
		Region					
		Head	Arms	Upper Torso	Lower Torso	Thighs	Lower Legs
SCHEDULE III†							
Standing	Mean	22.5	25.7	27.8	26.5	26.9	28.3
	Range	18.4-26.0	19.1-29.1	22.3-32.2	24.6-29.0	23.2-29.8	25.9-31.3
2 mph	Mean	19.5	25.3	25.1	26.7	25.3	28.3
	Range	16.6-25.1	19.7-30.1	22.1-29.5	23.4-29.0	21.9-30.4	25.8-33.4
4 mph	Mean	17.0	18.7	17.9	18.2	18.8	18.6
	Range	16.1-18.4	16.0-27.1	16.0-22.9	16.0-25.6	16.0-28.6	16.0-27.7
2 mph	Mean	19.5	22.0	19.2	21.0	23.8	20.2
	Range	16.3-25.2	16.5-27.2	16.5-23.0	16.6-25.6	16.7-32.5	16.6-27.8
Standing	Mean	21.6	22.5	21.6	24.1	25.3	21.7
	Range	16.3-28.4	16.5-28.6	16.5-24.9	16.8-29.2	19.4-33.5	16.6-29.3

†Averages of 5 runs.

(continued)

TABLE F.2 continued

Activity		Water Inlet Temperature, deg C — Region: Head	Arms	Upper Torso	Lower Torso	Thighs	Lower Legs
SCHEDULE IV†							
Standing	Mean	22.9	27.6	26.7	25.0	23.8	25.6
	Range	17.3-28.2	21.2-36.6	25.1-28.4	19.1-29.4	19.7-31.7	19.3-30.8
2 mph	Mean	23.3	25.1	26.0	24.8	22.4	24.2
	Range	17.1-32.1	19.0-31.3	22.6-28.3	20.1-27.7	20.7-25.0	20.4-30.5
3 mph	Mean	22.3	23.6	24.8	21.5	19.5	22.6
	Range	17.4-25.1	18.6-29.0	20.6-28.1	17.2-25.0	17.3-23.2	17.6-30.5
4 mph	Mean	16.9	19.7	19.6	18.5	18.1	18.2
	Range	16.2-17.3	16.6-30.3	17.0-29.0	16.5-25.8	16.6-23.4	16.6-23.9
2 mph	Mean	18.9	22.2	21.9	20.9	19.8	19.5
	Range	17.1-23.2	16.8-29.6	17.3-28.5	16.8-25.4	17.0-23.2	16.8-23.6
Standing	Mean	23.7	26.5	25.4	24.9	22.5	22.3
	Range	17.2-32.5	22.0-29.5	22.2-28.9	20.5-29.1	20.9-24.7	19.9-24.6

†Averages of 5 runs.

(continued)

TABLE F.2 continued

Activity		Water Inlet Temperature, deg C					
		Region					
		Head	Arms	Upper Torso	Lower Torso	Thighs	Lower Legs
SCHEDULE V†							
Standing	Mean	22.1	24.9	25.3	28.0	25.7	26.9
	Range	19.0-25.4	19.7-32.6	20.5-29.9	24.7-31.4	21.8-27.8	25.0-29.0
4 mph	Mean	17.0††	20.2	18.3	19.7	16.9	16.8
	Range	16.8-17.4	16.6-30.1	17.1-21.1	16.5-21.1	16.7-17.2	16.5-17.1
Standing	Mean	19.8	23.1	27.2	26.1	24.0	20.6
	Range	17.8-21.7	17.1-25.6	17.6-38.6	17.4-34.5	21.0-25.4	17.6-25.2
4 mph	Mean	19.6	23.0	27.0	23.2	21.9	18.6
	Range	17.2-21.5	16.8-25.5	17.3-38.0	16.8-34.4	16.9-25.4	16.8-22.5
Standing	Mean	19.7	22.9	25.9	23.3	21.9	18.5
	Range	17.0-21.8	16.7-25.4	17.2-33.6	16.7-35.0	16.8-25.4	16.6-22.0
4 mph	Mean	19.4	21.9	23.2	21.7	20.6	18.4
	Range	17.1-21.4	16.8-26.0	17.3-27.8	16.8-29.1	16.9-24.4	16.7-21.9

†Averages of 4 runs.

††Averages of 3 runs.

(continued)

TABLE F.2 continued

Activity		Water Inlet Temperature, deg C — Region: Head	Arms	Upper Torso	Lower Torso	Thighs	Lower Legs
SCHEDULE V cont.†							
Standing	Mean	19.2	21.7	22.8	21.4	20.3	17.9
	Range	16.8-21.3	16.6-25.6	17.1-26.9	16.5-28.5	16.7-24.2	16.5-21.4
4 mph	Mean	19.3	21.7	22.8	21.4	20.4	18.2
	Range	16.9-21.4	16.7-25.6	17.2-27.0	16.7-28.3	16.8-24.4	16.6-21.4
Standing	Mean	19.3	21.8	23.0	21.4	20.4	18.3
	Range	17.1-21.1	16.9-26.1	17.4-27.7	16.9-28.0	17.0-24.0	16.8-21.5
4 mph	Mean	18.1	21.8	20.3	19.8††	20.0	18.6
	Range	17.3-19.8	17.0-28.1	17.4-22.6	17.0-25.3	17.0-22.1	16.9-23.0
Standing	Mean	18.7	21.5	21.1	19.3††	20.3	18.4
	Range	17.2-20.1	16.9-26.3	17.5-22.8	17.0-24.1	17.0-22.7	16.9-22.3

†Averages of 4 runs.

††Averages of 3 runs.

LIST OF REFERENCES

1. Chambers, A. B., "Controlling Thermal Comfort in the EVA Space Suit," ASHRAE Journal, Vol. 12, 1970, pp. 33-38.

2. Billingham, J., "Heat Exchange Between Man and His Environment on the Surface of the Moon," Journal of the British Interplanetary Society, Vol. 17, 1959, pp. 297-300.

3. Best, C. H. and Taylor, N. B., The Living Body, Holt, Reinhardt and Winston, Fourth Edition, 1958, pp. 11-12, 377.

4. Lavoisier, A. L., "Experiences sur la Respiration des Animaux," Memoire de l'Academie des Sciences, 1777.

5. Burton, A. C., "The Application of the Theory of Heat Flow to The Study of Energy Metabolism," Journal of Nutrition, Vol. 7, 1934, pp. 497-533.

6. Eichna, L. W., Ashe, W. F., Bean, W. B., and Shelley, W. B., "The Upper Limits of Environmental Heat and Humidity Tolerated by Acclimatized Men Working in Hot Environments," Journal of Industrial Hygiene and Toxicology, Vol. 27, 1945, pp. 59-84.

7. Machle, W., and Hatch, T. F., "Heat: Men's Exchanges and Physiological Response," Physiological Review, Vol. 27, 1947, pp. 200-227.

8. Pennes, H. H., "Analysis of Tissue and Arterial Blood Temperature in the Resting Human Forearm," Journal of Applied Physiology, Vol. 1, 1948, pp. 93-122.

9. Wyndham, W., Bouwer, N., Devine, M. G., Patterson, H. E., and Macdonald, D. K. C., "Examination of Use of Heat Exchange Equations for Determining Changes in Body Temperature," Journal of Applied Physiology, Vol. 5, 1952, pp. 299-307.

10. Hertzman, A. B., "Some Relations between Skin Temperature and Blood Flow," American Journal of Physical Medicine, Vol. 32, 1953, pp. 233-251.

11. Taylor, C. L., "Heat Transfer Applications in the Human Body," Mechanical Engineering, Vol. 77, 1955, pp. 511-513.

12. Herrington, L. P., "The Biotechnical Problem of the Human Body as a Heat Exchanger," Transactions ASME, Vol. 80, 1958, pp. 343-346.

13. Herrington, L. P., "Full Scale Human-Body-Model Thermal Exchange Compared with Equational Condensation of Human Calorimetric Data," Journal of Heat Transfer, Vol. 81, Ser. C, 1959, pp. 187-194.

14. Westland, R. A., "A Biothermal Analog," U.C.L.A. Master's Thesis, 1958.

15. Osman, D. B., "An Electrical Analog of the Biothermal System," U.C.L.A. Master's Thesis, 1962.

16. Wyndham, C. H., and Atkins, A. R., "An Approach to the Solution of the Human Biothermal Problem with the Aid of an Analogue Computer," Proceedings of the Third International Conference on Medical Electronics, London, England, 1960, pp. 32-38.

17. Crosbie, R. J., Hardy, J. D., and Fessenden, E., "Electrical Analog Simulation of Temperature Regulation in Man," in Temperature, Its Measurement and Control in Science and Industry, J. D. Hardy, editor, Vol. 3, Part 3, Reinhold, New York, 1963, pp. 627-635.

18. Wissler, E. H., "Steady State Temperature Distribution in Man," Journal of Applied Physiology, Vol. 16, 1961, pp. 734-740.

19. Wissler, E. H., "An Analysis of Factors Affecting Temperature Levels in the Nude Human," in Temperature, Its Measurement and Control in Science and Industry, J. D. Hardy, editor, Vol. 3, Part 3, Reinhold, New York, 1963, pp. 603-612.

20. Wissler, E. H., "A Mathematical Model of the Human Thermal System," Bulletin of Mathematical Biophysics, Vol. 26, 1964, pp. 147-166.

21. Wissler, E. H., "Comparison of Computer Results from Two Mathematical Models--A Simple 14-Node Model and a Complex 250 Node Model," Symposium International de Thermoregulation Comportementale, Lyon, France, 7-11, September 1970.

22. Perl, W., "Heat and Matter Distribution in Body Tissues and the Determination of Tissue Blood Flow by Local Clearance Methods," Journal of Theoretical Biology, Vol. 2, 1962, pp. 201-235.

23. Perl, W., "An Extension of the Diffusion Equation to Include Clearance by Capillary Blood Flow," Annals of the New York Academy of Science, Vol. 108, 1963, pp. 92-105.

24. Perl, W., and Cucinell, S. A., "Local Blood Flow in Human Leg Muscle Measured by a Transient Response Thermoelectric Method," Biophysical Journal, Vol. 5, 1965, pp. 211-230.

25. Perl, W., and Hirsch, R. L., "Local Blood Flow in Kidney Tissue by Heat Clearance Measurement," Journal of Theoretical Biology, Vol. 10, 1966, pp. 251-280.

26. Brown, A. C., "Analog Computer Simulation of Temperature Regulation in Man," Technical Documentary Report AMRL-TDR-63-116, Aerospace Medical Research Laboratories, Wright-Patterson AFB, Ohio, 1963.

27. Brown, A. C., "Further Development of the Biothermal Analog Computer," Final Report AMRL-TR-66-197, Medical Research Laboratories, Wright-Patterson AFB, Ohio, 1966.

28. Layne, R. S., and Barker, R. S., "Digital Computer Simulation of the Biothermal Man," Paper No. 3369, Douglas Missile and Spacecraft Division, 1965.

29. Stolwijk, A. J. A., and Cunningham, D. J., "A Study of Heat Exchange between Man and His Environment in Project Apollo," Contract No. NAS-9-4522, Final Report, John B. Pierce Foundation.

30. Birkebak, R. C., Cremers, C. J., and Lafebre, E. A., "Heat Transfer Applied to Animal Systems," Transactions ASME, Ser. C., Vol. 88, 1966, pp. 125-130.

31. Stolwijk, A. J. A., and Hardy, J. D., "Temperature Regulation in Man--A Theoretical Study," Pflügers Archiv. f.d. gesamte Physiologie des Menschen und der Tiere, Vol. 291, 1965, pp. 129-162.

32. Guy, A. W., and Lehman, J. F., "Determination of Electromagnetic Heating Patterns in Human Tissue by Thermographic Studies on Phantom Models," Digest of the Seventh International Conference on Medical and Biological Engineering, Stockholm, Sweden, 1967.

33. Chan, A. K., Sigelmann, R. A., Guy, A. W., and Lehman, J. F., "Thermal Effect Due to Propagation of Acoustic Waves in Biological Materials," Proceedings of the Twenty-First Annual Conference on Engineering in Medicine and Biology, Houston, Texas, 1968, p. 19.3.

34. Ho, H. S., Guy, A. W., Sigelmann, R. A., and Lehman, J. F., "Electromagnetic Heating Patterns in Circular Cylindrical Models of Human Tissue," Proceedings of the Twenty-Second Annual Conference on Engineering in Medicine and Biology, 1969, Chicago, Illinois. p. 27.4.

35. Chan, A. K., Sigelmann, R. A., Guy, R. W., and Lehman, J. F., "Calculation of Temperature Distribution in Layered Tissue due to Distributed Thermal Sources by Finite Difference Method," Proceedings of the Twenty-Second Annual Conference on Engineering in Medicine and Biology, Chicago, Illinois, 1969, p. 27-3.

36. Richardson, P. D., and Whitelaw, J. H., "Transient Heat Transfer in Human Skin," Journal of The Franklin Institute, Vol. 286, 1968, pp. 169-181.

37. Gros, C., and Gautherie, "Etudi par Thermometrie Infrarouge de l'Evolution au Cours du Temps des Temperatures Cutnee's Humaines en Fonction de la Temperature Ambiante. Notion de'Adaptance Thermique Cutanee," Revue Francaise Etudes Cliniques et Biologiques, Vol.13, 1968, pp. 697-703.

38. Mitchell, J. W., and Myers, G. E., "Analytical Model of the Countercurrent Heat Exchange Phenomena," Biophysical Journal, Vol. 8, 1968, pp. 897-911.

39. Buchberg, H., and Harrah, C. B., "Conduction Cooling of the Human Body--A Biothermal Analysis," Thermal Problems in Biotechnology, ASME Symposium Series, New York, 1968, pp. 82-95.

40. Chato, J. C., "A Method for the Measurement of Thermal Properties of Biological Materials," Thermal Properties in Biotechnology, ASME Symposium Series, 1968, pp. 16-25.

41. Trezek, G. J., and Jewett, D. L., "Thermal Modeling of Cylindrical Source Transient Temperature Field in Brain," Proceedings of the Twenty-First Annual Conference on Engineering in Medicine and Biology, Houston, Texas, 1967, p. 53.4.

42. Trezek, G. J., and Cooper, T. E., "Analytical Determination of Cylindrical Source Temperature Fields and Their Relation to Thermal Diffusivity of Brain Tissue," Thermal Problems in Biotechnology, ASME Symposium Series, 1968, pp. 1-15.

43. Trezek, G. J., "Thermal and Electrical Modeling for Brain Surgical Probes," ASME Paper No. 69-WA/HT-40, 1969.

44. Cooper, T. E., "Bio-Heat Transfer Studies," University of California at Berkeley, Ph.D. Thesis, 1970.

45. Priebe, L., and Betz, E., "Wärmetransport in Homogen und Isotrop Durchbluteten Gewebe," Ärzliche Forschung, Vol. 10, 1969, pp. 18-30.

46. Keller, K. H., and Seiler, L., Jr., "An Analysis of Peripheral Heat Transfer in Humans," Simulation Council Meeting, Chicago, Illinois, March 9-10, 1970.

47. Nunneley, S. A., "Water Cooled Garments: A Review," to appear in Space Life Sciences.

48. Webb, P., editor, Bioastronautics Data Book, NASA Scientific and Technical Information Division, Washington, D.C., 1964.

49. Chato, J. C., "A Survey of Thermal Conductivity and Diffusivity Data on Biological Materials," ASME Paper No. 66-WA/HT-37, 1966.

50. Chato, J. C., "Heat Transfer in Bioengineering," in Advanced Heat Transfer, B. T. Chao, editor, University of Illinois Press, 1969, pp. 359-403.

51. Pond, J. B., "A Study of the Biological Action of Focused Mechanical Waves (Focused Ultrasound)," University of London, Ph.D. Thesis, 1968.

52. Cooper, T. E., and Trezek, G. J., "Thermal Properties of Human Organs via the Needle Probe Technique," Proceedings of the Twenty-Third Annual Conference on Engineering in Medicine and Biology, Washington, D.C., 1970, p.155.

53. Chato, J. C., Shitzer, A., and Fry, F. J., "Measurement of Thermal Properties of Living Tissue," Proceedings of the Twenty-Third Annual Conference on Engineering in Medicine and Biology, Washington, D.C., 1970, p. 156.

54. Ganong, W. F., Review of Medical Physiology, Third Edition, Lange Medical Publications, Los Altos, California, 1967, p. 450.

55. Bazett, H. C., "The Regulation of Body Temperatures," in Physiology of Heat Regulation and the Science of Clothing, L. H. Newburgh, editor, Hafner Publishing Co., New York, 1968, pp. 109-192.

56. Grollman, S., The Human Body--Its Structure and Physiology, Second Edition, The Macmillan Co., London, England, 1969, p. 166.

57. Nielsen, M., "Die Regulation der Körpertemperature bei Muskelarbeit," Skand. Arch. Physiol., Vol. 79, 1938, pp. 193-230.

58. Shitzer, A., and Chato, J. C., "Analytical Modeling of the Thermal Behavior of Living Human Tissue," Proceedings of the Fourth International Heat Transfer Conference, Versailles, France, 1970, pp. Cu-3.9.

59. Brad, P., Medical Physiology, The C. V. Mosby Co., St. Louis, Mo., 1956, p. 221.

60. Sokolnikoff, I. S., and Redheffer, R. M., Mathematics of Physics and Modern Engineering, McGraw-Hill Book Co., Second Edition, New York, 1966, p. 251.

61. Abramowitz, M., and Stegun, I. A., editors, Handbook of Mathematical Functions, Dover Publications, New York, 1965.

62. Chato, J. C., Hertig, B. A., Gammon, N. A., Streckert, J. H., and Lechner, P., "Physiological and Engineering Study of Advanced Thermoregulatory Systems for Extravehicular Space Suits," Semi-Annual Status Report No. 2, NASA Contract No. NGR 14-005-103, June, 1968.

63. Carslaw, H. S., and Jaeger, J. C., Conduction of Heat in Solids, Second Edition, Oxford University Press, London, England, 1959, pp. 30-32.

64. McLachlan, N. W., Bessel Functions for Engineers, Second Edition, Oxford University Press, London, England, 1941.

65. Chato, J. C., and Shitzer, A., "On The Dimensionless Parameters Associated with Heat Transport within Living Tissue," Aerospace Medicine, Vol. 41, 1970, pp. 390-393.

66. Johnson, R. E. Robbins, F., Schilke, R., Mole, P., Harris, J., and Wakat, D., "A Versatile System for Measuring Oxygen Consumption in Man," Journal of Applied Physiology, Vol. 22, 1967, pp. 377-379.

67. Molnar, S., "The Relationship between Cardiac Time Components, Maximal Oxygen Consumption and Endurance Performance," University of Illinois at Urbana-Champaign, Ph.D. Thesis, 1970.

68. Consolazio, F. C., Johnson, R. E., and Pecora, L. J., Physiological Measurements of Metabolic Functions in Man, McGraw-Hill Book Co., New York, 1963.

69. Dubois, D., and Dubois, E. F., "A Formula to Estimate the Approximate Surface Area if Height and Weight be Known," Archiv. International of Medicine, Vol. 17, 1916, pp. 863-871.

70. Carpenter, T. M., Tables, Factors and Formulas for Computing Respiratory Exchange and Biological Transformation of Energy, Third Edition, Carnegie Institute of Washington, Washington, D.C., 1939.

71. Webb, P., and Annis, J. F., "Bio-Thermal Responses to Varied Work Programs in Men Kept Thermally Neutral by Water Cooled Clothing," NASA Report No. CR-739, 1967.

72. Nunneley, S. A., "Head Cooling in Work and Heat Stress," Ohio State University, Master's Thesis, 1970.

73. Shvartz, E., "Effect of Cooling Hood on Physiological Responses to Work in a Hot Environment," Journal of Applied Physiology, Vol. 29, 1970, pp. 36-39.

74. Hatch, T., "Assessment of Heat Stress," in Temperature, Its Measurement and Control in Science and Industry, J. D. Hardy, editor, Vol. 3, Part 3, Reinhold, New York, 1963, pp. 307-318.

75. Craig, F. N., Medical Division Research Report No. 5, Chemical Corps Army Chemical Center, 1950.

76. Hall, J. F., and Polte, J. W., "Physiological Index of Strain and Body Heat Storage in Hyperthermia," Journal of Applied Physiology, Vol. 15, 1960, pp. 1027-1030.

77. Gold, A. J., and Zornitzer, A., "Effect of Partial Body Cooling on Man Exercising in a Hot, Dry, Environment," Aerospace Medicine, Vol. 39, 1968, pp. 944-946.

78. Hardy, J. D., "The 'Set-Point' Concept in Physiological Temperature Regulation," in Physiological Controls and Regulations, W. S. Yamamoto and J. R. Brobeck, editors, Saunders, Philadelphia, 1965, pp. 98-116.

79. Nagayama, T. H., Eisenman, J. S., and Hardy, J. D., "Single Unit Activity of Anterior Hypothalamus during Local Heating," Science, Vol. 134, 1961, pp. 560-561.

80. Hardy, J. D., Hellon, R. F., and Sutherland, K., "Temperature Sensitive Neurons in the Dog's Hypothalamus," Journal of Physiology, Vol. 175, 1964, pp. 242-253.

81. Robinson, S., Meyer, F. R., Newton, J. L., Ts'Ao, C. H., and Holgersen, L. O., "Relations Between Sweating, Cutaneous Blood Flow and Body Temperature in Work," Journal of Applied Physiology, Vol. 20, 1965, pp. 575-582.

82. Thauer, R.,"Der Nervose Mechanismus der Chemichen Temperaturregulation des Warmbluters," Naturwissenschaften, Vol. 51, 1964, pp. 73-80.

83. Bligh, J., "Localization of the Thermal Stimulus to Polypnoea," Journal of Physiology, Vol. 135, 1957, pp. 48p-49p.

84. Stoll, A. M., and Chianta, M. A., "Application of Biophysical Heat Transfer Studies in Protection Systems," Aerospace Research Department, NADC-MR-6722, 1967.

85. Chato, J. C., and Shitzer, A., "Thermal Modeling of the Human Body--Further Solutions of the Steady-State Heat Equation," to appear in AIAA Journal.